MULTI-OBJECTIVE OPTIMAL DESIGN OF STANDALONE HYBRID RENEWABLE ENERGY SYSTEM USING EVOLUTIONARY ALGORITHMS

© COPYRIGHT UPM

By

HUSSEIN MOHAMMED RIDHA

Thesis Submitted to the School of Graduate Studies, Universiti Putra Malaysia, in Fulfilment of the Requirements for the Degree of Doctor of Philosophy

May 2024

FK 2024 26

All material contained within the thesis, including without limitation text, logos, icons, photographs, and all other artwork, is copyright material of Universiti Putra Malaysia unless otherwise stated. Use may be made of any material contained within the thesis for non-commercial purposes from the copyright holder. Commercial use of material may only be made with the express, prior, written permission of Universiti Putra Malaysia.

Copyright © Universiti Putra Malaysia

Abstract of thesis presented to the Senate of Universiti Putra Malaysia in fulfilment of the requirement for the degree of Doctor of Philosophy

MULTI-OBJECTIVE OPTIMAL DESIGN OF STANDALONE HYBRID RENEWABLE ENERGY SYSTEM USING EVOLUTIONARY ALGORITHMS

By

HUSSEIN MOHAMMED RIDHA

May 2024

Chairman : Associate Professor Hashim bin Hizam, PhD
Faculty : Engineering

The most popular options for remote applications where a grid connection is not available are wind turbine (WT) generators and solar photovoltaic (PV) power systems. Selecting a desirable design of the WT/PV/Battery system among a wide range of configurations, particularly at a favorable level of reliability, lowering the total cost, and reducing surplus energy, remains a challenging task. Therefore, this study seeks to first explore the acquired approaches to solve the nonlinearity of the three-diode PV model's equation utilizing actual measured laboratory data collected at a variety of environmental conditions. Then, the optimum design of the hybrid standalone WT/PV/Battery system is chosen while considering three conflicting techno-economic criteria for power-isolated dwellings in Malaysia and South Africa.

The research presented in this thesis is divided into two phases, namely, modeling of the PV module and optimal sizing of the entire system to obtain reliability, cost-effectiveness, and reduce surplus energy for the WT/PV/Battery system. The robust adaptive arithmetic optimization algorithm based on the adaptive damping Berndt-Hall-Hall-Hausman ($RAOA_{AdBHHH}$) approach is used to efficiently determine the parameters of the three-diode PV model using two types of experimental data of the PV module technologies. In optimal sizing of the hybrid standalone WT/PV/Battery system, a unique improved two-archive approach was presented to develop diversity and convergence independently to find four optimum sets of Pareto front (PF) solutions. Additionally, a new integration based on the best-worst method (BWM) and preference ranking organization for enrichment evaluations (PROMETHEE II) method, along with a group decision-making (GDM) mechanism, was addressed to sort and rank the optimal sets of PF solutions. The objective functions were loss of load probability (LLP), life cycle cost (LCC), and dump power (Pdump) to analyze and evaluate the performance of the selected optimum design using hourly meteorological data for one year in Malaysia and South Africa. Finally, the proposed improved two-archive algorithm is verified using a hybrid numerical method.

The experimental results for the parameter extraction optimization problem demonstrate that the proposed $RAOA_{AdBHHH}$ approach successfully minimizes error to zero with rapid convergence, as determined by different statistical criteria and compared to experimental data of the two PV technologies. On the other hand, the theoretical results based on actual hourly meteorological data in Malaysia and South Africa indicated that the proposed improved two-archive-BWM-PROMETHEE II-GDM method is not only able to construct a uniform set of Pareto optimal solutions with fast convergence and high diversity but can also rank and select the most desired design for the WT/PV/Battery system. The optimum configurations of the two case studies are composed of a single WT, 105 PV modules, 69 battery storages at zero

© COPYRIGHT UPM

LLP, 60185 ($) of LCC, and 13548018 (KWh) of Pdump for the Malaysia case study. Meanwhile, it consists of 16 WTs, 80 PV modules, and 69 battery storages at zero LLP, 66073 ($) of LCC, and 31371 (KWh) of Pdump for the South Africa case study. Furthermore, the proposed improved two-archive-BWM-PROMETHEE II-GDM method is verified by utilizing a hybrid numerical method, which shows a high level of reliability, lowering overall cost, and reducing wasted energy. Therefore, the employment of WT in the Malaysia scenario is not recommended, while the WTs may considerably incorporate in supplying energy for the required load demand.

Keywords: Hybrid renewable energy; PV; Wind, Multi-objective optimization; Multi-criteria decision-making.

SDG: Parameter Extraction Accuracy, Conflicting Triple Objective Optimization, Techno-economic Perspectives.

© COPYRIGHT UPM

Abstrak tesis yang dikemukakan kepada Senat Universiti Putra Malaysia sebagai memenuhi keperluan untuk ijazah Doktor Falsafah

REKABENTUK OPTIMAL PELBAGAI OBJEKTIF SISTEM TENAGA BOLEH DIPERBAHARUI HIBRID STANDALONE MENGGUNAKAN ALGORITMA EVOLUSI

Oleh

HUSSEIN MOHAMMED RIDHA

Mei 2024

Pengerusi : Profesor Madya Hashim bin Hizam, PhD
Fakulti : Kejuruteraan

Pilihan paling popular untuk aplikasi jauh di mana sambungan grid tidak tersedia ialah penjana turbin angin (WT) dan sistem kuasa fotovoltaik solar (PV). Memilih reka bentuk yang diingini bagi sistem WT/PV/Bateri pelbagai konfigurasi, terutamanya pada tahap kebolehpercayaan yang baik, mengurangkan jumlah kos dan mengurangkan lebihan tenaga, kekal sebagai tugas yang mencabar. Oleh itu, kajian ini berusaha untuk terlebih dahulu meneroka pendekatan yang diperoleh untuk menyelesaikan persamaan tidak lurus model PV tiga diod menggunakan data makmal terukur sebenar yang dikumpul pada pelbagai keadaan persekitaran. Kemudian, reka bentuk optimum sistem WT/PV/Bateri kendiri hibrid dipilih sambil mempertimbangkan tiga kriteria tekno-ekonomi yang bercanggah untuk kegunaan kuasa kediaman terpencil di Malaysia dan Afrika Selatan.

Penyelidikan yang dibentangkan dalam tesis ini terbahagi kepada dua fasa iaitu pemodelan modul PV dan saiz optimum keseluruhan sistem untuk mendapatkan

© COPYRIGHT UPM

kebolehpercayaan, keberkesanan kos, dan mengurangkan lebihan tenaga untuk sistem WT/PV/Bateri. Algoritma pengoptimuman aritmetik adaptif teguh berdasarkan pendekatan *Berndt-Hall-Hall-Hausman* (RAOAAdBHHH) redaman adaptif digunakan untuk menentukan parameter model PV tiga diod dengan cekap menggunakan dua jenis data eksperimen teknologi modul PV. Dalam saiz optimum sistem WT/PV/Bateri kendiri hibrid, pendekatan dua arkib unik yang dipertingkatkan telah dibentangkan untuk membangunkan kepelbagaian dan penumpuan secara bebas untuk mencari empat set optimum penyelesaian hadapan Pareto (PF). Selain itu, penyepaduan baharu berdasarkan kaedah terbaik-terburuk (BWM) dan organisasi penarafan keutamaan untuk kaedah penilaian pengayaan (PROMETHEE II), bersama-sama dengan mekanisme membuat keputusan kumpulan (GDM), telah ditangani untuk mengisih dan menyusun set optimum Penyelesaian PF dengan nisbah ketekalan penuh pendapat tiga pakar dan tahap kestabilan yang tinggi dalam konfigurasi kedudukan. Fungsi objektif ialah kehilangan kebarangkalian beban (LLP), kos kitaran hayat (LCC), dan kuasa pembuangan (Pdump) untuk menganalisis dan menilai prestasi reka bentuk optimum terpilih menggunakan data meteorologi setiap jam selama setahun di Malaysia dan Afrika Selatan. Akhir sekali, algoritma dua arkib yang dicadangkan telah disahkan menggunakan kaedah berangka hibrid.

Keputusan eksperimen untuk masalah pengoptimuman pengekstrakan parameter menunjukkan bahawa pendekatan RAOAAdBHHH yang dicadangkan berjaya meminimumkan ralat kepada sifar dengan penumpuan pantas, seperti yang ditentukan oleh kriteria statistik yang berbeza dan dibandingkan dengan data eksperimen kedua-dua teknologi PV. Sebaliknya, keputusan teori berdasarkan data meteorologi setiap jam sebenar di Malaysia dan Afrika Selatan menunjukkan bahawa kaedah dua arkib-

© COPYRIGHT UPM

BWM-PROMETHEE II-GDM yang dicadangkan bukan sahaja mampu membina set seragam penyelesaian optimum Pareto dengan penumpuan pantas dan kepelbagaian tinggi tetapi juga boleh menentukan kedudukan dan memilih reka bentuk yang paling diingini untuk sistem WT/PV/Bateri. Konfigurasi optimum bagi dua kajian kes terdiri daripada satu WT, 105 modul PV, 69 storan bateri pada sifar LLP, 60185 ($) LCC dan 13548018 (KWj) Pdump untuk kajian kes Malaysia. Sementara itu, ia terdiri daripada 16 WT, 80 modul PV, dan 69 storan bateri pada sifar LLP, 66073 ($) LCC, dan 31371 (KWj) Pdump untuk kajian kes Afrika Selatan. Tambahan pula, kaedah dua arkib-BWM-PROMETHEE II-GDM yang dicadangkan telah disahkan dengan menggunakan kaedah berangka hibrid, yang menunjukkan tahap kebolehpercayaan yang tinggi, mengurangkan kos keseluruhan dan mengurangkan tenaga terbuang. Oleh itu, penggunaan WT dalam senario Malaysia tidak digalakkan, manakala WT mungkin banyak menggabungkan dalam membekalkan tenaga untuk permintaan beban yang diperlukan

Kata Kunci: Tenaga boleh diperbaharui hibrid; PV; Angin, Pengoptimuman berbilang objektif; Membuat keputusan pelbagai kriteria.

SDG: Ketepatan Pengekstrakan Parameter, Pengoptimuman Objektif Tiga Bercanggah, Perspektif Techno-economic.

© COPYRIGHT UPM

ACKNOWLEDGEMENTS

First and foremost, Alhamdulillah for giving me the courage, strength, patience, and determination in achieving this work. All thanks and graces belong to Almighty Allah. My Gratitude and Salam to Beloved Prophet Mohammed and his Household) Peace and Blessings of Allah Be Upon Him and His Household) who was sent by Allah to be a great teacher, leader, and commander of humankind.

I would like to express my heartfelt gratitude to my (main) supervisor, Assoc. Dr. Hashim Hizam, and my supervisors Assoc. Dr. Seyedali Mirjalili, Prof. Dr. Mohammad Lutfi Othman, and Dr. Mohammad Effendy Ya'acob for their motivation, enthusiasm, patient, and support. Their advice and guidance have inspired me to conduct a fruitful approach in achieving the objectives of this research. Without their effort, I would not be able to bring the research to completion.

I would like to thank my parents for encouraging me and pray to me as well as my sisters, my brothers, and my friends for their unconditional love and support. I treasure dearly their encouragement and moral support and I realize how lucky I am to have them. Also, I thank all my friends for keeping me and encourage me to do all my best.

© COPYRIGHT UPM

This thesis was submitted to the Senate of Universiti Putra Malaysia and has been accepted as fulfilment of the requirement for the degree of Doctor of Philosophy. The members of the Supervisory Committee were as follows:

Hashim bin Hizam, PhD
Associate Professor
Faculty of Engineering
Universiti Putra Malaysia
(Chairman)

Mohammad Lutfi bin Othman, PhD
Associate Professor, Ir
Faculty of Engineering
Universiti Putra Malaysia
(Member)

Mohammad Effendy bin Ya'acob, PhD
Senior Lecturer, Ir.
Faculty of Engineering
Universiti Putra Malaysia
(Member)

Seyedali Mirjalili, PhD
Associate Professor, Ir
Centre for Artificial Intelligence Research and Optimization
Torrens University Australia
(Member)

ZALILAH MOHD SHARIFF, PhD
Professor and Dean
School of Graduate Studies
Universiti Putra Malaysia

Date:

© COPYRIGHT UPM

TABLE OF CONTENTS

© COPYRIGHT UPM

LIST OF TABLES

© COPYRIGHT UPM

© COPYRIGHT UPM

LIST OF FIGURES

© COPYRIGHT UPM

LIST OF ABBREVIATIONS

ABC	Artificial bee colony
ABSO	Artificial bee swarm optimization
AC	Alternative current
AE	Absolute error
AEO	Ecosystem optimizer
AHP	Analytic hierarchy process
ALO	Ant lion optimizer
AMGA	Archive micro GA
ANN	Artificial neural network
BFA	Bacterial foraging algorithm
BHHH	Berndt-Hall-Hall-Hausman algorithm
BMA	Barnacles mating algorithm
BSA	Backtracking search algorithm
BWM	best worst method
CL	Comprehensive learning
CMAES	Covariance matrix adaption evolution strategy
COA	Coyote optimization algorithm
CRITIC	criteria importance though intercriteria correlation
DC	Direct current
DD	Double diode
DE	Differential evolution
DHS	Discrete harmony search
DSO	Drone squadron optimization
EA	Evolutionary algorithm
EENS	Expected energy not served

© COPYRIGHT UPM

ENSO	Energy not supplied probability
EPO	Emperor penguin optimization
EQE	External quantum efficiency
ESP	Energy shortfall probability
FA	Firefly algorithm
FF	Fill factor
FFA	Farmland fertility algorithm
FL	Fuzzy logic
FPA	Flower pollination algorithm
FUCOM	Full consistency method
GA	Genetic algorithm
GDM	Group decision making
GNDO	Generalized normal distribution optimization
GOL	Generalized opposition learning
GRG	Generalized reduced gradient
HHO	Harris hawk optimization
HOMER	Hybrid optimization model for electric renewable
HS	Harmony search
HSDEMFO	Hybrid symbiotic differential evolution moth-flame optimization
IAE	Individual absolute error
IBSO	Improved brain storming optimization
ICA	Imperialist competitive method
IEO	Improved equilibrium optimizer
IPM	Interior point method
LAB	Lead-acid battery
LCC	Life cycle cost

© COPYRIGHT UPM

LCE	Levelized cost of energy
LCOE	Levelized cost of energy
LHSSA	Locomotion hybrid salp swarm algorithm
LL	Loss of load
LLP	Loss of load probability
LM	Levenberg Marquardt
LOHE	Loss of healthy expectation
LOLE	Loss of load expectation
LPSP	Loss of power supply probability
LPS	Loss of power supply
LW	Lambert W function
MBA	Mine blast algorithm
MBE	Mean bias error
MCDM	Multi-criteria decision making
MCS	Monte Carlo simulation
MOEA-DM	Multi-objective evolutionary algorithm diversity-maintained scheme
MOO	Multiple objective optimization
MPA	Marine predictor algorithm
MPP	Maximum power point
MRF	Manta ray foraging optimization
MRFO	Manta ray foraging optimization
Multi-Si	Multi-crystalline silicon
MVA	Multi-verse algorithm
NM	Nelder-mead simplex algorithm
NPC	Net present cost
NR	Newton Raphson

© COPYRIGHT UPM

NSGA-II	Non-dominated sorting genetic algorithm
OBL	Opposition based learning
OFD	Objective function design
OL	Orthogonal learning
PBI	Penalty-Based boundary Intersection
PF	Pareto front
PGJAYA	Performance-guided JAYA algorithm
PROMETHEE II	Preference ranking organization for enrichment evaluations
PS	Pattern search
PSO	Particle swarm optimization
RaAOA	Robust adaptive arithmetic optimization algorithm
RETScreen	Clean energy management software
RMSE	Root mean square error
RVEA	Reference points guided evolutionary algorithm
SA	Simulated annealing
SAM	System advisor model
SD	Single diode
SFS	Stochastic fractal search
SFLBS	shuffled frog leaping with memory pool parameter
SGDE	Similarity-guided evolutionary multitask optimization with DE
SMA	Slim mould algorithm
SPB	Simple payback time
SPEA2	Strength Pareto evolutionary algorithm
SSE	Sum square error
SSO	Shark smell optimization
STC	Standard test condition

© COPYRIGHT UPM

STF	Special trans function
TAC	Total annual cost
TD	Three diode
TLBO	Teaching learning-based optimization
TOPSIS	Technique for order preference by similarity to ideal solution
TRANSYS	Transient system simulation model
TS	Test statistical
VIKOR	Vlsekriteriterijumska Optimizacija I Kompromisno Resenje
VRB	Vanadium redox battery
WDA	Wind driven algorithm
WOA	Whale optimization algorithm
WT	Wind turbine

© COPYRIGHT UPM

LIST OF SYMBOLS

d_{1-3}	Ideality factor of diodes
	Current conducted by the PV module (A)
I_{o1-03}	Saturation currents of the diodes (A)
V_e	Experimental voltage conducted by the PV module (V)
I_e	Experimental current conducted by the PV module (A)
I_P	Proposed current of the PV module (A)
I_{Ph}	Photocurrent (A)
N	Length of dataset
R_p	Shunt resistance (Ω)
KB	constant of Boltzmann (1.380603e-23 J/K)
R_s	Series resistance (Ω)
V	Voltage conducted by PV module (V)
R^2	Determination coefficient
V_{t1-t3}	Diodes thermal voltages (V)
d_i	Deviation of RMSE
$/$	*Division*
$\times$	*Multiplication*
$-$	*Subtraction*
$+$	*Addition*
X_L	Lower boundary variable
X_U	Upper boundary variable
$rand$	Random integer value between [0,1]
$MOA(C_i)$	Function's value in the current iteration
Max	Maximum value of MOA

© COPYRIGHT UPM

Min	Minimum value of the MOA
$best(x_j)$	Best optimal solution
r_2	Random number value
ϵ	Small number value
$\propto$	Critical parameter set to 5 for exploration accuracy
RL	Levy flight movement
A	Maximum value in OBL mechanism
B	Minimum value in OBL mechanism
X_{mean}	Mean value of X matrix
CMM	Covariance Matrix based Migration
Q_{xnew}	$D \times D$ matrix containing the eigenvector
A_{xnew}	Diagonal matrix
$\bar{M}$	Complement of multiplication operation
$\bar{D}$	Complement of division operation
β_i	Parameter estimate at current iteration
A_i	Variance-covariance matrix
$\propto_i$	Adaptive nonlinear damping parameter
V_{oc}	Open-circuit voltage
I_{sc}	Short-circuit current
I_{mpp}	Maximum power point current
λ_s	Reference values for solar radiation
T_r	Reference values for ambient temperature
β	Open-circuit coefficient
$v2$	WT's speed at the hub height ($h2$)
v_0	Refers to the WT's speed at reference height ($h2$)
$\propto$	Friction coefficient parameter (Hellmann exponent)

© COPYRIGHT UPM

V_{Ci}	Cut-in wind speed
V_{Co}	Cut-out wind speed
Pr	Rated power of the wind turbine
Vr	Nominal wind speed
C_{batt}	Capacity of the battery
$SOC_{(n)}$	State of charge at current iteration
DoD	Depth of discharge
$P_{L(n)}$	Energy demand
$\eta batt$	Efficiency of the battery
ηinv	Efficiency of the inverter
ηch	Efficiency of the charge controller
P_{WT}	Power of the wind turbine
P_{PV}	Power of thee PV modules
LLP	Loss of load probability
P_{dump}	Dumped power
LCC	Life cycle cost
I_c	Initial cost of the system
OM_c	Operation and maintenance expense of the system
LT	Lifespan of the system
f_r	Inflation rate
I_r	Interest rate
R_c	Replacement cost of the system
CA	Convergence archive
DA	Diversity archive
$I_{\varepsilon+}$	Indicator-based evolutionary algorithm (IBEA)
C_n	Criteria of the decision matrix

© COPYRIGHT UPM

A_B	Importance of the best criteria B over criteria $C_j, j = 1,2, \ldots, n$
W_j	Weight value of each objective
ξ^*	Consistency ratio
P_j	Preference function
δ_{it}	Difference in performance of the alternative of the criteria j
φ^+	Positive alternative criteria
φ^-	Negative alternative criteria
φ_j	Best sorting of the alternative
V_{bus}	Voltage of the bus system
V_{batt}	Voltage of the battery
v_i^*	Shortest distance from the positive-ideal solution
v_i^-	Farthest distance from the negative-ideal solutions
β_j^*	Euclidean distance from ideal-positive solution
β_j^-	Euclidean distance from ideal-negative solution
ϕ_j	Closeness to the ideal solution

© COPYRIGHT UPM

CHAPTER 1

INTRODUCTION

1.1 Research background

In the last decades, the population growth, global industrialization, and energy crisis around the world has resulted in huge usage of energy resources. Due to the ultimate progresses in all aspects of human life, the need to develop the renewable energy sources such as nuclear, wind turbine, and photovoltaic renewable energy sources is essential [8]. Therefore, the governments and scholars are motivated to change the strong dependability on the fossil fuels to clean, economical, inexhaustible, and efficient renewable energy resources. However, there are a number of economic and technical barriers must be overcome in order to improve the dependability and lower the capital cost of the hybrid PV systems [9]. In addition, the electrical hybrid systems have various benefits and drawbacks to balance between each involved component. This is attainable by accurately predicting the PV cells' output current utilizing genuine experimental data gathered at a range of environmental conditions. The performance of the PV system can be evaluated by extracting the parameters from the predefined PV model. Such parameters are strongly influenced by the solar irradiance, ambient temperature, wind speed, humidity, dust, and type of the PV technology. The degree of agreements between simulated and experimental currents using I-V and P-V curves indicates the correctness of the PV model [10].

The combination of wind turbine (WT) and photovoltaic (PV) energy systems is considered as a very economical option to generate electrical energy especially for remote areas owing to the complimentary nature and widely abundant, where the

© COPYRIGHT UPM

utility grid is expensive. These renewable energy sources are heavily impacted by the speed of the wind and amount of solar radiation, which are site-dependent. This system depends on the WT and PV technologies that converts the wind and solar radiation to electrical energy in order to fulfill the load demand energy. In addition, the use of batteries storage allows to store the excess energy during the day and restore it at the night.

1.2 Problem statement

The solar cells' performance under outside weather conditions are strongly dependent on their physical characteristics. Therefore, it is very necessary to address these parameters precisely while taking the range of environmental circumstances into consideration utilizing real experimental data [11]. In addition to that the nonlinearity behavior between each component of the standalone WT/PV/Battery system, and nonuniformity between the renewable energy sources and load demand make the selection to the optimal design more challenging and intricate. The high initial costs and loss of load are the major drawbacks of expansions of these systems. The system's dependability can be strengthened by utilizing an energy storage device as a backup supply, such as batteries, where the surplus energy can be stored [12].

To plot the I-V and P-V curves, the parameters of these models must be optimally estimated. As an outcome, such parameter may be determined either by minimizing the error between the simulated model and real experimental data, or by obtaining the three main reference points under ideal conditions: open-circuit (OC), short-circuit (SC), and maximum power point (MPP) [13]. Thus, the PV module's parameters take essential impacts on modeling and designing of the WT/PV/Battery system which can

© COPYRIGHT UPM

influence the availability and overall cost of the system [14]. Extracting the unknown parameters of the PV models utilizing actual experimental data gathered at a variety of weather circumstances is regarded to be more suitable and accurately represents the actual behavior of the PV cells. However, a significant hurdle to using these methods is a lack of broad and varied experimental data across a range of weather conditions [15]. The literature describes a number of approaches to parameter extraction optimization, involving analytical, numerical, stochastic, hybrid, and software tools [16,17]. The methods were utilized for modeling the PV model in the WT/PV/Battery systems are inaccurate and simple [18]. However, Hybrid methods have been proven their ability in extraction the parameters of the PV module in terms of efficiency, fast convergences, reducing the time of execution. The values of the parameters and I-V characteristics curve are determined under different weather conditions [19]. Consequently, inefficient modeling of the PV system can lead to undesirable performance and design of the WT/PV/Battery system which means that the system will be not only unreliable but also costly [20].

Another challenge is the current designing methods of the off-grid freestanding WT/PV/Battery system. Few research papers have considered multi-objective optimization (MOO) methods along with multi-criteria Decision making (MCDM) methods for optimal configuration of the WT/PV/Battery system in order to construct set of Pareto Front (PF) solutions and rank the configurations from the best to worst one. The MOO methods can be classified into single-objective methods which convert more than two objectives into single-objective, or optimizing more than two objectives synchronously by achieving a trade-off between them. The MOO methods generate two sets of solutions known as dominated and non-dominated solutions. In the

© COPYRIGHT UPM

dominated concept, the objectives are optimized without depriving the others. While, the non-dominated principle, the objectives cannot be further improved without prejudicing others [21]. Therefore, the set of PF solutions contains the best trade-off in the non-dominated solutions. Majority of researchers optimize the reliability and total cost of the system, while few of them address the reduction of the surplus energy, which may have a considerable impact on the overall system cost while ensuring a high level of dependability. Following that, It has observed that some of MCDM methods such as TOPSIS and VIKOR do not allow the decision maker to deal with unquantifiable facts in circumstances where the conflicting objectives are challenging to be organized [22]. Moreover, TOPSIS and VIKOR fail in ranking the set of optimal PF solutions when the dealing with complex three conflicting objectives due to their utilized structure. Finally, few research works pay attentions on how to choose the most appropriate configuration from a pool of optimal PF solutions' rather than providing further details on the consistency ratio of the expert or durability of the MCDM technique [23].

Therefore, an appropriate modeling method to identify the unknown parameters of the PV module is necessary to predict the output current of the WT/PV/Battery system. Optimization of the WT/PV/Battery system based powerful on multi-objective method is required to increase system reliability, minimizing the capital cost, and reducing the surplus energy. Finally, lack of studies were performed considering the selection of the best optimal solutions from the Pareto front set, especially when the objectives are complex and conflicting. Thus, the multi-criteria decision-making (MCDM) methods are very useful to handle this dilemma.

© COPYRIGHT UPM

1.3 Objectives

The objectives of this research study can be highlighted to achieve the following:

1. To develop an accurate method of parameters extraction of the PV module's model based on robust adaptive arithmetic optimization algorithm integrated with Berndt-Hall-Hall-Hausman technique ($RaAOA_{AdBHHH}$).
2. To optimize the size of the WT/PV/Battery system using improved two-archive algorithm by addressing convergence and diversity individually based on technoeconomic criteria considering Malaysia and South Africa case studies. The most desirable design of the WT/PV/Battery system from four sets of optimal PF solutions using advance hybrid multi-criteria decision methods.
3. To validate the proposed improved two-archive method for sizing of the WT/PV/Battery system using hybrid numerical method.

1.4 Significance and contribution of the study

According to the previous objectives, there are several theoretical gaps have been observed in this topic, which are summarized as follows:

- In this study, we have developed both methodology (algorithm itself) and objective function formulation by using innovative $RaAOA_{AdBHHH}$ model.
- This research study presents a new MOO principle by addressing convergence and diversity individually.
- This research introduces a fusion of the BWM and PROMETHEE II method groups.
- Finally, the proposed method is verified by combining with BWM-TOPSIS-GDM and BWM-PROMETHEE II-GDM methods, and the performance is assessed by hourly environmental data collected over the course of a year period in two distant places in Malaysia and South Africa.

© COPYRIGHT UPM

1.5 Scope and limitations of work

This thesis considers the improvements and developments of the WT/PV/Battery system by presenting a novel methodology to estimate the output current of the TD PV model based on real experimental data and an innovative hybrid improved two-archive algorithm for optimal sizing and selecting of the most desirable configuration from different sets of optimal PF solutions. The optimal design of hybrid standalone WT/PV/Battery system is strongly dependent on the availability of the meteorological data. In this study, we utilized the only the available data of the Malaysia and South Africa. In addition, it can support the viability, correctness, and capacity of the proposed method to solve three contradictory techno-economic criteria in diverse locations.

The scope of this work can be highlighted as follows:

- The $RaAOA_{AdBHHH}$ model is employed to estimate the nine parameters TD PV model of the standalone WT/PV/Battery system. The proposed $RaAOA_{AdBHHH}$ approach made significant advances in terms of methodology (algorithm itself) and design of the objective function. In terms of methodology, the improved opposition based learning (IOBL) was maintained to prevent local minima while teaching learning (TL) is obtained to improve the local search capability. Secondly, the exploration stage was developed by the use of complement division ($\overline{D}$) and subtraction (S) operators, along with Covariance Matrix based Migration (CMM) and levy flight (LF) techniques. Besides, the exploitation stage was augmented via the use of complement multiplication ($\overline{M}$) and addition (A) operators, as well as three unique vectors picked randomly from the population. Finally, winner principle was considered, which is based on two robust mutation procedures, in order to gradually improve the search capability. The $RaAOA_{AdBHHH}$ model's objective function was introduced for the first time for resolving the PV model's equation and to efficiently predict the initial roots of the PV

© COPYRIGHT UPM

models utilizing only first order derivative and half space expectation movements.

- A new fusion based on improved bi-archive multi-objective optimization algorithm for findings four well-constructed groups of optimal PF solutions and BWM-PROMETHEE II-GDM for sorting and ranking the optimized designs of the freestanding PV/WT/Battery system in two different locations: Malaysia and South Africa. The most desirable configurations for the freestanding PV/WT/Battery system are determined based on techno-economic-reliability assessments: LLP, LCC, and P_{dump} using hourly meteorological data over the course of one year. The improved two archive algorithm is presented to overcome the restrictions of the previous multi-objective methods by assigning two different selection concepts: Indicator-based and Pareto-based to the archive [24]. Furthermore, the diversity into the archive is increased by addressing the L_p-norm-based ($p < 1$) scheme. The description of the CA and DA are given in the Ref. [24]. In addition to that the hybrid MCDM method based on BWM-PROMETHEE II-GDM is presented to weight the three conflicting objectives based on three opinions of the three experts with full consistency ratio, to rank the configurations conducted by four optimal PF sets, and selecting the most desirable solutions by considering all opinions of the three experts.

- Finally, the proposed improved bi-archive multi-objective optimization method is validated by the usage of hybrid numerical methods.

The major limitations of this research work are given in the following:

- In extraction the parameters of the TD PV model, the proposed $RaAOA_{AdBHHH}$ needs more execution time owing to the complexity to determine its nine parameters. However, the accuracy, stability, and robustness are more important as the determined nine parameters of the TD PV model are based on off-line experimental data.

- Computing the output power of the WT is based on sequence of mathematical equations. More precise output power prediction of the WT can be performed

© COPYRIGHT UPM

using machine learning models. However, real experimental data of the output power of the WT is not available in this study.

- Dynamic behavior of the charging, discharging, and state of charge of the battery storage can be further developed in order to simulate the actual behavior of the battery storage.

1.6 Thesis outline

This thesis consists of five chapters, where chapter 1 includes an overview of the thesis and contains the introduction, research problem, objectives, research questions, significance and contribution of the study, and scope and limitations of work.

Chapter 2 contains the literature review, which includes types of the PV models, the employed methods to extract the parameters of the PV modules. In addition, kinds of typologies of the WT/PV/Battery system, the advantages and disadvantages of the WT, and optimal sizing methods of the WT/PV/Battery system. Finally, the weakness and challenges of the WT/PV/Battery system's performance are summarized.

Chapter 3 presents the methodology of this study. The proposed $RaAOA_{AdBHHH}$ model to extract the parameters of the TD PV model is discussed. The verification and assessments of the accuracy, stability, and reliability of the proposed $RaAOA_{AdBHHH}$ model are presented. Moreover, the proposed improved two-archive algorithm to construct set of optimal PF solutions is explained. The hybrid BWM-PROMETHEE II-GDM method is explained to weight and rank the configurations from best two worst. Loss of load probability (LLP), life cycle cost (LCC), and power dump (P_{dump}) are obtained to as techno-economic objectives to be optimized. Finally, the hybrid

© COPYRIGHT UPM

intuitive-numerical-MOO-BWM_TOPSIS-GDM method is employed to verify the accuracy of the proposed optimization method.

In chapter 4, the results and findings to determine the parameters of the TD PV model using two sets of the experimental data are presented. The proposed $RaAOA_{AdBHHH}$ model is verified by comparing with various well-published methods available in the literature under various conditions of the weather data using different statistical criteria. The optimization size of the WT/PV/Battery system using improved two-archive-BWM-PROMETHEE II-GDM is discussed using hourly meteorological data for one year with considering two case studies: Malaysia and South Africa. The most desirable optimal configuration is chosen for both scenarios and validated using hybrid numerical approach. The results and discussion are shown with figures and presented with tables in this chapter.

Chapter 5 summarizes the contributions of the is study and how the objectives are achieved. Finally, this chapter ends with future work direction of this study.

© COPYRIGHT UPM

CHAPTER 2

LITERATURE REVIEW

2.1 Introduction

Countless aspects have contributed to the rise in the energy consumption, indicating rapid population expansion, global warming, economic development, and industrialization. These changes can be attributed to major problems associated with the use of conventional fossil fuels, such as oil, gas, and coral [25]. In addition, commencement of the utility gird power for the remote areas has a number of technical and economic challenges, owning to lower energy consumption and costly initial expenditures. As a consequence, adopting alternative energy sources is crucial for reducing reliance on the fossil fuels and environmental damage [26]. Although renewable energy resources seem to be an excellent option, they still have many shortcomings, including their intermittent nature, weakness in some regions, and high initial expenses. Governments, research institutions, and businesses have spent decades developing renewable energy resources in order to enhance their dependability while maintaining low capital costs [27].

Both PV and WT generators are most widely utilized renewable energy sources, with 733 GW and 714 GW installed global capacity by the end of 2020 [28]. However, because to the intermittent nature, it is not practical to rely solely on the PV panels for the whole of the day. Therefore, the hybrid wind-photovoltaic system have been considered to remedy this issue. To provide more dependable and cost-effective options, the storage batteries are integrated in this system [29]. Designing hybrid systems is a difficult endeavor owning to nature’s stochastic behavior, integration

© COPYRIGHT UPM

between the components, and nonlinearity that directly impacts on the renewable energy sources. Moreover, such systems require to identify of the wind speed ratio and availability of the solar irradiation which are location dependent. Therefore, several researchers and designers have developed methodologies for determining the optimal designs depending on multiple objectives [30].

This study presents a review on parameters extraction of the PV models using different formulations of the objective functions. In addition to that, the methodologies for optimal sizing of the WT/PV/Battery system are explained. Finally, the limitations and challenges of the hybrid off-grid WT/PV/Battery system are discussed.

2.2 Hybrid off-grid WT/PV/Battery system

In general, the hybrid freestanding WT/PV/Battery system composes mainly of wind turbine, PV panels, bidirectional inverter, charge controller, storage battery, and load profile. According to a variety of variables, such as the accessibility of meteorological data, techno-economic criteria, and the desired power demand, these might vary significantly. The hybrid WT/PV/Battery system may be categorized based on system operation into two topologies: series topology [31,32], and parallel topology [33], as seen in Figure 1 and 2. In the series topology, the WT generator is connected to rectifier and PV panel linked to the charge controller. The battery storage can be charged through WT and PV panels through charge controller. The WT here cannot provide energy to the load demand directly. There several limitations in this topology and given by the following:

- The efficiency is low owning to energy loss during the changeover between the AC and DC busses.

© COPYRIGHT UPM

- The capacity of the inverter should be large, which is substantially larger than the maximum peak energy of the load demand.

- This topology is much expensive.

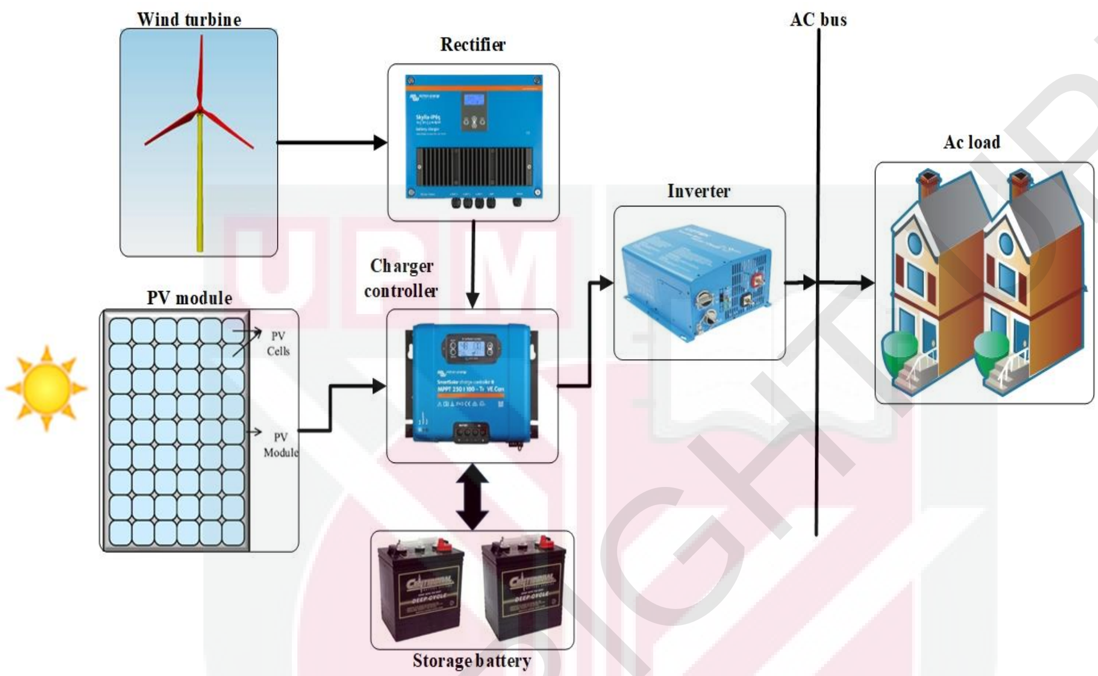

Figure 2.1 : Diagram of series topology for hybrid PV/WT/Battery system

On contrast, the parallel topology provides a superior performance compared with the previous one. This is because the WT can directly supply electricity to the required load demand, indicating a higher total efficiency for the WT/PV/Battery system, as illustrated in Figure 2.2. The main benefits of the this hybrid topology are [34]:

- There is no need to use many changeovers between the AC and DC busses, where the bi-directional allows the flow of electricity in both ways.

- Overall cost of the system is reduced.

- The capacities of the renewable energy sources, charge controller, and bi-inverter are minimized.

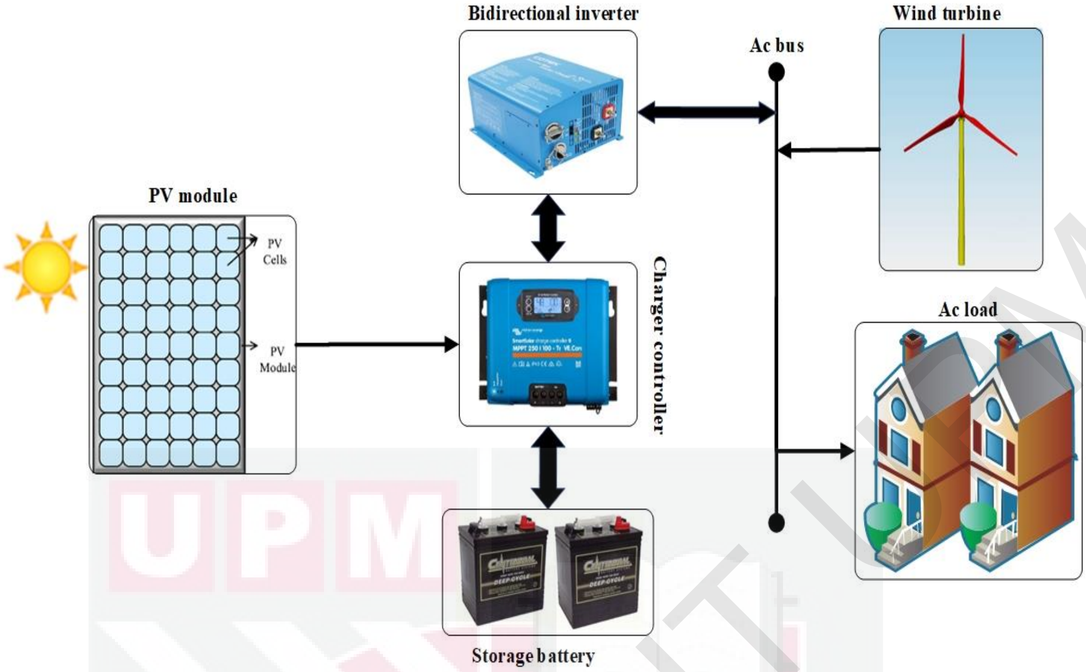

Figure 2.2 : Diagram of parallel topology for hybrid PV/WT/Battery system

In this chapter, the modeling components of the freestanding WT/PV/Battery system, optimization methods, and MCDM methods will be explored, and the challenges to this topic will be outlined in this chapter.

2.2.1 PV array model

In general, PV mathematical models are grouped into three broad categories: single diode (SD) model, double diode (DD) model, and three diode (TD) model. To plot the I-V and P-V curves, the parameters of these models must be optimally estimated. As an outcome, such parameter may be determined either by minimizing the error between the simulated model and real experimental data, or by obtaining the three main reference points under ideal conditions: open-circuit (OC), short-circuit (SC), and maximum power point (MPP) [13].

© COPYRIGHT UPM

- **Single-diode PV model**

The single diode model is the most often applied in prediction the output current of the PV cell in the literature owning to its simplicity, needing only five physical parameter to be optimality extracted. The five physical parameters are as follows: an ideality factor d linked in opposite direction to represent the PV cell's output voltage, a parallel-connected photovoltaic current source I_{Ph} in (A) parallelly connected, a diode saturation current I_o, a small series resistance R_s in (Ω), and a large shunt resistance R_p in (Ω) linked in parallel to describe the saturation current of the diode. Figure 2.3 illustrates the physical parameters of the SD PV model. Therefore, utilizing Kirchhoff's rule, the output current of the cell I in (A) can be calculated as follows:

$$I = I_{Ph} - I_d - I_p, \tag{2.1}$$

where I_d represents the current flowing through diode in (A) and I_p refers to the current flowing through the shunt resistor in (A). The I_d may be computed by deriving Shockley diode law in the following manner:

$$I = I_o \left[exp\left(\frac{V+IR_s}{V_t}\right) - 1 \right], \tag{2.2}$$

where V is the output voltage (V) and V_t refers to the thermal diode voltage (V). The V_t can be computed as follows:

$$V_t = \frac{dKBT_c}{q}, \tag{2.3}$$

where KB is the Boltzmann's constant $(1.38 \times 10^{-23}\, J/K)$, T_c refers to the cell temperature (K), and q is to the electron charge $(1.60 \times 10^{-19} C)$. The I_p is expressed by the following:

© COPYRIGHT UPM

$$I_p = \frac{V+IR_s}{R_p}, \tag{2.4}$$

As a result of solving Equations (2.1)-(2.4), the I is described using the following equation:

$$I = I_{Ph} - I_o \left[exp\left(\frac{V+IR_s}{V_{t1}}\right) - 1\right] - \frac{V+IR_s}{R_p}, \tag{2.5}$$

Therefore, the five parameters (d, I_{Ph}, I_o, R_s, and R_p) must be determined in order to plot the I-V and P-V characteristics curves [35].

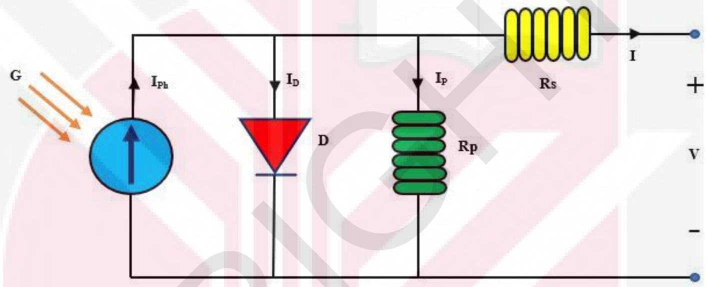

Figure 2.3 : The electrical circuit of the SD PV model

- **Double-diode PV model**

The DD PV model is employed to compensate the preceding PV model's poor accuracy. This model has a superior accuracy, especially at high solar irradiance conditions [35]. A second diode d_2 is inserted to reflect the recombination losses that occur in the depletion zone. Figure 2.4 depicts the physical electrical components of the DD PV model, whereas the output current is represented as follows:

$$I = I_{Ph} - I_{o1} \left[exp\left(\frac{V+IR_s}{V_{t1}}\right) - 1\right] - I_{o2} \left[exp\left(\frac{V+IR_s}{V_{t2}}\right) - 1\right] - \frac{V+IR_s}{R_p}, \tag{2.6}$$

© COPYRIGHT UPM

where I_{o1} and I_{o2} are reverse diode saturation currents, and V_{t1} and V_{t2} are diode thermal voltages written as follows:

$$V_{t1} = \frac{d_1 KBT_c}{q}, V_{t2} = \frac{d_2 KBT_c}{q}, \tag{2.7}$$

where d_1 and d_2 denote to the first and second ideality factors of the diodes, respectively. It is worth noting that extracting the seven parameters from the DD PV model involves additional computing time.

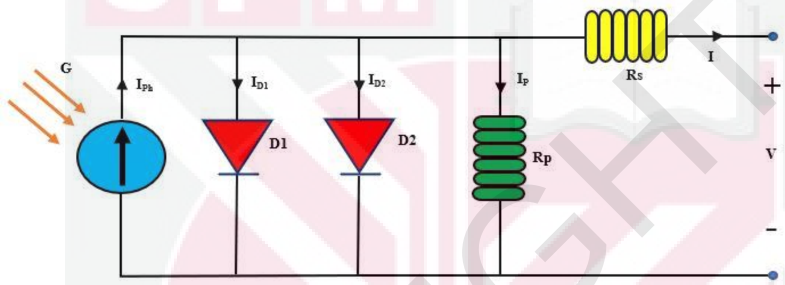

Figure 2.4 : The electrical circuit of the DD PV model

- **Three diode PV model**

The TD PV model has garnered more attention from scholars and academics due to its great accuracy in compared to prior PV models, which included another diode ideality factor d_3 and saturation dark current I_{o3}. Figure 2.5 exhibits the electrical equivalent circuit of the TD PV model, while the output current may be described as follows [35]:

$$I = I_{Ph} - I_{o1}\left[exp\left(\frac{V+IR_s}{V_{t1}}\right) - 1\right] - I_{o2}\left[exp\left(\frac{V+IR_s}{V_{t2}}\right) - 1\right] - I_{o3}\left[exp\left(\frac{V+IR_s}{V_{t3}}\right) - 1\right]\frac{V+IR_s}{R_p}, \tag{2.8}$$

where V_{t1}, V_{t2}, and V_{t3} are the diode's thermal voltage and expressed by the following:

© COPYRIGHT UPM

$$V_{t1} = \frac{d_1 KBT_c}{q}, V_{t2} = \frac{d_2 KBT_c}{q}, \text{and } V_{t3} = \frac{d_3 KBT_c}{q} \tag{2.9}$$

This model is complicated, and needs more computing time to extract its nine parameters.

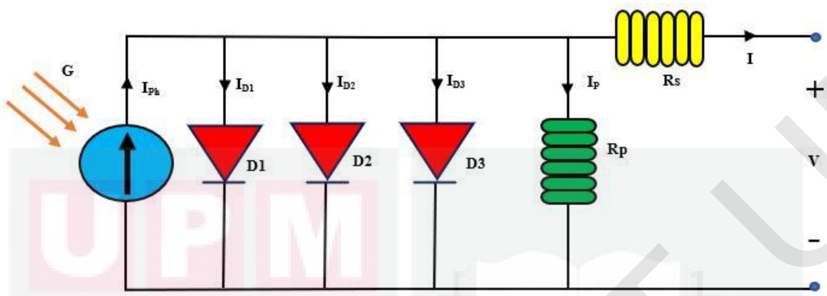

Figure 2.5 : The electrical circuit of the TD PV model

2.2.2 Objective function formulation

The PV model's equation is multivariable, nonlinear, and has multiple local minima owning to the impact of the natural behaviour of the solar radiation and ambient temperature. The majority of authors in the literature develop the methodology (algorithm itself) and immediately substituting the algorithm-estimated parameters into the main PV model's equation, resulting poor degree of accuracy [36]. On the other hand, the NR and LW function are most frequently utilized methods for solving this problem. The NR has fast convergence, whereas the LW function has a considerable accuracy, especially at heterogeneous operating temperature. However, the authors in [6] improved the NR method using LM's constant parameter [37]. The Root Mean Square Error (RMSE) is lowered by approximately 50% in this research. The following are the mathematical models of these approaches:

© COPYRIGHT UPM

A. NR method

For the SD PV model:

$$I = I - \frac{I_{Ph} - I - I_o\left(exp\left(\frac{V+R_SI}{dV_t}\right)-1\right) - \frac{V+R_SI}{R_p}}{-1 - I_o\left(\frac{R_S}{dV_t}\right) exp\left(\frac{V+R_SI}{dV_t}\right) - \frac{R_S}{R_p}}, \tag{2.10}$$

For the DD PV model:

$$I = I - \frac{I_{Ph} - I - I_{o1}\left(exp\left(\frac{V+R_SI}{d_1V_t}\right)-1\right) - I_{o2}\left(exp\left(\frac{V+R_SI}{d_2V_t}\right)-1\right) - \frac{V+R_SI}{R_p}}{-1 - I_{o1}\left(\frac{R_S}{d_1V_t}\right) exp\left(\frac{V+R_SI}{d_1V_t}\right) - I_{o2}\left(\frac{R_S}{d_2V_t}\right) exp\left(\frac{V+R_SI}{d_2V_t}\right) - \frac{R_S}{R_p}}, \tag{2.11}$$

For the TD PV model:

$$I = I - \frac{I_{Ph} - I - I_{o1}\left(exp\left(\frac{V+R_SI}{d_1V_t}\right)-1\right) - I_{o2}\left(exp\left(\frac{V+R_SI}{d_2V_t}\right)-1\right) - I_{o3}\left(exp\left(\frac{V+R_SI}{d_3V_t}\right)-1\right) - \frac{V+R_SI}{R_p}}{-1 - I_{o1}\left(\frac{R_S}{d_1V_t}\right) exp\left(\frac{V+R_SI}{d_1V_t}\right) - I_{o2}\left(\frac{R_S}{d_2V_t}\right) exp\left(\frac{V+R_SI}{d_2V_t}\right) - I_{o3}\left(\frac{R_S}{d_3V_t}\right) exp\left(\frac{V+R_SI}{d_3V_t}\right) - \frac{R_S}{R_p}}, \tag{2.12}$$

B. INR methods

$$I(i+1) = I(i) - \propto * \frac{F(i)}{F`(i)}, \tag{2.13}$$

For the SD PV model:

$$F(I) = I_{Ph} - I_o\left(\exp\left(\frac{(V+IR_S)}{d_1V_t}\right) - 1\right) - \frac{V+IR_S}{R_p} - I, \tag{2.14}$$

$$F`(I) = -I_o\frac{R_S}{dV_t}\left(\exp\left(\frac{(V+IR_S)}{d_1V_t}\right)\right) - \frac{R_S}{R_p} - 1, \tag{2.15}$$

For the DD PV model:

$$F(I) = I_{Ph} - I_{o1}\left(\exp\left(\frac{(V+IR_S)}{d_1V_t}\right) - 1\right) - I_{o2}\left(\exp\left(\frac{V+IR_S}{d_2V_t}\right) - 1\right) - \frac{V+IR_S}{R_p} - I, \tag{2.16}$$

$$F`(I) = -I_{o1}\frac{R_S}{d_1V_t}\left(\exp\left(\frac{(V+IR_S)}{d_1V_t}\right)\right) - I_{o2}\frac{R_S}{d_2V_t}\left(\exp\left(\frac{(V+IR_S)}{d_1V_t}\right)\right) - \frac{R_S}{R_p} - 1, \tag{2.17}$$

© COPYRIGHT UPM

For the TD PV model:

$$F(I) = I_{Ph} - I_{o1}\left(\exp\left(\frac{(V+IR_s)}{d_1V_t}\right) - 1\right) - I_{o2}\left(\exp\left(\frac{V+IR_s}{d_2V_t}\right) - 1\right) - I_{o3}\left(\exp\left(\frac{V+IR_s}{d_2V_t}\right) - 1\right) - \frac{V+IR_s}{R_p} - 1, \quad (2.18)$$

$$F`(I) = -I_{o1}\frac{R_s}{d_1V_t}\left(\exp\left(\frac{(V+IR_s)}{d_1V_t}\right)\right) - I_{o2}\frac{R_s}{d_2V_t}\left(\exp\left(\frac{(V+IR_s)}{d_1V_t}\right)\right) - I_{o3}\frac{R_s}{d_2V_t}\left(\exp\left(\frac{(V+IR_s)}{d_1V_t}\right)\right) - \frac{R_s}{R_p} - 1, \quad (2.19)$$

where $\propto$ is a static damping parameter and set to be 0.05 in the INR method. In the [38], the $\propto$ is given as follows:

$$\propto_i = e^{-\left(\frac{4.5C_i}{M_i}\right)^{2.5}}, \quad (2.20)$$

where C_i is the current iteration and M_i is the maximum iteration.

C. Lambert W function method

For the SD PV model:

$$I = \frac{R_p(I_{Ph}+I_o)-V}{R_p+R_s} - \frac{V_t}{R_s}[dW(\beta)], \quad (2.21)$$

For the DD PV model:

$$I = \frac{R_p(I_{Ph}+I_{o1}+I_{o2})-V}{R_p+R_s} - \frac{V_t}{R_s}[d_1W(\beta_1) + d_2W(\beta_2)], \quad (2.22)$$

For the TD PV model:

$$I = \frac{R_p(I_{Ph}+I_{o1}+I_{o2}+I_{o3})-V}{R_p+R_s} - \frac{V_t}{R_s}[d_1W(\beta_1) + d_2W(\beta_2) + d_3W(\beta_3)], \quad (2.23)$$

© COPYRIGHT UPM

where

$$\beta_1 = \frac{I_{o1} R_s R_p}{d_1 V_{t1}(R_s + R_p)} exp\left\{\frac{R_p(R_s I_{Ph} + R_s I_{o1} + V)}{d_1 V_{t1}(R_s + R_p)}\right\}, \quad (2.24)$$

$$\beta_2 = \frac{I_{o2} R_s R_p}{d_2 V_{t2}(R_s + R_p)} exp\left\{\frac{R_p(R_s I_{Ph} + R_s I_{o2} + V)}{d_2 V_{t2}(R_s + R_p)}\right\}, \quad (2.25)$$

$$\beta_3 = \frac{I_{o3} R_s R_p}{d_3 V_{t3}(R_s + R_p)} exp\left\{\frac{R_p(R_s I_{Ph} + R_s I_{o3} + V)}{d_3 V_{t3}(R_s + R_p)}\right\}, \quad (2.26)$$

Anyway, the PV array's output current is strongly affected by the meteorological data conditions. Therefore, the parameters of the TD PV model can be estimated based on the datasheet information given by the manufacturer under standard test conditions (STC). The manufacturer typically provides information for open-circuit (V_{oc}), short-circuit (I_{sc}), and maximum power point (I_{mpp}) at standard test conditions (STC) [39]. Following the determination of the optimum parameters of the d_{1-3}, R_s, and R_p, the I_{Ph} and I_{o1-3} parameters are computed as follows [39]:

$$I_{o1} = \frac{I_{sc} + \frac{R_s I_{sc}}{R_p} - \frac{V_{oc}}{R_p} -}{exp\left(\frac{qV_{oc}}{d_1 kbN_c T_c}\right) - exp\left(\frac{qR_s I_{sc}}{d_1 kbN_c T_c}\right)}, \quad (2.27)$$

$$I_{o2} = \frac{I_{sc} + \frac{R_s I_{sc}}{R_p} - \frac{V_{oc}}{R_p} - I_{o1}\left(exp\left(\frac{qV_{oc}}{d_1 kbN_c T_c}\right)\right) - I_{o1}\left(exp\left(\frac{qR_s I_{sc}}{d_2 kbN_c T_c}\right)\right)}{exp\left(\frac{qV_{oc}}{d_2 kbN_c T_c}\right) - exp\left(\frac{qR_s I_{sc}}{d_2 kbN_c T_c}\right)}, \quad (2.28)$$

$$I_{o3} = \frac{I_{sc} + \frac{R_s I_{sc}}{R_p} - \frac{V_{oc}}{R_p} - I_{o1}\left(exp\left(\frac{qV_{oc}}{d_1 kbN_c T_c}\right)\right) - I_{o1}\left(exp\left(\frac{qR_s I_{sc}}{d_1 kbN_c T_c}\right)\right) - I_{o2}\left(exp\left(\frac{qV_{oc}}{d_2 kbN_c T_c}\right)\right) - I_{o2}\left(exp\left(\frac{qR_s I_{sc}}{d_2 kbN_c T_c}\right)\right)}{exp\left(\frac{qV_{oc}}{d_2 kbN_c T_c}\right) - exp\left(\frac{qR_s I_{sc}}{d_2 kbN_c T_c}\right) - exp\left(\frac{qV_{oc}}{d_3 kbN_c T_c}\right) - exp\left(\frac{qR_s I_{sc}}{d_3 kbN_c T_c}\right)}, \quad (2.31)$$

© COPYRIGHT UPM

$$I_{ph} = I_{o1}\left(exp\left(\frac{qV_{oc}}{d_1 kbN_cT_c}\right) - 1\right) + I_{o2}\left(exp\left(\frac{qV_{oc}}{d_2 kbN_cT_c}\right) - 1\right) + I_{o3}\left(exp\left(\frac{qV_{oc}}{d_3 kbN_cT_c}\right) - 1\right) + \frac{R_sI_{sc}}{R_p}, \tag{2.29}$$

To construct I-V and P-V characteristics curves, the extracted nine parameters are substituted in the three key points: open-circuit [0, V_{oc}], short-circuit [I_{sc},0], and maximum power point [I_{mpp}, V_{mpp}]. The mathematical equations of the three key points are represented as follows [39]:

$$E_{oc} = I_{o1}\left(exp\left(\frac{qV_{oc}}{d_1 kbN_cT_c}\right) - 1\right) + I_{o2}\left(exp\left(\frac{qV_{oc}}{d_2 kbN_cT_c}\right) - 1\right) + I_{o3}\left(exp\left(\frac{qV_{oc}}{d_3 kbN_cT_c}\right) - 1\right) + \frac{V_{oc}}{R_p} - I_{ph}, \tag{2.30}$$

$$E_{sc} = I_{sc} + I_{o1}\left(exp\left(\frac{qR_sI_{sc}}{d_1 kbN_cT_c}\right) - 1\right) + I_{o2}\left(exp\left(\frac{qR_sI_{sc}}{d_2 kbN_cT_c}\right) - 1\right) + I_{o3}\left(exp\left(\frac{qR_sI_{sc}}{d_3 kbN_cT_c}\right) - 1\right) + \frac{R_sI_{sc}}{R_p} - I_{ph}, \tag{2.31}$$

$$E_{mpp} = I_{ph} - I_{o1}\left(exp\left(\frac{q(V_{mpp}+R_sI_{mpp})}{d_1 kbN_cT_c}\right) - 1\right) - I_{o2}\left(exp\left(\frac{q(V_{mpp}+R_sI_{mpp})}{d_2 kbN_cT_c}\right) - 1\right) - I_{o3}\left(exp\left(\frac{q(V_{mpp}+R_sI_{mpp})}{d_3 kbN_cT_c}\right) - 1\right) - \frac{V_{mpp}+R_sI_{mpp}}{R_p} - I_{mpp}, \tag{2.32}$$

The objective function is formed by adding the squared errors of the three critical points as given below:

$$E_R = {E_{oc}}^2 + {E_{sc}}^2 + {E_{mpp}}^2, \tag{2.33}$$

This enable us to extract and evaluate any type of the PV technology or mathematical PV model without requiring real experimental data.

© COPYRIGHT UPM

There are several approaches in the literature for parameter determining optimization problem exist, including analytical, numerical, stochastic, hybrid, and software tools [16]. The analytical approaches are fast and straightforward, relying on a series of mathematical equations to derive each parameter of the PV model. However, such methodologies acquire manufacturer's ideal datasheet information at standard test condition. Moreover, any tiny inaccuracy in derivation of one of these equations may conduct a substantial error. Finally, the intricacy of these approaches is evident when the DD and TD PV models are implemented [40]. The numerical procedures are more accurate and are recommended for solving the PV model's equation. In addition, these methods may uncover a large portion of the feature space of the problem due to their ability to handle the nonlinear and multivariable equations effectively. These methods, however, need a lengthy execution time and adequate initial solutions [6]. By contrast, the stochastic approaches are extensively employed to determine the parameters of the PV models due to their numerous advantages, including the following: the set of solutions is randomly generated from the search space of the problem, and control parameters, if used, can synchronously balance between exploration and exploitation phases [41]. However, these methods have a number of drawbacks, such as the following: they the problem as a black box, with their accuracy dependent on the formulated objective function, number of evaluations, population size, the inappropriate usage of control parameters, and exploration/exploitation stages [42]. Additionally, robust and powerful strategies for dealing with a large number of nonlinear and multimodal variables, especially for extracting the parameters of the TD PV model. This is because these methods are inspired by the nature, physics, biology, swarm, and evolutionary algorithms with their own strengths and weaknesses based on their inspirations [43]. Therefore, the hybrid approaches are developed to address

© COPYRIGHT UPM

all the limitations of the prior methods by combining two or more than benefits and lessening the negatives [44,45]. The readers may refer to the recent a comprehensive overview of the meta-heuristic and hybrid methods for the parameter extraction of the PV models [46].

The hybrid approaches can be classified into parts: the first one is by improving the algorithm itself by enhancing the control parameters, and exploration and/or exploitation stages. While there are a few approaches concentrate on developing the objective function, the resultant degree of precision is restricted. Some of the most well-published methods that concern on only the methodology include the performance-guided JAYA (PGJAYA) algorithm [47], hybrid symbiotic differential evolution moth-flame optimization (HSDEMFO) algorithm [48], improved brain storming optimization (IBSO) algorithm [49], locomotion hybrid salp swarm algorithm (LHSSA) [50], shuffled frog leaping with memory pool parameter (SFLBS) [51], similarity-guided evolutionary multitask optimization with DE (SGDE) [52], and more research works can be found in [41,46,53].

In PGJAYA [47], quantifies the probability parameter in order to self-adapt individual solutions and balance the exploration and exploitation tactics. While the chaotic mechanism is handled in order to explore more promising solutions and replace them with worst ones. The HSDEMFO is improved by dividing the population into two groups: soybean group focuses on exploration in the DE algorithm, and rhizobium group emphasizes on the exploitation in the MFO algorithm. Furthermore, chaotic strategy is established to refine the solutions' quality. The IBSO performs two significant improvements: it uses improved periodic individual clustering (IPIC) in

© COPYRIGHT UPM

conjunction with K-means to compute the distance between the solutions, and it utilizes improve individual generation (IIG) to share the information among the population [49]. In LHSSA, the opposition-based learning (OBL) is addressed to enhance the exploratory process [54]. Moreover, the leader particle based on particle swarm optimization (PSO) is introduced in serialized scheme to provide more valuable information [55]. The SFLBS has been equipped with crossover and mutation mechanisms. In addition, the memory-pool is obtained in order to store the high-quality of the solutions. The SGDE is advanced by subdividing the population into subpopulations, each of which performs a specific task. The DE is employed for improving the subpopulations, whereas the local search technique is defined to discover a better solution [52]. An improved equilibrium optimizer (IEO) for determining unknown parameters of the SD, DD, and TD PV models is presented in [56]. The improvements in IEO are achieved by employing the back propagation neural network for predicting the output current of the PV model. In addition, various selection probabilities are addressed for enhancing the solutions quality. The statistical results indicated that the IEO outperformed well-published methods mentioned in the literature.

The second categorization of the hybrid approaches is accomplished for the purpose of formulating the algorithm and objective function [57]. Since extracting the parameters of the TD PV model requires a sufficiently robust explorer-exploiter mechanism capable of avoiding stagnation in local minima and obtaining high-quality of solutions, as well as reliable objective function to precisely solving PV model's equation. Several numerical methods have been utilized to solve PV model's equation, including Newton Raphson (NR) method [58], Lambert W function (LW) [59],

© COPYRIGHT UPM

Levenberg-Marquardt (LM) method [60,61], and special trans function (STF) method. In addition, the ant lion optimizer in linked with LW function (ALO_{LW}) in [62]. The authors of [63] improved PSO algorithm by incorporating chaotic with heterogeneous comprehensive learning processes and then integrating it with NR method ($CHCLPSO_{NR}$). The DE algorithm is based on electromagnetism (EM) method concept of attraction-repulsion [64]. The mutant and crossover control parameters are adjusted using logistic sigmoid function. Then, the $DEAM_{NR}$ algorithm is associated with NR to solve the PV model's equation. The authors of [55] alleviated the premature convergence of the PSO algorithm by using five successive mutation scheme, then the NR is obtained as objective function ($ELPSO_{NR}$). An updated LSHADE algorithm is presented in [6] using chaotic-guided tactic with improved NR method ($ELSHADE_{INR}$). The authors of [65] proposed farmland fertility algorithm and linked with NR method (FFA_{NR}).

El-Fergany [66] improved slime mould algorithm utilizing levy flight (LF) and random distribution strategies and the output current equation is solved based on LW function ($ImSMA_{LW}$). Marine predators algorithm is associated with LW function to estimate unknown parameters of the PV models in [45,67]. In [68], mutation scheme is hybridized with PSO algorithm and the PV model equation solved by NR method ($MPSO_{NR}$) [68]. The authors of [69] and [70] present manta ray foraging optimization and the PV model's equation is handled by NR method ($MRFO_{NR}$). In [71], two control parameters are updated based personal and social acceleration using PSO and the PV model's equation is treated by NR method ($TVACPSO_{NR}$). A modified flower pollination algorithm is presented using dynamic switch probability and step size function to enhance overall performance of the local and global search. The output

© COPYRIGHT UPM

current is using NR method [72]. Despite the contributions made to algorithm itself and objective function formulation, the aforementioned research investigations do not provide realistic performance of the PV model. This is because of that the classic NR and LW methods struggle to present adequate initial root solutions, especially at MPP and hard edges regions. The methodologies of extraction the parameters of the PV model can be illustrated in Figure 2.6. As a reason, we will discuss the methodology and OFD concurrently in this research study. The existing work and their contributions as presented in Table 2.1.

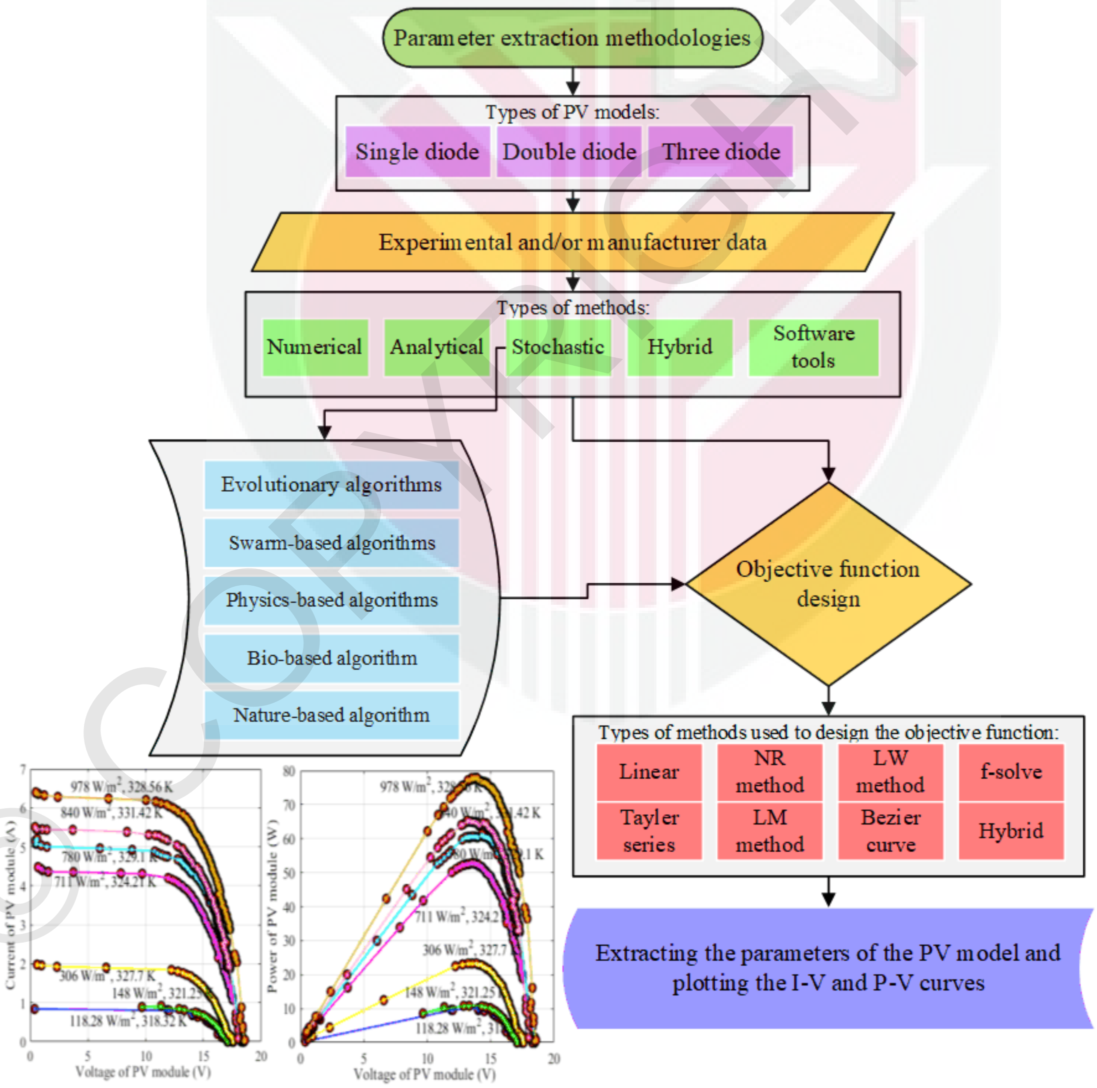

Figure 2.6 : Diagram of parameter extraction methodologies

Table 2.1 : The utilized methods in designing the objective function of the PV models

Reference	Model	OFD	Method	Contribution
[58]	SD	NR with adaptive LM parameter	Numerical	The initial parameters are calculated iteratively. Then, using NR with an adjustable LM parameter, the PV current is forecasted.
[73]	SD, DD	LM	Analytical	The analytical expressions serve as initial values for the parameters of PV models.
[74]	SD	NR	Analytical	These parameters are extracted analytically by employing three critical points.
[75]	SD, DD	NR	Stochastic	COA is obtained to forecast the current for both PV models.
[76]	TD	NR	Hybrid	Two methods are presented: RWOA updates the population using ranking method. While HWOA incorporates cyclical exploration and exploitation stages with RWOA. HWOA outperforms other algorithms.
[77]	DD	LW	Hybrid	rbcNM algorithm is demonstrated to be more accurate while being more time intensive.
[78]	DD	Derivative of power at MPP	Hybrid	I_{ph}, I_{o1}, and R_p are analytically computed, while d_1, d_2, I_{o2}, and R_s are computed using DE algorithm.
[79]	TD	NR	Hybrid	HMPA is a hybrid algorithm that combines the MPA and SMA algorithms. HMPA provides a minimum RMSE and consistency.
[80]	SD, DD	NR	Stochastic	DSO is offered as a method for extracting parameter from PV models. OFD is evaluated using both Linear and NR methods.
[81]	SD, DD	NR	Hybrid	ISA is integrated with DE to enhance local and global search capabilities. The parameters extending the limits of the PV cells displays more accuracy.
[82]	SD	Derivative of power at MPP	Hybrid	The R_s, G_{sh}, and d parameters are determined using PS algorithm, while the I_{ph} and I_o parameters are analytically derived. The performance is verified by monitoring the current and power faults at MPP regions.
[83]	SD, DD, TD	LW	Hybrid	The SMA is improved by the LF mechanism, resulting more diversity of population.
[84]	SD, DD,	NR	Stochastic	FFO is employed to find the parameters of the PV models.
[85]	SD	LW	Analytical	The data-driven method is considered for solving PV model problem analytically.
[86]	SD	LW	Analytical	The PV model's parameters are analytically derived from three key points.

© COPYRIGHT UPM

Table 2.1 : Continued

[87]	SD	LW	Analytical	The reduced form method is obtained to extract the five parameters.
[88,89]	SD and DD	Splitting I-V curve	Stochastic	FA is presented, and the OFD is solved by separating the I-V curve into two regions: one for computation current and another for the voltage computation.
[90]	SD and DD	NR	Stochastic	DSO is used to tackle the challenge of optimizing PV model. The authors investigate the accuracy of the Linear and NR methods.
[91]	SD	MOOP	Hybrid	The GA combined with IPM methods to extract the following parameters: d, R_s, and R_p, whereas I_{Ph} and I_o are analytically derived. The STC and NOCT is consult as input information. The two objectives are treated as single objective function to be optimized.
[92,93]	SD, TD	NR	Hybrid	AWDO and IWDO are employed in this study. The Chenlo's model is used to shift from one meteorological state to another. The IWDO is enhanced by mutation and CMAES techniques.
[94]	DD	LW	Hybrid	ITLBO is improved by the use of elite learning with hybrid learning strategies.
[95,96]	SD	Derivative of power at MPP	Hybrid	DE is used to extract d, R_s, and R_P, on the other hand, I_{Ph} and I_o are analytically computed. By BFA.
[97]	TD	NR	Stochastic	AEFA is presented to predict the nine parameters of the PV model.
[98]	SD, DD	NR	Hybrid	GA is employed to extract d_1, d_2, R_s, and R_P, whereas, I_{Ph}, I_{o1}, and I_{o2} are analytically computed. The OFD is treated by NR using datasheet information and its operations are simulated by MATLAB software.
[99]	SD, DD	NR	Hybrid	WDAWOAPSO is proposed based on combination of several meta-heuristic algorithms.
[54]	SD, DD	NR	Hybrid	NLBMA incorporates with Laplacian-based crossover search and neighborhood wandering search to better exploration and exploitation tactics.
[100]	SD	NR	Hybrid	Improved EM takes the benefit of the nonlinear formula to adjust the particle's length and total force formula is omitted.

© COPYRIGHT UPM

Table 2.1 : Continued

[43]	SD, DD	NR	Hybrid	Chaotic based on Rao-1 algorithm is presented in this study for more solution diversity.
[101]	SD	LW and NR	Numerical	LSM based on NR method shows a better accuracy compared with other methods.
[102]	SD, DD, TD	NR	hybrid	Fractional chaos maps are addressed for FC-EPSO algorithm to prevent premature convergence and improve the exploration phase.
[103]	TD	Sum of SC, OC, and MPP absolute differences	Hybrid	I_{Ph} and R_P are mathematically determined first, then the SFO is applied to extract seven parameters.
[104]	SD	LSM	Stochastic	PSO is used to reduce the sum of absolute errors of the PV model's current by using LSM and FF. LSM is a function built in MATLAB.
[105]	DD	Derivative of power at MPP	Hybrid	Social learning is utilized to improve DE algorithm (SL-DE), which is used to extract the $d_{1,2}$ and R_s, whilst the I_{Ph}, $I_{o1,2}$, and R_p are derived analytically. OFD is based on NR which obtains I_{sc} as starting point.
[106]	SD	LM	Analytical	The SA is employed to find best value of λ of the LM algorithm.
[107]	SD	Modified TS	Analytical	The parameters are analytically computed using main three key points from datasheet which is much faster than LW method.
[108]	SD	LM	Analytical	The parameters are analytically computed based on three key points. Then, the OFS is based on LM method using 'fsolve' function.
[109]	SD, DD	LM	Analytical	The parameters two models are analytically calculated then 'fsolve' command is used as ready function in MATLAB based on LM method.
[55]	SD, DD	NR	Hybrid	Enhanced leader PSO (ELPSO) is proposed as a result of five successive mutations based on best fitness function obtained so far.
[110]	DD	NR	Hybrid	R_s and R_p are numerically computed, whilst the others five parameters are estimated using datasheet information obtained by MATLAB simulator.

Table 2.1 : Continued

[111]	SD	LW	Analytical	The PV model's parameters are extracted based on Laplace transfer function and integral based linear square system using datasheet information.
[112]	DD	LW	Analytical	This model is separated into two parts: linear, which is solved by Thevenin's theorem, and nonlinear, which is solved by piecewise linear model.
[113]	SD	GRG	Analytical	The five parameters are analytically estimated.
[114]	SD	LW	Analytical	The parameters are analytically computed from datasheet information.
[115]	SD	NR	Hybrid	I_{Ph} and I_o are analytically analyzed, whereas R_p, R_s, and d are computed by EPO.
[116]	SD	Piecewise method	Numerical	The parameters are mathematically computed from template data.
[117]	DD	NR	Analytical	The seven parameters are extracted analytically from datasheet information.
[118][119]	SD, DD	NR	Hybrid	I_{Ph} and $I_{o1,2}$ are analytically analyzed, while R_p, R_s, and $d_{1,2}$ are calculated by BPFPA.
[7,120]	SD, DD	NR	Hybrid	DEIM and DEAM are improved using mutation scaling factor and crossover rate is updated by new formula.
[121]	SD, DD	NR	Hybrid	Guaranteed convergence PSO is improved by using adjusting the movements of the particles. The hyperbolic strategy is used to prevent the particles from traveling outside the search space.
[122]	SD, DD	NR	Stochastic	FPA is employed to extract the parameters of PV models.
[123]	SD, DD	NR and LM	Analytical	A comparative study of NR, LW, and GA is given. The parameters of these models are reduced to three. LW is used to analyze the R_p, R_s, and $d_{1,2}$ parameters.
[124]	SD	NR	Stochastic	MVO is employed to extract the five parameters under uniform and ununiform weather conditions.
[125,126]	SD, DD	NR	Stochastic	AEO is proposed to estimate the parameters of the PV models.

© COPYRIGHT UPM

Table 2.1 : Continued

[127]	SD	Sum of SC, OC, and MPP absolute differences	Stochastic	BFO is obtained to extract the five parameters of PV model using the summation error of the key points between the expected and datasheet information.
[128]	SD	NR	Software	TRR least square algorithm implemented in MATLAB using "Fmincom" command is proposed to extract the parameters at MPP under STC.
[129]	SD	Derivative of power at MPP	Software	At STC, Powell's method is obtained to extract the parameters by PSIM software tools. R_p, R_s, and d are taken from datasheet information, and then I_{Ph} and I_o are analytically derived.
[130]	SD	LW	Hybrid	The d is iteratively computed, while others derived from template data.
[62]	SD	LW	Stochastic	ALO is used to extract the five parameter of PV model.
[131]	SD, DD	NR	Hybrid	Multiswarm spiral leader PSO is multi-search mechanisms is proposed, which each swarm has a leader who provides directions to optimal solutions.
[132]	SD	LW	Analytical	The parameters are determined via three key points. The variation of d is employed to extract the other parameters.
[133]	SD, DD	Error at MPP	Stochastic	ICA is applied to determine the parameters of both models at STC.
[39]	SD, DD	Sum of SC, OC, and MPP absolute differences	Hybrid	LSHADE is employed to extract R_p, R_s, and d parameters, meanwhile I_{Ph} and I_o are determined analytically. The 'fsolve' command is employed to plot I-V curve for set of optimal solutions.
[134]	SD, DD	LW	Stochastic	Several approaches are utilized to verify performance of the PV models using different types of objective function. The results indicate that the R^2 has minimal error and LW is best OFD but takes prolong time.
[135]	DD	Derivative of power at MPP	Hybrid	FWA is utilized to calculate R_p, R_s, and d parameters, while the I_{Ph} and I_o are computed manually under STC.

Table 2.1 : Continued

[136]	TD	Sum of SC, OC, and MPP absolute differences	Hybrid	HHO is used to optimize R_p, R_s, and $d_{1,2,3}$, while I_{Ph} and $I_{o1,2,3}$ are derived analytically at STC and NOCT.
[68]	SD, DD	NR	Hybrid	An improved mutated PSO algorithm is proposed to determine the parameters of PV models. MPSO shows better performance in terms of accuracy and stagnation avoidance.
[137]	SD, DD	NR	Hybrid	HPSOSA algorithm is proposed, the SA is connected for preventing PSO from converging prematurely. The complexity and processing time have been increased.
[138]	SD	Fit-curve method	Hybrid	Improved SSO is proposed based on three critical points obtained by manufacturer. ISSO divides the population into two parts: global and local searches. ISSO verified by using R.T.C France experimental data.
[139]	SD, DD	LW	Stochastic	The basic DE is applied to experimentally extract the parameters of PV models.
[140]	SD	LW	Hybrid	R_s and d are firstly analyzed, while R_p, I_{Ph}, and I_o are calculated by using LSM under STC and experimental data.
[141]	SD, DD	NR	Hybrid	MFPA obtains a dynamic switch probability as well as dynamic step size function to improve overall performance of the proposed algorithm.
[45]	SD, DD, TD	NR and LW	Stochastic	Several meta-heuristic algorithms are employed to estimate the parameters of PV models. MPA outperformed others models. The authors prove that NR and LW can significantly enhance the performance of PV models.
[142]	SD	NR	Analytical	ACT is used to extract the parameters of PV models. The parameters are analytically derived, then five-loop iterations are used for adjustments.
[143]	SD	LW	Analytical	The five parameters of PV models analytically extracted from datasheet information.

Table 2.1 : Continued

[144]	SD	Reduced form	Analytical	Based on the main three points equations, the five equation is reduced to two R_s and d, then graphical optimization method is employed to solve the PV equation. The other parameters are derived mathematically.
[63]	SD, DD	NR	Hybrid	Chaotic heterogeneous comprehensive learning PSO is proposed to extract the parameters of static and dynamic PV models. The population is divided into two parts. A comprehensive learning and learning probability procedures are obtained to improve its performance. While chaotic tactics is used to avoid premature convergence.
[145]	SD, DD	NR	Hybrid	Hybrid Rao is proposed to extract the parameters of the static and dynamic PV models. The chaotic map and performance learning strategies are employed to improve the exploration and exploitation phases.
[146]	SD	LW	Analytical	R_p, R_s, I_{Ph}, and I_o parameters are firstly derived by LW. Then, these equations are obtained to be solved by NR method. The d parameter is analytically determined. This method is complicated due to procedure obtained to extract the parameters of PV model.
[71]	SD, DD	NR	Hybrid	TVACPSO is presented to extract the parameters of PV models. An acceleration coefficient is linearly increased to improve its performance using large number of population size.
[147]	SD	STF	Numerical	Ranking based branch selection and modified NM algorithm is proposed in this study. When the STF objective function was replaced with LW, the accuracy improved. However, the distinction is trivial between them.
[67]	SD, DD	LW and NR	Stochastic	MPA is employed with seven levels of experimental. The results show that the LW has better convergence at high voltage ranges.
[148]	SD	NR	Hybrid	Boosted HHO method is improved using Levy flight and mutation trajectories. The exploration and exploitation phases are significantly improved.

Table 2.1 : Continued

[6]	TD	Improved NR	Hybrid	Enhanced LSHADE method is proposed by using guided-chaotic strategy to enrich the population diversity during the second half of iterations.
[149]	TD	NR	Hybrid	Improved AVO is enhanced by obtaining OBL and OL. IAVO boosts the convergence rate.
[150]	SD, DD	NR	Stochastic	The traditional SFS algorithm is introduced to experimentally optimize the PV models.
[69]	SD, DD, TD	NR	Stochastic	MRFO is proposed to experimentally estimate the parameters of PV models.
[151]	TD	NR	Hybrid	Premature convergence and ranking based updating methods are integrated to enhance the GNDO algorithm.
[152]	DD	NR	Hybrid	Hybridized WDO's exploitation and Fruit Fly's exploration are presented in this study.
[153]	SD	ImLM	Analytical	A new reduced form based on Brent's algorithm is implemented to calculate the initial values.

© COPYRIGHT UPM

2.3 Wind turbine

It is necessary to select the appropriate model for forecasting the performance of a single WT, which is characterized by its power curve. To precisely evaluate wind energy potential, specific statistical characteristics of wind speed should be considered. For example, the Weibull probability distribution function is employed for finding the monthly frequency distribution of the wind speed measurement. Huang et al. [154] assumed that the wind turbine velocity at various height ranged between 10-12 m. The output of the WT generators is strongly dependent on their types, heights, and speed of wind. In general, the WT output can be computed based on its start power generation at the cut-in wind speed, after that the power increases linearly according to the speed of the wind from the cut-in wind speed to the rated value. The WT will be shut down if the produced rated power is more than the cut-out wind speed for safety considerations [155]. Some of authors assumed the calculation of the WT output power as follows [156]:

$$\textit{Kinetic energy} = \frac{1}{2} MV^2, \tag{2.34}$$

$$\frac{M}{S} = V(\text{m/s})\ A_W(\text{m}^2)\ \text{air density}\ (\text{kg/m}^3), \tag{2.35}$$

where M is the mass of wind molecules (kg), V is wind speed (m/s) [157]. Substituting (2.34) in (2.35), the output power of the wind hitting wind turbine for a certain swept area is presented as follows:

$$P_{WT} = \frac{1}{2}\ \text{air density}\ r^2 \pi V^3, \tag{2.36}$$

The above formula is based on linear calculation, which cannot reflect the actual behavior of the WT performance [158].

© COPYRIGHT UPM

The advantage of WT generator are:

- It is a free, environmental friendly, and inexhaustible renewable energy source.
- Wind flow naturally occurs, and utilizing wind motion has little effect on wind currents and cycles.
- It lessens the greenhouse impact.

The disadvantages of WT generator are:

- Wind speed is changeable in nature.
- When load power is required, wind may not always blow at the anticipated time.

2.4 Charge controller

In partial shading cases such as trees, clouds, building cover or planets, the sunshine is entirely or partially absent. Therefore, the charge controller has three main functions: first is to track the maximum power point (MPP) at peak value during the day. The second function is to reduce the battery charging time to fast back up the PV array. Finally, it can be used to protect the battery from overcharged, hence increasing its efficiency and longevity. The battery power delivered to the load through the charge controller and inverter may be stated as follows [159,160]:

$$P_L = E_{batt} \times \eta batt \times \eta inv \times \eta ch, \tag{2.37}$$

This charge controller is chosen to regulate the voltages differences between the produced power from inverter and the battery voltage.

© COPYRIGHT UPM

2.5 Inverter

The primary usage of the inverters are conversion of DC into AC, modifying the frequency of conducted AC power, and controlling the effective output voltage value. The main features of a PV inverter are the reliability and efficiency. In general, the inverter output waveform can be categorized into three types: a square wave inverter, modified sine wave inverter, and pure sine wave inverter. The square wave inverter is simple and it has poor efficiency owing to the large harmonics content, which may be connected with electromagnetic filed in conductive components. The modified sine wave inverter offers higher level of accuracy than previous one. However, this kind of inverter is expensive and more suitable for the grid-connected applications [161]. Finally, the pure sine wave inverter has been utilized in many applications due to its several benefits: higher efficiency, reducing the needed numbers of DC voltage source, and less cost and complexity. The efficiency of the inverters are assumed within ranges of 90% to 97% at full load demand [162].

2.6 Battery storage

The intermittency of the WT generator and PV array is due the output power reduction caused by low wind speed and motion of clouds over PV panels. The intermittency results undesired effects such as voltage variations, increase the losses and power factor modification, and overall cost of the system. Therefore, a reliable battery storage size design for the hybrid WT/PV/Battery system is required to ensure the stability of the generated power, efficiency, and prevent high costs. The primary purpose of using battery storage is to deliver the stored power when the WT generator or PV array is not enough to meet the required load demand.

© COPYRIGHT UPM

There are several kinds of the batteries storage regarding to their applications. The lead-acid battery is mostly utilized in the standalone PV system due to high-reliability and low cost. The lead-acid batteries can be categorized into three types which are: flooded type, gelled electrolyte sealed type, and absorbent glass mat (AGM) type [161]. The flooded batteries are economically and widely used in the hybrid WT/PV/Battery system. However, these type of batteries require continuous maintenance and must be placed in ventilated area. The gelled electrolyte and AGM types are more economical owning to few maintenance and free of venting [163]. Deep cycle batteries are required in the renewable energy system as they can provide consistent performance, longer life time, over/under charging or discharging, higher temperature, and good maintenance [29]. Lately, the usage of the lithium-ion batteries have been broadly increased due to their high reliability and long lifetime [164]. However the main obstacle of these kind of batteries storage are very costly compared with lead-acid batteries. Moreover, the lithium-ion batteries are more suitable for grid-connected systems due to their highly reliability in terms of highly variations in currents and voltages.

2.7 Sizing methods of hybrid WT/PV/Battery system

The freestanding hybrid WT/PV/Battery system is economical and reliable feasible solution for providing areas where the grid utility is not accessible. There are many difficulties associated with optimization of the hybrid renewable energy system such as large variable, fluctuation of renewable energy sources, and meeting the load demand at reliable and economical perspectives. All of the above complexities make the optimal sizing of the WT/PV/Battery system more challenging. The aim of utilizing the optimization methods in this system is to reduce the overall cost and

© COPYRIGHT UPM

increasing the reliability [165]. The sizing optimization methods can be classified into intuitive, numerical, analytical, stochastic, hybrid, and software tools [166]. The optimal sizing of the WT/PV/Battery system can be achieved by using singe-objective or multi-objective method. In single-objective method, only technical or economic criteria is obtained to be optimized [167]. In these methods, one optimal solutions is conducted at each execution.

The multi-objective optimization methods can be categorized into: aggregation methods that combine two objective or more objectives and convert them to a single-objective, such as Penalty-Based boundary Intersection (PBI) [168–170] and ε-constraint method [171], or by simulating several objectives concurrently by generating a set of PF optimal solutions [172]. The reliability and efficiently of the MOO methods can be verified by their capacity to create the Pareto optimal solutions with high levels of convergence, coverage, and diversity [173]. The PF optimization methods are categorized in single set PF solution and two sets PF solutions such as non-dominated sorting genetic algorithm (NSGA-II) [174], multi-objective particle PSO (MOPSO) [175], strength Pareto evolutionary algorithm (SPEA2) [176], multi-objective evolutionary algorithm (MOEA/D) [168], improved multi-objective evolutionary algorithm method by developing a diversity-maintained scheme (MOEA-DM) [33], archive micro GA (AMGA) [177], reference points guided evolutionary algorithm (RVEA) , Bi-goal evolution (BiGE) [178], ∅-dominace-based evolutionary algorithm (∅-DEA) [179], multi-objective metaheuristic R_2 indicator-II (MOMBI-II) [180], and two sets PF solutions [181–183]. Selecting desirable configuration from a collection of PF solutions is considered a difficult undertaking, much more so when conflicting objectives require a trade-off. As a result, Multi-criteria Decision-making (MCDM) methods are essential for boosting the energy efficiency and lowering the capital costs of the system by guiding to designer to the most optimum solution [184,185]. The most well-known MCDM methods are: multi-attribute border approximation area comparison (MABAC) [186], decision making trial and evaluation laboratory model (DEMATEL) [187], multi-objective optimization by ratio analysis (MORRA) [188], integrated analytic hierarchy process (AHP) [189], technique for order preference by similarity to ideal solution (TOPSIS) [189], weighted aggregated sum product assessment (WASPAS) [190], preference ranking organization method for enrichment evaluations (PROMETHEE) [191], Vlsekriteriterijumska Optimizacija I Kompromisno Resenje (VIKOR) [22], complex proportional assessment method (COPRAS) [192], best-worst method (BWM) [193], criteria importance though intercriteria correlation (CRITIC) [174], and full consistency method (FUCOM) [194]. The sizing methodologies of the hybrid WT/PV/Battery system are presented in Figure 2.7.

© COPYRIGHT UPM

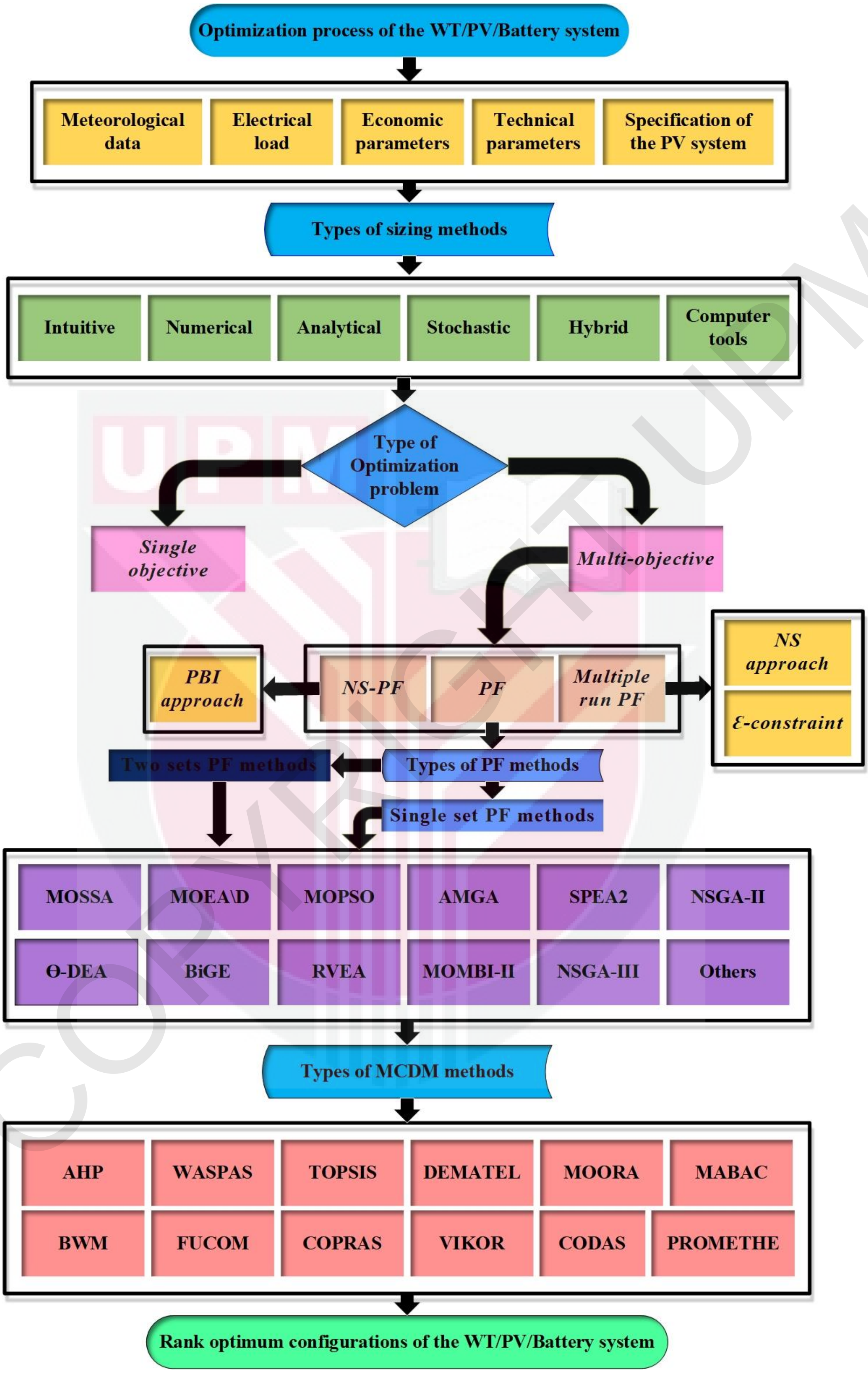

Figure 2.7 : Sizing methods of the hybrid standalone WT/PV/Battery system

© COPYRIGHT UPM

A. Intuitive method

The simplest method for developing the WT/PV/Battery system is the intuitive method, which ignores the interaction between multiple subsystems and randomness of solar radiation and wind speed. This method utilizes information about the weather, such as the worst month's average, monthly data, or the yearly average. During the sizing procedure, which is based on the safety factor given by the designers, the production of the WT and PV model is calculated. This method only covers the necessary need load demand, which results in an expensive/unreliable system. Therefore, this method is helpful for preliminary estimation and an approximate assessment of the design of the WT/PV/Battery system [195].

Borowy and Salameh [196] presented an intuitive method for finding an optimal combination of the WT/PV/Battery system based on long-term information data for typical load campus of the University of Massachusetts Lowell. The average output power of WT and PV module is computed based on average monthly production. At desired level of loss power supply probability (LPSP), the optimum design is selected. In [197], a simple methodology based on only two seasons: summer and winter is presented to find optimal design of the WT/PV/Battery system. However, this method do not present accurate capacity of the renewable energy sources, which is not flexible and it is based on different approximations.

B. Numerical method

The iterative method is assumed to be quite accurate, since it can generate multiple configurations in the design space of the WT, PV, and battery. Then, based on hourly climatic data, each configuration is simulated, and the dependability is first computed

© COPYRIGHT UPM

for all potential system configurations. The optimum design is selected based on the required reliability and low cost. This approach, however, takes very long time [198].

Kellogg et al. [199,200] proposed simple iterative method to minimize only the cost of the hybrid WT/PV/Battery system using hourly environmental data for a hypothetical site in Montana. The optimal design is chosen based on required storage capacity to satisfy the load demand. The authors of [157] proposed an iterative procedure for optimal size of the WT/PV/Battery system in Kula Terengganu, Malaysia. The loss of load probability (LLP) is used to evaluate the system's reliability. Then, the optimum design is determined based on lowest cost. However, simple mathematical models were obtained for estimating the output power of the WT and PV module. Ferrer-Marti et al. [201] proposed a mixed integer linear programming for optimal size and location of the WT/PV/Battery system in El Alumbre and Alto Peru, which are located in Spain and USA, respectively. The objective function is to reduce the initial cost of the system. However, the reliability assessment is ignored in this project. Yang et al. [27] presented an iterative method for sizing of WT/PV/Battery system in China. The LPSP and levelized cost of energy (LCE) are employed as a techno-economic criteria. The best optimal solution is chosen based on the intersection of the two curves of LPSP and LCE values. However, the authors stated that increasing the number of PV arrays and WTs is better choice than only increasing the number of batteries. Diaf et al. [202] proposed optimal sizing numerical method for the hybrid WT/PV/Battery system to supply residential house located in Corsica Island. The LPSP is set to be zero, while the optimal design is chosen based on minimum LCE. In [203], an iterative procedure is presented to find optimal size of the hybrid renewable energy system for the site Pompuhar, India. The

© COPYRIGHT UPM

reliability of the system is verified by deficiency power supply probability (DPSP), unutilized energy probability (UEP), and relative excess power generated (REPG). While the economic criteria are LCE and life cycle unit cost (LUC). However, the optimal design is chosen based on the interest of designer. Giallanza et al. [204] proposed an iterative procedure based on fuzzy logic interface system to optimal size of the WT/PV/Battery system to provide electricity for three different areas in Sicily. The annualized cost of system (ACS), LLP, and seasonal LLP are considered as techno-economic objectives to be minimized. However, average monthly weather data were obtained in this study, which may results over/under sizing. Ma et al. [205] optimize the size of the WT/PV/Battery system using numerical method to supply energy for the required load demand located near Shanghai in China. The LPSP is used as a technical parameter, while NPC and simple payback time (SPB) are considered as economic criteria. Different WT sizes were investigated in this study. The performance results indicated that the WT with 2kW is most viable choice for the proposed system.

C. Analytical method

The relationship in algebraic equation methods is related to the system's size and dependability. The performance of the WT/PV/Battery system is assessed by utilizing several sets of feasible-sized components of the system. The optimal design is then chosen by comparing one or more performance indicators from various configurations' combinations. The advantages of these methods are simple, use sequence of mathematical equations, and do not need prolong processing time. However, these method suffer from provide accurate equation's coefficients of the WT/PV/Battery system in local site [166].

© COPYRIGHT UPM

In [206], an analytical procedure for optimal design of the hybrid renewable energy system is presented in Kandla, India, in an effort to lower the system's overall cost. The results are verified by the use of the analytical method and Monte Carlo simulation (MCS). The system is verified using two technical parameters: loss of healthy expectation (LOHE) and loss of load expectation (LOLE). The results indicated that the proposed method needs less computational time with reasonable accuracy. The authors of [207] proposed an analytical method to optimize the size the of the PV/wind system in South Africa. The equations of the PV and WT variables are used to minimize the LCE. However, the technical assessment has not been mentioned, which makes the reliability of the system questionable. Rathore et al. [208] proposed a probabilistic upper reservoir multi-state model (MSM_{UR}) to maintain reliability for WT/PV/pumped storage hydro system in Kandle, India. Loss of load expected (LOLE) and expected energy not served (EENS) criteria are used as technical indicators based on analytical method and MCS. However, there is no economic evaluation in this study, which may make the results questionable. Kerboua et al. [209] proposed an analysis meteorological data and load demand to find optimal size of the WT/PV/Battery system based on hourly 16 days in February to supply energy for the required load demand in Algeria. Techno-economic criteria are derived, including LPSP and LCE. The results indicated that investing in hybrid system requires a significant increase in the quantity of the batteries storage. In addition to that, the LEC analysis stated that the batteries' cost represented 52% of the total cost, while the WT and PV panels required 42% and 2%, respectively. Hadi et. al [31] proposed WT/PV/Battery system for rural area in Sarawak, Malaysia, with lowering two objectives: LPSP and LCC. On the basis of monthly average data, the probabilistic method is used for sizing the hybrid system. Due to the fact that the Ref. [31] proposes a probabilistic method based on analytical assumptions, few optimal solutions are obtained.

D. Stochastic method

In order to overcome the limitations of the previous approaches and to address the lack of the weather data, stochastic approaches may use heuristic and metaheuristic methods. These methods can indeed handle the nonlinear solar irradiation intermittentness. These method fall under the category of population-based methods that explore a search space for the best possible solutions [210].

The authors of [211] proposed a GA to find optimal size of hybrid PV/WT/battery system using hourly weather data in Spain. The NPC is addressed as an objective function to be minimized. However, the technical objective has not defined in this study. Maleki et al. [212] proposed PSO based on constriction factor (PSO-CF) to find optimal size of the WT/PV/Battery system in three typical regions in Iran. The objective function is based on TAC as an economic criteria. However, the authors do not consider the reliability of the system. In [213], presented grey wolf optimizer (GWO) to optimal size of the WT/PV/Battery system. The TAC is used as an objective function to be minimized, while considering the power balance constraint (PBC) and LPSP as a static technical criteria. Tito et al. [214] proposed GA to find optimal size of the hybrid renewable energy system to supply power for load demand in New Zealand. TAC is defined as an objective function to be optimized, while addressing LPSP at 0. The authors also investigated the influence of the socio-demographic factors on sizing of the system. The results indicated that optimizing the system to the customers socio-demographic factors can considerably savings the cost. In [215],

© COPYRIGHT UPM

imperial competitive algorithm based on multi-objective optimization method is presented to optimize the size of the WT/PV/FC system for supplying energy for the required load located in the northwest region of Iran. Based on hourly weather data for one year, the NPC is used as an economic factor, while equivalent loss factor (ELF), LPSP, and loss of load expectation (LOEE) are considered as reliability parameters to be optimized. These objectives are normalized and converted to a single objective using fuzzy logic approach.

In [216], mine blast algorithm (MBA) is implemented to find optimal design of the WT/PV/FC system to meet the requirement of the load demand in a remote area in Egypt. The output power of the PV module is computed using DD PV model. Based on hourly weather condition, the total cost of the system is minimized. However, the authors do not consider the reliability of the system. Hassan et al. [217] proposed modified PSO (MPSO) to size optimization of the WT/PV/Battery system for providing energy in Mansoura University, Egypt. Monthly average data were used in this study to minimize the total investment cost (TIC) without considering the technical perspective. In addition, simple mathematical models of the WT and PV array, which may significantly impact of the generated power. Naderipour et al. [218] proposed artificial electric filed algorithm (AEFA) to optimize the size of the WT/PV/Battery system to meet required load demand using hourly weather conditions at Ardabil region in Iran. Two types of batteries storage were carried out in this study, which are lead-acid battery (LAB) and vanadium redox battery (VRB). The objectives function to be optimized are energy not supplied probability (ENSO) and cost of system lifespan (CSLS). The two objectives are normalized and converted to a single objective function. The performance results indicated that The optimal design of the

© COPYRIGHT UPM

proposed system is cost-effective and more reliable with VRB than using LAB. Javed et al. [219] proposed GA to optimal the size of the WT/PV/Battery system to supply required energy in rural area located near Shanghai in China. Based on average monthly weather conditions, the LPSP and COE are considered as techno-economic criteria. The results showed the superiority of the GA against HOMER software in terms of less computational time, precise results, and more flexibility. In [220], GA based on multi-objective optimization method is proposed to find optimal size of the WT/PV/Battery system. Based on hourly climatic conditions, the LPSP and LCE are employed as techno-economic criteria. However, the LPSP and LCE are converted into single-objective.

E. Hybrid method

The shortcoming of the sizing previous methods have been improved by combining two or more separate methods. Since the WT/PV/Battery system design might be seen as a multi-objective optimization, the hybrid technique is much better to precisely handle the constraint objectives [164]. However the major obstacle of these methods is complexity to design the components of the hybrid system since they rely on intricate algorithms [221].

Maleki et al. [222] combined MCS and PSO in order to optimize the size of the WT/PV/Battery system using hourly meteorological data to provide energy for required load demand in Iran. MCS is used to generate stochastic demand and supply profiles, while PSO is used to optimize the total annual cost (TAC) of the system. However, the reliability of the system is not mentioned. In [223], proposed an improved NSGA-II to find optimal design of the WT/PV/Battery system using hourly

© COPYRIGHT UPM

weather data in Iran. The INSGA-II is developed by utilizing a new diversity maintenance method based dynamic crowding distance, simulated binary crossover (SBX), and polynomial mutation (PM). The INSGA-II is used to optimize the reliability index, cost of the system, and cost of the environmental. Then, fuzzy decision-making (FDM) is applying to sort the set of PF solution from best to worst. The authors of [224] proposed NSGA-II to find optimal design of the WT/PV/Battery system using historical hourly data from 2000-2008 to supply load for a household in Kent, UK. The TAC and DPSP are used as techno-economic criteria. The results indicated that proposed method yields a higher reliability compared with MCS. The authors of [225] proposed cuckoo search (CS) algorithm based on Pareto ε-constraint multi-objective method to find optimal design of the WT/PV/Battery system in Algeria. The technical and economic objectives required to be minimized are grid power absorption probability (GPAP) is considered as a technical indicator and total cost of the system. The proposed method outperformed PSO in terms of higher accuracy, faster convergence, and less processing time.

Ahmadi et al. [226] combined big-big crunch algorithm with PSO to discover optimal design of the WT/PV/Battery system utilizing hourly weather data for one year to supply electricity to a village in Qazvin, in Iran. The mutant scheme is employed for local minima avoidance and exploring new promising area. The total present cost (TPC) is considered as an objective function to be optimized, while the technical indicator is based on energy not supplies (ENS) based on minimum and maximum charge quantity of the battery storage. The results of the proposed method is compared with PSO and discrete harmony search (DHS). Fetanat et al. [227] proposed ant colony optimization based on integer programming (ALO_R) for size optimization of the

© COPYRIGHT UPM

WT/PV/Battery system. The objective function is addressed by the minimizing the total design cost. However, the reliability indicator is not considered in this study. In [228] combined the binary-coded GA (BCGA) with support vector machine (SVM) to investigate a proper power management for the WT/PV/Battery system for a typical residential house located in Turkey. However, this study optimized only the total cost of the system, while ignored the technical parameter.

In [229], a chaotic simulated annealing algorithm (HSA) for size optimization of the hybrid renewable energy system for increasing the fresh water availability and to provide load demand using hourly climatic data in Fedeshk, Iran. LPSP and LCC are designed as techno-economic objectives to be minimized. The proposed method is verified its superiority by comparing with CS and SA. The authors of [230] combined chaotic search (CS), SA, harmony search (HS), and ANN algorithm to optimal size of the WT/PV/Hydrogen system to supply electricity in Iran. LCC and LPSP are employed as economic and technical objectives based on hourly weather data. The performance results are compared with basic methods mentioned in the literature. Ghorbani et al. [231] proposed a hybrid GA-PSO to size optimization of the WT/PV/Battery system to supply energy for a house in Teheran, Iran. Based on hourly environmental data, the total cost and LPSP are employed as techno-economic criteria. The results of the GA-PSO are compared with HOMER software results. However, simple PV model is utilized to predict the output power. The authors of [232] proposed Iterative-Pareto-Fuzzy (IPF) method to find optimal size of WT/PV/Battery system to provide energy for the location of Kula Terengganu, Malaysia. Total cost of the system, energy index of reliability (EIR), and minimizing dump power are the objective function to be optimized.

© COPYRIGHT UPM

Ma et al. [233] a multi-objective optimization based on natural selection PSO and weight coefficient transform method to find optimal size of the WT/PV/battery system. The load demand is randomly generated using probability density function. Using hourly weather data for one year, the LPSP, loss of energy probability and LCC are objectives function to be optimized. The penalty function and a weight function transformation method are used to optimize the techno-economic criteria. Tahani et al. [234] combined flower pollination algorithm (FPA) and SA (FPASA) to optimally size of the WT/PV/Battery system using hourly weather data to supply power building located in Tehran, Iran. Computational fluid dynamics (CFD) is presented to predict the speed of the WT. LPSP and cumulative hybrid system savings (CHSS) are considered techno-economic factors to be optimized. Weighted sum method is applied to convert the two objective to single objective.

Houssem et. al [168] proposed a hybrid system for establishing a set of optimal configurations for a limited number of dwellings in Yanbu, Saudi Arabia using multi-objective evolutionary algorithm (MOEA/D). Loss of power supply probability (LPSP) and the cost of electricity (COE) are obtained as objective functions to be optimized. However, the obtained set of PF solutions is unequally distributed along with objectives and lacks of diversity. In addition, there was no consideration of MCDM methods, which casts doubt on the selection of the desirable optimal designs for decision makers. In Ref. [174], a modified NSGA-II algorithm using reinforcement learning method is addressed to optimize the WT/PV/hydrogen system in Gansu province, China. LCE, LPSP, and power abandonment rate (PAR) are the criteria to be optimized for lowering the capital costs and enhancing the reliability. The criteria importance though correlation (CRITIC) method is then included for weighting the objectives, and order preference by similarity to ideal solution (TOPSIS) method is used to choose the most optimal configuration. Sun et al. [235] presented mix of MOPSO and TOPSIS approaches in order to develop a collection of optimum PF solutions and to select an optimal design in Inner Mongolia, China. The pollution emissions and COE were objectives to be reduced for the PV/WT/Battery system. However, there is no mentioned to the technical aspect casting doubt on the dependability of the system.

F. Software tools method

The size of the standalone WT/PV/Battery system has recently optimized by the use of a variety of software tools. These tools have benefits of being user-friendly, able to solve multi-objective optimization methods, and suitable for studies of feasibility, sensitivity, and other factors [236]. However, these tools are unable to improve the components of the system [237].

Hybrid Optimization by Genetic Algorithm (HOGA) [238], Integrated Simulation Environment Language (INSEL) [237], Hybrid Optimization Model for Electric Renewable (HOMER) [239], In [238], HOGA software is presented to size optimization of the hybrid renewable energy system based hourly environmental data for two different locations in Zaragoza Airport and Jaca. The HOGA software uses SPEA and SPEA 2 methods, which are employed to minimize the costs and emissions, while GA method is used to choose the best control strategy with lowest cost for each pair of components. The objective function to be minimized are: LCE, CO_2, and life cycle emissions. However, the reliability indicator has not considered in this study. The authors of [240] proposed a simulation based on propriety simulation optimization

© COPYRIGHT UPM

engine (OptQuest) software for optimal design of the WT/PV/Battery system for supplying load demand in Izmir Institute of Technology Campus area, Turkey. The LLP is obtained as a technical criteria, while the optimal design is chosen based on different auxiliary energy unit cost. Ma et al. presented [241] a feasibility of the WT/PV/Battery system using HOMER software to provide electricity in in remote island. Nest present cost (NPC) and cost of energy (COE) are employed as technical criteria, whilst the cycles-to-failure curve of the battery is used as a technical parameter. Abbes et al. [242] proposed NSGA-II to size optimization of the WT/PV/Battery system using Matlab/Simulink to provide energy to a residential home. Based on half-hourly information data, LPSP, LCC, and embodied energy (EE) are considered objectives function to be minimized, then these objectives are converted to a single objective. However, simple mathematical models of WT and PV array were obtained, which may significantly affect on the generated power. Khan et al. [239] proposed optimal sizing of the WT/PV/Battery system using HOMER software based on average hourly environmental conditions to meet the required load demand in rural Indian area. The simulation optimization method is carried out using techno-economic-social parameters.

The summary of optimal design methods for sizing of WT/PV/Battery system is listed in Appendix 1.

2.8 Summary

In this chapter, more than 200 articles in the period of 2013-2022 related to the parameters extraction of the PV model and sizing of the WT/PV/Battery system were reviewed in this chapter. The focus in this chapter is on the developing in the parameter

© COPYRIGHT UPM

extracting optimization problem in terms improving the algorithm itself and objective function formulations. In addition, the optimal sizing methods of the WT/PV/Battery system have been covered. Prior analysis and studied is required for the availability of the meteorological data and load demand for the selected site in order to determine proper components of the WT/PV/Battery system. The technical and economic criteria that employed to evaluate the performance of the hybrid renewable energy sources system have been considered. The intuitive methods are rarely used to optimizing the size of the WT/PV/Battery system, while the numerical methods are considered very accurate and recommended to be utilized for validation of other methods. Most of the multi-objective optimization methods are based on single-objective principle, which produce only one solution during the optimization process. In addition to that these methods are subjective to the weights given to each objective. Finally, most of authors use hybrid methods owning to their ability to handle nonlinear, complex, and multi-variable optimization problem. However, the employment of the MCDM methods are limited on the use of the AHP, TOPSIS, VIKOR methods.

© COPYRIGHT UPM

CHAPTER 3

RESEARCH METHODOLOGY

3.1 Introduction

The combination of wind turbine (WT) and photovoltaic (PV) energy systems is considered as a very economical option to generate electrical energy especially for remote areas owing to the complimentary nature and widely abundant, where the utility grid is expensive. These renewable energy sources are heavily impacted by the speed of the wind and amount of solar radiation, which are site-dependent. In addition, the use of batteries storage allows to store the excess energy during the day and restore it at the night. This integration can significantly reduce the total cost of the system by reducing the amount of the batteries storage and efficiently meet the required load demand. The nonlinearity behavior between each component of the system, and nonuniformity between the renewable energy sources and load demand make the selection to the optimal design more challenging and intricate. The high initial costs and loss of load are the major drawbacks of expansions of these systems.

An accurate modeling of the PV module is necessary to accurately reflect the actual behavior of the output. The mathematical model of the PV equivalent circuit has several physical factors that influence directly on the performance of the PV cell. Therefore, these parameters must be optimally extracted based on advanced methodology which includes the developments in the algorithm and objective function design. The optimal design based on techno-economic criteria can not only reduce the total cost of the system and increasing the reliability, but also contribute in mitigating the world crisis such as global warming, reducing the dependability on the traditional

© COPYRIGHT UPM

energy sources, and these resources are free and inexhaustible. In this chapter, there are two main sections to explain the methodology of this research, as depicted in Figure 3.1. The first section is the parameter extraction of the TD PV model's method. The proposed a robust adaptive Arithmetic Optimization Algorithm based on the adaptive damping Berndt-hall-hall-Hausman ($RaAOA_{AdBHHH}$) approach is employed to determine the parameters of the TD PV module under various weather conditions of the real experimental data. The second section is optimal sizing of the WT/PV/Battery system using improved two-achieve algorithm to construct sets of the optimal PF solutions for two cases study: Malaysia and South Africa. The most desirable configurations from the sets of optimal PF solutions is chosen based on integration of BWM-PROMETHEE II-GDM method. Finally, the proposed method is validated based on intuitive-numerical-MOO-BWM-TOPSIS-GDM method.

© COPYRIGHT UPM

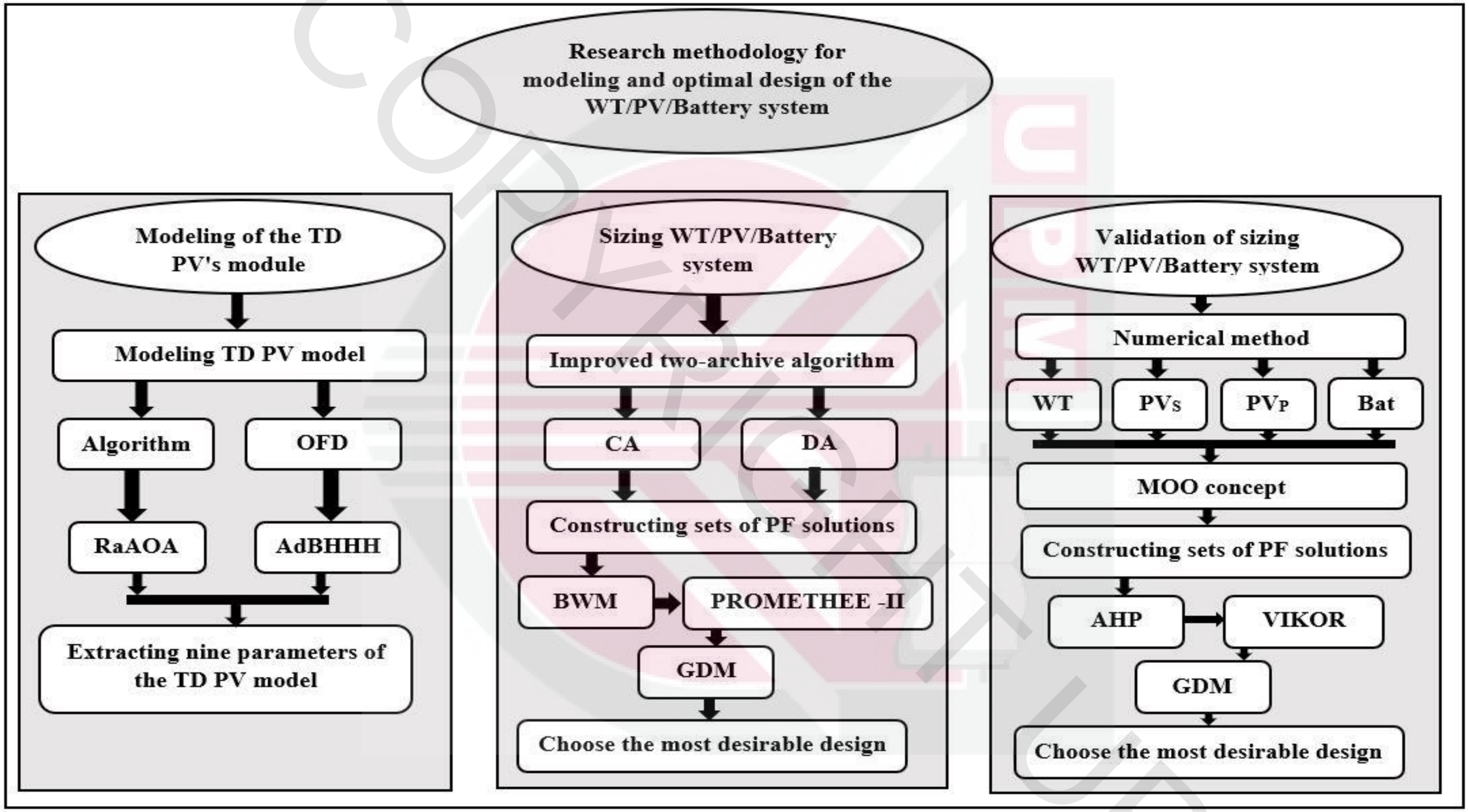

Figure 3.1 : Research methodology description

3.2 Modeling of the PV system output power

There are primarily mainly three types of PV models described in the literature: single-diode (SD), double-diode (DD), and three-diode (TD) PV models [151]. The simplest PV model is the single-diode, which requires only five physical parameters to define the electrical equivalent circuit. The double-diode PV model is sophisticated and precise than the previous one, which needed optimal estimation of seven physical parameters. On the other hand, the third-diode PV model is more complicated and needs an extensive computation in order to extract its nine parameters. This model is appropriate for practical and industrial applications of the PV system, exhibiting good accuracy at low and high solar radiation levels [243,244]. In the literature, simple mathematical PV models were employed to predict the output power without considering their physical factors elements that were directly influenced by the fluctuations of the nature. Whereas, the TD PV model has not applied yet for sizing of the hybrid standalone WT/PV/Battery system, which is considered the most realistic and accurate model to date. The $RaAOA_{AdBHHH}$ approach has never been utilized in the literature and its presented to extract nine unknown parameters of the TD PV model using actual measured experimental data.

3.2.1 Three-diode PV model

The analogous circuit of the TD PV model is illustrated in Figure 3.2. The TD PV model consists of nine physical properties: a parallel current source I_{Ph} in (A), diodes ideality factor d_{1-3}, connected in the reverse way to mirror the output voltage of the PV cell, three diode absorption current I_{o1-3}, in (A), a small series resistor R_s in (Ω),

© COPYRIGHT UPM

and a big shunt resistance R_p in (Ω). Kirchhoff's law may be used to compute the PV cell's output current in (A), which is denoted as follows [245]:

$$I = I_{Ph} - I_d - I_p, \tag{3.1}$$

where I_d is the forward diode current in (A) and I_p is the shunt resistor current in (A), respectively. Therefore, the output current of the TD PV model can be described by the following equation:

$$I = I_{Ph} - I_{o1}\left[exp\left(\frac{V+IR_s}{V_{t1}}\right)-1\right] - I_{o2}\left[exp\left(\frac{V+IR_s}{V_{t2}}\right)-1\right] - I_{o3}\left[exp\left(\frac{V+IR_s}{V_{t3}}\right)-1\right] - \frac{V+IR_s}{R_p}, \tag{3.2}$$

where V_{t1-t3} define the thermal voltage of the diodes and computed as follows:

$$V_{t1} = \frac{d_1 KBT_c}{q},\ V_{t2} = \frac{d_2 KBT_c}{q},\ \text{and } V_{t3} = \frac{d_3 KBT_c}{q} \tag{3.3}$$

where KB denotes to constant of the Boltzmann $\left(1.38 \times 10^{-23}\, J/_K\right)$, T_c is the cell temperature (K), and q refers to the electron charge ($1.60 \times 10^{-19} C$).

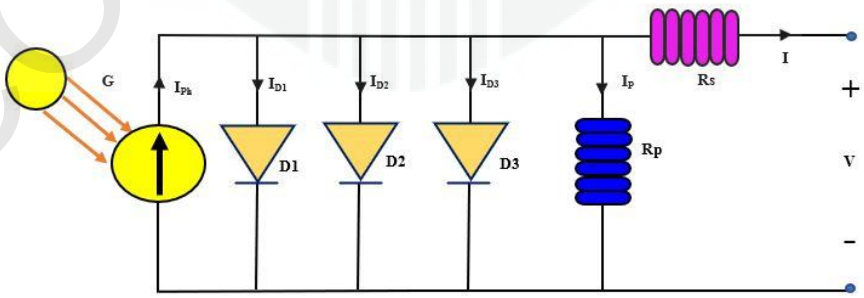

Figure 3.2 : The electrical circuit for the TD PV model

It must be highlighted that the nine parameters of the TD PV model are dependent on operating environment and must be estimated appropriately to plot I-V and P-V curves [246].

3.3 Proposed method for extracting the parameters of the TD PV model

In this thesis, we present a robust adaptive Arithmetic Optimization Algorithm based on the adaptive damping Berndt-hall-hall-Hausman ($RaAOA_{AdBHHH}$) approach to efficacity determine the parameters of the three diode PV model.

3.3.1 Arithmetic optimization algorithm (AOA)

The AOA is developed to determine the parameters of the TD PV model [247]. Algebra, geometry, and analysis are the main inspiration of the numerical theory and the essential aspects of the modern mathematics. The four arithmetic operators: (*Division* "$/$", *Multiplication* "$\times$", *Subtraction* "$-$", and *Addition* "$+$") are employed to represent the exploration and exploitation phases [247]. The following outlines the procedure and modalities of the AOA:

A. Initialization

At first, a random collection of solutions is generated (X). The most optimum solution is kept, along with its position, for the next step.

$$X = X_L + rand(X_U - X_L), \tag{3.4}$$

where $rand$ is a randomly number between [0,1], X_U and X_L define problem's the upper and lower boundaries. The AOA selects the exploration and exploitation stages using Math Optimizer Accelerated (MOA) function as follows:

© COPYRIGHT UPM

$$MOA(C_i) = Min + C_i \times \left(\frac{Max - Min}{M_i}\right), \tag{3.5}$$

where $MOA(C_i)$ is the function's value in the current iteration. Max and Min are minimum and maximum values of the *MOA* function. The changeover between the exploration and exploitation strategies is handled according to the random value of r_1 and *MOA* function value.

B. Exploration stage

The *Division* (*D*) and *Multiplication* (*M*) operators are responsible on the exploratory process, with *D* executing when the $r_2 > 0.5$, *M* acting otherwise. The AOA traverses the search space randomly between the lower and upper variables, as modelled in the following equation:

$$x_{i,j}(C_i + 1) = \begin{cases} best(x_j) \div (MOP + \epsilon) \times \left((U_j - L_j) \times \mu + L_j\right) & r_2 > 0.5 \\ best(x_j) \times MOP \times \left((U_j - L_j) \times \mu + L_j\right) & otherwise \end{cases}, \tag{3.6}$$

where $best(x_j)$ is the most optimum solution, r_2 is randomly selected value, ϵ is a small value, U_j and L_j are the lower and upper bounds of the j th position, and MOP is Math Optimizer Probability coefficient and it is expressed as follows:

$$MOP(C_i) = 1 - \frac{{C_i}^{1/\propto}}{{M_i}^{1/\propto}}, \tag{3.7}$$

where $\propto$ is a critical parameter set to 5 and determine the exploration accuracy across iterations.

© COPYRIGHT UPM

C. Exploitation stage

In this step, the *Subtraction* (*S*) and *Addition* (*A*) operators are utilized to search propensity. The *S* and *A* operators are constrained by the random r_3 value to conduct in-depth search in various dense locations and to produce high-quality solutions.

$$x_{i,j}(C_i+1)=\begin{cases} best(x_j)-MOP\times\left(\left(U_j-L_j\right)\times\mu+L_j\right) & r_3>0.5 \\ best(x_j)+MOP\times\left(\left(U_j-L_j\right)\times\mu+L_j\right) & otherwise \end{cases}, \qquad (3.8)$$

The original AOA has several limitations such as:

- Its exploration and exploitation phases are not mature, it can easily trap in local minima.
- The *D* and *M* operators are highly scattering, presence a large number of improper random solutions in the feature space during the optimization process.
- The population's updating structure is strongly depend on the lower and upper limits, convergence to nonlinear and multivariable optimization problems is challenging.
- There is no effective mechanism to obtain high-quality solutions. Therefore, being trapped in suboptimal solutions is much easily.

3.3.2 The proposed robust adaptive AOA procedure

The classical AOA has a number of shortcomings, such as premature convergence and stagnation in local minima, which are exacerbated when employed to solve the multivariable and high-dimensional optimization problems. From this vantage view, the proposed developments try to overcome the previous restrictions, beginning with newly modified control parameters and modified explorer-exploiter mechanisms and ending with the lunch of innovative strategies to ensure a high capability of

© COPYRIGHT UPM

discovering new regions with globally convergence. The following details the subsequent developments:

- **An adaptive explorer-exploiter mechanism**

Opposition based learning is considered one of the most promising techniques for effectively discovering unknown areas in the search space [248]. This technique may be further refined by drawing inspiration from levy flight (RL) motion. The improved OBL (IOBL) is able of escaping from non-optimal areas by concurrently searching both randomly directions and its opposites. The IOBL is employed to explore the first half of population, whereas the teaching learning (TL) mechanism is proposed for the rest iterations. Hence, the TL technique is successful at exploitation by learning from other neighbourhood particles [249]. The adaptive explorer-exploiter mechanism is expressed as follows:

$$xnew_i^{new} = \begin{cases} xnew_i + RL_i \times (rand \times (A+B) - xnew_i) & i > N/2 \\ xnew_i + MOP \times (best(x) - rand \cdot (X_{mean})) & otherwise \end{cases}, \quad (3.9)$$

where $xnew_i^{new} \in [A, B]; j = 1, 2, \ldots, D$

where RL_i is the LF mechanism, A and B are the iteration's lowest and maximum values, and X_{mean} is mean of the X matrix.

- **Improved exploration stage**

The original AOA's four operators are highly reliant on the design variables bounds, which may converge prematurely to non-optimality areas. It should be noted that the optimization problem of the PV model requires large step sizes for solution movement in the feature space. To alleviate the weaknesses and deficiencies of searching based

© COPYRIGHT UPM

on only upper and lower bounds, the Covariance Matrix based Migration (CMM) strategy is integrated with *D* and *M* arithmetic operators. The CMM's fundamental component is the rotation of the original coordinate solutions into eigenvector-based solutions, which enables efficient information sharing between the particles. The mathematical model for the CMM is as follows [250]:

$$CMM_{i,j} = \frac{\sum_{k=1}^{N}\left(xnew_{i,k}^{C_i} - \overline{xnew}_i^{C_i}\right)\left(xnew_{k,j}^{C_i} - \overline{xnew}_{,j}^{C_i}\right)}{N-1}, \tag{3.10}$$

where $\overline{xnew}_i^{C_i} = \sum_{k=1}^{N} xnew_{i,k}^{C_i} \,/\, N$ refers to the variables in the current iteration. The covariance matrix is stated as follows:

$$CMM_{i,j} = \left[CMM_{i,j}\right]_{D\times D}, \tag{3.11}$$

where *D* is the problem's dimension. The eigenvector is computed by factoring the covariance into its canonical formulas, as shown in [250]:

$$CMM_{i,j} = Q_{xnew} A_{xnew} Q_{xnew}^{T}, \tag{3.12}$$

where Q_{xnew} is the $D \times D$ matrix containing the eigenvector, A_{xnew} is the diagonal matrix. Following eigenvector decomposition, the coordinate solutions are rotated into eigenvector-based solutions. The migration is then performed and structure is rotated back to its original shape as follows [250]:

$$CMM_{i,j} = eigxnew_{i,k}^{C_i+1} \times Q_{xnew}^{T}, \tag{3.13}$$

where the rotating habitant is denoted by $eigxnew_{i,k}^{C_i}$. Each iteration in the exploration step is tuned by only *D* and *M* factors, along with upper and lower boundaries, resulting very poor convergence. These *D* and *M* operations always conduct

© COPYRIGHT UPM

indisputable solutions that are beyond the search space. The results of loss several rounds without increasing the exploration inclination, hence limiting the population diversity. To address these shortcoming, the *D* and *M* operators have been revised to include a complement rule that enabling broader exploration while preventing diversity loss throughout the optimization process [251]. Additionally, the new strategy is not dependent on the bounds variable of the optimization problem, which may substantially aid in avoiding convergence difficulties. The newly singed $\overline{D}$ and $\overline{M}$ operators are as follows:

$$xnew_i^{new} = \begin{cases} best(x) - (-1) \cdot MOP \times \left(RL_i \times \left((CMM_i - xnew_1) + rand \cdot (xnew_i - xnew_3)\right)\right) & r_2 > 0.5 \\ best(x) - MOP \times \left(RL_i \times \left((CMM_i - xnew_1) + rand \cdot (xnew_i - xnew_3)\right)\right) & otherwise \end{cases}, \tag{3.14}$$

- **Improved exploitation stage**

In the exploitation stage, three distinct vectors are picked up from the current iteration in order to enrich the diversity of population while maintaining high-quality solutions. Therefore, the MOP and LF techniques are included to prevent stagnation in the locality. As a consequence, a more robust explorer-exploiter tactic is involved for the four arithmetic operators, as written:

$$xnew_i^{new} = \begin{cases} best(x) + (-1) \cdot MOP \times \left(RL_i \times \left((xnew_1 - xnew_3) + rand \cdot (xnew_2 - xnew_i)\right)\right) & r_3 > 0.5 \\ best(x) + MOP \times \left(RL_i \times \left((xnew_1 - xnew_3) + rand \cdot (xnew_1 - xnew_i)\right)\right) & otherwise \end{cases}, \tag{3.15}$$

In this upgraded algorithm, the exploration is carried out by the complement $\overline{D}$ and S operators as a result of their moves into new optimal regions. Whereas, the

© COPYRIGHT UPM

complement $\overline{M}$ and A operators perform the exploitation stage as a result of their motions to near-optimal and best-optimum positions discovered so far, as demonstrated in Figure 3.3. The iteration is classified to promote the diversity in the first half of iterations using the CMM mechanism, while increasing the capacity to explore in small regions surrounding the most optimum solution.

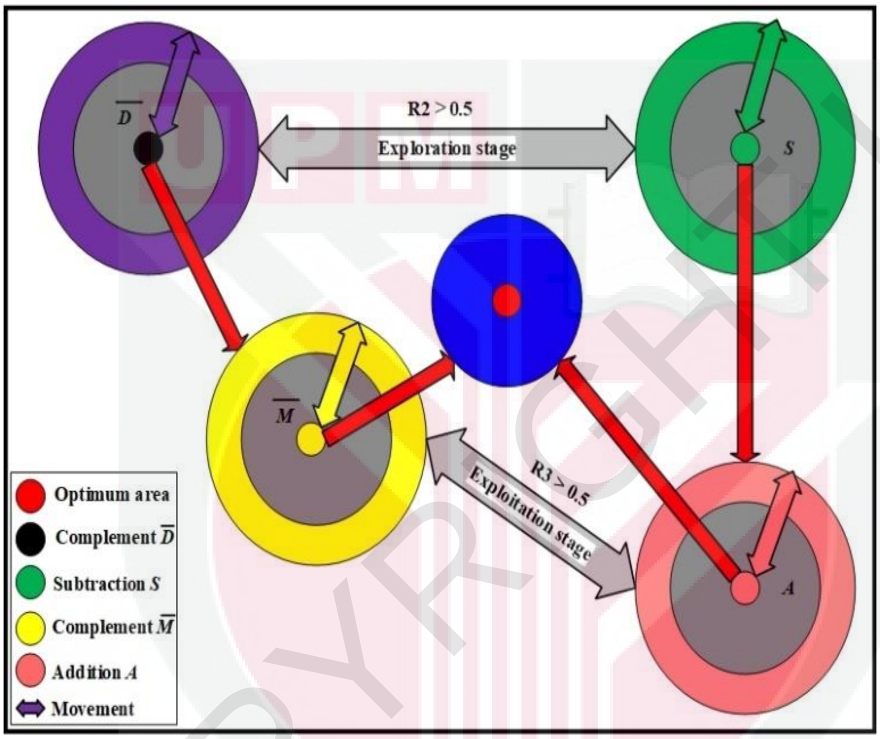

Figure 3.3 : Mathematical model of RaAOA operators to optimal regions

- **Winner-based mutant schemes**

Two schemes: DE/current/1 and DE/best/2 are proposed in this study based on the minimum cost function. In the current iteration, the winning mutation strategy is selected. In the other sense, the proposed $RaAOA_{AdBHHH}$ processes in two directions, simultaneously using the advantages of the local and global searches [252,253]. If none of these strategies produces a winner, the best-optimal fitness and its position will be placed in the current iteration, as expressed by,

© COPYRIGHT UPM

$$x_i(C_i + 1) = xnew_i - rand \times (xnew_1 - xnew_2), \tag{3.16}$$

$$x_i(C_i + 1) = best(x) - L \times \left(B + (xnew_1 - xnew_2)\right), \tag{3.17}$$

The main aims of proposing the $\text{RaAOA}_{\text{AdBHHH}}$ model is overcome the shortcoming in the original AOA. The flowchart of the proposed $\text{RaAOA}_{\text{AdBHHH}}$ is illustrated in Figure 3.4.

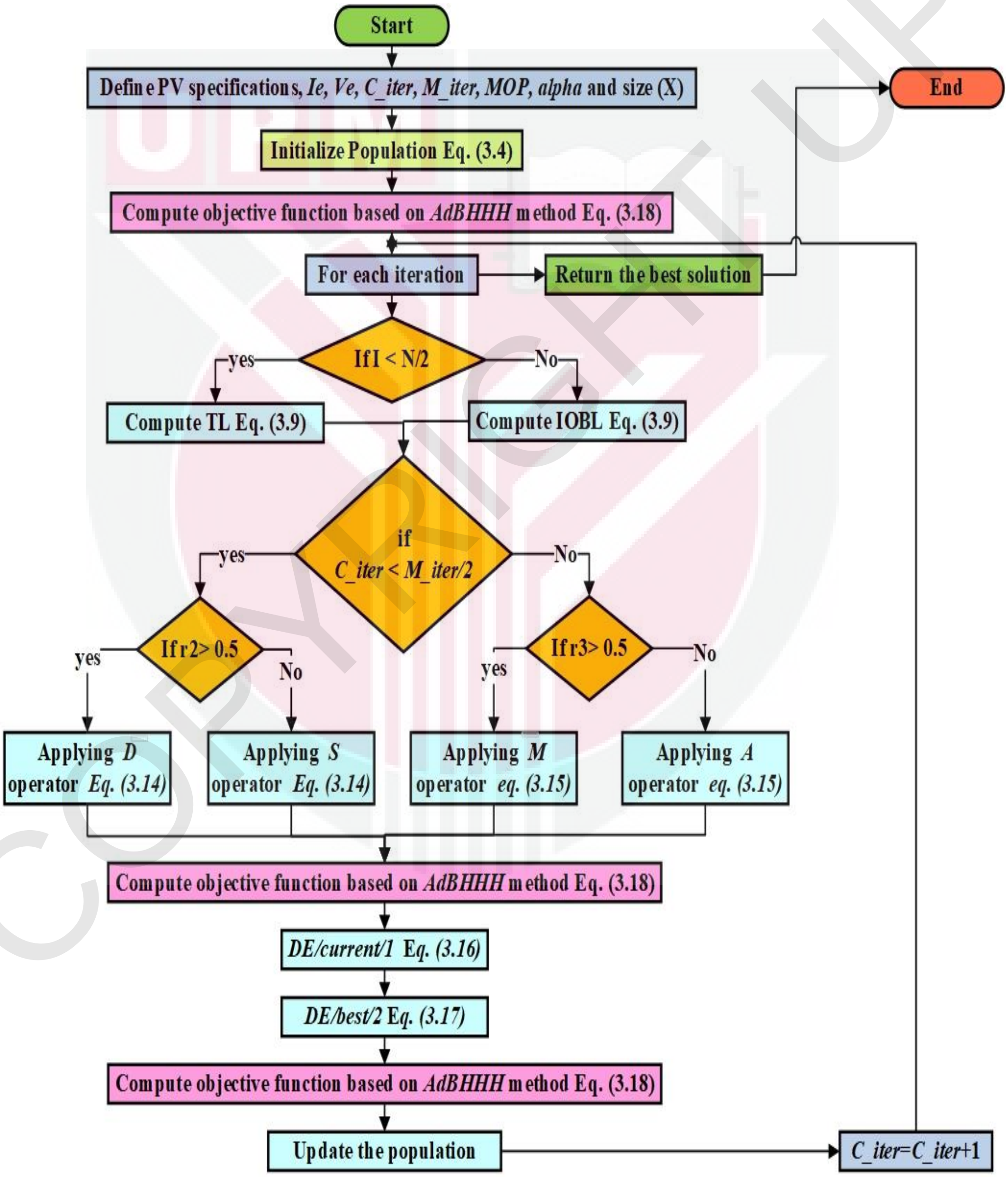

Figure 3.4 : Flowchart of the proposed $\text{RaAOA}_{\text{AdBHHH}}$ approach

© COPYRIGHT UPM

This benefits of the proposed improvements can be highlights as follows:

- The balancing between the exploration and exploitation tendencies are achieved by addressing the powerful IOBL mechanism at first-half of iterations, while TL is considered in the second one.

- Promoting a new and successful explorer tactic for ensuring the local minima avoidance. The CMM and complements of the $\overline{D}$ operators are presented. The LF strategies can significantly enhance the diversity of the population.

- The complement $\overline{M}$ operator along with three distinct-mutant vectors are applied in the exploitation stage. The high-quality of solutions is included for the rest of optimization process.

- The winner-principle is defined by including the best fitness function found so far. If there is no winner from Equations (3.15) and (3.16), the best optimal solution and its location will be obtained in the current iteration. This process can affectively assist the decision-maker to choose most optimum solution in the search space.

- The novel objective function formulation is proposed based on AdBHHH method in order not only to reduce the oscillations and noise effects, but also half-space distance in the search space will be chosen to provide very precisely initial root solutions.

- The nonlinearity and intermittent of the nature are handled by employing adaptive damping control parameter of the LM's method. This formulae assists to minimize the error between the experimental data points to zero.

3.3.3 The novel Berndt-Hall-Hall-Hausman based on adaptive damping parameter (AdBHHH) method

The BHHH is one of the numerical methods and similar to the NR method, but it uses only the first derivative order to efficiently solve the nonlinear equations, restricting its model to small mathematical steps. The BHHH method computes minimum

© COPYRIGHT UPM

distance estimator rather than maximum likelihood, which it selects the half-space as a direction at each iteration. If the process moves intentionally toward critical point (local maximum), several initial root variables are chosen to figure out the actual shape of the objective function carefully until the global maximum is located. The mathematical model of the BHHH can be represented as follows [254]:

$$\beta_{i+1} = \beta_i - \propto_i A_i \frac{\partial \varrho}{\partial \beta}(\beta_i), \tag{3.18}$$

where β_i is the parameter estimate at current iteration and A_i is calculated within a current iteration as follows:

$$A_i = \left[\sum_{t=1}^{N} \frac{\partial ln\varrho_i}{\partial \beta}(\beta_i) \frac{\partial ln\varrho_i}{\partial \beta}(\beta_i)'\right]^{-1}, \tag{3.19}$$

The main advantages of the AdBHHH are: it requires only first-order derivative. Also, it computes the variance-covariance matrix (A_i) from the previous iteration, which the initial solutions are provided by RaAOA algorithm. The convergence of the (A_i) matrix is depicted in Figure 3.5. The adaptive nonlinear damping parameter ($\propto_i$) of Eq. (7) enables the search direction to global region. The RMSE is calculated as follows:

© COPYRIGHT UPM

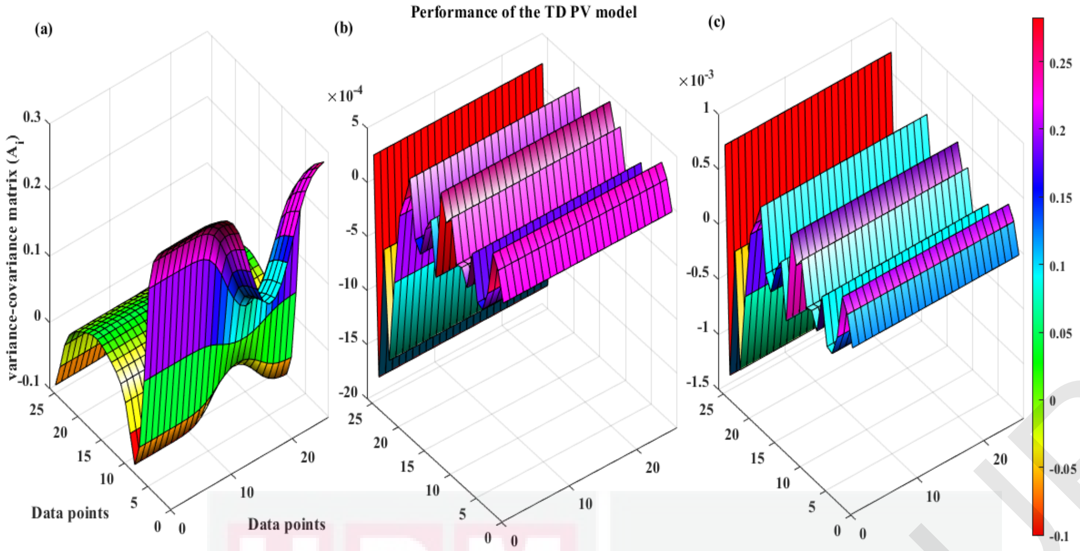

Figure 3.5 : Performance of the variance-covariance matrix (A_i) at (a) first iteration, (b) 500 iteration, and (c) 950 iteration for the TD PV model

$$RMSE = \sqrt{\frac{1}{N}\sum_{i=1}^{N} P(I_e - I_p)^2}, \tag{3.20}$$

where N is the total number of the I-V characteristic data curve, I_e and I_p signify the experimental and proposed currents with considering the experimental length of voltage V_e for the PV model, respectively.

3.4 Output current and voltage of the TD PV model using datasheet information

The experimental data for the Yingli PV module are not readily available in this study. The manufacturer typically provides information for open-circuit (V_{oc}), short-circuit (I_{sc}), and maximum power point (I_{mpp}) at standard test conditions (STC) [39]. To solve this dilemma, the parameters of the TD Yingli PV module are extracted by using the methodology of the GCAOA to minimize the errors at the three main points. The following equation of the TD PV model based on Yingli module at MPP is used to forecast the output current and voltage for the given solar radiation and ambient temperature at any location [255]:

$$I(k) = I_{sc} \cdot \lambda(k) - \frac{I_{sc}}{e^{\frac{qd_1}{n_c KBT_C(k)}}} \cdot \left[e^{\frac{qd_1}{n_c KBT_C(k)}} \cdot e^{\frac{V(k)}{V_{oc}}} - 1\right] - \frac{I_{sc}}{e^{\frac{qd_2}{n_c KBT_C(k)}}} \cdot \left[e^{\frac{qd_2}{n_c KBT_C(k)}} \cdot e^{\frac{V(k)}{V_{oc}}} - 1\right] - \frac{I_{sc}}{e^{\frac{qd_3}{n_c KBT_C(k)}}} \cdot \left[e^{\frac{qd_3}{n_c KBT_C(k)}} \cdot e^{\frac{V(k)}{V_{oc}}} - 1\right] - \frac{V(k)+I_{sc}R_s}{R_p}, \quad (3.21)$$

where λ is the variation of the solar radiation, T_c =273+T , T is the ambient temperature, V is determined by the following:

$$V = V_{mpp} + V_t \cdot \ln\left(\frac{\lambda}{\lambda_s}\right) + \beta \cdot (T - T_r), \quad (3.22)$$

where λ_s and T_r are the reference values for solar radiation and ambient temperature, respectively. β is the open-circuit coefficient (V/K). The authors of [255] ignored the effects of $\frac{V(k)+I_{sc}R_s}{R_p}$ in Equation (3.21), resulting in erroneous current and voltage outputs predictions.

3.5 Wind turbine model

Wind is a renewable energy source that is accessible for free. WT generator converts the wind speed to electricity. In this research, a small-scale WT generator with 800 W is considered for the design of the WT/PV/Battery system due to its low start-up wind speed, where the WT generator can operate efficiently. Since wind speed varies with height, it is necessary to position the WT at a specified hub height. The following formula is used to determine the wind speed at a 20-meter height [256]:

$$\frac{v2}{v1} = \left(\frac{h2}{h1}\right)^{\propto}, \quad (3.23)$$

© COPYRIGHT UPM

where $v2$ denotes the WT's speed at the hub height ($h2$) and v_1 refers to the WT's speed at reference height ($h2$). $\propto$ is the friction coefficient parameter (Hellmann exponent), which is typically between 0.14 and 0.25 [257,258]. The WT generator's output power may be computed as follows:

$$WT = \begin{cases} 0 & V < V_{Ci}, V > V_{Co} \\ V^3\left(\frac{Pr}{V^3 - V_{Ci}^3}\right) - Pr\left(\frac{V_{Ci}^3}{V_r^3 - V_{Ci}^3}\right) & V_{Ci} \leq V < Vr, \\ \mathrm{Pr} & Vr \leq V \leq V_{Co} \end{cases} \tag{3.24}$$

where V refers to the current wind speed, V_{Ci} and V_{Co} are the cut-in and cut-out wind speeds, respectively. Pr and Vr are the rated power and nominal wind speed. Table 3.1. contains the specification for the WT generator.

Table 3.1 : WT's specifications [1]

Parameter	Characteristic
Model	SS-800
Rated power	800 W
wheel diameter	1.3 m
Start-up wind speed	1.3 m/s
Rated wind speed	13 m/s
Survival wind speed	50 m/s
Number of blades	6
Blades length	580 mm
Design life	20 years

3.6 Battery mathematical model

Due to its acceptable degree of reliability, efficiency, and cheaper cost than other types [259,260], the lead-acid battery is chosen for the proposed system [4]. Whenever the electrical power supplied by the renewable power sources: PV panels ($P_{PV(n)}$) and WT generator ($P_{WT(n)}$), is inadequate to meet the required power demands, the storage battery will be utilized, where its capacity is calculated as follows:

© COPYRIGHT UPM

$$C_{batt} = \frac{E_L * A_d}{DoD * \eta_{bat} * \eta inv}, \tag{3.25}$$

where E_L is the average daily amount of energy needed, DoD refers to the depth of the discharge, η_{bat} indicates the battery efficiency equal to 85%; ηinv denotes to the inverter efficiency equal to 95%, A_d is the number of the autonomy (usually 3 days), and $C_{batt}$is the battery's nominal capacity. The battery's charging, discharging, and state of charge ($SOC_{(n)}$) status are represented as follows :

For charging:

$$E_{batt_{(n)}} = SOC_{(n-1)} + \left[\left(P_{WT(n)} + P_{PV(n)}\right) - P_{L(n)}\right] \times \eta_{bat}, \tag{3.26}$$

For discharging:

$$E_{batt_{(n)}} = SOC_{(n-1)} + \left[P_{L(n)} - \left(P_{WT(n)} + P_{PV(n)}\right)\right] \times \eta_{bat} \tag{3.27}$$

For the SOC status:

$$SOC_{(n)} = \begin{cases} SOC_{min} & E_{batt} < SOC_{min} \\ E_{batt} & SOC_{min} < E_{batt} < SOC_{max}, \\ SOC_{max} & E_{batt} > SOC_{max} \end{cases} \tag{3.28}$$

For the minimum SOC value:

$$E_{min} = SOC_{max} \times (1 - DoD), \tag{3.29}$$

where $E_{batt_{(n)}}$ refers to the battery's current capacity and $P_{L(n)}$ denotes to the energy demand. The terms SOC_{min} and SOC_{max} represent, respectively, the lowest and highest battery's capacities.

© COPYRIGHT UPM

3.7 Charge controller

The battery power supplied to the load requirement through the charge controller and inverter can be expressed as follows [159,160]:

$$P_L = E_{batt} \times \eta batt \times \eta inv \times \eta ch, \tag{3.30}$$

where ηch is the efficiency of the charge controller, which is 99 %. The charge controller is used to protect the battery from overcharged, hence increasing its efficiency and longevity. This charge controller is chosen to regulate the voltages differences between the produced power from inverter and the battery voltage. The specifications of the charger controller is given in Table 3.2.

Table 3.2 : Specification of the charger controller [2]

Parameter	Characteristic
Model	MPP 250/100-Tr VE.Can
Battery voltage	12/24/48 V
Rated charge current	70/85/100 A
Max. efficiency	99%

3.8 Bidirectional inverter

To save costs and simplify the optimization process, the use of converters is omitted. The PV generates DC current and WT generates AC power, the bidirectional inverter converts the DC electricity to AC power to satisfy the required load profile, while converting the AC power to DC power to charge the battery. This bidirectional inverter has various features, including DC/AC power, input/output protection, internal over temperature, and battery over temperature. The inverter/charger's specifications are given in Table 3.3. The amount of energy supplied to the load is expressed as follows [258]:

© COPYRIGHT UPM

$$P_L = (E_{batt} + P_{WT} + P_{PV}) \times \eta inv, \tag{3.31}$$

Table 3.3 : Specifications of the bidirectional inverter [3]

Parameter		Characteristic
Model		SL-3000
Inverter mode	Input voltage range	9~17 V DC
	Max. DC input current	400 A DC
	AC output power	3000 VA
	Max. efficiency	> 90%
	Output voltage	12 V AC
Charger mode	AC input voltage	120 V AC
	AC input current	5~50 A
	AC nominal current	18 A
	Charger efficiency	85%
	Charging current range	0~125 A

3.9 Data collection and techno-economic assessments

Two hourly climatological collected data for a one year period in South Africa and Malaysia are investigated in this research. The effectiveness and potency of the suggested approaches for optimal sizing of the PV/WT/Battery system are examined via two different case studies.

- **Load profile**

This study produces a constant load requirement for 24 hours then duplicated for an entire year in a distant Malaysian area. In order to power the client appliances such as lamps, TVs, fans, laptops and refrigerator, this load may only use up to 5 KW of electricity [261].

- **Malaysia**

The Subang climatic center in Malaysia, which is situated at longitude of a 101.6° east and latitude of 3.12° north, was responsible for the data collection in Kang Valley. The solar radiation transmitter has a high-stability PV sensor with a +/-1 %, type

© COPYRIGHT UPM

WE300. The PV array's surface has a detector temperature precision of 0.25 ℃. The WE700 type air thermometer has an accuracy of +/-0.1℃ across an ambient temperature of +/-50 ℃. The electrical transducer model of the CTH-50 type, including an output range 4-20 mA and an input range of 0-50 A DC [262].

- **South Africa**

Every hour, time-stamped data were collected at neighboring station in Johannesburg, South Africa, at -26.2° latitude north and -28° west longitude using the HOMER[TM] and RETScreen software, from a neighboring [263,264].

In order to improve the dependability, lower system costs overall, and use less energy, three competing factors were considered for the freestanding PV/WT/Battery system [265]. The problem formulation of the three conflicting objectives is given is as follows:

Min $F(X) = \{LLP, LCC, P_{dump}\}$, (3.32)

$X = (WT, N_S, N_P, B_S)$

where X represents the vector of the decision variables: WT, N_S, N_P, and B_S that must be optimized by improved bi-archive algorithm.

- **Loss of load probability**

The LLP define as the percentage of the annual load demand power to the total electricity shortfalls across a time period as follows:

$$LLP = \frac{\sum_{t=1}^{8759} deficit\ energy_t}{\sum_{t=1}^{8759} demand\ energy_t}, \quad (3.33)$$

© COPYRIGHT UPM

- **Dumped power**

One of the key constraints in building an off-grid PV/WT/Battery system is surplus energy. As a result, the second technical objective is to decrease lost energy via resistive loads while simultaneously boosting system dependability. The following model is obtained to compute the dumped power:

$$P_{dump} = \begin{cases} \sum_{t=1}^{t=8760} P_{WT}(t) + P_{PV}(t) - P_L(t) & if\ P_{WT}(t) + P_{PV}(t) > \ P_L(t) \\ otherwise & 0 \end{cases}, \quad (3.34)$$

- **Life cycle cost**

The second objective is Life Cycle Cost (LCC), which is applied for computing the overall expense of the power produced by the freestanding PV/WT/Battery system for a specific amount of time. The initial outlay (I_c), operation and maintenance (OM_c), and the replacement cost (R_c) make up the LCC, which is computed as follows [224,232]:

$$LCC(\$) = I_c + OM_c + R_c, \quad (3.35)$$

The initial investment of the independent PV/WT/Battery system, in addition to the cost of cabling, construction, and civil work, are included, which are presented as follows:

$$I_c\ (\$) = U_{PV} \times C_{PV} + U_{WT} \times C_{WT} + U_B \times C_B + U_{Inv} \times C_{Inv} + U_{ch} \times C_{ch} + C_c, \quad (3.36)$$

where U_B and C_B are the unit cost and capacity of the battery bank, U_{WT} and C_{WT} are the unit cost and capacity of the wind turbine, U_{PV} and C_{PV} are the unit cost and capacity of the PV array, U_{Inv} and C_{Inv} are the unit cost and capacity of the bi-

© COPYRIGHT UPM

directional inverter, U_{ch} and C_{ch} are the unit cost and capacity of the charge controller, and C_c indicates the civil work and outlay cost which is considered to be 6000 $ [224,266]. Additionally, the cost of operation and maintenance is calculated throughout the system lifespan (LT). The following formulas are utilized in the OM_c to determine the inflation rate (f_r) and interest rate (I_r) [265]:

$$OM_c(\$) = \begin{cases} OM_{f,c} \times \left(\frac{1+f_r}{I_r-f_r}\right)\left(1 - \left[\frac{1+f_r}{I_r+I_r}\right]^{LT}\right) & for\ f_r \neq I_r \\ OM_{f,c}\ \times\ LT & for\ f_r = I_r \end{cases}, \tag{3.37}$$

where $OM_{f,c}$ represents first-year operating and maintenance expenses. The following is the calculation of the replacement cost:

$$R_c\ (\$) = U_r \times \left(\sum_{i=1}^{N} \left[\frac{1+f_r}{1+I_r}\right]^{\left(\frac{LF\times i}{f_r+1}\right)}\right), \tag{3.38}$$

where U_r is the is the element's initial purchase price. N is the total number of times an unit will need to be changed over the course of the system's life [267]. The financial statistics for the WT/PV/Battery system is given in Table 3.4.

Table 3.4 : Financial statistics for the WT/PV/Battery system [4]

Component	Unit cost ($)	LF	OM	R	In_R	Ir_c
WT	0.33345	20	0.02	0	0.04	0.08
PV	0.91836	25	0.01	0		
Battery	0.12544	2	0.03	0.042		
Inverter	0.45833	20	0	0		
Charge controller	0.84798	10	0	1		

© COPYRIGHT UPM

3.10 The proposed methodology sizing for the WT/PV/Battery system

This section is divided into three phases: the energy power flow management of the proposed freestanding PV/WT/Battery system is given in phase 1. Phase 2 includes the improved bi-archive algorithm to construct two sets of PF solutions while optimizing the three conflicting objectives. Phase 3 presents the selection of the most desirable design using hybrid MCDM method for both case studies.

3.10.1 Energy management procedure of the proposed WT/PV/Battery system

The energy-management is set up to satisfy the necessary load requirements while considering the dynamic energy flow of all the system components. The simulation firstly starts checking the state of conducted energy by the WT generators, PV modules, and SOC of the battery. There are three possible status for the net energy (E_{net}):

- Scenario 1: if the E_{net} is equal to 0, the PV models (E_{PV}) and wind turbines (E_{WT}) completely satisfy the needed load demand (E_{load}), eliminating the requirement for the battery storage. There is either surplus or deficit energy.
- Scenario 2: the E_{PV} and E_{WT} provide the E_{load}, if the E_{net} is higher than 0. Any excess energy will be used to recharge the battery bank if the SOC is below than SOC_{max}; otherwise, it will be kept as P_{dump}.
- Scenario 3: if the E_{net} is less than 0, the system will check the SOC whether it is larger than SOC_{min}, if it is yes, the E_{PV} and E_{WT} will provide the E_{load} with the help of the battery bank. Meanwhile, if the SOC is less than SOC_{min}, the system falls to provide the needed energy to the load demand. Each cycle routinely computes the LLP, LCC, and P_{dump} objectives. The proposed PV/WT/Battery system's operational flowchart process is shown in Figure 3.6.

© COPYRIGHT UPM

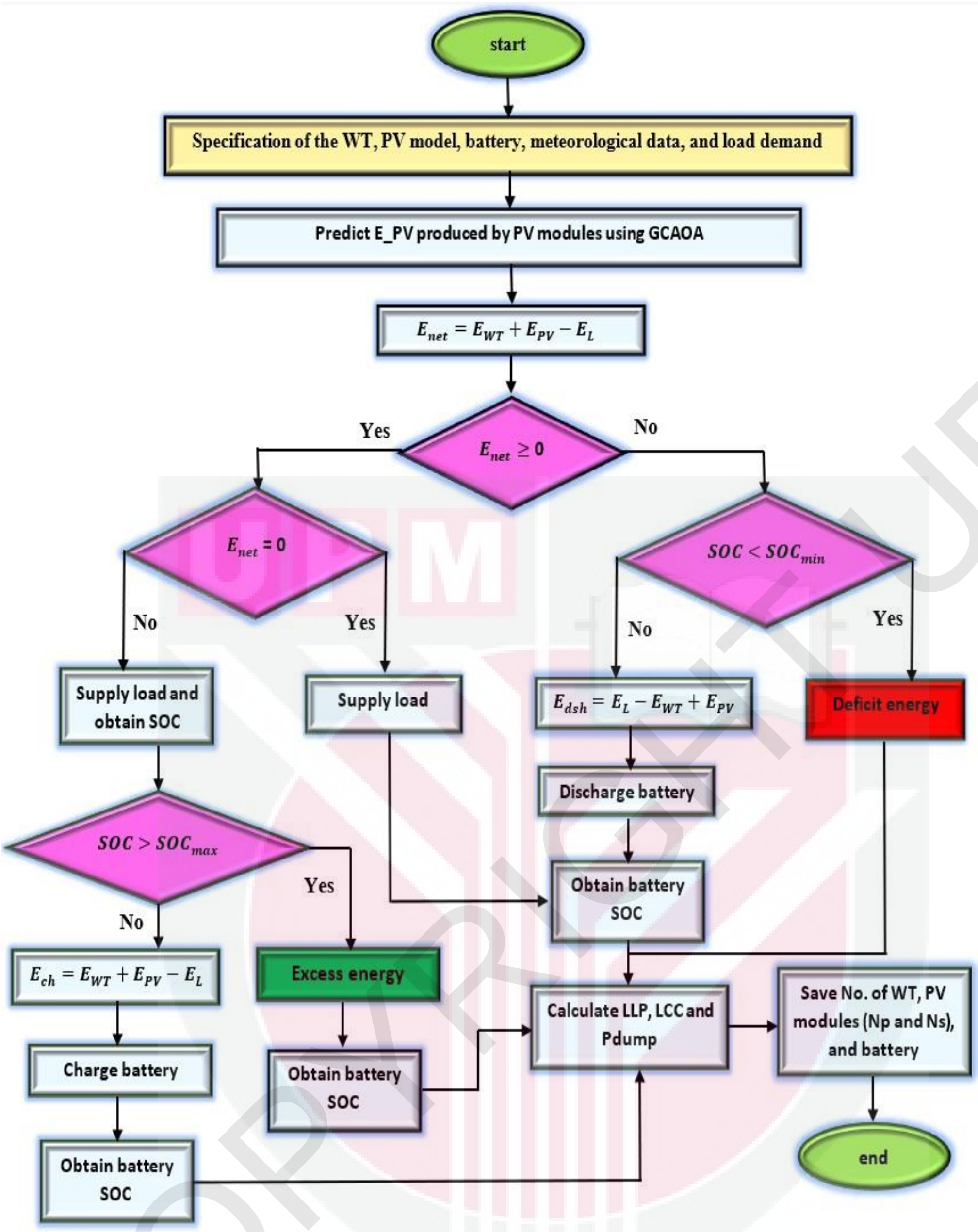

Figure 3.6 : Energy management of the hybrid PV/WT/Battery system

The energy management of the PV/WT/Battery system is essential to address the power flow during the optimization process.

3.10.2 The improved bi-archive algorithm

Maintaining the multi-objective optimization methods poses challenges in terms of convergence, diversity, and efficiency in developing a collection set of PF solutions.

© COPYRIGHT UPM

Most MOO method attempt to enhance the diversity and convergence concurrently, resulting unsatisfactory optimal PF solutions in the large objectives optimization problem. Therefore, the core idea of the bi-archive algorithm is to focus on convergence and diversity separately. The bi-archive algorithm employs two archives during the optimization process named as: Convergence archive (CA) and diversity archive (DA) [268]. Despite the fact that the idea is attractive, the original bi-archive algorithm has limited performance in large scale optimization problems such as: the CA does not include diversity maintenance during the convergence process, where the CA and DA cannot be updated when they are full. Therefore, the improved two archive algorithm is presented to overcome the restrictions of the original one by assigning two different selection concepts: Indicator-based and Pareto-based to the archive [24]. Moreover, the diversity into the archive is increased by addressing the L_p-norm-based ($p < 1$) scheme. The description of the CA and DA are given in the following subsection [24].

A. Convergence archive

The primary principle selection of the CA is based on indicator $I_{\varepsilon+}$ in Indicator-based evolutionary algorithm (IBEA) [269], which computes the minimal distance required for one solution to dominate another one in the objective feature. The following is the mathematical model of the $I_{\varepsilon+}$ [24]:

$$I_{\varepsilon+}(x_1, x_2) = min_{\varepsilon}(f_i(x_1) - \varepsilon \leq f_i(x_2), 1 \leq i \leq m), \tag{3.39}$$

$$F(x_1) = \sum_{x_2 \in P \setminus \{x_1\}} -e^{-I_{\varepsilon+}}(x_1, x_2)/0.05, \tag{3.40}$$

where m is the number of objectives. The Equation (3.39) is the measure of the $I_{\varepsilon+}$ if x_1 is omitted from the population. To update the CA, the offspring are firstly included

© COPYRIGHT UPM

in the CA, then the two archive algorithms eliminate the extra solution depending on their fitness. The solution with the smallest $I_{\varepsilon+}$ is discarded from the archive, and the $I_{\varepsilon+}$ values of the remaining solutions in the CA are updated for in each iteration according to the predetermined number of solutions in the archive.

B. Diversity archive

It is challenging with MOO methods to maintain the diversity of solutions distributed over the whole high-dimensional design space in order to handle all conceivable information in the PF. The diversity mechanism of the two archive is performed by firstly selecting the minimum and maximum solutions of each objective. Then, additional different solutions are chosen and incorporated to the DA. As a result, the improved two archive algorithm employs the L_p-norm based ($p < 1$) scheme, where $p = 1/\text{m}$. Both CA and DA are updated independently in each iteration. The final set of PF solutions are included in DA because the diversity of the CA is limited [24].

3.10.3 Hybridization of the MCDM methods

A decision-maker is essential to determine the independent PV/WT/Battery system's optimal design based on different techno-economic perspectives. The decision-maker gives the ability to rank these optimal solutions in accordance with the opinions of the three experts. The three objectives are weighted by BWM, while the PROMETHEE II is obtained for ranking these solutions. Finally, the GDM concept is applied to select the most ideal design and the analysis its performance and feasibility for the case studies, leading to a final and more reliable solution.

3.10.3.1 The BWM method

Rezaei et al. first proposed BWM, which is a comparison-based technique that uses two vectors of pairwise comparisons for weighting the objectives, in 2015 [193]. The first vector pits the best (highest important) criteria against the rest, and the worst (lowest important) criteria against the rest [270]. In contrast to the AHP technique, which needs n(n − 1) / 2 paired comparisons to weight the criteria, the BMW gives a high degree of stability and only needs for only 2n − 3 pairwise comparisons. As a consequence, the BWM can provide more trustworthy outcomes since each objective's priority is determined by view of experts. The following is a description of the BMW's steps:

- Deciding on a set of criteria for making decisions $(C_1, C_2, \dots, C_n)$.
- The decision-maker identifying the best criteria and worst criteria.
- The numbers between 1 to 9 are used to rank the importance of the best criteria in relation to others. The following expression explains the vector of the best criteria to others:

$A_B = (a_{B1}, a_{B2}, \dots, a_{Bn})$, where a_{B1} refers to the importance of the best criteria B over criteria $C_j, j = 1,2, \dots, n$.

- Resolving the preceding model to determine the optimal weight for each criteria:

$$\min max\left\{\left(\left|\frac{W_B}{W_j} - a_{Bj}\right|, \left|\frac{W_j}{W_w} - a_{Wj}\right|\right),\right. \tag{3.41}$$

S. t.

$\left|\frac{W_B}{W_j} - a_{Bj}\right| \leq \xi^*$, for all j

$\left|\frac{W_j}{W_w} - a_{Wj}\right| \leq \xi^*$, for all j

© COPYRIGHT UPM

$W_j \geq 0$, for all j.

where ξ^* denotes to the consistency ratio, the more closely zero value of ξ^*, the more consistently judgement is made, as shown by the following:

consistency Ratio=$\frac{\xi^*}{CI}$, (3.42)

where the CI stands for consistency index and is given in Table 3.5.

Table 3.5 : Values for the consistency index CI

a_{BW}	1	2	3	4	5	6	7	8	9
Consistency index (max ξ)	0.00	0.44	1.00	1.63	2.30	3.00	3.73	4.47	523

3.10.3.2 The PROMETHEE II method

The PROMETHEE method, which includes PROMETHEE I and II, is well-known outranking MCDM model that was firstly developed by Brans [271], The PROMETHEE I can be applied for partial ranking, but the PROMETHEE II may be utilized for a complete ranking of coordinate alternatives. Due to their ease-of-use, simplicity, and stability, they have been implemented in a wide range of applications. The steps of the PROMETHEE II method are given as follows [272]:

- Define the decision maker matrix as well as criterion j, alternative *m*, and the weights for each objective.

- The type of the preference function to be employed. Here, the regular preference function is optimally chosen after several attempts to achieve better stability.

- Calculate the preference function of each criterion for each alternatives' pair, as follow:

© COPYRIGHT UPM

$$P_j(x_i, x_t) = P_j\left(u_j(x_i) - u_j(x_t)\right) = P_j(\delta_{it}), \tag{3.43}$$

where P_j is the preference function, $u_j(x_i) - u_j(x_t)$ correspond to the objective value j for the alternatives x_i and x_t. The δ_{it} refers to the difference in performance of the alternatives considering the criteria j, and its equation is given below:

$$\delta_{it} = u_j(x_i) - u_j(x_t), \tag{3.44}$$

Calculate the preference index δ_{it} by comparing the alternatives, where the sum of P_j in which x_i is preferable to x_t. Then, the sum is weighted as presented by the following:

$$\delta_{it} = \frac{\sum_j w_j P_j(\delta_{it})}{\sum_j w_j}, \tag{3.45}$$

The positive (φ^+) and negative (φ^-) are calculated for each alternative, where $\varphi +$ denotes to how the x_i alternative surpasses others, while φ^- refers to how the x_i alternative is surpassed by others, as shown below:

$$\varphi_j^+ = \frac{1}{n-1}\sum_j \delta_{it}\left(x_i - u_{j'}\right),$$

$$\varphi_j^- = \frac{1}{n-1}\sum_j \delta_{it}\left(u_{j'} - x_t\right), \tag{3.46}$$

- Compute the overall net flow for each alternative, as follows:

$$\varphi_j = \varphi_j^+ - \varphi_j^- \tag{3.47}$$

The largest φ_j is the most dominated alternative to others.

© COPYRIGHT UPM

3.10.3.3 GDM technique

It is difficult to exclude or depend just on one expert. Therefore, the GDM makes a decision from a list of alternatives by compiling final decisions that are not specific to one expert and considering the knowledge and judgement of all experts [273]. The PROMETHEE II algorithm is extended to a group aggregation scenario, where it depends on the three experts' differing viewpoints. To lessen the differences in the final weights assigned to each expert, the arithmetic mean is addressed [274,275].

3.11 The numerical method for validation of proposed sizing method

The WT/PV/Battery system is designed optimally utilizing intuitive-numerical-MOO-BWM-TOPSIS methods for validation of the improved two archive-BWM-PROMETHEE II-GDM method.

3.11.1 Intuitive method

To reduce the very long computational time and processing of the numerical method, the intuitive method is employed. The intuitive can be successfully applied to estimate the initial ranges of the search space for the WT/PV/Battery system. Therefore, the numbers of the WT generators, PV modules, and storage batteries are computed intuitively as follows:

$$P_{WT} = \frac{1}{2}\text{Air density } r^2 \pi V^3, \tag{3.48}$$

where r is wind turbine rotor radius and air density s around 1.23 Kg/m^3 [276]. The number of the PV modules is computed as follows:

$$N_{PV} = \frac{E_L}{PSH * \eta inv * \eta batt * A} S_F, \tag{3.49}$$

© COPYRIGHT UPM

where PSH is the peak sunshine hours, S_F is the design safety factor, and A is the area of the PV array. The capacity of the storage battery is computed according the Equation (3.25). Moreover, the number of the storage batteries in series and parallel may be determined as follows:

$$N_{Sbatt} = \frac{V_{bus}}{V_{batt}} \text{ and } N_{Pbatt} = \frac{C_{batt}}{C_{batt},Wh}, \tag{3.50}$$

where V_{bus} and V_{batt} are the voltages of the bus system and battery, respectively. C_{batt}, Wh is the days of autonomy and Wh is the capacity of the battery.

3.11.2 Numerical method

The optimization process of the numerical method is boosted by roughly determining the ranges of the search space of the proposed system. The numerical method starts by iterating each variable (WT, Ns, Np, Batt), from minimum to maximum based on defined ranges. To compute the output energy from renewable energy sources, the energy management system is configured to satisfy the required load demand with a high degree of reliability and at the lowest possible total cost. After specifying each component of the WT/PV/Battery system, the simulation checks the state of conducted energy by using the WT and PV models. The net energy (E_{net}) may take one of three forms:

- Case 1: if the E_{net} equals 0, the load demand (E_{load}) is fully met by the wind turbines (E_{WT}) and PV models (E_{PV}), without requirement for a storage battery. The surplus and deficit energy are zero.
- Case 2: if the E_{net} is greater than 0, the E_{WT} and E_{PV} provide the E_{load}. If the state of charge is less than SOC_{max}, any surplus energy will be utilized for charging the battery; otherwise, it is stored as dump energy.

© COPYRIGHT UPM

- Case 3: if the E_{net} is less than 0, the E_{WT} and E_{PV} provide the E_{load} with storage battery after ensuring that the SOC is more than SOC_{min}. If the SOC is less than SOC_{min}, the system cannot supply the required load profile with the energy available, and the deficit energy is stored. The LLP, LCC, and P_{dump} objectives are regularly computed at each iteration. The management flowchart procedure for the proposed WT/PV/Battery system is depicted in Figure 3.7.

© COPYRIGHT UPM

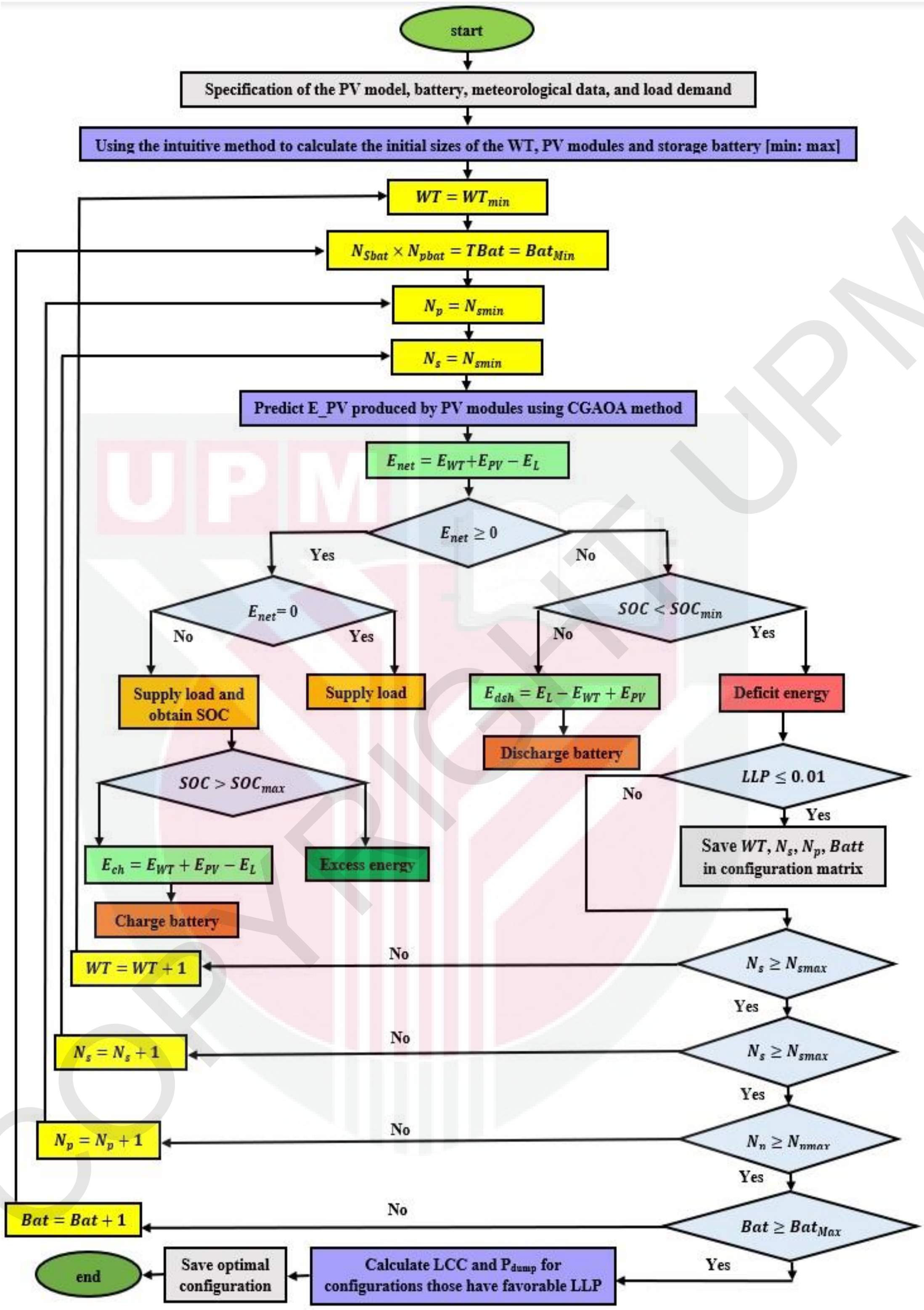

Figure 3.7 : Energy management of the hybrid numerical method for the WT/PV/Battery system

© COPYRIGHT UPM

3.11.3 MOO

In this study, a multi-objective based on non-dominated Pareto Front concept is used to maintain the three objectives required to be optimally minimized. The numerical method can accurately discover all possible solutions in the search space. The number of configurations that resulted by the numerical method is very large which is 315337 configurations. Therefore, it is essential to choose the most optimum configurations by constructing set of optimal PF solutions. This concept is derived from the study of Coello Coello et. al [277]. The implementation steps of the proposed multi-objective optimization method are presented as follow:

- At first, we have divided the huge number of configurations into eight groups and each group has approximately 40000 configurations to be processed by multi-objective optimization method.
- The initialization of population is performed by including resulted groups of the numerical methods with their objectives individually.
- A dominated concept is introduced for the three objective functions: LLP, LCC, and P_{dump}, as given below:

Rule: X_1 (solution 1) is dominated over X_2 (solution 2) if: 1;

$f_i\ (X_1) \leq f_i\ (X_2)$ for the three objectives from 1 to i; 2. $f_i\ (X_1) < f_i\ (X_2)$ for at least one of the three objectives from 1 to i.

- The non-dominated solutions are separated and stored in the archive (repository).
- When the number of solutions in the achieve are exceeded, the most crowded and dominated solutions are removed.

© COPYRIGHT UPM

This process will continue until examined all possible solutions of all eight groups. Then, the eight sets of optimal PF solutions will be obtained to select the most optimum configuration by using MCDM methods.

3.11.4 TOPSIS method

The TOPSIS method is a MCDM method which as firstly developed by Hwang and Yoon and has been successfully applied in tackle various applications [278,279]. The main concept of this method is that the best alternative must have the shortest distance from the positive-ideal solution (v_i^*) simultaneously and the farthest distance from the negative-ideal solutions (v_i^-). Therefore, the positive-ideal solution maximizes the benefit and minimizes the cost criteria, whilst the negative-ideal solution has reverse process. The steps of the TOPSIS method is expressed as follows:

- Normalize the decision matrix $\left(F = [f_{ij}]_{n\times m}\right)$. The normalized decision matrix is defined as $H = [h_{ij}]_{n\times m}$, and the normalized criterion value h_{ij} may be computed as follows:

$$h_{ij} = \frac{f_{ij}}{\sqrt{\sum_{j=1}^{m}(f_{ij})^2}}, \text{ where } i = 1,2,\dots,n; j = 1,2,\dots,m. \tag{3.51}$$

- The weighted matrix (W_i) by BWM method is normalized $V = [V_{ij}]_{n\times m}$ and can be expressed as follows:

$$V_{ij} = W_i h_{ij} \tag{3.52}$$

- The positive-ideal and negative-ideal solutions are then computed by the following equations:

$$A^* = \{v_1^*, \dots, v_n^*\} = \left\{\left(\underset{i}{max} v_{ij} \middle| i \in \Omega_b\right), \left(\underset{i}{min} v_{ij} \middle| i \in \Omega_c\right)\right\}, \tag{3.53}$$

© COPYRIGHT UPM

$$A^- = \{v_1^-, \dots, v_n^-\} = \left\{\left(\underset{i}{min} v_{ij} \middle| i \in \Omega_b\right), \left(\underset{i}{max} v_{ij} \middle| i \in \Omega_c\right)\right\}, \tag{3.54}$$

where $i = 1,2, \dots, n; j = 1,2, \dots, m$.

- Compute the Euclidean distance from the ideal-positive and ideal-negative solutions. The Euclidean distance is determined as follows:

$$\beta_j^* = \sqrt{\sum_{i=1}^{n} \left(v_{ij} - v_i^*\right)^2}, \text{ where } j = 1,2, \dots, m, \tag{3.55}$$

$$\beta_j^- = \sqrt{\sum_{i=1}^{n} \left(v_{ij} - v_i^*\right)^2}, \text{ where } j = 1,2, \dots, m, \tag{3.56}$$

- Closeness to the ideal solution is then computed as follows:

$$\phi_j = \frac{\beta_j^-}{\beta_j^* + \beta_j^-}, \text{ where } j = 1,2, \dots, m, \text{ and } 0 \leq \phi_j \leq 1. \tag{3.57}$$

- Ranking the solutions based on the relative closeness to the ideal solution. The best solution is the one that has large ϕ_j value.

In this step the solution with the largest ϕ_j value is sorted along with their criteria. In this regard, the best solution is the one that has a very short distance from β_j^* and definitely furthest distance from β_j^-. The explanation of the proposed intuitive-numerical-MOO-BWM-TOPSIS-GDM methods are illustrated in Figure 3.8.

© COPYRIGHT UPM

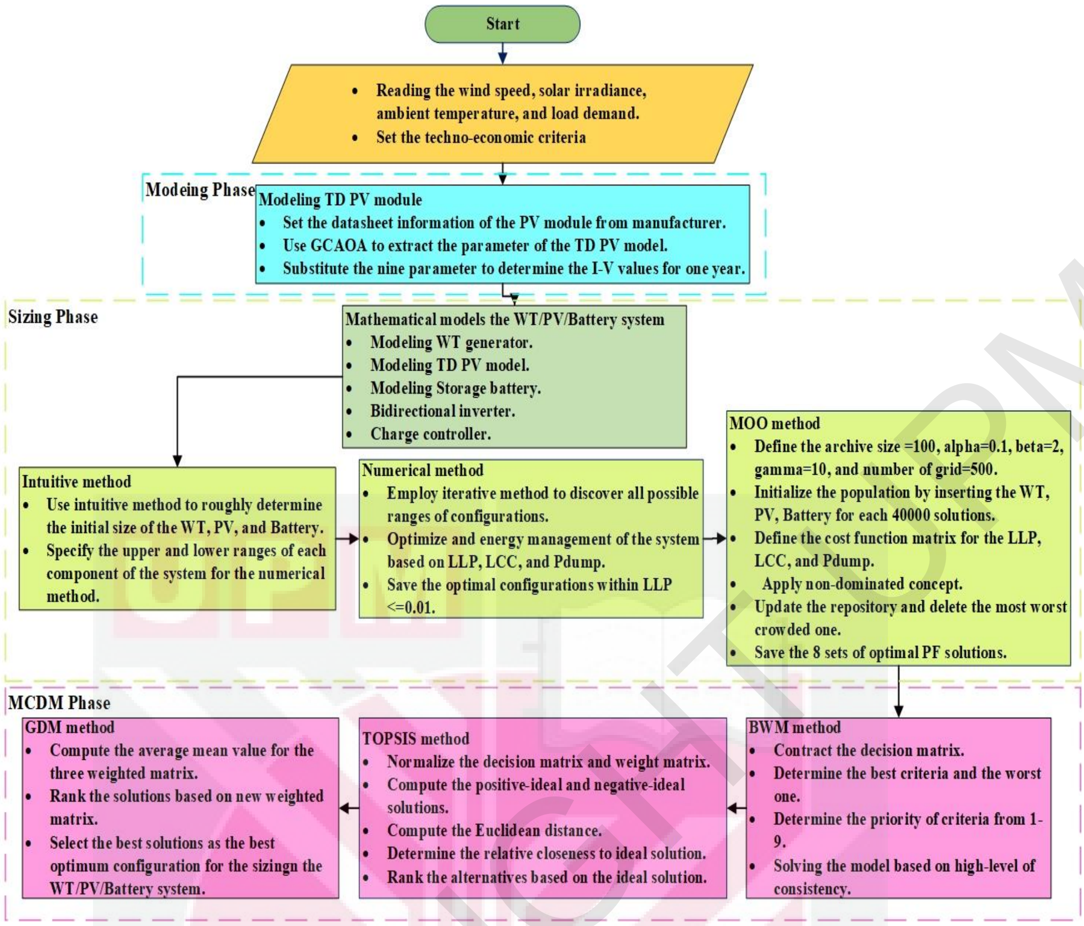

Figure 3.8 : Flowchart of the proposed hybridized numerical model

3.12 Summary

This chapter presents the methodology of extracting the parameter of the TD PV module's model using $\mathrm{RaAOA}_{\mathrm{AdBHHH}}$ method in the first phase, while the second one presents the methodology of sizing hybrid WT/PV/Battery system using improved two-archive-BWM-PROMETHEE II-GDM method, and its validated by intuitive-numerical-MOO-BWM-TOPSIS-GDM method. The proposed $\mathrm{RaAOA}_{\mathrm{AdBHHH}}$ approach developed the (algorithm itself) and design of the objective function. In terms of methodology, the IOBL was maintained to prevent local minima while TL is obtained to improve the local search capability. Secondly, the exploration stage was developed by the use of complement $\overline{D}$ and S operators, along with CMM and LF

© COPYRIGHT UPM

techniques. Besides, the exploitation stage was augmented via the use of $\bar{M}$ and A operators, as well as three unique vectors picked randomly from the population. Finally, winner principle was considered, which is based on two robust mutation procedures, in order to gradually improve the search capability. The $\text{RaAOA}_{\text{AdBHHH}}$ model's objective function was introduced for the first time for resolving the PV model's equation and to efficiently predict the initial roots of the PV models utilizing only first order derivative and half space expectation movements. In second phase, a unique improved bi-archive approach to develop the diversity and convergence independently in order to find four optimum sets of PF solutions. In addition, a new integration based on BWM and PROMETHEE II method along with GDM mechanism are addressed to sort and rank the optimal sets PF solutions with full consistency ratios of the three experts opinions and high degree of stability in ranking configurations. Finally, the proposed two-archive-BWM-PROMETHEE II-GDM method is validated based on by intuitive-numerical-MOO-BWM-TOPSIS-GDM method.

© COPYRIGHT UPM

CHAPTER 4

RESULT AND DISCUSSION

4.1 Introduction

The parameters extraction of the TD PV model based on $RaAOA_{AdBHHH}$ approach and optimal sizing of the WT/PV/Battery system based on improved two-archive algorithm integrated with hybrid MCDM method have been presented in this chapter. In modelling phase, the $RaAOA_{AdBHHH}$ approach is proposed to determine the parameters of the TD PV model via R.T.C France experimental data and validate the findings using a variety of statistical criteria and comparisons to previously approaches in the literature. Moreover, the most desirable configuration of the WT/PV/Battery system has been optimally determined utilizing hybrid improved two-archive algorithm to construct four sets of optimal PF solutions using three conflicting techno-economic criteria. The BWM is obtained to determine the weights value for each objective with full consistency ratios, and then the PROMETHEE-II method is utilized to rank the four sets of optimal PF solutions from best to worst according to the opinions of the experts judgements. Finally, the best design is chosen using GDM with considering all experts' view. The validation of the proposed optimal sizing method is accomplished via intuitive-Numerical-BWM-TOPSIS-GDM method.

4.2 Experimental data description

The parameters extraction of the TD PV models are evaluated and determined using two kinds of the experimental data. The first set is based on seven weather conditions using A Kyocera KC120-1 multi-crystalline (Multi-Si) of 120 Wp PV module [7]. The technical specifications and experimental data points of the proposed PV module at a variety ranges of the environmental conditions are demonstrated in Tables 4.1 and Figure 4.1 [7].

Table 4.1 : Kyocera KC120-1 PV module's technical specifications [7]

Characteristics	Value
Maximum power at STC (P_{mp})	120 Wp
Open-circuit voltage (V_{oc})	16.9 V
Short-circuit current (I_{sc})	7.45 A
MPP's current (I_{mp})	7.1 A
MPP's voltage (V_{mp})	16.9 V
Number of connected cells in series	36
Nominal Operation Cell Temperature (NOCT)	43.6 ℃
Temperature coefficient of I_{sc} (α)	1.325 mA/k
Temperature coefficient of V_{sc} (β)	-77 mV/k

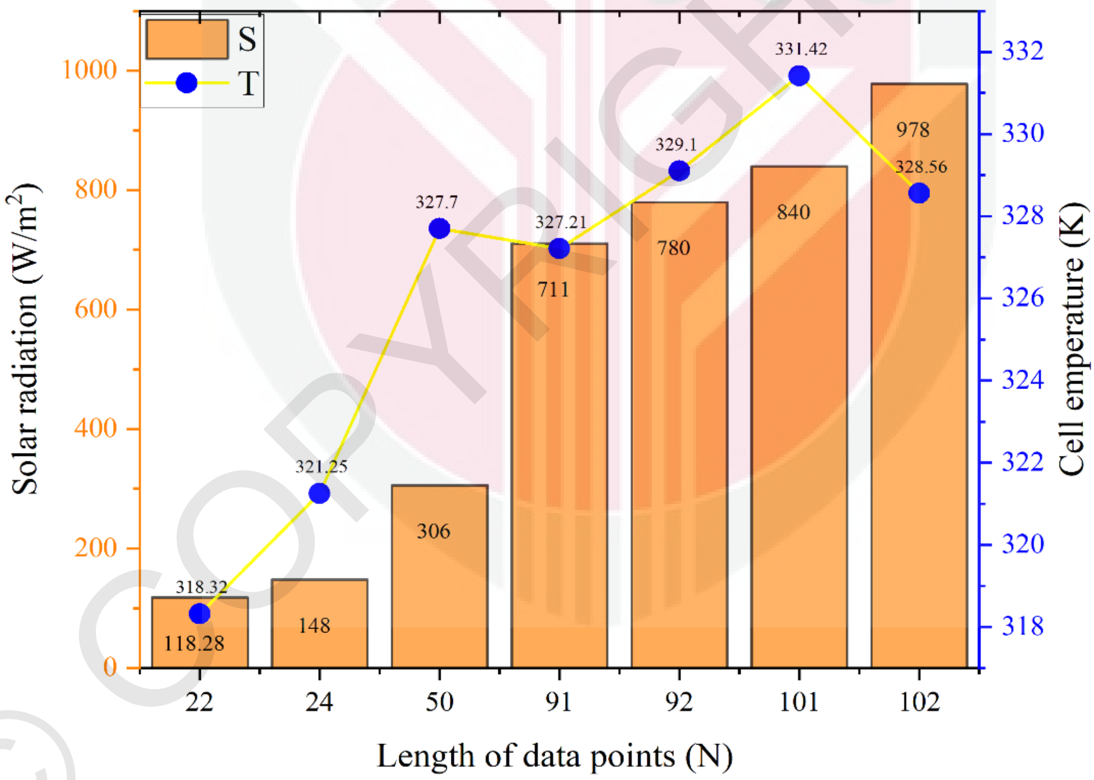

Figure 4.1 : Experimental data under seven climatic conditions [7]

The second experimental data set is from R.T.C France a 57 mm diameter silicon PV cell operating at 1000 W/m^2 solar irradiance and 33℃ ambient temperature [5]. The I-

V and P-V curves of the R.T.C France PV module are shown in Figure 4.2, while the its technical specifications is tabulated in Table 4.2.

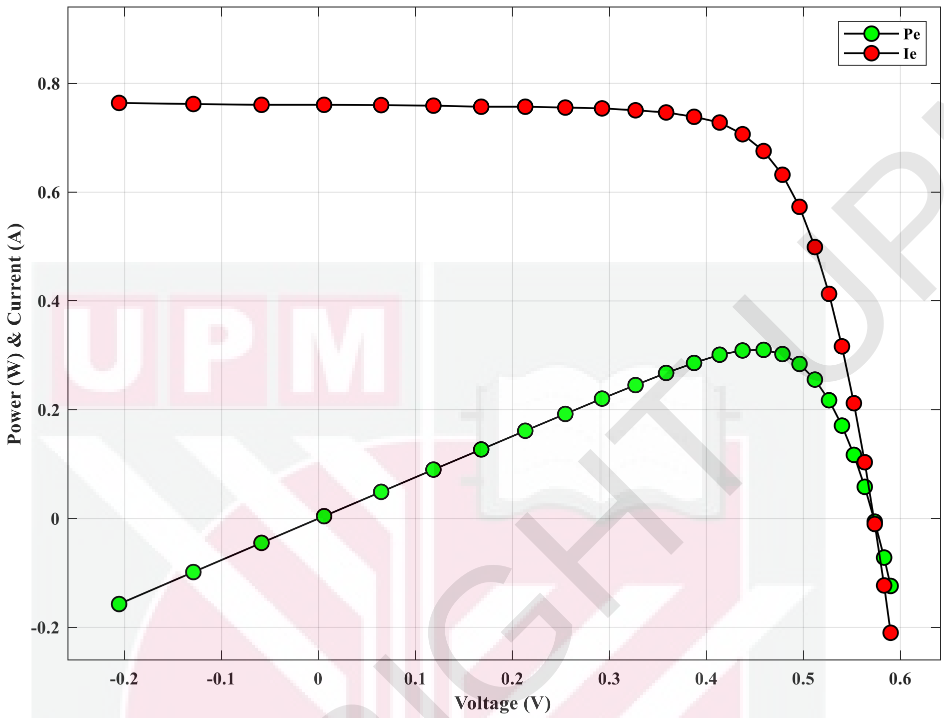

Figure 4.2 : The I-V and P-V data curves of the R.T.C France PV module [5]

Table 4.2 : R.T.C France silicon PV module's technical specifications [5]

Characteristics	Value
Open-circuit voltage (V_{oc})	0.5728 V
Short-circuit current (I_{sc})	0.7603 A
MPP's current (I_{mp})	0.6894 A
MPP's voltage (V_{mp})	0.4507 V
Number of connected cells in series	1

The hourly meteorological data of the sizing of the WT/PV/Battery system considers two case studies: Malaysia and South Africa. Figure 4.3 displays Their hourly wind velocity, solar irradiance, and temperature difference for one year for the Malaysia and South Africa.

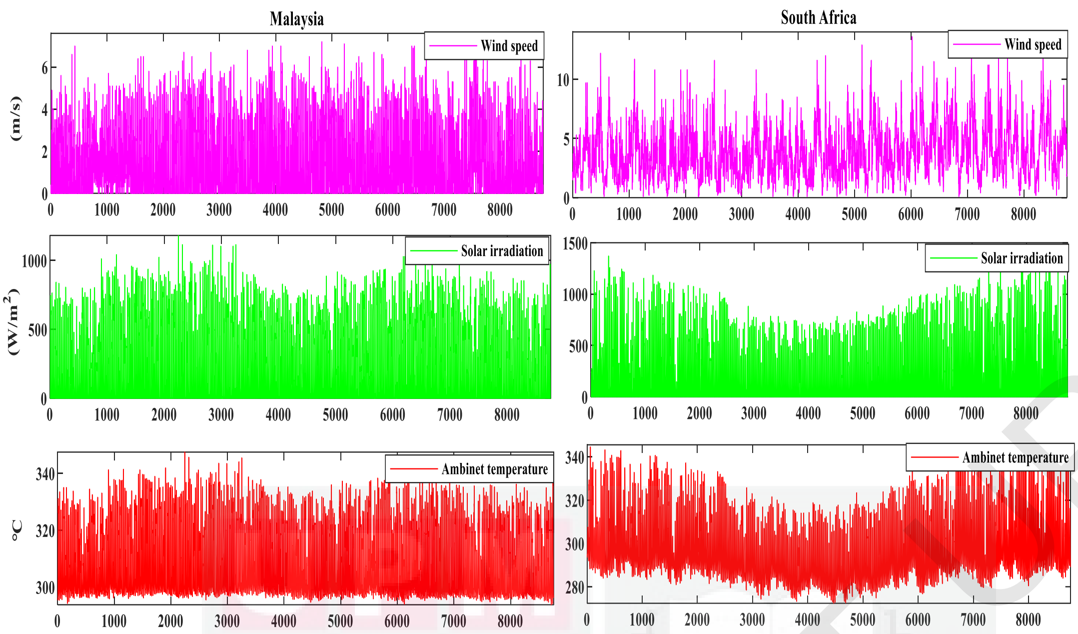

Figure 4.3 : Hourly weather data for the Malaysia and South Africa via a year

4.3 Performance of the Kyocera KC120-1 TD PV module

The proposed RaAOA$_{AdBHHH}$ model is applied to forecast the nine parameters of the TD PV model at various climatic conditions utilizing several criterion analyses. In addition to the experimental data from the Kyocera (KC120-1) PV module, comparisons are made with four distinct objective function design for the RaAOA, which are: RaAOA$_{mBHHH}$, RaAOA$_{BHHH}$, GCAOA$_{INR}$, RaAOA$_{NR}$, and RaAOA$_{LW}$, respectively. Meanwhile, the papers are selected from literature according to their synchronous dealing with the methodology and objective function design. These methods are: AEO$_{NR}$ [125], ELPSO$_{NR}$ [55], ELSHADE$_{INR}$ [6], MPA$_{LW}$ [45,67], MPSO$_{NR}$ [68], MRFO$_{NR}$ [69], ALO$_{LW}$ [62], CHCLPSO$_{NR}$ [63], and DEAM$_{NR}$ [120]. The utilized statistical criteria to experimentally assess the performance of these methods are: RMSE, MBE, d_i, R^2, TS, AE, and CPU-execution time. All environmental settings are assumed to be the same for fair comparison, including the search space of the nine variables [6,67], where the maximum number of iterations

© COPYRIGHT UPM

(M_{iter}) is 500, size of the population is 30 (N), dimension (Dim) of the problem is 9, and each algorithm is executed 30 times for each level of weather conditions (S_{1-7}). The search space of the TD PV model are given in Table 4.3 [67,120,280].

Table 4.3 : The search space ranges for the TD PV model

Parameter	Three PV diode	
	LB	UB
d_1 d_2	1	2
d_3	1	5
I_{Ph}	0.5	8
I_{o1}, I_{o2}	e^{-12}	$1e^{-5}$
R_s	0.1	2
R_p,	10	8000

The estimated nine parameters of the TD PV model at variety of sunshine and ambient temperature conditions utilizing the proposed RaAOA$_{\text{AdBHHH}}$ model and other peers are given in Table 4.4. For the diode ideality factors RaAOA$_{\text{AdBHHH}}$ model, the extracted parameters are within the predefined physical upper and lower boundary ranges. The I_{Ph} is proportionally correlated with the increases of solar irradiance within range of 0.8703-6.4222 A. Keeping in mind that these parameters are determined by pairings of I-V data points and the obtained RaAOA$_{\text{AdBHHH}}$ model. The differences in parameters from one execution to the next are due to natural fluctuations, where the RaAOA always provides the most suitable initial conditions and the AdBHHH explores the feature space of the PV model optimization problem in great depth. The I_{o1-3} are substantial influenced by the ambient temperature and the values of the diode ideality factors. Finally, the R_s and R_p values tend to decrease as the solar irradiance increase, with the exception of the S_2, where their values are somewhat larger than other levels.

© COPYRIGHT UPM

The extracted parameters using NR and LW methods almost exhibit the similar values and level of accuracy, while the parameters values are changed when the objective function method is changed. This variation is belong to the ability of each objective function's method on discovering the search space for providing most accurate initial root solutions for the main equation of the TD PV model. Therefore, both the optimizer and nonlinear PV model equation's method play an important role in increasing the accuracy, stability, and convergence rate to simulate the real behaviour of the PV model and can practically simulate each data point at I-V and P-V data curves. This issue encourages the scholars and researchers to further develop the optimization problem of the PV model in terms of methodology and OFD.

© COPYRIGHT UPM

Table 4.4 : The extracted parameters of the TD PV model utilizing different approaches

Parameter	Method	S_1	S_2	S_3	S_4	S_5	S_6	S_7
	$RaAOA_{AdBHHH}$	**1.3946**	**1.4892**	**1.9565**	**1.7140**	**1.3448**	**1.4923**	**1.4421**
	$RaAOA_{BHHH}$	1.7742	1.2027	1.9226	1.7243	1.28614	1.3087	1.5870
	$GCAOA_{INR}$	1.0000	1.9535	1.0000	1.1759	1.6250	1.4702	1.4989
	$RaAOA_{NR}$	1.0000	1.0000	1.9999	1.9663	1.00002	1.4702	1.4990
	$RaAOA_{LW}$	2.0000	1.9909	1.0000	1.0409	1.55971	1.6051	1.4676
	AEO_{NR}	1.4814	1.7393	1.2794	1.9524	1.3065	1.5193	1.6667
	$ELPSO_{NR}$	1.0000	1.3262	1.4876	1.1783	1.4467	1.9710	1.4258
d_1	$ELSHADE_{INR}$	1.1911	1.4063	1.0000	1.2305	1.5681	1.4713	1.5008
	MPA_{LW}	1.9751	1.3113	1.8659	1.5888	1.8416	1.5819	1.4864
	$MPSO_{NR}$	1.0000	1.8059	1.9497	2.0000	1.6418	1.4015	1.9930
	$MRFO_{NR}$	1.0000	1.3556	1.6783	1.2311	1.2384	1.4479	1.4608
	ALO_{LW}	1.4317	1.3966	1.8058	1.2877	1.9115	1.2242	1.7314
	$CHCLPSO_{NR}$	1.3470	1.6431	1.1488	1.7010	1.2643	1.4897	1.4295
	$DEAM_{NR}$	1.0000	1.6000	1.2765	1.2065	1.2292	1.4813	1.4808
	$RaAOA_{AdBHHH}$	**1.9850**	**1.4807**	**1.3292**	**1.3962**	**1.8831**	**1.3712**	**1.4828**
	$RaAOA_{BHHH}$	1.2956	1.9150	1.4029	1.3849	1.5602	1.9073	1.6345
	$GCAOA_{INR}$	1.0000	1.3741	1.0000	1.4238	1.5555	1.4702	1.4989
	$RaAOA_{NR}$	2.0000	1.9996	1.0000	1.1764	1.590	1.4702	1.4990
	$RaAOA_{LW}$	1.0000	1.0000	2.0000	1.5246	1.00000	1.5245	1.0000
	AEO_{NR}	1.9121	1.4832	1.5169	1.2677	1.3851	1.1118	1.3586
d_2	$ELPSO_{NR}$	2.0000	1.8908	1.8873	1.6052	1.9679	1.3183	1.5076
	$ELSHADE_{INR}$	1.1604	1.0418	1.9861	1.1748	1.6745	1.4662	1.4961
	MPA_{LW}	1.0000	1.5588	1.0615	1.0424	1.2719	1.5878	1.6432
	$MPSO_{NR}$	1.9553	1.0273	2.0000	1.3404	1.9582	1.8856	1.6607
	$MRFO_{NR}$	1.0000	1.7695	1.0238	1.9001	1.8729	1.4551	1.5006
	ALO_{LW}	1.7481	1.9419	1.0948	1.4967	1.3251	1.4523	1.5028
	$CHCLPSO_{NR}$	1.3374	1.3934	1.5941	1.2816	1.6712	1.5078	1.5247
	$DEAM_{NR}$	1.3386	1.2830	1.0000	1.2626	1.7393	1.4480	1.5152

© COPYRIGHT UPM

Table 4.4 : Continued

d_3	$RaAOA_{AdBHHH}$	**3.8558**	**3.4265**	**1.4432**	**4.5799**	**3.5266**	**3.1958**	**4.2823**
	$RaAOA_{BHHH}$	4.3528	4.9367	2.1800	3.6735	1.6727	1.8505	1.4042
	$GCAOA_{INR}$	3.8876	1.0000	4.9869	4.9996	1.0000	1.4701	1.4989
	$RaAOA_{NR}$	4.9925	4.9999	4.9999	4.9990	1.5919	1.4702	1.4990
	$RaAOA_{LW}$	4.9991	4.9906	4.9845	2.2242	4.9600	1.0000	1.0000
	AEO_{NR}	3.9046	1.4451	3.8436	4.1820	2.7305	4.4589	2.8591
	$ELPSO_{NR}$	5.0000	1.9723	1.1733	1.8766	1.1852	1.4895	1.7401
	$ELSHADE_{INR}$	1.0038	3.8006	1.0000	2.0432	1.0162	1.4730	1.5000
	MPA_{LW}	5.0000	4.1940	4.4438	4.4012	1.2334	1.5446	1.6154
	$MPSO_{NR}$	1.0000	1.0026	1.0000	5.0000	1.0000	1.4314	1.3830
	$MRFO_{NR}$	4.4739	3.4585	4.3919	5.0000	1.9431	1.4710	1.5588
	ALO_{LW}	4.4292	2.3308	2.1603	2.4057	3.8910	2.8442	1.6931
	$CHCLPSO_{NR}$	1.9909	1.6556	1.6603	1.6556	1.5509	1.4214	1.5251
	$DEAM_{NR}$	4.3885	3.9779	2.1735	3.0259	2.0768	1.4853	1.5039
I_{Ph}	$RaAOA_{AdBHHH}$	**0.8703**	**0.9177**	**1.9282**	**4.3806**	**4.9005**	**5.6612**	**6.4222**
	$RaAOA_{BHHH}$	0.8466	0.9250	1.9851	4.3751	4.9609	5.4381	4.6206
	$GCAOA_{INR}$	0.8406	1.0560	1.9714	4.4472	5.1602	5.5268	6.4461
	$RaAOA_{NR}$	0.8402	1.0557	1.9713	4.4472	5.1615	5.5278	6.4480
	$RaAOA_{LW}$	0.8402	1.0557	1.9713	4.4646	5.1842	5.5447	6.4373
	AEO_{NR}	0.6046	1.0760	2.1704	4.0972	5.2606	5.1130	6.6604
	$ELPSO_{NR}$	0.8348	0.9713	1.9461	4.4098	5.1639	5.5504	6.4216
	$ELSHADE_{INR}$	0.8461	1.0035	1.9714	4.4471	5.1639	5.5252	6.4459
	MPA_{LW}	0.8402	0.9735	1.9609	4.4442	5.1719	5.5220	6.4817
	$MPSO_{NR}$	0.8402	0.9675	1.9580	4.3918	5.2399	5.3335	6.4831
	$MRFO_{NR}$	0.8402	0.9426	1.9637	4.4369	5.1601	5.5267	6.4256
	ALO_{LW}	0.8639	0.9140	1.9294	4.3918	5.1474	5.5380	6.2238
	$CHCLPSO_{NR}$	0.8516	0.9298	1.9514	4.4194	5.1514	5.5284	6.4476

Table 4.4 : Continued

	$DEAM_{NR}$	0.8402	0.9656	1.9692	4.4415	5.1581	5.5274	6.4470
I_{o1}	$RaAOA_{AdBHHH}$	**2.79E-06**	**7.83E-06**	**3.15E-07**	**3.56E-06**	**6.30E-06**	**5.73E-06**	**9.98E-06**
	$RaAOA_{BHHH}$	8.82E-06	5.13E-07	1.70E-06	4.48E-06	3.55E-06	4.26E-06	3.10E-06
	$GCAOA_{INR}$	1.97E-08	1.00E-12	6.16E-08	6.76E-07	1.00E-05	1.00E-05	1.00E-05
	$RaAOA_{NR}$	1.95E-08	2.96E-08	1.00E-12	1.00E-12	4.22E-08	1.00E-05	1.00E-05
	$RaAOA_{LW}$	1.00E-12	1.00E-12	6.15E-08	6.33E-08	9.62E-06	1.00E-05	1.00E-05
	AEO_{NR}	3.64E-06	9.31E-06	2.91E-06	4.88E-06	4.91E-06	1.45E-07	8.83E-06
	$ELPSO_{NR}$	1.94E-08	2.01E-06	1.33E-06	6.16E-07	3.30E-06	1.00E-05	1.00E-05
	$ELSHADE_{INR}$	1.61E-07	1.39E-06	1.00E-12	4.08E-08	9.97E-06	1.00E-05	1.00E-05
	MPA_{LW}	2.41E-11	1.85E-06	1.65E-07	2.85E-06	2.31E-06	9.70E-06	9.77E-06
	$MPSO_{NR}$	1.07E-09	9.69E-06	1.00E-05	7.25E-06	8.65E-06	1.00E-05	9.53E-06
	$MRFO_{NR}$	1.95E-08	2.55E-06	5.74E-06	1.38E-06	2.08E-06	7.61E-06	1.00E-05
	ALO_{LW}	2.50E-06	4.26E-06	3.73E-06	3.38E-07	2.47E-06	5.67E-07	9.84E-06
	$CHCLPSO_{NR}$	1.01E-06	3.66E-06	5.57E-07	4.20E-06	2.56E-06	9.96E-06	7.62E-06
	$DEAM_{NR}$	1.95E-08	1.35E-07	1.23E-07	9.67E-07	1.79E-06	1.00E-05	1.00E-05
I_{o2}	$RaAOA_{AdBHHH}$	**2.45E-08**	**1.29E-06**	**1.74E-06**	**8.01E-06**	**8.62E-06**	**1.00E-05**	**9.84E-06**
	$RaAOA_{BHHH}$	8.82E-07	3.32E-06	8.84E-06	7.36E-06	1.19E-06	2.40E-06	9.39E-06
	$GCAOA_{INR}$	2.31E-11	1.00E-12	1.00E-12	1.00E-12	9.95E-06	1.00E-05	1.00E-05
	$RaAOA_{NR}$	1.00E-12	1.00E-12	6.15E-08	6.80E-07	1.00E-05	1.00E-05	1.00E-05
	$RaAOA_{LW}$	1.95E-08	2.96E-08	1.00E-12	3.85E-07	8.59E-09	1.00E-05	1.24E-09
	AEO_{NR}	3.50E-07	3.22E-06	6.46E-06	2.21E-06	5.55E-07	5.66E-07	5.60E-06
	$ELPSO_{NR}$	1.00E-12	6.52E-06	-2.55E-06	4.21E-06	1.37E-06	5.12E-06	1.00E-05
	$ELSHADE_{INR}$	7.97E-08	4.19E-08	2.97E-11	6.46E-07	1.00E-05	1.00E-05	1.00E-05
	MPA_{LW}	1.95E-08	1.00E-12	1.68E-07	1.20E-08	9.10E-11	9.69E-06	8.00E-06
	$MPSO_{NR}$	1.00E-12	5.29E-09	1.00E-05	4.68E-06	9.09E-07	5.96E-08	9.75E-06
	$MRFO_{NR}$	1.00E-12	6.94E-06	8.55E-08	3.13E-07	8.51E-06	9.54E-06	1.00E-05
	ALO_{LW}	3.88E-06	4.20E-07	2.40E-07	1.77E-06	5.51E-06	6.79E-06	8.95E-06
	$CHCLPSO_{NR}$	7.77E-07	3.28E-06	1.07E-06	2.27E-06	1.71E-06	9.86E-06	9.99E-06

Table 4.4 : Continued

	$DEAM_{NR}$	1.45E-12	1.38E-06	5.88E-08	9.07E-08	9.19E-06	9.98E-06	1.00E-05
I_{o3}	$RaAOA_{AdBHHH}$	**2.57E-06**	**6.87E-06**	**8.94E-06**	**3.87E-06**	**7.66E-06**	**2.15E-06**	**1.05E-06**
	$RaAOA_{BHHH}$	4.75E-07	1.95E+06	4.16E-06	4.53E-06	3.44E-06	4.11E-06	9.98E-06
	$GCAOA_{INR}$	1.00E-12	2.96E-08	1.00E-12	1.02E-12	4.16E-08	1.00E-05	1.00E-05
	$RaAOA_{NR}$	1.00E-12	1.48E-12	1.00E-12	1.00E-12	1.00E-05	1.00E-05	1.00E-05
	$RaAOA_{LW}$	1.00E-12	1.01E-12	1.00E-12	3.67E-09	3.81E-10	3.24E-09	1.24E-09
	AEO_{NR}	6.97E-06	4.16E-06	2.98E-06	5.52E-06	9.85E-07	2.51E-06	5.18E-07
	$ELPSO_{NR}$	1.00E-12	1.00E-12	7.62E-07	1.00E-05	9.02E-07	1.00E-05	1.00E-05
	$ELSHADE_{INR}$	3.88E-09	9.91E-06	6.16E-08	2.60E-12	6.03E-08	1.00E-05	1.00E-05
	MPA_{LW}	4.11E-06	9.96E-06	9.31E-06	6.39E-06	1.94E-06	1.00E-05	5.21E-06
	$MPSO_{NR}$	1.84E-08	2.45E-08	5.85E-08	2.39E-06	5.95E-08	8.90E-06	9.70E-06
	$MRFO_{NR}$	1.00E-12	5.31E-06	1.00E-12	1.00E-05	2.86E-06	1.00E-05	9.86E-06
	ALO_{LW}	2.72E-06	4.13E-08	2.80E-06	1.98E-06	1.54E-06	6.62E-06	9.63E-06
	$CHCLPSO_{NR}$	3.31E-06	1.49E-07	1.18E-07	6.67E-07	1.00E-05	8.04E-09	2.79E-09
	$DEAM_{NR}$	1.37E-09	7.83E-07	4.08E-08	1.20E-06	7.52E-06	1.00E-05	9.99E-06
	$RaAOA_{AdBHHH}$	**0.8858**	**0.2721**	**0.3732**	**0.4783**	**0.3133**	**0.1329**	**0.2617**
	$RaAOA_{BHHH}$	0.7106	1.0772	0.6040	0.4627	0.3225	0.4435	0.2393
	$GCAOA_{INR}$	1.9091	0.6910	0.7763	0.5642	0.3122	0.1525	0.1568
	$RaAOA_{NR}$	1.9327	0.6927	0.7778	0.5638	0.3146	0.1520	0.1557
	$RaAOA_{LW}$	1.9324	0.6927	0.7778	0.7008	0.5790	0.4708	0.4271
	AEO_NR	0.8456	1.0260	0.5875	0.4145	0.3945	0.2353	0.5052
R_s	$ELPSO_{NR}$	2.0000	0.2131	0.6700	0.5478	0.2951	0.1783	0.1639
	$ELSHADE_{INR}$	1.6970	0.5289	0.7763	0.5640	0.3170	0.1525	0.1569
	MPA_{LW}	1.9328	0.3157	0.7430	1.0100	0.3009	0.3796	0.3252
	$MPSO_{NR}$	1.9330	0.6771	0.7659	0.5184	0.3046	0.1763	0.1664
	$MRFO_{NR}$	1.9324	0.2374	0.7464	0.5450	0.2876	0.1497	0.1724
	ALO_{LW}	1.8680	0.3216	0.8169	0.9940	0.2730	0.3944	0.4065
	$CHCLPSO_{NR}$	1.4059	0.1864	0.6731	0.5171	0.2759	0.1561	0.1603

Table 4.4 : Continued

	$DEAM_{NR}$	1.9324	0.3562	0.7712	0.5524	0.2868	0.1525	0.1561
R_p	$RaAOA_{AdBHHH}$	**322.53**	**4609.05**	**2976.61**	**3706.70**	**2258.71**	**22.95**	**71.16**
	$RaAOA_{BHHH}$	2056.14	7388.86	3382.26	7336.38	357.42	2296.22	65.52
	$GCAOA_{INR}$	1034.72	67.60	141.51	102.44	41.50	43.11	35.55
	$RaAOA_{NR}$	1117.57	67.73	141.91	102.32	41.21	42.77	35.07
	$RaAOA_{LW}$	1115.59	67.73	141.92	83.79	44.75	52.93	53.09
	AEO_{NR}	3652.69	2548.11	911.00	5034.11	7189.20	2714.65	4789.23
	$ELPSO_{NR}$	8000.00	151.46	518.81	216.50	38.77	36.55	36.36
	$ELSHADE_{INR}$	7766.18	103.16	141.53	102.67	40.25	43.33	35.59
	MPA_{LW}	1134.36	149.63	193.99	144.57	37.67	56.43	37.14
	$MPSO_{NR}$	1125.30	151.03	225.68	3497.55	25.02	118.70	31.12
	$MRFO_{NR}$	1116.16	284.82	210.52	133.06	39.91	40.75	41.67
	ALO_{LW}	7160.18	1176.46	2048.51	5473.90	44.35	42.45	1669.66
	$CHCLPSO_{NR}$	7793.37	431.19	370.21	241.98	42.59	42.80	34.51
	$DEAM_{NR}$	1117.07	161.29	150.73	116.85	40.77	42.81	35.15

Several statistical metrics, including RMSE, MBE, R^2, d_i, TS, and CPU, are obtained to verify and assess the models' correctness, stability, and reliability, as presented in Table 4.5. The proposed $\mathrm{RaAOA_{AdBHHH}}$ model states zeros values for RMSE, MBE, d_i, TS, and one for the R^2. This experimental findings confirms that the proposed $\mathrm{RaAOA_{AdBHHH}}$ model dominates other contemporaries in every quantifiable criterion assessments except for the CPU-execution time, where it is 10 times slower than the faster one which is $\mathrm{ELSHADE_{INR}}$. This is due to the proficient linear reduction strategy obtained by the $\mathrm{ELSHADE_{INR}}$. However, the commotional of the $\mathrm{RaAOA_{AdBHHH}}$ model is still acceptable, with an average time value of 88.60 s. Furthermore, in such optimization problems applicable to real-world PV applications, the accuracy, stability, and reliability are more important than computing speed. Hence, this problem is considered as off-line measurements, while the online measurements take very prolong time and are highly costly.

The $\mathrm{RaAOA_{BHHH}}$ is ranked second, followed by $\mathrm{GCAOA_{INR}}$, and $\mathrm{ELSHADE_{INR}}$, with average RMSE values of zero, 0.0056, 0.0057, respectively. The $\mathrm{RaAOA_{AdBHHH}}$ has a higher level of accuracy compared with other models. This is due to the employing an efficient nonlinear damping control parameter of LM method. In addition, this variation is belong to the ability of each objective function's method on discovering the search space for providing most accurate initial root solutions for the main equation of the TD PV model. This confirms the effectiveness and superiority, and well-employing methodology and objective function design to solve the TD PV model optimization problem. This, however, illustrates the powerful, economical, and successful employed exploration and exploitation strategies, which can deliver improved precision and a guaranteed convergence rate. The $\mathrm{RaAOA_{LW}}$ came in sixth rank, followed by MPA_{LW}, $RaAOA_{NR}$, $DEAM_{NR}$, $MRFO_{NR}$, $CHCLPSO_{NR}$, $ELPSO_{NR}$, ALO_{LW}, and $MPSO_{NR}$, with average RMSE values of 0.0563, 0.0579, 0.0584, 0.0586, 0.0589, 0.0593, 0.0594, 0.0610, 0.0623, respectively. Previous results demonstrate that the conventional LW has superior prediction initial root solutions than the basic NR method, as observed between the $GCAOA_{LW}$ and $GCAOA_{NR}$ models. Despite using NR as OFD, the AEO_{NR} is ranked as poorest method owning to the inadequate methodology, as given in Table 4.5. Similar analysis and ranking can be observed for MBE, d_i, TS, and R^2 statistical criteria, with the exception of the CPU execution time, which is strongly reliant on the intricacy of the methodology and resulting OFD.

© COPYRIGHT UPM

Table 4.5 : Statistical criteria of different algorithms for the TD PV model

Parameter	Method	S_1	S_2	S_3	S_4	S_5	S_6	S_7	Average
RMSE	$RaAOA_{AdBHHH}$	**0.0000**	**0.0000**	**0.0000**	**0.0000**	**0.0000**	**0.0000**	**0.0000**	**0.0000**
	$RaAOA_{BHHH}$	0.0000	0.0000	0.0000	0.0000	0.0000	0.0000	0.0000	0.0000
	$GCAOA_{INR}$	0.0033	0.0012	0.0024	0.0027	0.0087	0.0096	0.0116	0.0056
	$RaAOA_{NR}$	0.0329	0.0123	0.0252	0.0280	0.0903	0.0997	0.1201	0.0584
	$RaAOA_{LW}$	0.0329	0.0123	0.0252	0.0277	0.0903	0.0979	0.1079	0.0563
	AEO_{NR}	0.1219	0.0669	0.1337	0.1087	0.2031	0.2149	0.3507	0.1714
	$ELPSO_{NR}$	0.0330	0.0133	0.0271	0.0286	0.0907	0.1017	0.1215	0.0594
	$ELSHADE_{INR}$	0.0033	0.0012	0.0024	0.0027	0.0087	0.0096	0.0116	0.0057
	MPA_{LW}	0.0329	0.0130	0.0258	0.0281	0.0908	0.0983	0.1161	0.0579
	$MPSO_{NR}$	0.0329	0.0128	0.0257	0.0297	0.0996	0.1095	0.1255	0.0623
	$MRFO_{NR}$	0.0329	0.0132	0.0259	0.0282	0.0907	0.1003	0.1214	0.0589
	ALO_{LW}	0.0354	0.0135	0.0277	0.0298	0.0910	0.1030	0.1264	0.0610
	$CHCLPSO_{NR}$	0.0342	0.0133	0.0268	0.0289	0.0908	0.1000	0.1209	0.0593
	$DEAM_{NR}$	0.0329	0.0129	0.0253	0.0281	0.0907	0.0998	0.1202	0.0586
MBE	$RaAOA_{AdBHHH}$	**0.0000**	**0.0000**	**0.0000**	**0.0000**	**0.0000**	**0.0000**	**0.0000**	**0.0000**
	$RaAOA_{BHHH}$	**0.0000**	**0.0000**	**0.0000**	**0.0000**	**0.0000**	**0.0000**	**0.0000**	**0.0000**
	$GCAOA_{INR}$	1.08E-05	1.45E-06	5.90E-06	7.44E-06	7.54E-05	9.24E-05	1.35E-04	4.68E-05
	$RaAOA_{NR}$	1.08E-03	1.51E-04	6.38E-04	7.84E-04	8.17E-03	9.96E-03	9.96E-03	1.44E-02
	$RaAOA_{LW}$	1.08E-03	1.51E-04	6.38E-04	7.71E-04	8.15E-03	9.60E-03	1.17E-02	4.58E-03
	AEO_{NR}	1.49E-02	4.47E-03	1.79E-02	1.18E-02	4.12E-02	4.62E-02	1.23E-01	3.71E-02
	$ELPSO_{NR}$	1.09E-03	1.76E-04	7.32E-04	8.16E-04	8.22E-03	1.03E-02	1.48E-02	5.16E-03
	$ELSHADE_{INR}$	1.11E-05	1.51E-06	5.90E-06	7.44E-06	7.54E-05	9.24E-05	1.35E-04	4.69E-05
	MPA_{LW}	1.08E-03	1.69E-04	6.64E-04	7.91E-04	8.25E-03	9.66E-03	1.35E-02	4.87E-03
	$MPSO_{NR}$	1.08E-03	1.65E-04	6.60E-04	8.85E-04	9.92E-03	1.20E-02	1.58E-02	5.78E-03
	$MRFO_{NR}$	1.08E-03	1.74E-04	6.70E-04	7.93E-04	8.23E-03	1.01E-02	1.47E-02	5.11E-03
	ALO_{LW}	1.25E-03	1.82E-04	7.68E-04	8.88E-04	8.28E-03	1.06E-02	1.60E-02	5.42E-03
	$CHCLPSO_{NR}$	1.17E-03	1.77E-04	7.20E-04	8.34E-04	8.24E-03	9.99E-03	1.46E-02	5.11E-03
	$DEAM_{NR}$	1.08E-03	1.67E-04	6.42E-04	7.87E-04	8.22E-03	9.97E-03	1.44E-02	5.05E-03
R^2	$RaAOA_{AdBHHH}$	**1.0000**	**1.0000**	**1.0000**	**1.0000**	**1.0000**	**1.0000**	**1.0000**	**1.0000**
	$RaAOA_{BHHH}$	**1.0000**	**1.0000**	**1.0000**	**1.0000**	**1.0000**	**1.0000**	**1.0000**	**1.0000**

Table 4.5 : Continued

	$GCAOA_{INR}$	0.9998	1.0000	1.0000	1.0000	1.0000	1.0000	0.9999	0.9999
	$RaAOA_{NR}$	0.9835	0.9980	0.9981	0.9993	0.9949	0.9946	0.9938	0.9946
	$RaAOA_{LW}$	0.9835	0.9980	0.9981	0.9993	0.9949	0.9948	0.9950	0.9948
	AEO_{NR}	0.7751	0.9420	0.9477	0.9903	0.9746	0.9752	0.9473	0.9360
	$ELPSO_{NR}$	0.9835	0.9977	0.9979	0.9993	0.9949	0.9944	0.9937	0.9945
	$ELSHADE_{INR}$	0.9998	1.0000	1.0000	1.0000	1.0000	1.0000	0.9999	0.9999
	MPA_{LW}	0.9836	0.9978	0.9981	0.9994	0.9949	0.9948	0.9942	0.9947
	$MPSO_{NR}$	0.9836	0.9979	0.9981	0.9993	0.9939	0.9936	0.9933	0.9942
	$MRFO_{NR}$	0.9836	0.9977	0.9980	0.9994	0.9949	0.9946	0.9937	0.9946
	ALO_{LW}	0.9810	0.9976	0.9978	0.9993	0.9949	0.9943	0.9932	0.9940
	$CHCLPSO_{NR}$	0.9823	0.9977	0.9979	0.9993	0.9949	0.9946	0.9937	0.9944
	$DEAM_{NR}$	0.9836	0.9978	0.9981	0.9994	0.9949	0.9946	0.9938	0.9946
d_i	$RaAOA_{AdBHHH}$	**0.0000**	**0.0000**	**0.0000**	**0.0000**	**0.0000**	**0.0000**	**0.0000**	**0.0000**
	$RaAOA_{BHHH}$	0.0000	0.0000	0.0000	0.0000	0.0000	0.0000	0.0000	0.0000
	$GCAOA_{INR}$	-0.0024	-0.0044	-0.0032	-0.0029	0.0030	0.0040	0.0059	0.0000
	$RaAOA_{NR}$	-0.0254	-0.0460	-0.0331	-0.0303	0.0319	0.0413	0.0617	0.0018
	$RaAOA_{LW}$	-0.0234	-0.0440	-0.0311	-0.0285	0.0339	0.0416	0.0516	0.0016
	AEO_{NR}	-0.0495	-0.1045	-0.0377	-0.0627	0.0316	0.0435	0.1793	0.0090
	$ELPSO_{NR}$	-0.0264	-0.0461	-0.0323	-0.0308	0.0313	0.0423	0.0621	0.0019
	$ELSHADE_{INR}$	-0.0023	-0.0044	-0.0032	-0.0029	0.0030	0.0040	0.0059	0.0000
	MPA_{LW}	-0.0249	-0.0449	-0.0321	-0.0297	0.0330	0.0404	0.0582	0.0018
	$MPSO_{NR}$	-0.0293	-0.0494	-0.0366	-0.0325	0.0373	0.0473	0.0633	0.0022
	$MRFO_{NR}$	-0.0260	-0.0457	-0.0331	-0.0308	0.0318	0.0413	0.0625	0.0019
	ALO_{LW}	-0.0256	-0.0475	-0.0333	-0.0312	0.0300	0.0420	0.0654	0.0020
	$CHCLPSO_{NR}$	-0.0251	-0.0459	-0.0324	-0.0304	0.0315	0.0407	0.0616	0.0019
	$DEAM_{NR}$	-0.0256	-0.0456	-0.0332	-0.0305	0.0321	0.0413	0.0616	0.0019
TS	$RaAOA_{AdBHHH}$	**0.0000**	**0.0000**	**0.0000**	**0.0000**	**0.0000**	**0.0000**	**0.0000**	**0.0000**
	$RaAOA_{BHHH}$	**0.0000**	**0.0000**	**0.0000**	**0.0000**	**0.0000**	**0.0000**	**0.0000**	**0.0000**
	$GCAOA_{INR}$	0.0151	0.0058	0.0170	0.0259	0.0835	0.0971	0.1179	0.0518

© COPYRIGHT UPM

Table 4.5 : Continued

	$RaAOA_{NR}$	0.1560	0.0597	0.1813	0.2733	0.9477	1.1085	1.3722	0.5855
	$RaAOA_{LW}$	0.1560	0.0597	0.1813	0.2709	0.9468	1.0862	1.2163	0.5596
	AEO_{NR}	0.6360	0.3438	1.0806	1.1573	2.4306	2.7380	5.4292	1.9736
	$ELPSO_{NR}$	0.1564	0.0645	0.1943	0.2800	0.9520	1.1142	1.4023	0.5948
	$ELSHADE_{INR}$	0.0153	0.0059	0.0170	0.0259	0.0836	0.0971	0.1179	0.0518
	MPA_{LW}	0.1561	0.0631	0.1852	0.2745	0.9530	1.0901	1.3199	0.5774
	$MPSO_{NR}$	0.1561	0.0624	0.1845	0.2908	1.0551	1.2300	1.4426	0.6316
	$MRFO_{NR}$	0.1561	0.0642	0.1860	0.2750	0.9515	1.1142	1.3887	0.5908
	ALO_{LW}	0.1682	0.0656	0.1995	0.2914	0.9549	1.1485	1.4542	0.6118
	$CHCLPSO_{NR}$	0.1622	0.0647	0.1930	0.2821	0.9527	1.1107	1.3821	0.5925
	$DEAM_{NR}$	0.1561	0.0629	0.1820	0.2738	0.9514	1.1090	1.3728	0.5869
CPU	$RaAOA_{AdBHHH}$	83.78	85.31	83.92	92.98	90.95	91.55	91.70	88.60
	$RaAOA_{BHHH}$	86.19	81.45	90.28	98.61	98.73	98.92	96.22	92.92
	$GCAOA_{INR}$	19.00	18.53	19.92	22.97	22.09	22.58	22.80	21.13
	$RaAOA_{NR}$	52.86	41.52	44.03	60.14	50.05	49.77	50.06	49.77
	$RaAOA_{LW}$	2118.33	2807.19	4617.63	6822.16	10264.81	13126.05	15216.83	7853.28
	AEO_{NR}	19.64	17.52	18.45	20.98	19.47	19.59	20.06	19.39
	$ELPSO_{NR}$	12.78	13.53	14.67	14.23	14.75	22.16	14.25	15.20
	$ELSHADE_{INR}$	**8.56**	**8.59**	**8.55**	**9.16**	**8.89**	**8.88**	**9.36**	**8.85**
	MPA_{LW}	250.48	1352.31	2846.45	5631.59	11101.31	1261.05	849.52	3327.53
	$MPSO_{NR}$	10.92	12.56	12.09	11.58	11.14	11.39	13.83	11.93
	$MRFO_{NR}$	18.14	19.31	17.92	19.42	19.86	23.05	19.44	19.59
	ALO_{LW}	1827.64	553.27	1383.69	1882.30	5615.73	345.59	3644.34	2178.94
	$CHCLPSO_{NR}$	15.53	11.80	12.84	13.42	12.67	11.89	11.88	12.86
	$DEAM_{NR}$	11.19	11.41	11.20	13.08	13.66	12.30	12.22	12.15

The best optimizer model is chosen to simulate the I-V and P-V data curves, where the planned and experimental data points completely overlap, as illustrated in Figure 4.4. The proposed $RaAOA_{AdBHHH}$ model has an exceptionally high degree of correctness to predict all the experimental current even at sharp and zigzag edges. This is a result of the effective hybridization of the RaAOA algorithm (itself) and the mechanism of the BHHH algorithm in estimating the initial roots solutions of the TD PV model. This optimization problem is not a simple process, therefore using solely numerical, analytical, or stochastic methods without addressing the nonlinearity and multidimensionality of the PV model's equation might result in extremely low accuracy. Keeping in mind that the complexity of predicting the parameters of the TD PV model is notably increased when the number of the parameters are large and the I-V and P-V experimental data points curves are not straightforward and include various stochastic distributions, as seen in zoomed-figures of Figure 4.4.

© COPYRIGHT UPM

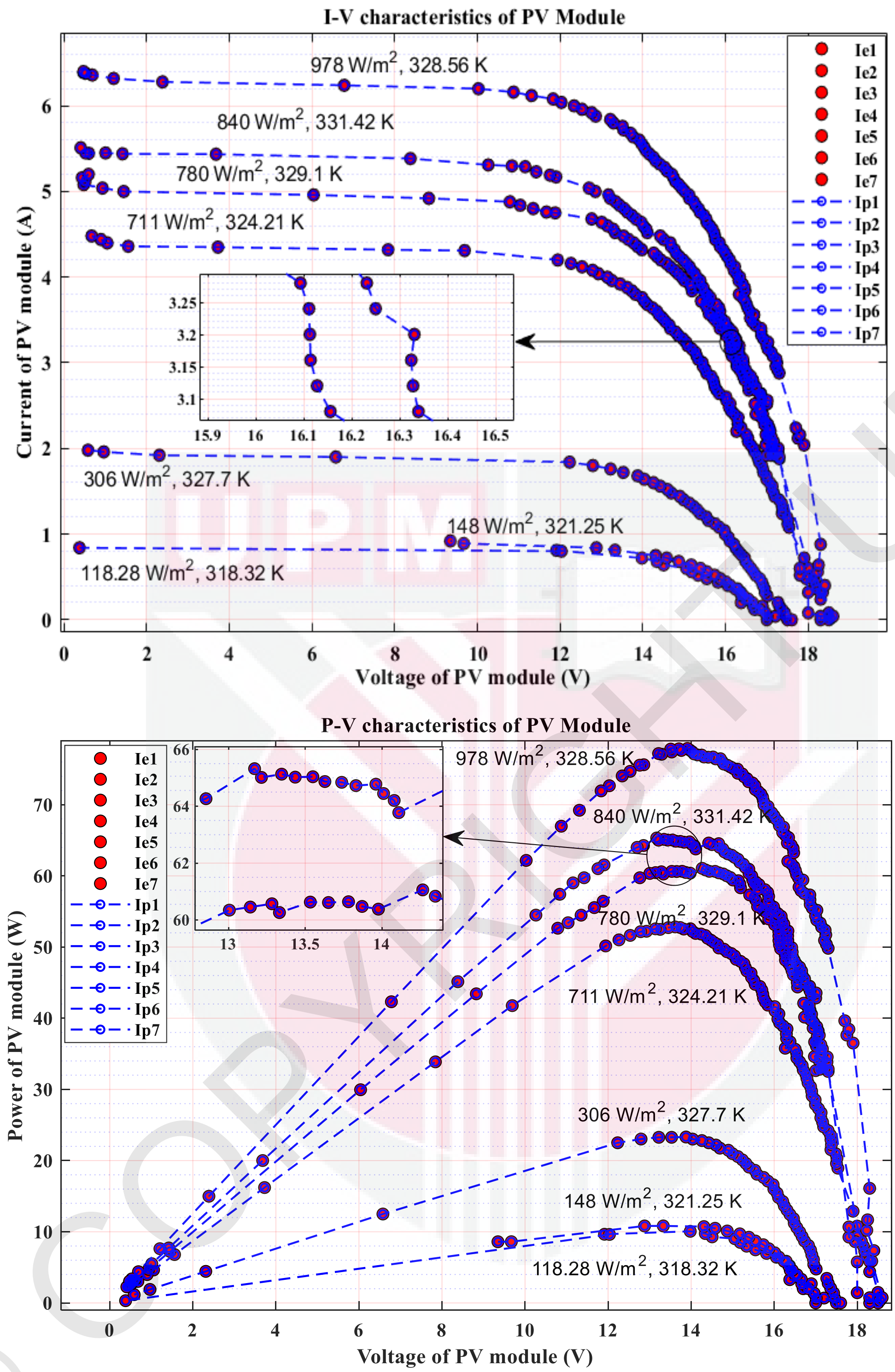

Figure 4.4 : The experimental and proposed I-V and P-V data curves for the TD PV model under various environmental circumstances

The average AE values of the proposed $RaAOA_{AdBHHH}$ and other models under seven environmental conditions is given by Table 4.6. There is no doubt that the proposed $RaAOA_{AdBHHH}$ offers an efficient methodology and a distinctive OFD, as confirmed by promising results. $RaAOA_{BHHH}$ has the second lowest average AE value according to the developed objective function values, followed by $GCAOA_{INR}$, $ELSHADE_{INR}$, $RaAOA_{LW}$, MPA_{LW}, $RaAOA_{NR}$, $DEAM_{NR}$, $CHCLPSO_{NR}$, $MRFO_{NR}$, $ELPSO_{NR}$, ALO_{LW}, and $MPSO_{NR}$. Their average AE values are as follows: 0.0039, 0.0075, 0.0382, 0.0410, 0.0412, 0.0413, 0.0420, 0.0422, 0.0423, 0.0434, and 0.0465, respectively. AEO_{NR} once again has worst average AE, with a value of 0.1452. This is owing to the poor performance of the utilized methodology of the AEO model. Form these findings, it can be analyzed that the damping control parameter of the LM plays a crucial rule in simulating the nonlinearity behavior of the TD PV model's equation by reducing the oscillations and noise effects to trivial errors values.

© COPYRIGHT UPM

Table 4.6 : Average AE values of the proposed $RaAOA_{AdBHHH}$ model and other models

Method	S_1	S_2	S_3	S_4	S_5	S_6	S_7	Average
$RaAOA_{AdBHHH}$	**0.000000**	**0.000000**	**0.000000**	**0.000000**	**0.000000**	**0.000000**	**0.000000**	**0.000000**
$RaAOA_{BHHH}$	**0.000000**	**0.000000**	**0.000000**	**0.000000**	**0.000000**	**0.000000**	**0.000000**	**0.000000**
$GCAOA_{INR}$	0.002227	0.000779	0.001643	0.001956	0.005971	0.006722	0.008649	0.003992
$RaAOA_{NR}$	0.022617	0.007961	0.016998	0.020109	0.061901	0.069523	0.089629	0.041248
$RaAOA_{LW}$	0.022619	0.007961	0.017000	0.019751	0.061110	0.066060	0.073455	0.038279
AEO_{NR}	0.100252	0.055546	0.114293	0.074017	0.175293	0.188907	0.308128	0.145205
$ELPSO_{NR}$	0.023226	0.008871	0.019093	0.020194	0.062148	0.072364	0.090526	0.042346
$ELSHADE_{INR}$	0.002331	0.000797	0.001643	0.001955	0.005999	0.031323	0.008648	0.007528
MPA_{LW}	0.023533	0.010037	0.017905	0.021597	0.062221	0.066473	0.085902	0.041096
$MPSO_{NR}$	0.023532	0.009560	0.017884	0.022659	0.072620	0.082783	0.096830	0.046553
$MRFO_{NR}$	0.023528	0.010342	0.018140	0.021780	0.062148	0.070069	0.089677	0.042240
ALO_{LW}	0.026401	0.009700	0.019999	0.020929	0.061281	0.073658	0.092224	0.043456
$CHCLPSO_{NR}$	0.024489	0.009100	0.018846	0.020412	0.061392	0.069771	0.090431	0.042063
$DEAM_{NR}$	0.022619	0.008654	0.017064	0.020070	0.061651	0.069564	0.089618	0.041320

© COPYRIGHT UPM

Figure 4.5 shows the development convergence speed to the optimal solutions of the proposed $RaAOA_{AdBHHH}$ model and alternative approaches at variety of the environmental scenarios. It is evident that the proposed $RaAOA_{AdBHHH}$ ends with zero values for all meteorological circumstances. The $RaAOA_{AdBHHH}$ model has the quickest convergence rate when compared to other models, where its RMSE values at the first iteration under seven weather circumstances are $2.98e^{-8}$,$2.04e^{-8}$, $2.54e^{-5}$, $5.61e^{-5}$, $4.05e^{-4}$, $8.26e^{-4}$, and $5.49e^{-5}$, respectively. As depicted in Figure 4.5, the $RaAOA_{AdBHHH}$ model only requires 16, 18, 21, 16, 18, 37, and 38 iterations to achieve RMSE of zero. Therefore, the $RaAOA_{AdBHHH}$ model presents a potent hybrid stochastic algorithm and a unique objective function design for forecasting the TD PV model's output current.

© COPYRIGHT UPM

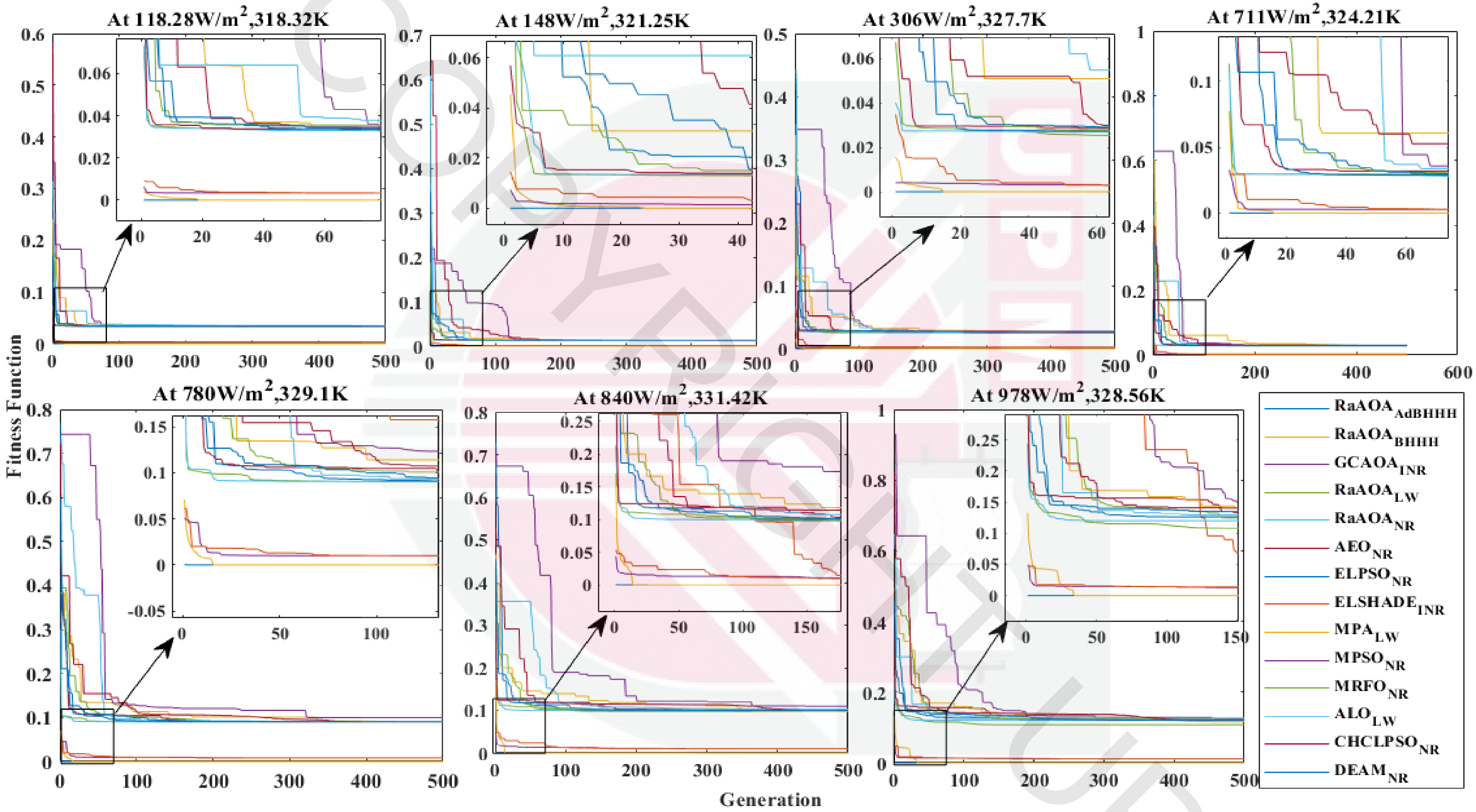

Figure 4.5 : Development of the OFD using $RaAOA_{AdBHHH}$ and other models at seven weather conditions

4.4 Performance of the R.T.C France silicon TD PV module

The second data set is based on experimental I-V data gathered from R.T.C France a 57 mm diameter silicon PV cell operating at 1000 W/m^2 solar irradiance and 33℃ ambient temperature [5]. The RaAOA$_{AdBHHH}$ model is compared to peer-reviewed research publications using a number of statistical criteria that take into account assessments of accuracy, dependability, consistency, and stability. The proposed RaAOA$_{AdBHHH}$ approach is also verified with five versions objective function formulations: RaAOA$_{BHHH}$, RaAOA$_{INR}$, RaAOA$_{NR}$, RaAOA$_{LW}$, and RaAOA$_{L}$. Whereas the peer-reviewed approaches are chosen from the literature according to the utilized objective function design, they are as follows: AEO$_{NR}$ [125], ALO$_{LW}$ [62], CHCLPSO$_{NR}$ [63], DEAM$_{NR}$ [64], ELPSO$_{NR}$ [55], ELSHADE$_{INR}$ [6], FFA$_{NR}$ [65], HSDEMFO$_{L}$ [48], ImSMA$_{LW}$ [66], MPA$_{LW}$ [45], MPSO$_{NR}$ [68], MRFO$_{NR}$ [69,70], PGJAYA$_{L}$ [47], and TVACPSO$_{NR}$ [71].

For fair comparisons, all algorithms are performed in the same environment, with population size (N) set to 30. The maximum iterations number (M_i) set is 1000. Besides, each algorithm is run independently for all algorithms, and the results are selected based on best optimum fitness function identified so far. The ranges of TD PV models is given in Table 4.7 [45]. It is necessary to emphasize that the NR approach described in the literature solves the PV model equation suing a set of vectors, and its drawback is that it does not take into account the individual imperfection between couples of the I-V data curves. As an outcome, the individual pairs of the data points is computed for the RaAOA$_{NR}$ and RaAOA$_{INR}$.

Table 4.7 : Search space ranges for the TD PV models [6]

Parameter	TD	
	LB	UB
d_1 d_2	1	2
d_3	1	5
I_{Ph}	0	1
I_{o1}, I_{o2}, I_{o3}	0	$1e^{-6}$
R_s	0	0.5
R_p	0	100

This thesis focus on the parameters extraction of the TD PV model as it has a far higher degree of precision due to the inclusion of two extra parameters. Furthermore, this model is better suited for industrial PV systems since it provides a high current value and the current degrades very slowly, even during the partial shading and overcast days. Table 4.8 provides the determined unknown parameters of the TD PV model utilizing the $RaAOA_{AdBHHH}$ model and other approaches. Their I-V and P-V curves are displayed in Figure 4.6. Despite the intricacy of the TD PV mode, the $RaAOA_{AdBHHH}$ extracts the nine parameter affectively, as seen by the I-V and P-V curves. In accordance to the Table 4.8, the majority of the algorithms determine the parameters within the feasible search space ranges. However, the algorithm's the accuracy, stability, and reliability can be indicated by the manner in which it simulates the whole experimental data points domains. The zoomed-in graphics in the Figure 4.8 indicate that the $RaAOA_{AdBHHH}$ model is definitely overlapped all the experimental data points, which may be derived with confidence for the practical applications of the PV systems.

© COPYRIGHT UPM

Table 4.8 : The extracted parameters of the $RaAOA_{AdBHHH}$ and other methods

Method	d_1	d_2	d_3	I_{o1}	I_{o2}	I_{o3}	I_{Ph}	R_s	R_p
$RaAOA_{AdBHHH}$	**1.8570**	**1.2696**	**1.8898**	**9.97E-07**	**2.03E-07**	**1.00E-06**	**0.7176**	**0.0396**	**59.4389**
$RaAOA_{BHHH}$	1.8675	1.2581	1.8626	1.00E-06	1.70E-08	1.00E-06	0.7606	0.0398	59.0876
$RaAOA_{INR}$	2.0000	1.4520	2.4314	4.54E-07	2.32E-07	1.00E-06	0.7607	0.0367	55.8059
$RaAOA_{LW}$	1.1968	1.9745	1.9748	2.78E-09	1.00E-06	1.00E-06	0.7613	0.0809	62.0120
$RaAOA_{NR}$	1.9508	1.1715	1.8114	1.00E-06	3.56E-09	9.62E-07	0.7609	0.0521	60.8402
$RaAOA_{L}$	1.9999	1.4554	2.4047	3.59E-07	2.43E-07	1.00E-06	0.7607	0.0367	55.6880
AEO_{NR}	1.7750	1.3725	2.3874	7.61E-07	7.93E-08	1.00E-06	0.7608	0.0376	56.8647
ALO_{LW}	1.4676	1.1887	2.4278	2.81E-07	0.00E+00	3.78E-09	0.7614	0.0367	43.7674
$CHCLPSO_{NR}$	1.8174	1.4386	2.3226	3.20E-07	1.94E-07	8.77E-07	0.7607	0.0369	55.4818
$DEAM_{NR}$	1.4021	1.9998	2.1208	1.26E-07	9.90E-07	9.99E-07	0.7608	0.0376	57.1156
$ELPSO_{NR}$	1.9184	1.4009	1.8373	0.00000	1.17E-07	8.78E-07	0.7608	0.0373	55.3628
$ELSHADE_{INR}$	2.0000	1.4520	2.4315	4.54E-07	2.32E-07	1.00E-06	0.7607	0.0367	55.8060
FFA_{NR}	1.9713	1.4773	3.0822	3.08E-09	3.11E-07	9.93E-07	0.7607	0.0364	54.2642
$HSDEMFO_{L}$	1.9999	1.4890	4.8877	3.73E-11	3.51E-07	0.00E+00	0.7607	0.03603	65.1906
$ImSMA_{LW}$	1.8929	1.3924	2.1210	4.22E-07	9.07E-08	7.91E-07	0.7609	0.0506	53.9121
MPA_{LW}	1.4563	1.9612	4.9999	2.52E-07	1.47E-08	9.99E-07	0.7608	0.0375	48.8690
$MPSO_{NR}$	1.7564	1.4376	1.4213	1.06E-08	9.25E-10	1.72E-07	0.7613	0.0386	40.4563
$MRFO_{NR}$	1.9425	1.4278	3.2703	8.74E-07	1.71E-07	7.18E-07	0.7608	0.0372	54.6809
$PGJAYA_{L}$	1.9998	1.4598	4.8260	5.67E-07	2.52E-07	8.70E-07	0.7607	0.0365	55.3108
$TVACPSO_{NR}$	1.4449	1.9634	2.3840	2.14E-07	4.26E-07	9.99E-07	0.7607	0.0369	55.1450

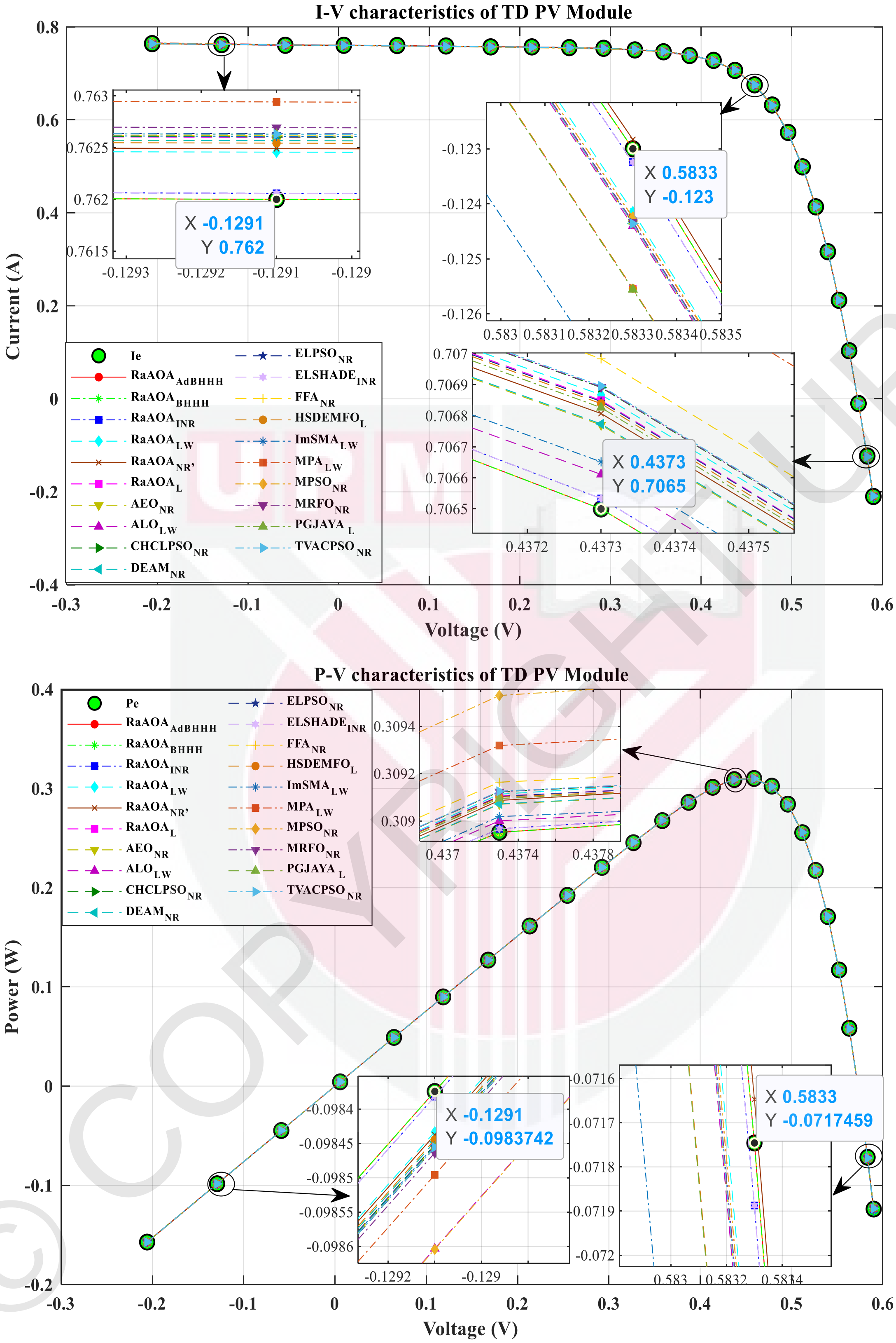

Figure 4.6 : The I-V and P-V data characteristic curves using the RaAOA$_{AdBHHH}$ and alternative approaches based on experimental data

Another perspective to verify the efficacy of the proposed $RaAOA_{AdBHHH}$ model and other methods is by addressing the statical analysis quantitively as tabulated in Table 4.9. According to this table, the $RaAOA_{AdBHHH}$ has zero values for all statistical criteria, and the R^2 is one, indicating the originality of the proposed approach for extracting the parameters even for the complicated model. In contrast, the $RaAOA_{AdBHHH}$ requires a substantial amount of processing time owning to its structure's complexity in terms of algorithm and the objective function formulation. Note that the CPU execution time is somewhat unimportant in this optimization problem. This is due to the offline nature of the measured experimental data. In comparison, online measurement is initially costly and time-consuming. The $RaAOA_{AdBHHH}$ differs in that it has quick convergence and the extracted parameters are more stable, allowing it to affectively imitate real current at different voltages ranges. Importantly, the basic BHHH approach presents very accurate initial root values by computing half-distance in the search space without any further improvements, as evidenced by the $RaAOA_{BHHH}$ findings, where RMSE is 2.9894E-07. The ranking of the approaches are as follows: $RaAOA_{AdBHHH}$, $RaAOA_{BHHH}$, $RaAOA_{INR}$, $ELSHADE_{INR}$, $RaAOA_{NR}$, $RaAOA_{LW}$, $DEAM_{NR}$, AEO_{NR}, $ELPSO_{NR}$, $MRFO_{NR}$, $TVACPSO_{NR}$, $CHCLPSO_{NR}$, FFA_{NR}, MPA_{LW}, $ImSMA_{LW}$, ALO_{LW}, $RaAOA_{L}$, $PGJAYA_{L}$, $HSDEMFO_{L}$, and $MPSO_{NR}$ as observed in Table 4.9, respectively. The faster method is $DEAM_{NR}$ with only 17.8 second.

© COPYRIGHT UPM

Table 4.9 : Statistical findings of the $RaAOA_{AdBHHH}$ and other PV models

Method	RMSE	MBE	R^2	TS	STD	AE	CPU
$RaAOA_{AdBHHH}$	**0.000000**	**0.000000**	**1.000000**	**0.000000**	**0.000000**	**0.000000**	151.04
$RaAOA_{BHHH}$	2.9894E-07	8.9366E-14	**1.000000**	1.4947E-06	2.5624E-07	2.1911E-07	150.64
$RaAOA_{INR}$	9.4417E-05	8.9145E-09	**1.000000**	4.7213E-04	8.0929E-05	5.4084E-05	198.76
$RaAOA_{LW}$	5.9326E-04	3.5196E-07	0.999996	2.9681E-04	5.0851E-04	3.7580E-04	3411.45
$RaAOA_{NR}$	4.9877E-04	2.4877E-07	0.999997	2.4951E-04	4.2752E-04	3.8664E-04	94.28
$RaAOA_{L}$	9.8033E-04	9.6105E-07	0.999989	4.9065E-03	8.4028E-04	5.5833E-04	66.46
AEO_{NR}	7.3854E-04	5.4544E-07	**1.000000**	3.6954E-03	6.3303E-04	4.9539E-04	31.01
ALO_{LW}	9.1978E-04	8.4600E-07	0.999990	4.6032E-03	7.8839E-04	6.3692E-04	7864.71
$CHCLPSO_{NR}$	7.5050E-04	5.6325E-07	0.999994	3.7553E-03	6.4328E-04	5.0758E-04	26.73
$DEAM_{NR}$	7.3376E-04	5.3841E-07	0.999994	3.6715E-03	6.2894E-04	4.9104E-04	**17.87**
$ELPSO_{NR}$	7.4514E-04	5.5524E-07	0.999994	3.7285E-03	6.3869E-04	5.0224E-04	22.79
$ELSHADE_{INR}$	9.4417E-05	8.9145E-09	**1.000000**	4.7213E-04	8.0929E-05	5.4084E-05	57.18
FFA_{NR}	7.6966E-04	5.9237E-07	0.999999	3.8512E-03	6.5971E-04	5.2640E-04	32.89
$HSDEMFO_{L}$	9.9948E-04	9.9895E-07	0.999989	5.0024E-03	8.5669E-04	5.9103E-04	100.04
$ImSMA_{LW}$	8.4191E-04	2.8748E-06	0.999968	1.7132E-02	7.2164E-04	7.6606E-04	371.25
MPA_{LW}	8.2348E-04	6.7811E-07	0.999993	4.1208E-03	7.0584E-04	5.7424E-04	8956.71
$MPSO_{NR}$	1.1942E-03	1.4261E-06	0.999984	5.9780E-03	1.0236E-03	8.6430E-04	18.35
$MRFO_{NR}$	7.4664E-04	5.5748E-07	0.999994	3.7360E-03	6.3998E-04	5.0610E-04	30.23
$PGJAYA_{L}$	9.8334E-04	9.6695E-07	0.999989	4.9215E-03	8.4286E-04	5.6712E-04	24.20
$TVACPSO_{NR}$	7.4856E-04	5.6034E-07	0.999994	3.7456E-03	6.4162E-04	5.0690E-04	21.39

© COPYRIGHT UPM

Figure 4.7 illustrates the IAE of the between each data points between the forecasted currents and experimental currents utilizing the $RaAOA_{AdBHHH}$ and other models for the TD PV model. According to Figure 4.7, the $RaAOA_{AdBHHH}$ may plainly deteriorate the errors up to zero for all measured data points. The IAE value for the $RaAOA_{BHHH}$ is 2.1911E-07, which represents an acceptable level of accuracy when compared to other models. The MPA_{LW} method clearly demonstrates the difficulties of extracting the parameters of the TD PV model, since its performance is marginally with an IAE of 5.7424E-04. The worst IAE value is registered with $MPSO_{NR}$ method, where its value is 8.6430E-04. Therefore, the solving the parameter extraction optimization problem must be solved by efficiently considering the exploration and exploitation phases in terms of algorithm and by accurately picking initial root solutions from the search space in terms of the formulation of the objective function, as indicated by the $RaAOA_{AdBHHH}$ approach.

© COPYRIGHT UPM

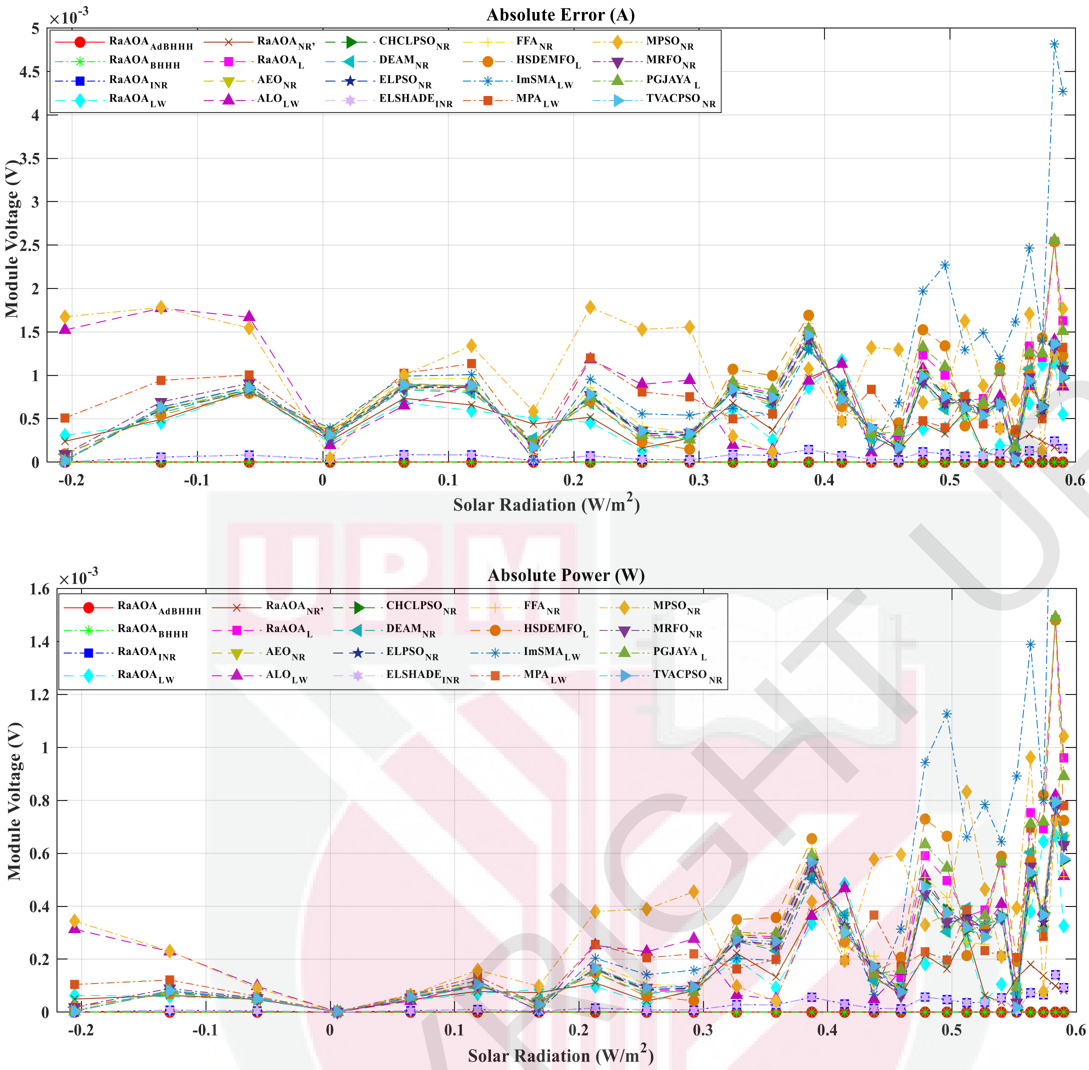

Figure 4.7 : The IAE of current and power for the TD PV model using differernt models

Figure 4.8 depicts the convergence velocity of the RaAOA$_{AdBHHH}$ and its counterparts. The RaAOA$_{AdBHHH}$ may swiftly converge, followed by RaAOA$_{BHHH}$. The RMSE value for the first iteration is 0.000468; however, it drops drastically as the number of iterations increases, eventually reaching zero after 838 iterations. The RaAOA$_{AdBHHH}$ beats other methods in terms of accuracy, stability, and convergence rate.

© COPYRIGHT UPM

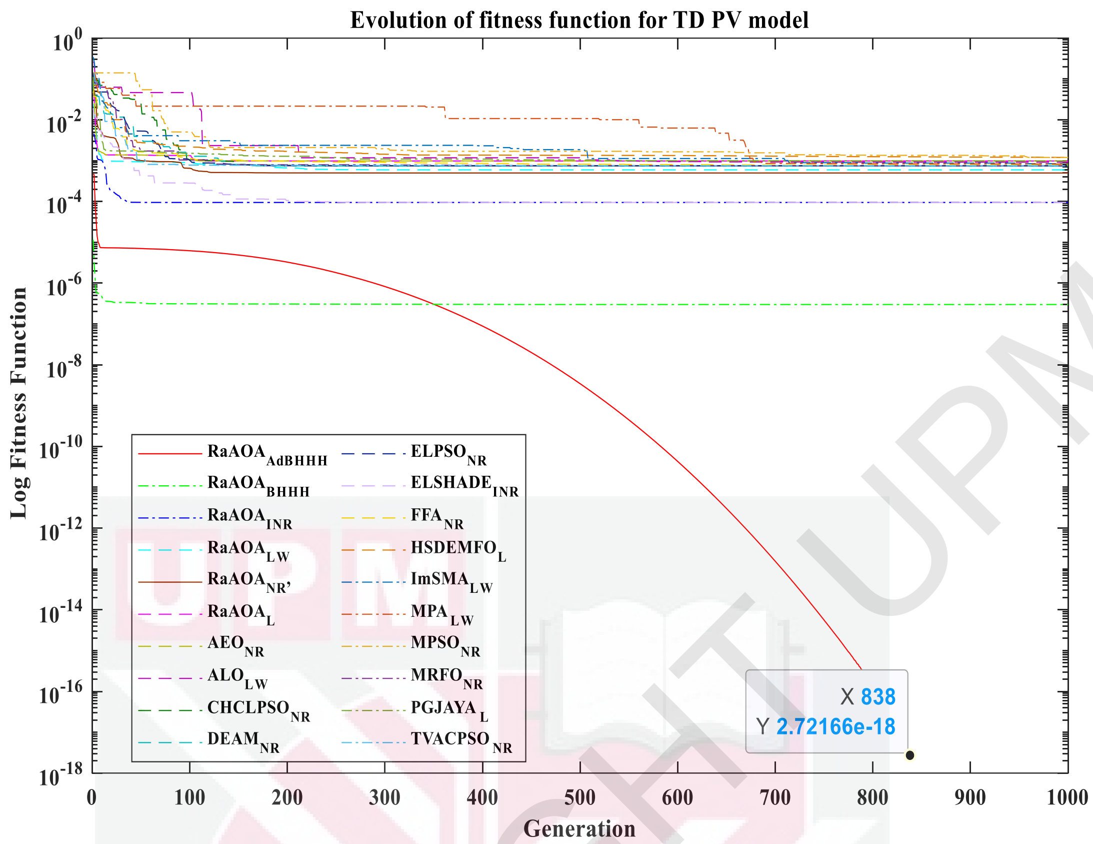

Figure 4.8 : The development of the fitness function for the TD PV model under varoius methods

As a result, the proposed RaAOA$_{AdBHHH}$ exhibits an excellent performance in extracting the parameters for the three types of the PV models. This is a sufficient application of IOBL and LF techniques for avoiding local minima, and strong use of exploitation tactics to improve the quality of the solutions offered by CMM and winner principle.

4.5 Optimization of the standalone WT/PV/Battery system

The optimal design of the freestanding PV/WT/Battery system is presented in this study to illustrate the most effective way to meet the load requirement for two scenarios in Malaysia and South Africa. The experimental data of the Yingli PV module is not available. Therefore, the GCAOA is employed to estimate the parameters of the TD PV model by minimizing errors at three critical points using information given by the manufacture at STC. The population size (N) is 30, the number of maximum iterations is 1000, and the problem dimension is 5. The d_{1-3}, R_s, and R_P are successfully optimized by the GCAOA approach, while the parameters I_{Ph} and I_{o1-3} are then mathematically computed form the optimized parameters. The extracted parameters of the TD PV model based on three key points are given in Table 4.10. The I-V and P-V curves of the TD PV model of the Yingli PV module at MPP are depicted in Figure 4.9. The most optimal solutions are determined by their lowest error value over a period of 30 individual runs.

Table 4.10 : The extracted parameters of TD PV model of the Yingli PV module

d_1	d_2	d_3	I_{Ph}	I_{o1}	I_{o2}	I_{o3}	R_s	R_p	E_R
1.0045	1.9999	4.9997	8.6457	2.02E-06	2.29E-14	4.73E-14	0.0429	67.7787	2.361E-19

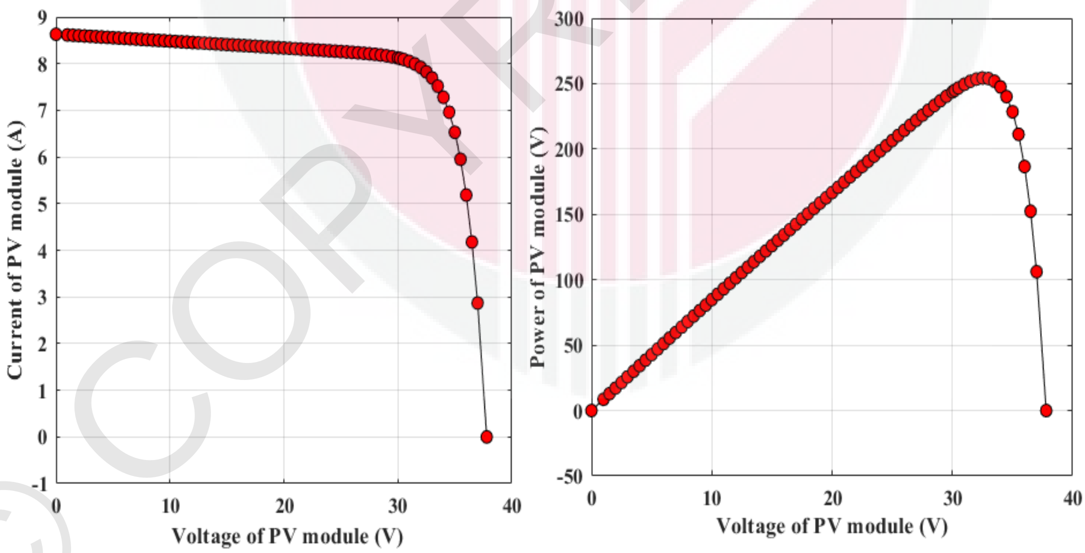

Figure 4.9 : I-V and P-V data characteristics curves of the TD PV model of the Yingli PV module

The output power of TD PV model of the Yingli PV module across a one-year period using climatic data from Malaysia and South Africa are demonstrated in Figure 4.10.

© COPYRIGHT UPM

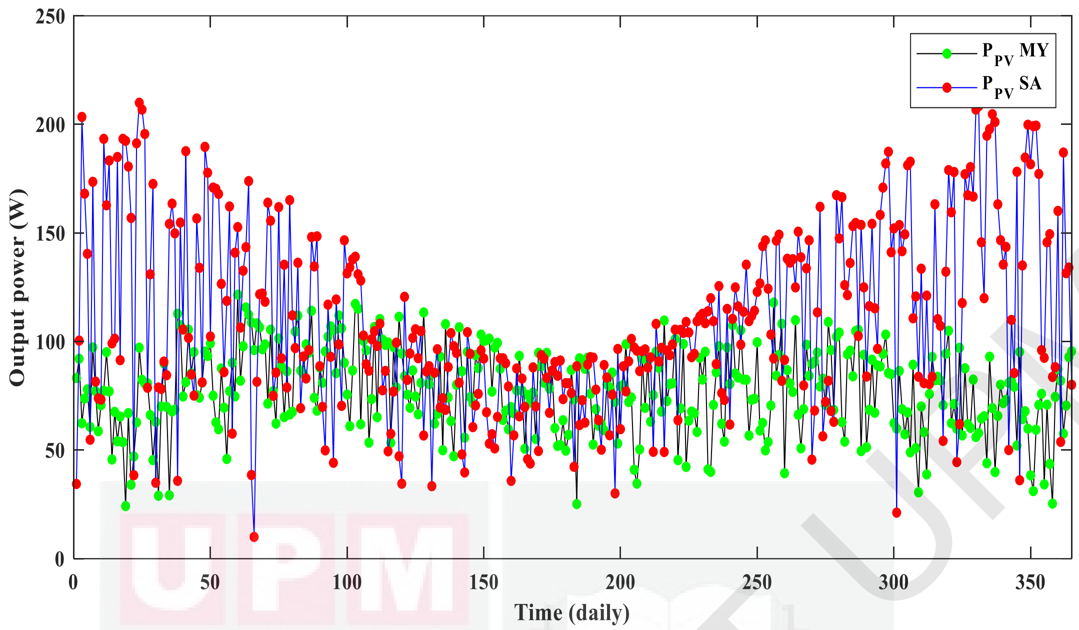

Figure 4.10 : The output power average (daily) of the TD PV model of the Yingli PV module for Malaysia and South Africa

4.6 Results on the improved bi-archive algorithm

In this section, the improved two archived algorithm is employed to construct four collections of optimal PF solutions of the proposed independent PV/WT/Battery system for both Malaysia and South Africa scenarios. The improved two archived method has a parameter setting of 100 for population and archived sizes, as well as the maximum iteration. The upper and lower boundaries variables are derived based on mathematical analysis equations for the WT, PV (N_T) (in series (N_S) and parallel (N_P)), and battery storage (B_S) are [1,17], [2,35], and [3,69], respectively. For the Malaysia case study, the results of four sets optimal PF solutions based on the improved two archive algorithm are illustrated in Figure 4.11**.** (a) for the three objectives: LLP, LCC, and P_{dump}, and their corresponding solutions for the WT, PV, Battery storage are presented in part (b). The final output optimal solutions are maintained in DA, which contains the most diversified solutions, while the CA directs to the fastest converge. Thus, the interaction between DA and CA may notably impact on the efficiency of the improved two archive algorithm. It can be clearly seen that the optimal sets of the DA has the most desirable solutions of the proposed system. This is due to the efficient use of the $I_{\varepsilon+}$ indicator and mutation mechanism, where the $I_{\varepsilon+}$ indicator prevents the stagnation and the mutation scheme delivers some of best solutions in DA to guide CA.

(a)

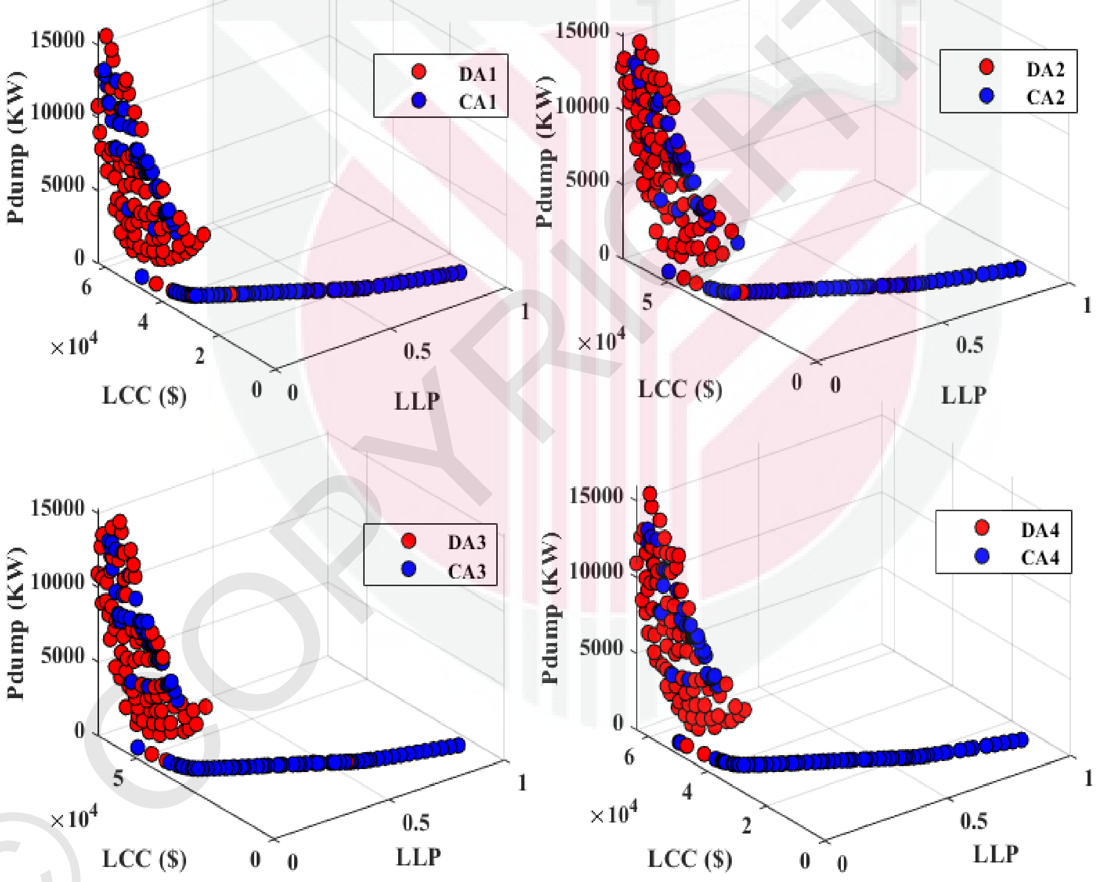

© COPYRIGHT UPM

(**b**)

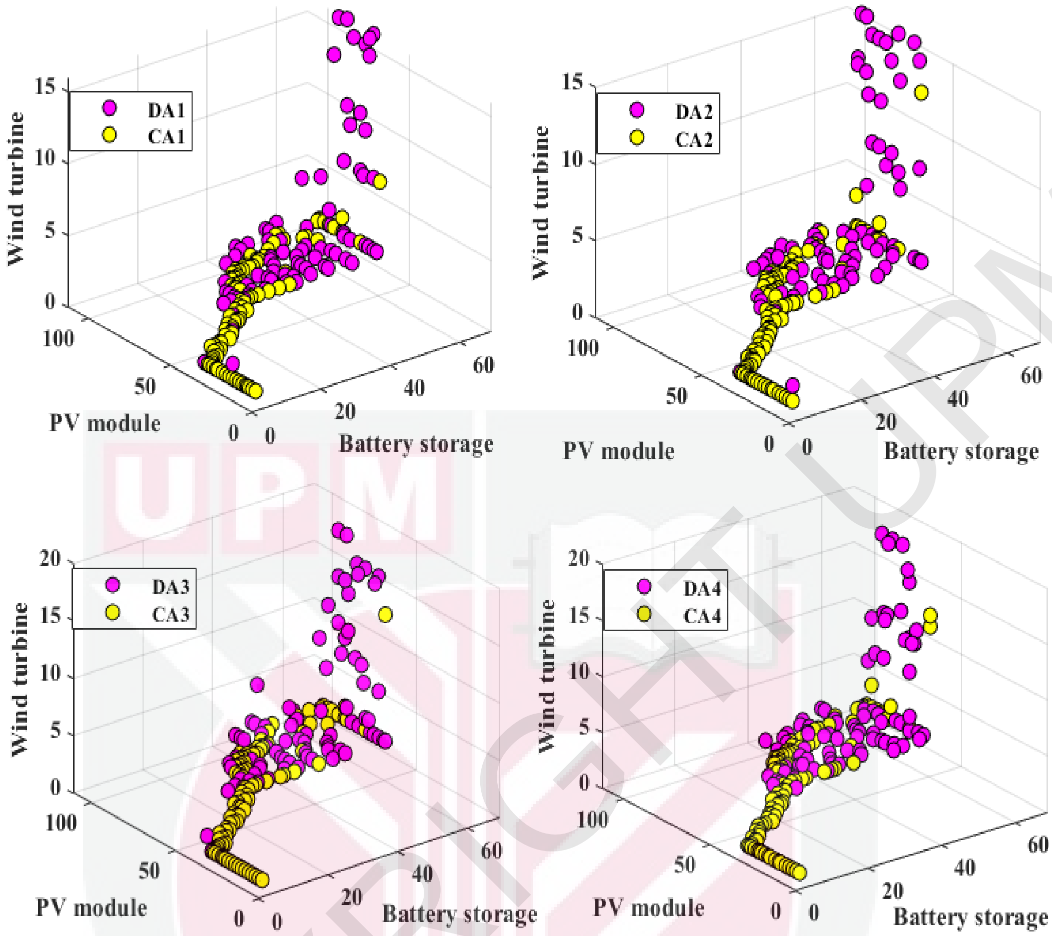

Figure 4.11 : Results of the multi-objective improved two archive algorithm in Malaysia (a) LLP, LCC, and P_{dump}, and (b) WT, PV, and battery storage

For the South Africa scenario, the four sets of the optimal PF solutions are exhibited in Figure 4.12, where the three competing objectives are demonstrated in part (**a**) and their variables are shown in part (**b**). From Figure 4.11, both the diversity and convergence are successfully achieved by taking the benefits of the $I_{\varepsilon+}$ indicator for boosting the convergence and L_p-norm based distance for increasing the diversity. The justification of that is clarified in Figures 4. 11 and 4. 12 part (b), where the DA is well-distributed along the dimensions of the search space.

(a)

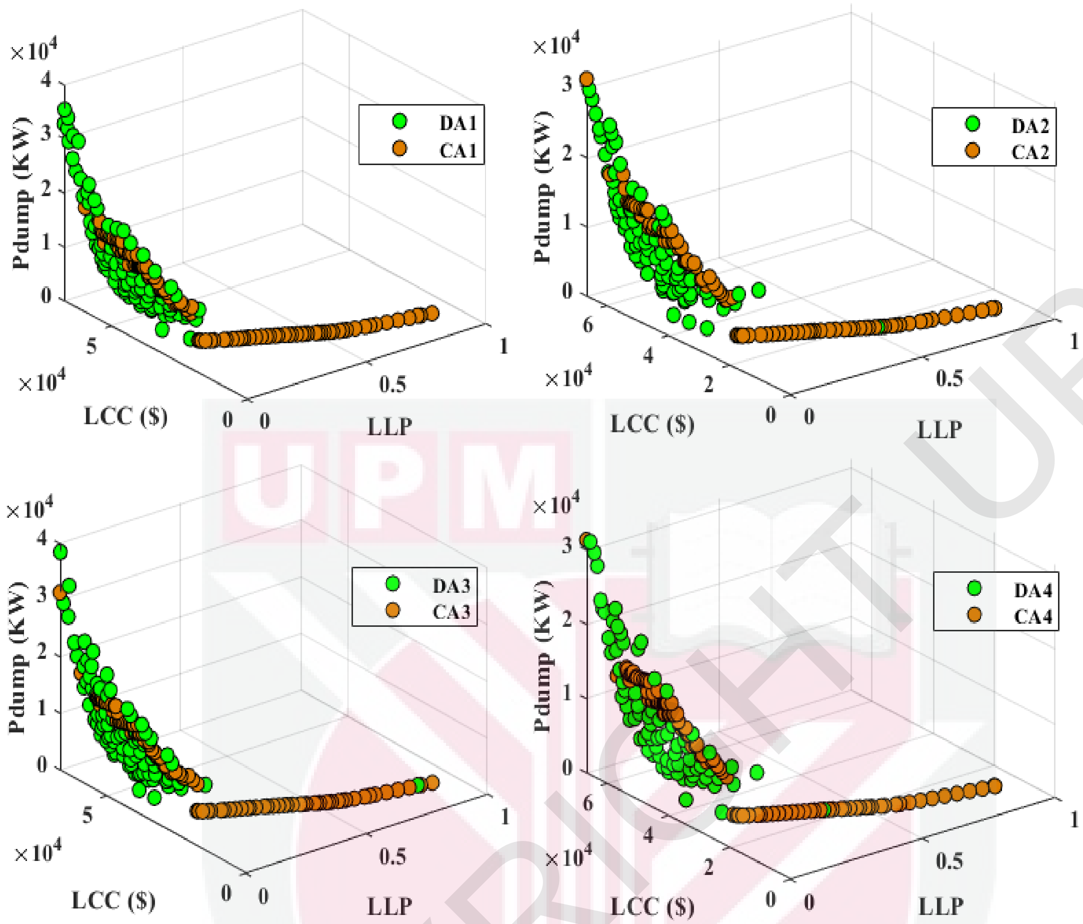

© COPYRIGHT UPM

(**b**)

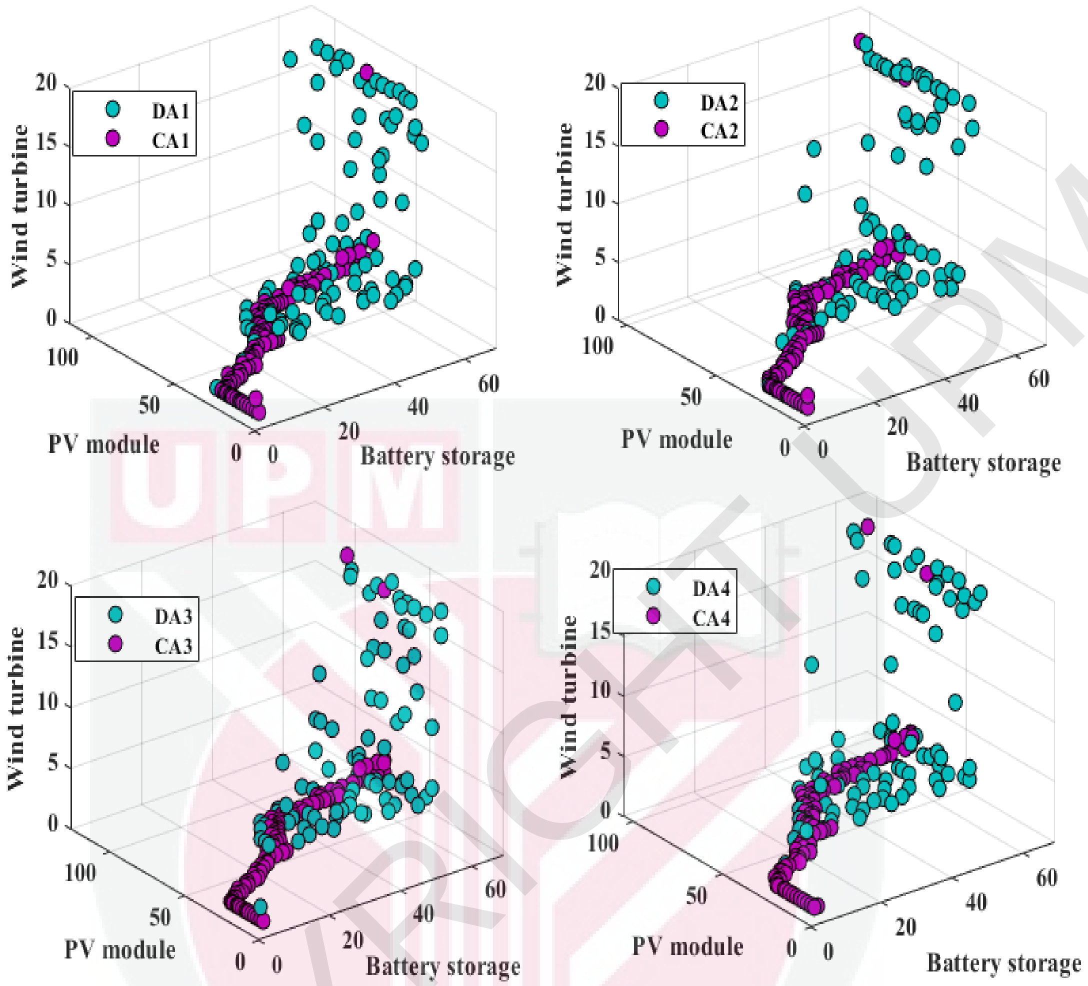

Figure 4.12 : Results of the multi-objective improved two archive algorithm in South Africa (a) LLP, LCC, and Pdump, and (b) WT, PV, and battery storage

4.7 Results on Intuitive-Numerical-MOO method

The bottom and higher search spaces for the WT, PV modules, storage batteries are determined by the intuitive method. The numerical method is then employed to iterate these variables, conducted by intuitive method, from 1 to 17 for the WT, 2 to 35 for the PV module in series and parallel, and 3 to 69 for the storage batteries. With predefined ranges, the numerical method may exactly find all possible configurations in the search space. The ranges of the LLP is between 0 to 0.01, which is regarded as the most desirable value for an off-grid system. The numerical technique yields configurations of 624045 and 668884 for Malaysia and South Africa, whereas their CPU processing times are 276883.98 s and 145547.45 s, respectively. Figure 4.13 demonstrates the search space (left) and the design space (right) of the numerical findings for the both Malaysia and South Africa. According to the Figure 4.13, the search space comprises several optimum solutions for the WT, PV modules, and storage batteries, while their LLP, LCC, and P_{dump} objectives illustrate the simulation iterations of the numerical approach. In addition, this optimization problem for the hybrid WT/PV/Battery system is multivariable, nonlinear, and consists of several local minima. Therefore, the challenging task is to pick a single best design to reflect the performance of the Malaysia and South Africa. From this perspective, the non-dominated multi-objective concept is obtained to construct sets of optimal PF solutions and excluding the undesirable solutions from the vast search space.

© COPYRIGHT UPM

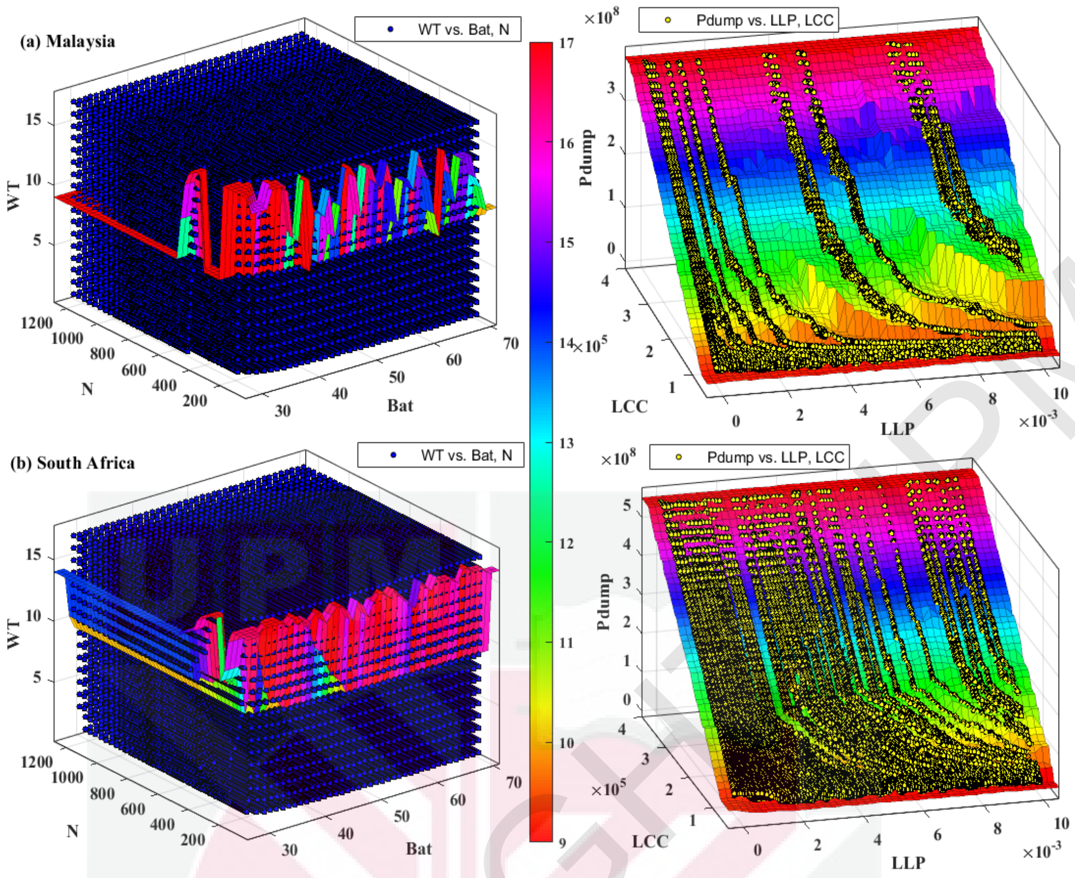

Figure 4.13 : The exploratory numerical results analysis of the storage batteries, PV modules, and WT along with their LLP, LCC, and P_{dump} objectives for (a) Malaysia and (b) South Africa

The non-dominated principle is implemented afterwards by including approximately 40.000 configurations to conduct only one optimal set of the PF solutions. As seen in Figure 4.14, there are 16 optimal sets of PF solutions generated by this method for the Malaysia case study, and there are 17 optimal sets of the PF solutions for the South Africa. There optimal sets PF solutions for the Malaysia and South Africa differ due to the greater likelihood of including optimal solutions with LLP values smaller than 1% in South Africa than Malaysia, confirming that this optimization problem is highly sensitive on the availability of the meteorological data. Despite the non-dominated concept has reduced the number of optimum solutions, it is still difficult to choose the most unique solution for each case study, where each set has 100 optimal PF solutions.

In this regard, the MCDM method is essential ranking these solutions according to their importance, considering the opinions views of the three experts.

© COPYRIGHT UPM

(a)

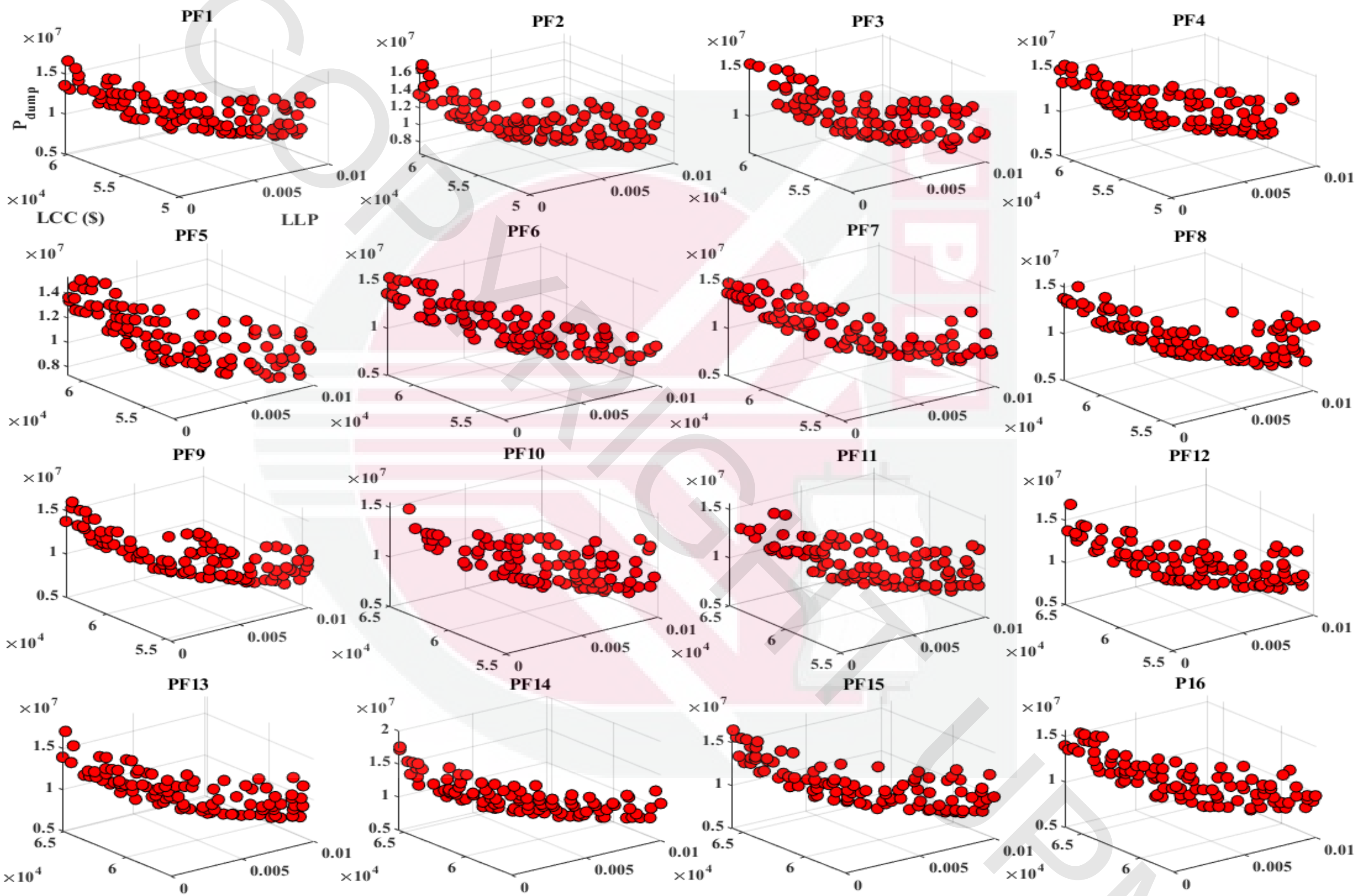
PF1
PF2
PF3
PF4
PF5
PF6
PF7
PF8
PF9
PF10
PF11
PF12
PF13
PF14
PF15
P16
P_{dump}
LCC ($)
LLP
$\times 10^7$
$\times 10^4$

(b)

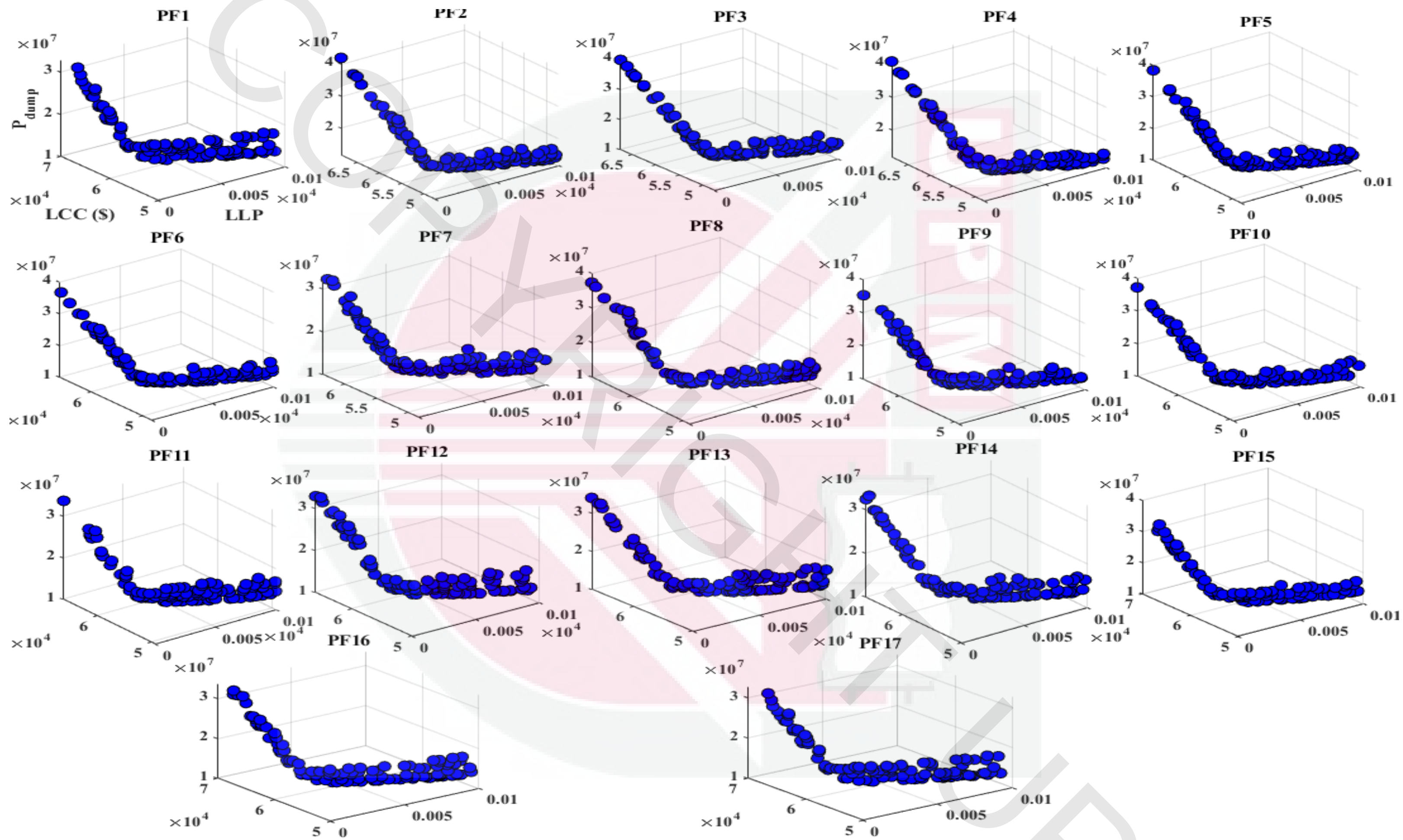

Figure 4.14 : Optimal sets of the PF solutions based on non-dominated concept for both Malaysia and South Africa

© COPYRIGHT UPM

4.8 Results on the improved bi-archive-BWM-PROMETHEE II-GDM methods

The hybrid MCDM methods are applied for the best optimum group PF solutions for the improved two archive and hybrid numerical-nondominated methods. The weights of the objectives are given to each objective using BWM method by considering full consistency ratios of the three experts opinions. Firstly, the weights of the objectives are assigned by the judgements of the three experts. Full consistency ratios are achieved, as tabulated in Table 4.11, indicating a high stability to select the most desirable configuration. The consistency ratio demonstrates the stability of the BWM method; hence, when one objective is improved, the other objectives deteriorate. These assigned weights are included into PROMEHEE II method in order to overcome its constraints. According to Table 4.11, the first expert view gives the LLP a higher priority than the LCC and P_{dump} in order to ensure that the WT/PV/Battery system operates with a degree of confidence and that the provided energy does not fluctuate throughout the year, while paying more attention to the total cost of the system. The second expert favors reducing the total cost of the system while maintaining an favorable levels of dependability. The main obstacle of the off-grid WT/PV/Battery system is that the wasted energy is large, resulting over sizing and the system become more expensive. Consequently, the P_{dump} should take into account. Lastly, the third expert is more concerned with the system's reliability than the first exert, with lowering the overall cost of the system.

© COPYRIGHT UPM

Table 4.11 : BWM's evolutions of the three criteria based on three experts' opinions

1st expert	Best to others	LLP	LCC	P_{dump}
	LLP	1	2	4
	Others to worst	LLP	LCC	P_{dump}
	P_{dump}	4	2	1
	Weights	0.5714	0.2857	0.1429
	ξ^*		0.0000	
2nd expert	Best to others	LLP	LCC	P_{dump}
	LLP	3	1	9
	Others to worst	LLP	LCC	P_{dump}
	P_{dump}	3	9	1
	Weights	0.2307	0.6923	0.07692
	ξ^*		0.0000	
3rd expert	Best to others	LLP	LCC	P_{dump}
	LLP	1	3	9
	Others to worst	LLP	LCC	P_{dump}
	P_{dump}	9	3	1
	Weights	0.6923	0.2308	0.0769
	ξ^*		0.0000	
GDM	Weights	LLP	LCC	P_{dump}
		0.4982	0.4029	0.0989

The top ten designs in Malaysia and South Africa are selected according to the three experts' opinions, as seen in Table 4.12 (a) and (b), respectively. From Table 4.12, it can be clearly observed that the three experts and BWM-PROMETHEE-II method favor configurations with a high number of batteries storage in both scenarios. This is because the stored and conducted energy in batteries storage have a lower overall cost, high degree of dependability, and less lost energy rather than increasing the quantity of renewable energy sources. In this regard, the over/under sizing is guaranteed to be avoided. Furthermore, the employment of the WTs is not advised in the Malaysian case study owing to the low potential of the wind speed and conducted energy, however it WTs may considerably assist to provide energy in the South Africa scenario. Finally, the φ_j is almost high, with a value more than 0.96, indicating that reflects the hybridization of the MCDM methods is very reliable and stable.

© COPYRIGHT UPM

Table 4.12 (a) : Ranking of improved two archive-BWM-PROMETHEE II method for the three experts in Malaysia

Expert	φ_j^+	φ_j^-	φ_j	WT	N_T	N_S	N_P	B_S	LLP	LCC	P_{dump}	T
1st expert	0.9864	0.0079	0.9785	12	104	8	13	69	0.000000	64362.20	13535.46	1.06 s
	0.9792	0.0208	0.9585	7	105	5	21	68	0.000031	62320.09	13724.89	
	0.9696	0.0276	0.9420	15	102	34	3	69	0.000252	65011.63	12941.75	
	0.9699	0.0286	0.9413	5	104	8	13	69	0.000032	61523.87	13366.74	
	0.9631	0.0279	0.9352	1	105	7	15	69	0.000000	60185.47	13548.02	
	0.9631	0.0279	0.9352	1	105	7	15	69	0.000000	60185.47	13548.02	
	0.9631	0.0279	0.9352	1	105	35	3	69	0.000000	60185.47	13548.02	
	0.9631	0.0279	0.9352	1	105	15	7	69	0.000000	60185.47	13548.02	
	0.9663	0.0322	0.9341	4	104	8	13	69	0.000032	61118.40	13324.97	
	0.9653	0.0319	0.9334	10	102	6	17	69	0.000252	62984.25	12841.84	
2nd expert	0.9921	0.0056	0.9865	12	104	8	13	69	0.000000	64362.20	13535.46	1.84 s
	0.9861	0.0127	0.9734	15	102	34	3	69	0.000252	65011.63	12941.75	
	0.9771	0.0218	0.9553	10	102	6	17	69	0.000252	62984.25	12841.84	
	0.9722	0.0278	0.9445	7	105	5	21	68	0.000031	62320.09	13724.89	
	0.9722	0.0278	0.9445	15	99	33	3	69	0.000810	64161.14	11912.71	
	0.9699	0.0289	0.9410	9	102	34	3	69	0.000252	62578.78	12823.49	
	0.9626	0.0374	0.9252	12	100	25	4	67	0.000898	62631.74	12156.72	
	0.9622	0.0372	0.9250	5	104	8	13	69	0.000032	61523.87	13366.74	
	0.9566	0.0409	0.9158	17	96	16	6	69	0.001489	64121.59	10894.19	
	0.9566	0.0409	0.9158	17	96	12	8	69	0.001489	64121.59	10894.19	
3rd expert	0.9886	0.0044	0.9842	12	104	8	13	69	0.000000	64362.20	13535.46	0.97 s
	0.9815	0.0185	0.9630	7	105	5	21	68	0.000031	62320.09	13724.89	
	0.9738	0.0245	0.9493	5	104	8	13	69	0.000032	61523.87	13366.74	
	0.9697	0.0210	0.9487	1	105	7	15	69	0.000000	60185.47	13548.02	
	0.9697	0.0210	0.9487	1	105	7	15	69	0.000000	60185.47	13548.02	
	0.9697	0.0210	0.9487	1	105	35	3	69	0.000000	60185.47	13548.02	
	0.9697	0.0210	0.9487	1	105	15	7	69	0.000000	60185.47	13548.02	
	0.9711	0.0254	0.9456	15	102	34	3	69	0.000252	65011.63	12941.75	
	0.9711	0.0272	0.9439	4	104	8	13	69	0.000032	61118.40	13324.97	
	0.9678	0.0287	0.9391	10	102	6	17	69	0.000252	62984.25	12841.84	

Table 4.12 (b) : Ranking of improved two archive-BWM-PROMETHEE II method for the three experts in South Africa

Expert	φ_j^+	φ_j^-	φ_j	WT	N_T	N_S	N_P	B_S	LLP	LCC	P_{dump}	T
1st expert	0.9943	0.0014	0.9928	17	108	6	18	68	0.000000	67225.33	32772.66	1.08 s
	0.9932	0.0068	0.9864	16	114	6	19	63	0.000089	67029.67	35472.44	
	0.9893	0.0039	0.9853	17	105	21	5	69	0.000000	66673.07	31370.82	
	0.9893	0.0039	0.9853	17	105	5	21	69	0.000000	66673.07	31370.82	
	0.9893	0.0039	0.9853	17	105	7	15	69	0.000000	66673.07	31370.82	
	0.9850	0.0150	0.9699	2	126	6	21	69	0.000179	66544.40	38550.41	
	0.9850	0.0150	0.9699	10	114	6	19	67	0.000179	65789.76	34361.17	
	0.9839	0.0161	0.9678	14	108	6	18	68	0.000179	66008.91	32288.38	
	0.9828	0.0168	0.9660	17	102	17	6	69	0.000096	65822.58	30010.81	
	0.9764	0.0226	0.9538	17	105	7	15	65	0.000182	65480.13	31370.82	
2nd expert	0.9975	0.0008	0.9967	17	108	6	18	68	0.000000	67225.33	32772.66	1.20 s
	0.9958	0.0042	0.9915	16	114	6	19	63	0.000089	67029.67	35472.44	
	0.9894	0.0048	0.9846	17	105	21	5	69	0.000000	66673.07	31370.82	
	0.9894	0.0048	0.9846	17	105	5	21	69	0.000000	66673.07	31370.82	
	0.9894	0.0048	0.9846	17	105	7	15	69	0.000000	66673.07	31370.82	
	0.9867	0.0133	0.9734	2	126	6	21	69	0.000179	66544.40	38550.41	
	0.9846	0.0154	0.9692	14	108	6	18	68	0.000179	66008.91	32288.38	
	0.9823	0.0175	0.9647	17	102	17	6	69	0.000096	65822.58	30010.81	
	0.9823	0.0177	0.9645	10	114	6	19	67	0.000179	65789.76	34361.17	
	0.9759	0.0239	0.9520	17	102	6	17	68	0.000185	65524.34	30010.81	
3rd expert	0.9940	0.0008	0.9933	17	108	6	18	68	0.000000	67225.33	32772.66	0.92 s
	0.9906	0.0025	0.9880	17	105	21	5	69	0.000000	66673.07	31370.82	
	0.9906	0.0025	0.9880	17	105	5	21	69	0.000000	66673.07	31370.82	
	0.9906	0.0025	0.9880	17	105	7	15	69	0.000000	66673.07	31370.82	
	0.9923	0.0077	0.9846	16	114	6	19	63	0.000089	67029.67	35472.44	
	0.9846	0.0152	0.9693	17	102	17	6	69	0.000096	65822.58	30010.81	
	0.9846	0.0154	0.9692	10	114	6	19	67	0.000179	65789.76	34361.17	
	0.9834	0.0166	0.9668	14	108	6	18	68	0.000179	66008.91	32288.38	
	0.9832	0.0168	0.9665	2	126	6	21	69	0.000179	66544.40	38550.41	
	0.9767	0.0227	0.9539	17	105	7	15	65	0.000182	65480.13	31370.82	

© COPYRIGHT UPM

The new sorted top 10 configurations is given in Table 4.13 based on GDM technique, with the most optimum design highlighted in black **boldface**. In most desirable configuration, the PV/WT/Battery system operates with high confidence, at a minimal cost, and with little wasted energy. It is vital to notice that this optimization problem has numerous variables and multiple local minima. This is owning to the three conflicting objectives, wherein improving one objective causes the others to deteriorate.

Table 4.13 (a) : Ranking of improved two archive-BWM-PROMETHEE II-GDM method in Malaysia

φ_j^+	φ_j^-	φ_j	WT	N_T	N_S	N_P	B_S	LLP	LCC	P_{dump}	T
0.9890	0.0060	0.9831	12	104	8	13	69	0.000000	64362.20	13535.46	4.19 s
0.9777	0.0223	0.9553	7	105	5	21	68	0.000031	62320.09	13724.89	
0.9756	0.0219	0.9537	15	102	34	3	69	0.000252	65011.63	12941.75	
0.9700	0.0275	0.9426	10	102	6	17	69	0.000252	62984.25	12841.84	
0.9686	0.0301	0.9385	5	104	8	13	69	0.000032	61523.87	13366.74	
0.9658	0.0317	0.9340	9	102	34	3	69	0.000252	62578.78	12823.49	
0.9641	0.0346	0.9295	4	104	8	13	69	0.000032	61118.40	13324.97	
0.9560	**0.0353**	**0.9207**	**1**	**105**	**7**	**15**	**69**	**0.000000**	**60185.47**	**13548.02**	
0.9560	0.0353	0.9207	1	105	7	15	69	0.000000	60185.47	13548.02	
0.9560	0.0353	0.9207	1	105	35	3	69	0.000000	60185.47	13548.02	

Table 4.13 (b) : Ranking of improved two archive-BWM-PROMETHEE II-GDM method in South Africa

φ_j^+	φ_j^-	φ_j	WT	N_T	N_S	N_P	B_S	LLP	LCC	P_{dump}	T
0.9953	0.0010	0.9943	17	108	6	18	68	0.000000	67225.33	32772.66	0.94 s
0.9937	0.0063	0.9875	16	114	6	19	63	0.000089	67029.67	35472.44	
0.9897	**0.0038**	**0.9860**	**17**	**105**	**21**	**5**	**69**	**0.000000**	**66673.07**	**31370.82**	
0.9897	0.0038	0.9860	17	105	5	21	69	0.000000	66673.07	31370.82	
0.9897	0.0038	0.9860	17	105	7	15	69	0.000000	66673.07	31370.82	
0.9850	0.0150	0.9699	2	126	6	21	69	0.000179	66544.40	38550.41	
0.9840	0.0160	0.9679	14	108	6	18	68	0.000179	66008.91	32288.38	
0.9839	0.0161	0.9679	10	114	6	19	67	0.000179	65789.76	34361.17	
0.9832	0.0165	0.9667	17	102	17	6	69	0.000096	65822.58	30010.81	
0.9762	0.0231	0.9531	17	105	7	15	65	0.000182	65480.13	31370.82	

© COPYRIGHT UPM

4.9 Results on validation of the proposed hybrid MCDM method

The BWM-TOPSIS-GDM methods are developed to in order to justifiably rank the sets of optimal PF solutions for the WT/PV/Battery system. The outcomes of the BWM-TOPSIS method based on the view of the three experts for both Malaysia and South Africa are presented in Table 4.14 (a) and Table 4.14 (b).

The 16 and 17 sets optimal PF solutions for Malaysia and South Africa are ultimately narrowed down to 10 configurations. The largest $\phi_j$values denotes to the best ideal solutions found so far. Regarding the ranked top 10 configurations, the differences in $\phi_j$values are negligible, and the clients has option to choose the configuration that best meets their needs. From Table 4.14 (a) and (b)., it can evident that most of configurations have favorable levels of dependability, with primary objective being to choose the configuration with the lowest LCC.

© COPYRIGHT UPM

Table 4.14 (a) : Ranking based on BWM-TOPSIS method for the three experts in Malaysia

Experts	WT	N	Ns	Np	Batt	LLP	LCC	P_{dump}	β_j^*	β_j^-	ϕ_j	Time
1st expert	1	104	4	26	69	0.000121	59901.97	13206.37	0.0025	0.0260	0.9137	2.12 s
	2	102	6	17	69	0.000342	59740.45	12623.91	0.0024	0.0255	0.9127	
	2	104	4	26	69	0.000121	60307.45	13247.61	0.0025	0.0260	0.9127	
	4	104	26	4	69	0.000032	61118.40	13324.97	0.0025	0.0263	0.9118	
	1	105	21	5	69	0.000000	60185.47	13548.02	0.0025	0.0263	0.9118	
	2	105	21	5	69	0.000000	60590.95	13586.22	0.0026	0.0263	0.9107	
	5	102	17	6	69	0.000342	60956.88	12677.201	0.0025	0.0255	0.9101	
	5	104	8	13	68	0.000160	61225.64	13366.74	0.0026	0.0259	0.9092	
	6	104	8	13	68	0.000121	61631.11	13383.27	0.0026	0.0260	0.9090	
	6	102	3	34	69	0.000342	61362.35	12715.86	0.0025	0.0255	0.9090	
2nd expert	1	105	3	35	63	0.000607	58396.06	13548.02	0.0025	0.0103	0.8026	0.89 s
	1	104	4	26	63	0.000800	58112.56	13231.24	0.0025	0.0101	0.8020	
	1	105	7	15	65	0.000338	58992.53	13548.018	0.0026	0.0105	0.8004	
	1	102	6	17	65	0.000916	58142.04	12602.37	0.0025	0.0100	0.8000	
	1	102	34	3	63	0.001208	57545.56	12613.15	0.0025	0.0097	0.7957	
	1	100	4	25	68	0.000988	58469.75	11850.97	0.0026	0.0099	0.7949	
	1	105	35	3	60	0.001147	57501.35	13567.19	0.0025	0.0098	0.7944	
	1	108	6	18	63	0.000208	59246.55	14571.46	0.0028	0.0106	0.7938	
	2	105	5	21	62	0.000798	58503.30	13593.87	0.0026	0.0101	0.7938	
	2	105	35	3	61	0.000923	58205.06	13593.87	0.0026	0.0100	0.7936	
3rd expert	1	105	21	5	69	0.000000	60185.47	13548.02	0.0015	0.0319	0.9545	1.10 s
	1	104	4	26	69	0.000121	59901.97	13206.37	0.0015	0.0315	0.9543	
	2	105	21	5	69	0.000000	60590.95	13586.22	0.0016	0.0319	0.9536	
	4	104	26	4	69	0.000032	61118.40	13324.97	0.0016	0.0318	0.9535	
	2	104	4	26	69	0.000121	60307.45	13247.61	0.0015	0.0315	0.9535	
	6	105	7	15	68	0.000031	61914.61	13678.84	0.0016	0.0318	0.9507	
	6	104	8	13	68	0.000121	61631.11	13383.27	0.0016	0.0315	0.9507	
	5	105	21	5	67	0.000121	61210.90	13657.08	0.0016	0.0315	0.9504	
	5	104	8	13	68	0.000160	61225.64	13366.74	0.0016	0.0314	0.9503	
	8	104	13	8	69	0.000032	62740.30	13446.26	0.0017	0.0318	0.9501	

© COPYRIGHT UPM

Table 4.14 (b) : Ranking based on BWM-TOPSIS method for the three experts the in South Africa

Experts	WT	N	Ns	Np	Batt	LLP	LCC	P_{dump}	β_j^*	β_j^-	ϕ_j	Time
1st expert	16	80	20	4	69	0.000688	59180.15	19174.16	0.0028	0.0253	0.9008	0.70 s
	15	81	3	27	69	0.000702	59058.18	19456.79	0.0028	0.0253	0.8993	
	17	81	27	3	68	0.000672	59570.89	19890.65	0.0029	0.0253	0.8987	
	16	81	3	27	69	0.000687	59463.65	19698.78	0.0029	0.0253	0.8986	
	16	84	7	12	69	0.000591	60314.15	21251.52	0.0029	0.0255	0.8972	
	14	80	4	20	69	0.000807	58369.20	18754.85	0.0029	0.0250	0.8955	
	17	87	29	3	69	0.000451	61570.11	22802.71	0.0030	0.0258	0.8951	
	16	85	5	17	69	0.000590	60597.64	21772.73	0.0030	0.0255	0.8947	
	17	77	7	11	69	0.000846	58735.14	17909.31	0.0030	0.0249	0.8940	
	16	81	3	27	68	0.000770	59165.42	19698.78	0.0030	0.0251	0.8937	
2nd expert	2	80	16	5	69	0.001606	53503.50	16403.69	0.0027	0.0105	0.7977	0.60 s
	1	81	9	9	67	0.001784	52785.05	16740.48	0.0026	0.0104	0.7975	
	2	81	3	27	69	0.001515	53787.00	16923.42	0.0027	0.0105	0.7975	
	2	81	3	27	66	0.001759	52892.29	16923.42	0.0027	0.0104	0.7972	
	2	80	10	8	68	0.001716	53205.27	16414.52	0.0027	0.0104	0.7959	
	1	81	3	27	68	0.001739	53083.29	16740.48	0.0027	0.0104	0.7959	
	3	80	5	16	66	0.001759	53014.27	16630.02	0.0027	0.0104	0.7958	
	2	81	3	27	67	0.001715	53190.53	16923.42	0.0027	0.0104	0.7955	
	1	80	20	4	69	0.001758	53098.03	16269.07	0.0027	0.0104	0.7952	
	3	80	8	10	67	0.001737	53312.51	16630.02	0.0027	0.0104	0.7927	
3rd expert	17	87	29	3	69	0.000451	61570.11	22802.71	0.0024	0.0311	0.9292	0.73 s
	16	95	5	19	69	0.000295	63432.62	26481.67	0.0024	0.0315	0.9284	
	17	96	16	6	69	0.000232	64121.59	27141.12	0.0024	0.0317	0.9284	
	17	92	23	4	69	0.000361	62987.60	25207.24	0.0024	0.0313	0.9283	
	17	88	22	4	69	0.000450	61853.61	23263.85	0.0024	0.0311	0.9282	
	16	96	6	16	69	0.000269	63716.12	26955.29	0.0024	0.0316	0.9281	
	17	96	4	24	68	0.000266	63823.36	27141.12	0.0025	0.0316	0.9277	
	17	93	31	3	68	0.000360	62972.87	25685.75	0.0024	0.0313	0.9276	
	17	98	7	14	69	0.000189	64688.59	28091.82	0.0025	0.0319	0.9270	
	15	90	10	9	69	0.000466	61609.66	23905.00	0.0025	0.0310	0.9267	

To arrive at the final decision, it is fair to apply GDM by computing the weighted mean of all experts views. It may be justified on the justified that it is unreasonable to rely just on expert and exclude the others. Therefore, it is possible to identify the most desired option in the expert's list. The sorted solutions based on BWM-TOPSIS-GDM methods for both case studies are presented in Table 15 (a) and (b). The best ideal solution is selected with the highest ϕ_j value of 0.9121, which is rated second for Malaysian scenario, and the first optimal solution with the highest ϕ_j value of 0.8848 for South African scenario; both best solutions are highlighted by black **boldface** in Table 4.15.

© COPYRIGHT UPM

Table 4.15 : (a) Ranking based on BWM-TOPSIS-GDM method in Malaysia

WT	N	Ns	Np	batt	LLP	LCC	P_{dump}	β_j^*	β_j^-	ϕ_j	Time
1	104	4	26	69	0.000121	59901.97	13206.37	0.0021	0.0227	0.9137	1.20 s
1	**105**	**21**	**5**	**69**	**0.000000**	**60185.47**	**13548.02**	**0.0022**	**0.0230**	**0.9121**	
2	104	4	26	69	0.000121	60307.45	13247.61	0.0022	0.0227	0.9116	
2	102	6	17	69	0.000342	59740.45	12623.91	0.0022	0.0222	0.9112	
2	105	21	5	69	0.000000	60590.95	13586.22	0.0023	0.0230	0.9101	
1	105	7	15	65	0.000338	58992.53	13548.02	0.0022	0.0222	0.9093	
4	104	26	4	69	0.000032	61118.40	13324.97	0.0023	0.0229	0.9088	
1	108	6	18	63	0.000208	59246.55	14571.46	0.0023	0.0225	0.9061	
5	104	8	13	68	0.000160	61225.64	13366.74	0.0023	0.0226	0.9060	
4	105	21	5	66	0.000248	60507.19	13635.53	0.0023	0.0224	0.9055	

Table 4.15 : (b) Ranking based on BWM-TOPSIS-GDM method in South Africa

WT	N	Ns	Np	batt	LLP	LCC	P_{dump}	β_j^*	β_j^-	ϕ_j	Time
16	**80**	**20**	**4**	**69**	**0.000688**	**59180.15**	**19174.16**	**0.0029**	**0.0220**	**0.8848**	0.68 s
15	81	3	27	69	0.000702	59058.18	19456.79	0.0029	0.0220	0.8841	
16	81	3	27	69	0.000687	59463.65	19698.78	0.0029	0.0220	0.8826	
17	81	27	3	68	0.000672	59570.89	19890.65	0.0029	0.0220	0.8825	
14	80	4	20	69	0.000807	58369.20	18754.85	0.0029	0.0217	0.8819	
12	81	9	9	69	0.000841	57841.75	18919.38	0.0029	0.0217	0.8817	
13	81	3	27	69	0.000824	58247.23	19051.42	0.0029	0.0217	0.8809	
16	84	7	12	69	0.000591	60314.15	21251.52	0.0030	0.0222	0.8806	
12	85	17	5	69	0.000741	58975.74	20852.74	0.0030	0.0219	0.8797	
16	81	3	27	68	0.000770	59165.42	19698.78	0.0030	0.0218	0.8791	

© COPYRIGHT UPM

From Tables 15, it can be clearly seen that the hybrid off-grid WT/PV/Battery system operates at a high degree of confidence and almost same economic outlook, while minimizing the excess energy to the greatest extent feasible. In contrast, the South Africa scenario operates at almost identical levels of system dependability and total cost. Moreover, the majority of the variables and their competing techno-economic optimization criteria are identical. Due to the usage of the BWM method in terms of weighted objectives by the three experts view and TOPSIS method in terms of ranking the ideal solutions, a trivial difference exists. Noting that this optimization problem involves several variables and non-linearity, which are directly impacted by the weighted objectives values and ranking structure. As an outcome, the picked optimum configurations are addressed based on a complete consistency ratio for both methods to guarantee that the system performance is evaluated based on very high degree of stability.

4.10 Evaluation the performance of optimal design for Malaysia and South Africa

The performance of the independent PV/WT/Battery system is assessed and verified during a one year period based on the most desired configurations selected utilizing the improved two archive-BWM-ROMEETHEE II-GDM method. For the Malaysian case study, the most desired design is consisted of a single WT, and 105 PV modules (7 in series and 15 in parallel), and 69 batteries storage with zero LLP, 60185.5 $ of LCC, and 13548.02 of P_{dump}, respectively. Therefore, the usage of the WT generator is not recommended in Malaysian zone. The monthly performance of solar radiation (W/m^2), ambient temperature ℃, WT generator (W), PV modules (KWh), SOC of the batteries (KWh), load demand (KWh), dumped energy (KWh), and deficit energy

© COPYRIGHT UPM

(KWh) is shown in Figure 4.15. The maximum and minimum conductivities of the of the solar radiation was occurred in March and December with values of 5131.5 (W/m^2) and 3779.8 (W/m^2), respectively. Therefore, the maximum produced energy by PV modules was 110.50 KWh, while the lowest energy was 79.86 KWh in November. The challenge in sizing of the off-grid PV/WT/Battery system is not only to increase the dependability and reducing the overall cost, but also to reduce the surplus energy to minimum. Thus, the values of the Pdump for the aforementioned dates were 56.13 KWh and 23.59 KWh, respectively. The minimum and maximum conductivities of the WT were occurred in January and June with values of 39 W and 106.32 W. The large number of the batteries storage plays a crucial rule in boosting dependability, lowering overall cost, and keeping the lost energy at minimum, where the SOC levels are high throughout the year and there is no deficit energy.

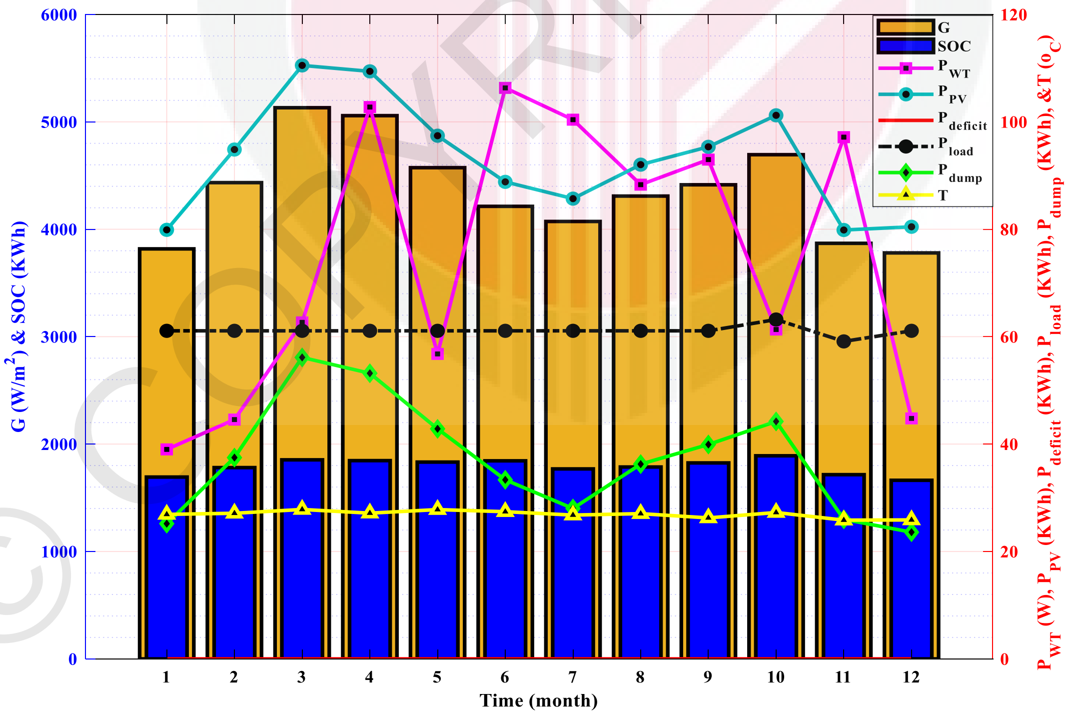

Figure 4.15 : Monthly performance of the G, T, P_{WT}, P_{PV}, SOC, P_{load}, P_{dump}, and $P_{deficit}$ during a one year period in Malaysia

On the other hand, the most desirable selected design of the independent PV/WT/Battery system for the South Africa case study is composed of 17 WT generators, 105 PV modules (21 in series and 5 in parallel), and 69 batteries storage with zero LLP, 66673.07 $ of LCC, and 31370.82 of P_{dump}, respectively. The monthly performance based on the optimum design for the G (W/m^2), T ℃, WT generator (KWh), PV modules (KWh), SOC of the batteries (KWh), P_{load} (KWh), P_{dump} (KWh), and $P_{deficit}$ (KWh) is illustrated in Figure 4.16. The highest and lowest solar radiation levels were 7028.93 (W/m^2) and 3906.66 (W/m^2) in December and June, respectivly. For the aforementioned dates, the conductivity of the PV modules were 167.23 KWh and 87.77 KWh, while the wasted energy were 122.29 KWh and 38.53 KWh, respectively. As previously indicated, the WTs have made a significant contribution in increasing the reliabily, cutting total costs, and reducing the surplus energy of the system, where its maximum and minmim conductivies recorded in October and May, respectivly, with values of 14 KWh and 5.82 KWh. As a result, the aim of the study is to select the most desirable configuration by merging improved two archeive mathod with BWM-PROMETHEE II-GDM method in order to maximize reliability, deccrease overall cost, and minimize the surplus energy.

© COPYRIGHT UPM

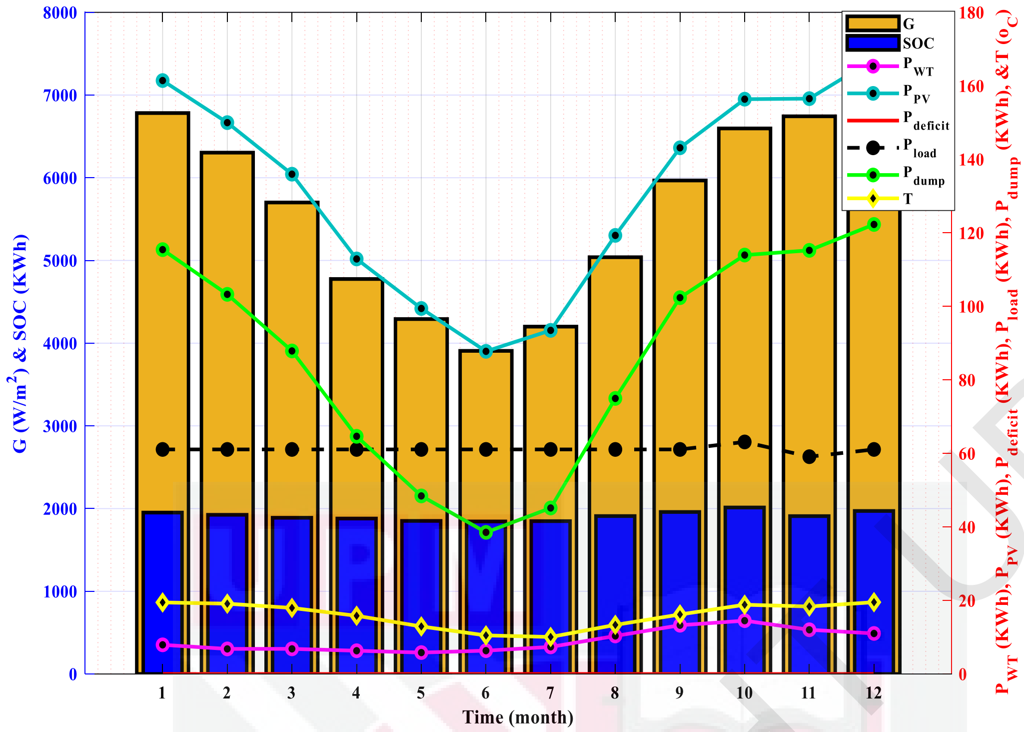

Figure 4.16 : Monthly performance of the G, T, P_{WT}, P_{PV}, SOC, P_{load}, P_{dump}, and $P_{deficit}$ during a one year period in South Africa

The simulation starts synchronously computing the three objectives: LLP, LCC, and P_{dump}, respectively for input variables came from optimization algorithm. The best optimum configurations based on BWM-PROMETHEE II-GDM approach is obtained to assess the performance of the WT/PV/Battery system during a one-year period in Malaysia and South Africa as shown in Figures 4.17 and 4.18. In Malaysian scenario, the total energy generated by a single WT, referred by purple color, during one year is 27.31 KWh, while the energy generated by 105 PV modules, referred by dark orange color, is 3.3902e^4 KWh. As can be clearly seen, the PV modules are far recommended for meeting the required load demand in Malaysia than wind turbine installation. The total energy needed to meet the load demand during the same period of time is 22.298 KWh as demonstrated in Figure 4.17. The storage batteries ensure that the reliability of the system operates at very high degree of assurance throughout the year without any deficit energy, with energy stored in the storage batteries totaling $6.5364e^5$ KWh. The dump's energy content is $1.3548e^4$ KWh, as seen by green hue. At 1 WT, 105 PV modules, and 69 storage batteries, the freestanding WT/PV/Battery regimen performs excellently in terms of availability, overall cost, and surplus energy.

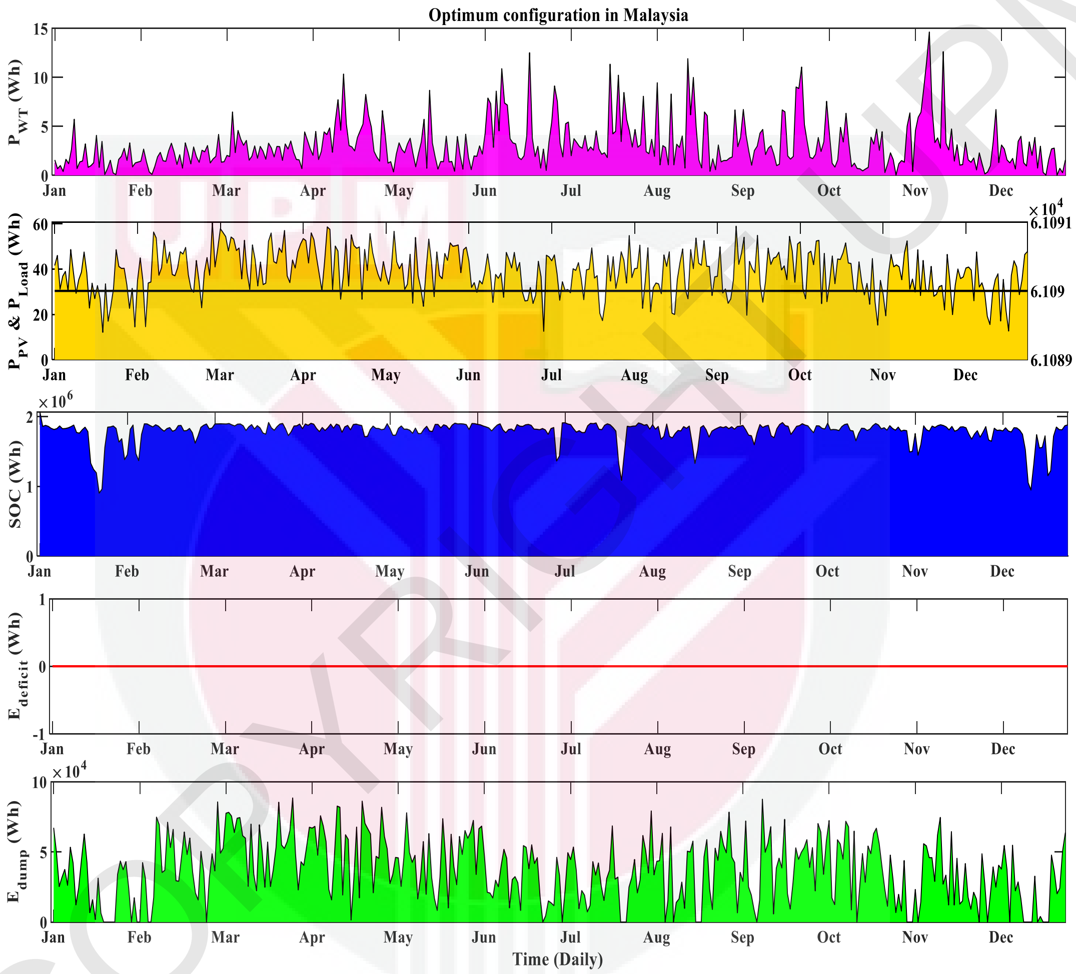

Figure 4.17 : Daily productivity of the optimal design of the WT/PV/Battery regimen in Malaysia

In the South African scenario, the total energy carried by the 17 WT is $3.308e^3$ KWh, whereas the total energy generated by 105 PV modules is $4.814e^4$ KWh. WT generators can notably help to strengthening the dependability of the WT/PV/Battery system, as well as PV modules and storage batteries. Bearing in mind that increasing

© COPYRIGHT UPM

the number of the PV modules above the optimum number results in an increase in the system's capital cost and wasted energy. Therefore, the optimum amount of the WT and PV modules should be carefully addressed to prevent over- or under-sizing. With 69 number of storage batteries, the energy produced by the storage batteries over a year is $6.979e^5$ KWh. As demonstrated in Figure 4.18, there is no deficit energy during the year based on the optimum design, whilst the dump energy is $3.137e^4$ KWh. According to earlier findings, the optimum designs in both Malaysia and South Africa are strongly reliant on the availability of the solar irradiance and wind speed ratio.

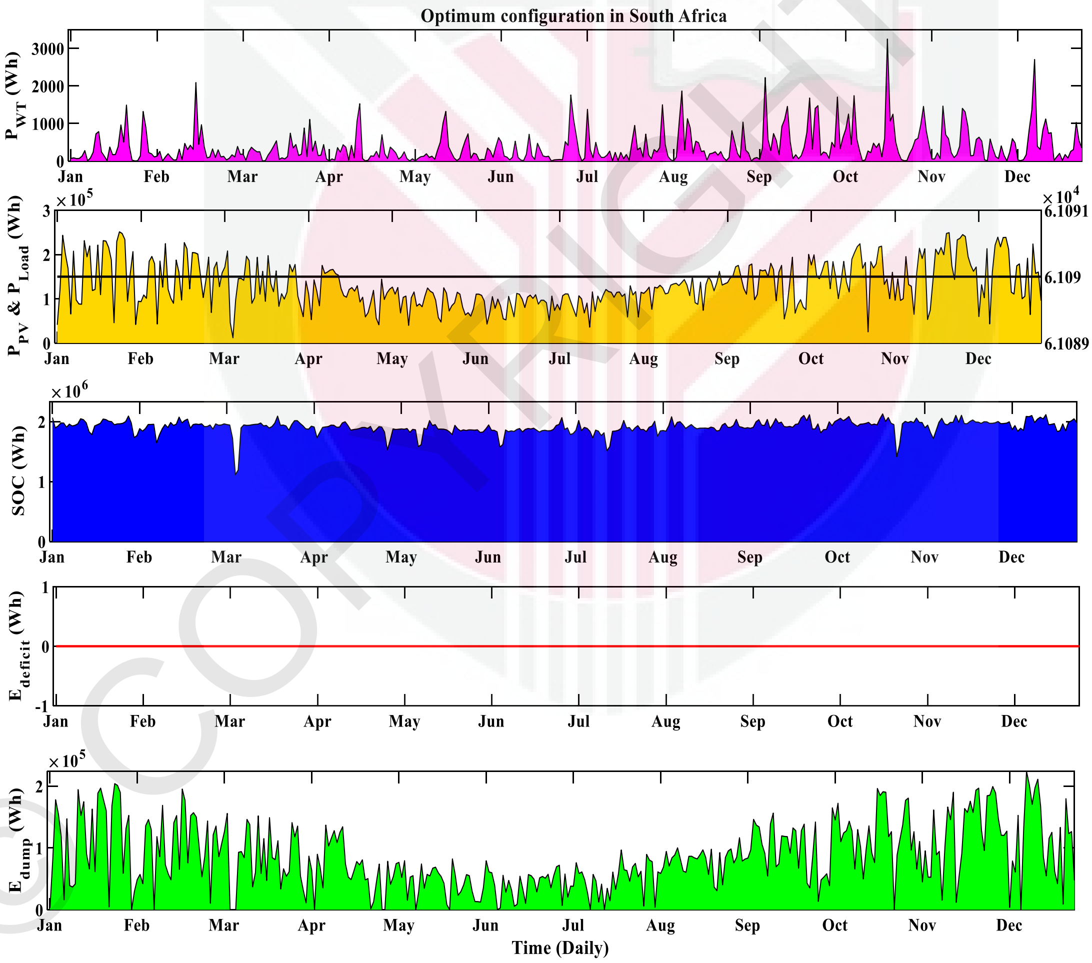

Figure 4.18 : Daily productivity of the optimal design of the WT/PV/Battery regimen in South Africa

© COPYRIGHT UPM

4.11 Summary

In this chapter, an innovative $\text{RaAOA}_{\text{AdBHHH}}$ model for accurately determining the parameter of the TD PV model utilizing experimental data form Kyocera (KC120-1) and R.T.C France PV modules. The results of the proposed $\text{RaAOA}_{\text{AdBHHH}}$ model were validated by comparing it to well-known published approaches using numerous statistical criteria. The proposed approach made significant advances in terms of methodology (algorithm itself) and design of the objective function. In terms of methodology, the IOBL was maintained to prevent local minima while TL is obtained to improve the local search capability. Secondly, the exploration stage was developed by the use of complement $\overline{D}$ and S operators, along with CMM and LF techniques. Besides, the exploitation stage was augmented via the use of $\overline{M}$ and A operators, as well as three unique vectors picked randomly from the population. Finally, winner principle was considered, which is based on two robust mutation procedures, in order to gradually improve the search capability. The $\text{RaAOA}_{\text{AdBHHH}}$ model's objective function was introduced for the first time for resolving the PV model's equation and to efficiently predict the initial roots of the PV models utilizing only first order derivative and half space expectation movements. With the exception of the CPU processing time, the experimental results indicated that the proposed $\text{RaAOA}_{\text{AdBHHH}}$ beats all well-published models in terms of accuracy, reliability, and convergence rate.

In the second phase of this thesis, a new fusion based on improved bi-archive multi-objective optimization algorithm for findings four well-constructed groups of optimal PF solutions and BWM-PROMETHEE II-GDM for sorting and ranking the optimized designs of the freestanding PV/WT/Battery system in two different locations: Malaysia and South Africa. The most desirable configurations for the freestanding

© COPYRIGHT UPM

PV/WT/Battery system are determined based on techno-economic-reliability assessments: LLP, LCC, and P_{dump} using hourly meteorological data over the course of one year. Full consistency ratios of the experts' judgements are attained using the BWM, along with a high stability of the outstanding PROMETHEE II procedure for rating the top ten configurations. The best optimal solution in Malaysia consists of a single WT, and 105 PV modules (7 in series and 15 in parallel), and 69 batteries storage with zero LLP, 60185.5 $ of LCC, and 13548.02 of P_{dump}, respectively. Therefore, the employment of WT in this scenario is not recommended. In South Africa case study, the best optimal configuration composes of 17 WT generators, 105 PV modules (21 in series and 5 in parallel), and 69 batteries storage with zero LLP, 66673.07 $ of LCC, and 31370.82 of P_{dump}, respectively. This scenario stated that the WTs may considerably incoorpatrate as in supplying energy for the required load demand. The integration of the hybrid numerical BWM-TOPSIS-GDM approach is utilized to verify the improved bi-archive-BWM-PROMETHEE II-GDM approach. The results indicated that both aforementioned hybrid methods can be applied to find the most suitable design for the PV/WT/Battery system at any site. However, the PROMETHEE II offers a high stability and less sensitivity rather than TOPSIS method, owning to the simple normalization of the TOPSIS method.

© COPYRIGHT UPM

CHAPTER 5

CONCLUSION AND FUTURE WORK

5.1 Conclusion

In this thesis, the parameters determination of the TD PV model and optimal sizing of the WT/PV/Battery system have been presented and the results are discussed. According to the findings, the following conclusion are carried out.

The $\text{RaAOA}_{\text{AdBHHH}}$ model was presented to optimally estimated unknown parameters of the TD PV model using two sets of the experimental data under various environmental conditions. First, an improved generalized opposition based learning and teacher learning are proposed to mitigate the premature convergence and low-quality of solutions. Moreover, complements of the $\overline{D}$ and $\overline{M}$ operators are employed to generate more desirable solutions rather than using the simple D and M operators of the AOA. In addition, complement $\overline{D}$ and S operators are retained to perform exploratory mechanism in the early stages of the optimization process, while complement $\overline{M}$ and A operators execute the exploitation phase in order to maintain a balance between the explorer-exploiter tactics. Furthermore, the CMM algorithm and LF mechanism are proposed to address information from rotated solutions and stagnation in local minima avoidance. Finally, the winner concept based on two mutant schemes is used to ensure globally solutions during the optimization process. The objective function is further developed by using BHHH algorithm, which can roughly search for the initial root solutions in the feature space with minimum number of iterations. Additionally, a nonlinear damping parameter of the LM technique is proposed to reduce the oscillations and noises in the PV model and to simulate its

© COPYRIGHT UPM

outdoor behavior. Finally, only first order derivative of the NR method is considered to simply the computations with guaranteed convergence. The results of the proposed $RaAOA_{AdBHHH}$ model the error is reduced to zero for both of sets of the experimental data and accurately predict the output current of the PV model. With the exception of the CPU processing time, the experimental results indicated that the proposed $RaAOA_{AdBHHH}$ beats all well-published models in terms of accuracy, reliability, and convergence rate.

In the second phase of this thesis, a unique improved bi-archive approach is presented to develop the diversity and convergence independently in order to find four optimum sets of PF solutions. In addition, a new integration based on best worst method (BWM) and preference ranking organization for enrichment evaluations (PROMETHEE II) method along with group decision making (GDM) mechanism are addressed to sort and rank the optimal sets PF solutions with full consistency ratios of the three experts opinions and high degree of stability in ranking configurations. The theoretical results based on actual hourly meteorological data in Malaysia and South Africa indicated that the suggested improved two-archive-BWM-PROMETHEE II-GDM method is not only able to construct a uniform set of Pareto optimal solutions with fast convergence and high diversity, but can also rank and select the most desired design for the PV/WT/Battery system. The most desirable configurations for the freestanding PV/WT/Battery system are determined based on techno-economic-reliability assessments: LLP, LCC, and P_{dump} indicators. The best optimal solution in Malaysia consists of a single WT, and 105 PV modules (7 in series and 15 in parallel), and 69 batteries storage with zero LLP, 60185.5 \$ of LCC, and 13548.02 of P_{dump}, respectively. Therefore, the employment of WT in this scenario is not recommended.

© COPYRIGHT UPM

In South Africa case study, the best optimal configuration composes of 17 WT generators, 105 PV modules (21 in series and 5 in parallel), and 69 batteries storage with zero LLP, 66673.07 $ of LCC, and 31370.82 of P_{dump}, respectively. This scenario stated that the WTs may considerably incoorpatrate as in supplying energy for the required load demand. The integration of the hybrid numerical BWM-PROMETHEE II-GDM and BWM-TOPSIS-GDM approaches are utilized to verify the improved bi-archive-BWM-PROMETHEE II-GDM approach. The results indicated that both aforementioned hybrid methods can be applied to find the most suitable design for the PV/WT/Battery system at any site. However, the PROMETHEE II offers a high stability and less sensitivity rather than TOPSIS method, owning to the simple normalization of the TOPSIS method.

5.2 Future Work

The research studies carried out in developing new method to estimate the parameters of the TD PV mode using two sets of the experimental data at various weather conditions. In addition to that an improved two-archive-BWM-PROMETHEE II-GDM method to select the most desirable solution for the WT/PV/Battery system for the two case studies: Malaysia and South Africa. However, more advancement of this research study can be accomplished by the following future directions:

1. The parameters extraction of the PV model can be optimized using multi-objective optimization problem by solving the PV mode's equation in terms of current and voltage outputs.
2. The optimization of the WT/PV/Battery system can be further developed by considering the grid-connected system. It can significantly increase the investment of the employing renewable energy sources with considering the feedback time for returning the total cost of the system.

© COPYRIGHT UPM

3. Hybrid energy storage such as hydrogen fuel cell (HFC) can be investigated in order to increase the reliability, lowering the total cost, and reduce the wasted energy.

© COPYRIGHT UPM

REFERENCES

[256] Borhanazad, H., Mekhilef, S., Ganapathy, V. G., Modiri-Delshad, M., & Mirtaheri, A. (2014). Optimization of micro-grid system using MOPSO. *Renewable energy, vol. 71*, pp.295-306.

Abbassi, A., Mehrez, R. B., Abbassi, R., Saidi, S., Albdran, S., & Jemli, M. (2022). Improved off-grid wind/photovoltaic/hybrid energy storage system based on new framework of Moth-Flame optimization algorithm. *International Journal of Energy Research, vol. 46, no.* 5, pp.6711-6729.

Abbassi, A., Mehrez, R. B., Abbassi, R., Saidi, S., Albdran, S., & Jemli, M. (2022). Improved off-grid wind/photovoltaic/hybrid energy storage system based on new framework of Moth-Flame optimization algorithm. *International Journal of Energy Research, vol. 46, no.* 5, pp.6711-6729.

Abbassi, R., Abbassi, A., Jemli, M., & Chebbi, S. (2018). Identification of unknown parameters of solar cell models: A comprehensive overview of available approaches. *Renewable and Sustainable Energy Reviews*, vol. *90*, pp.453-474.

Abbes, D., Martinez, A., & Champenois, G. (2014). Life cycle cost, embodied energy and loss of power supply probability for the optimal design of hybrid power systems. *Mathematics and Computers in Simulation*, *vol. 98*, pp.46-62.

Abdel-Basset, M., El-Shahat, D., Chakrabortty, R. K., & Ryan, M. (2021). Parameter estimation of photovoltaic models using an improved marine predators algorithm. *Energy Conversion and Management, vol. 227*, pp.113491.

Abdel-Basset, M., Mohamed, R., El-Fergany, A., Abouhawwash, M., & Askar, S. S. (2021). Parameters identification of PV triple-diode model using improved generalized normal distribution algorithm. *Mathematics*, *vol. 9*, no. 9, pp.995.

Abdel-Basset, M., Mohamed, R., El-Fergany, A., Askar, S. S., & Abouhawwash, M. (2021). Efficient ranking-based whale optimizer for parameter extraction of three-diode photovoltaic model: Analysis and validations. *Energies*, *vol. 14,* no. 13, pp. 3729.

Abdulrazzaq, A. K., Bognár, G., & Plesz, B. (2020). Evaluation of different methods for solar cells/modules parameters extraction. *Solar Energy*, *vol. 196*, pp.183-195.

Abualigah, L., Diabat, A., Mirjalili, S., Abd Elaziz, M., & Gandomi, A. H. (2021). The arithmetic optimization algorithm. *Computer methods in applied mechanics and engineering*, *vol. 376*, pp.113609.

© COPYRIGHT UPM

Afrouzi, H. N., Hassan, A., Wimalaratna, Y. P., Ahmed, J., Mehranzamir, K., Liew, S. C., & Malek, Z. A. (2021). Sizing and economic analysis of stand-alone hybrid photovoltaic-wind system for rural electrification: A case study Lundu, Sarawak. *Cleaner engineering and technology*, vol. *4*, pp.100191.

Agwa, A. M., El-Fergany, A. A., & Maksoud, H. A. (2020). Electrical characterization of photovoltaic modules using farmland fertility optimizer. *Energy conversion and management*, *vol. 217*, pp.112990.

Agwa, A. M., El-Fergany, A. A., & Maksoud, H. A. (2020). Electrical characterization of photovoltaic modules using farmland fertility optimizer. *Energy conversion and management*, *vol. 217*, pp.112990.

Ahmadi, S., & Abdi, S. (2016). Application of the Hybrid Big Bang–Big Crunch algorithm for optimal sizing of a stand-alone hybrid PV/wind/battery system. *Solar Energy*, *vol. 134*, pp.366-374.

Akram, M., Noreen, U., & Pamucar, D. (2023). Extended PROMETHEE approach with 2-tuple linguistic m-polar fuzzy sets for selection of elliptical cardio machine. *Expert Systems*, *vol. 40*, no. 3, pp. e13178.

Alam, D. F., Yousri, D. A., & Eteiba, M. B. (2015). Flower pollination algorithm based solar PV parameter estimation. *Energy Conversion and Management*, *vol. 101*, pp.410-422.

Al-Falahi, M. D., Jayasinghe, S. D. G., & Enshaei, H. J. E. C. (2017). A review on recent size optimization methodologies for standalone solar and wind hybrid renewable energy system. *Energy conversion and management*, *vol. 143*, pp.252-274.

Alghamdi, M. A., Khan, M. F. N., Khan, A. K., Khan, I., Ahmed, A., Kiani, A. T., & Khan, M. A. (2021). PV model parameter estimation using modified FPA with dynamic switch probability and step size function. *IEEE Access*, vol. *9*, pp.42027-42044.

Alghamdi, M. A., Khan, M. F. N., Khan, A. K., Khan, I., Ahmed, A., Kiani, A. T., & Khan, M. A. (2021). PV model parameter estimation using modified FPA with dynamic switch probability and step size function. *IEEE Access*, vol. *9*, pp.42027-42044.

Ali, E. E., El-Hameed, M. A., El-Fergany, A. A., & El-Arini, M. M. (2016). Parameter extraction of photovoltaic generating units using multi-verse optimizer. *Sustainable Energy Technologies and Assessments*, *vol. 17*, pp. 68-76.

AliExpress, (accessed June 7, 2022), Available online: https://www.aliexpress.com/item/1005002185320613.html.

Anoune, K., Bouya, M., Astito, A., & Abdellah, A. B. (2018). Sizing methods and optimization techniques for PV-wind based hybrid renewable energy system: A review. *Renewable and Sustainable Energy Reviews*, *vol. 93*, pp.652-673.

© COPYRIGHT UPM

Anoune, K., Ghazi, M., Bouya, M., Laknizi, A., Ghazouani, M., Abdellah, A. B., & Astito, A. (2020). Optimization and techno-economic analysis of photovoltaic-wind-battery based hybrid system. *Journal of Energy Storage*, vol. *32*, pp.101878.

Appelbaum, J., & Peled, A. (2014). Parameters extraction of solar cells–A comparative examination of three methods. *Solar energy materials and solar cells*, *vol. 122*, pp.164-173.

Ayang, A., Wamkeue, R., Ouhrouche, M., Saad, M., Andy Tameghe, T., Deli, K., & Tchakoua Takoutsing, P. (2021). Least square estimator and IEC-60891 procedure for parameters estimation of single-diode model of photovoltaic generator at standard test conditions (STC). *Electrical Engineering*, *vol. 103*, pp.1253-1264.

Azab, M. (2015, March). Identification of one-diode model parameters of PV devices from nameplate information using particle swarm and least square methods. In *2015 First Workshop on Smart Grid and Renewable Energy (SGRE)* (pp. 1-6). IEEE.

Azimoh, C. L., Klintenberg, P., Wallin, F., Karlsson, B., & Mbohwa, C. (2016). Electricity for development: Mini-grid solution for rural electrification in South Africa. *Energy Conversion and Management*, *vol. 110*, pp.268-277.

Azimoh, C. L., Wallin, F., Klintenberg, P., & Karlsson, B. (2014). An assessment of unforeseen losses resulting from inappropriate use of solar home systems in South Africa. *Applied energy*, vol. *136*, pp.336-346.

Babu, T. S., Ram, J. P., Sangeetha, K., Laudani, A., & Rajasekar, N. (2016). Parameter extraction of two diode solar PV model using Fireworks algorithm. *Solar energy*, *vol. 140*, pp.265-276.

Bai, J., Liu, S., Hao, Y., Zhang, Z., Jiang, M., & Zhang, Y. (2014). Development of a new compound method to extract the five parameters of PV modules. *Energy Conversion and Management*, vol. *79*, pp.294-303.

Bansal, A. K. (2022). Sizing and forecasting techniques in photovoltaic-wind based hybrid renewable energy system: A review. *Journal of Cleaner Production*, *vol. 369*, pp.133376.

Bañuelos-Ruedas, F., Angeles-Camacho, C., & Rios-Marcuello, S. (2010). Analysis and validation of the methodology used in the extrapolation of wind speed data at different heights. *Renewable and Sustainable Energy Reviews*, *vol. 14*, no. 8, pp.2383-2391.

Barakat, S., Ibrahim, H., & Elbaset, A. A. (2020). Multi-objective optimization of grid-connected PV-wind hybrid system considering reliability, cost, and environmental aspects. *Sustainable Cities and Society*, vol. *60*, pp.102178.

© COPYRIGHT UPM

Barzegarkhoo, R., Moradzadeh, M., Zamiri, E., Kojabadi, H. M., & Blaabjerg, F. (2017). A new boost switched-capacitor multilevel converter with reduced circuit devices. *IEEE Transactions on Power Electronics, vol. 33, no.* 8, pp.6738-6754.

Batzelis, E. I., Routsolias, I. A., & Papathanassiou, S. A. (2013). An explicit PV string model based on the lambert $ W $ function and simplified MPP expressions for operation under partial shading. *IEEE Transactions on Sustainable Energy*, vol. *5*, no. 1, pp.301-312.

Belouda, M., Hajjaji, M., Sliti, H., & Mami, A. (2018). Bi-objective optimization of a standalone hybrid PV–Wind–battery system generation in a remote area in Tunisia. *Sustainable Energy, Grids and Networks*, *vol. 16*, pp.315-326.

Bencherif, M., & Brahmi, N. (2022). Solar cell parameter identification using the three main points of the current–voltage characteristic. *International Journal of Ambient Energy*, vol. *43, no.* 1, pp.3064-3084.

Biswas, P. P., Suganthan, P. N., Wu, G., & Amaratunga, G. A. (2019). Parameter estimation of solar cells using datasheet information with the application of an adaptive differential evolution algorithm. *Renewable energy*, *vol. 132*, pp.425-438.

Borowy, B. S., & Salameh, Z. M. (1996). Methodology for optimally sizing the combination of a battery bank and PV array in a wind/PV hybrid system. *IEEE Transactions on energy conversion*, *vol. 11*, *no.* 2, pp.367-375.

Bouchekara, H. R. E. H., Javaid, M. S., Shaaban, Y. A., Shahriar, M. S., Ramli, M. A. M., & Latreche, Y. (2021). Decomposition based multiobjective evolutionary algorithm for PV/Wind/Diesel Hybrid Microgrid System design considering load uncertainty. *Energy Reports*, vol. *7*, pp.52-69.

Brano, V. L., & Ciulla, G. (2013). An efficient analytical approach for obtaining a five parameters model of photovoltaic modules using only reference data. *Applied Energy*, *vol. 111*, pp.894-903.

Brans, J. P., Vincke, P., & Mareschal, B. (1986). How to select and how to rank projects: The PROMETHEE method. *European journal of operational research*, *vol. 24, no.* 2, pp.228-238.

Brauers, W. K., & Zavadskas, E. K. (2006). The MOORA method and its application to privatization in a transition economy. *Control and cybernetics, vol. 35, no.* 2, pp.445-469.

Büyüközkan, G., & Çifçi, G. (2012). A novel hybrid MCDM approach based on fuzzy DEMATEL, fuzzy ANP and fuzzy TOPSIS to evaluate green suppliers. *Expert Systems with Applications*, *vol. 39, no.* 3, pp.3000-3011.

© COPYRIGHT UPM

Ćalasan, M., Aleem, S. H. A., & Zobaa, A. F. (2020). On the root mean square error (RMSE) calculation for parameter estimation of photovoltaic models: A novel exact analytical solution based on Lambert W function. *Energy conversion and management*, *vol. 210*, pp.112716.

Chaibi, Y., Salhi, M., El-Jouni, A., & Essadki, A. (2018). A new method to extract the equivalent circuit parameters of a photovoltaic panel. *Solar Energy*, *vol. 163*, 376-386.

Chauhan, A., & Prakash, S. (2021). A new emperor penguin optimisation-based approach for solar photovoltaic parameter estimation. *International Transactions on Electrical Energy Systems*, vol. *31*, no. 7, pp.e12917.

Chen, S., Farkoush, S. G., & Leto, S. (2020). Photovoltaic cells parameters extraction using variables reduction and improved shark optimization technique. *International Journal of Hydrogen Energy*, *vol. 45*, *no.* 16, pp.10059-10069.

Chen, T. Y. (2019). A novel PROMETHEE-based method using a Pythagorean fuzzy combinative distance-based precedence approach to multiple criteria decision making. *Applied Soft Computing*, vol. *82*, pp.105560.

Chen, X., Tianfield, H., Du, W., & Liu, G. (2016). Biogeography-based optimization with covariance matrix based migration. *Applied Soft Computing*, *vol. 45*, pp.71-85.

Chen, Y., Sun, Y., & Meng, Z. (2018). An improved explicit double-diode model of solar cells: Fitness verification and parameter extraction. *Energy conversion and management*, *vol. 169*, pp.345-358.

Cheng, R., Jin, Y., Olhofer, M., & Sendhoff, B. (2016). A reference vector guided evolutionary algorithm for many-objective optimization. *IEEE Transactions on Evolutionary Computation*, *vol. 20*, *no.* 5, pp.773-791.

Chin, V. J., & Salam, Z. (2019). Coyote optimization algorithm for the parameter extraction of photovoltaic cells. *Solar Energy*, vol. *194*, pp.656-670.

Chin, V. J., Salam, Z., & Ishaque, K. (2016). An accurate modelling of the two-diode model of PV module using a hybrid solution based on differential evolution. *Energy conversion and management*, *vol. 124*, pp.42-50.

Chiu, W. Y., Tzeng, G. H., & Li, H. L. (2013). A new hybrid MCDM model combining DANP with VIKOR to improve e-store business. *Knowledge-based systems*, *vol. 37*, pp.48-61.

Coello, C. C., & Lechuga, M. S. (2002, May). MOPSO: A proposal for multiple objective particle swarm optimization. In *Proceedings of the 2002 Congress on Evolutionary Computation. CEC'02 (Cat. No. 02TH8600)* (Vol. 2, pp. 1051-1056). IEEE.

© COPYRIGHT UPM

Cui, Y., Geng, Z., Zhu, Q., & Han, Y. (2017). Multi-objective optimization methods and application in energy saving. *Energy*, *vol. 125*, pp.681-704.

Dehghanzadeh, A., Farahani, G., & Maboodi, M. (2017). A novel approximate explicit double-diode model of solar cells for use in simulation studies. *Renewable energy*, *vol. 103*, pp. 468-477.

Derick, M., Rani, C., Rajesh, M., Farrag, M. E., Wang, Y., & Busawon, K. (2017). An improved optimization technique for estimation of solar photovoltaic parameters. *Solar Energy*, *vol. 157*, pp.116-124.

Dhabi, A. (2020). Irena. *Renewable energy statistics*. Available online: https://www.irena.org/media/files/irena/agency/publication/2019/dec/irena_rra_azerbaijan_2019.pdf

Diaf, S., Diaf, D., Belhamel, M., Haddadi, M., & Louche, A. (2007). A methodology for optimal sizing of autonomous hybrid PV/wind system. *Energy policy*, *vol. 35, no.* 11, pp.5708-5718.

Dizqah, A. M., Maheri, A., & Busawon, K. (2014). An accurate method for the PV model identification based on a genetic algorithm and the interior-point method. *Renewable Energy*, *vol. 72*, pp.212-222.

Dkhichi, F., Oukarfi, B., Fakkar, A., & Belbounaguia, N. (2014). Parameter identification of solar cell model using Levenberg–Marquardt algorithm combined with simulated annealing. *Solar Energy*, *vol. 110*, pp.781-788.

Dkhichi, F., Oukarfi, B., Fakkar, A., & Belbounaguia, N. (2014). Parameter identification of solar cell model using Levenberg–Marquardt algorithm combined with simulated annealing. *Solar Energy*, *vol. 110*, pp.781-788.

Dufo-López, R., Bernal-Agustín, J. L., Yusta-Loyo, J. M., Domínguez-Navarro, J. A., Ramírez-Rosado, I. J., Lujano, J., & Aso, I. (2011). Multi-objective optimization minimizing cost and life cycle emissions of stand-alone PV–wind–diesel systems with batteries storage. *Applied Energy*, *vol. 88*, no. 11, pp.4033-4041.

e Silva, D. P., Salles, J. L. F., Fardin, J. F., & Pereira, M. M. R. (2020). Management of an island and grid-connected microgrid using hybrid economic model predictive control with weather data. *Applied energy*, *vol. 278*, pp.115581.

Easwarakhanthan, T., Bottin, J., Bouhouch, I., & Boutrit, C. (1986). Nonlinear minimization algorithm for determining the solar cell parameters with microcomputers. *International journal of solar energy*, *vol. 4*, no. 1, pp. 1-12.

Easwarakhanthan, T., Bottin, J., Bouhouch, I., & Boutrit, C. (1986). Nonlinear minimization algorithm for determining the solar cell parameters with microcomputers. *International journal of solar energy*, *vol. 4, no.* 1, pp.1-12.

© COPYRIGHT UPM

Ekren, B. Y., & Ekren, O. (2009). Simulation based size optimization of a PV/wind hybrid energy conversion system with battery storage under various load and auxiliary energy conditions. *Applied Energy*, *vol. 86*, *no.* 9, pp.1387-1394.

El Achouby, H., Zaimi, M., Ibral, A., & Assaid, E. M. (2018). New analytical approach for modelling effects of temperature and irradiance on physical parameters of photovoltaic solar module. *Energy conversion and management*, *vol. 177*, pp.258-271.

Elbaset, A. A., Ali, H., & Abd-El Sattar, M. (2014). Novel seven-parameter model for photovoltaic modules. *Solar energy materials and Solar cells*, *vol. 130*, pp.442-455.

El-Fergany, A. A. (2021). Parameters identification of PV model using improved slime mould optimizer and Lambert W-function. *Energy Reports*, *vol. 7*, pp.875-887.

El-Fergany, A. A. (2021). Parameters identification of PV model using improved slime mould optimizer and Lambert W-function. Energy Rep vol. 7, pp.875–887.

El-Hameed, M. A., Elkholy, M. M., & El-Fergany, A. A. (2020). Three-diode model for characterization of industrial solar generating units using Manta-rays foraging optimizer: Analysis and validations. *Energy conversion and management*, *vol. 219*, pp.113048.

Elkholy, M. M., El-Hameed, M. A., & El-Fergany, A. A. (2021). Artificial ecosystem-based optimiser to electrically characterise PV generating systems under various operating conditions reinforced by experimental validations. *IET Renewable Power Generation*, *vol. 15, no.* 3, pp.701-715.

Emovon, I., & Oghenenyerovwho, O. S. (2020). Application of MCDM method in material selection for optimal design: A review. *Results in Materials*, *vol. 7*, pp.100115.

Essalaimeh, S., Al-Salaymeh, A., & Abdullat, Y. (2013). Electrical production for domestic and industrial applications using hybrid PV-wind system. *Energy conversion and management*, *vol. 65*, pp.736-743.

Farhoodnea, M., Mohamed, A., Khatib, T., & Elmenreich, W. (2015). Performance evaluation and characterization of a 3-kWp grid-connected photovoltaic system based on tropical field experimental results: new results and comparative study. *Renewable and Sustainable Energy Reviews*, *vol. 42*, pp.1047-1054.

Fathy, A. (2016). A reliable methodology based on mine blast optimization algorithm for optimal sizing of hybrid PV-wind-FC system for remote area in Egypt. *Renewable energy*, vol. *95*, pp.367-380.

Fathy, A., & Rezk, H. (2017). Parameter estimation of photovoltaic system using imperialist competitive algorithm. *Renewable Energy*, *vol. 111*, pp.307-320.

© COPYRIGHT UPM

Ferrer-Martí, L., Domenech, B., García-Villoria, A., & Pastor, R. (2013). A MILP model to design hybrid wind–photovoltaic isolated rural electrification projects in developing countries. *European Journal of Operational Research, vol. 226, no.* 2, pp.293-300.

Fetanat, A., & Khorasaninejad, E. (2015). Size optimization for hybrid photovoltaic–wind energy system using ant colony optimization for continuous domains based integer programming. *Applied Soft Computing*, vol. *31*, pp.196-209.

Gao, X., Cui, Y., Hu, J., Tahir, N., & Xu, G. (2018). Performance comparison of exponential, Lambert W function and Special Trans function based single diode solar cell models. *Energy conversion and management*, *vol. 171*, pp.1822-1842.

Gao, X., Cui, Y., Hu, J., Xu, G., & Yu, Y. (2016). Lambert W-function based exact representation for double diode model of solar cells: Comparison on fitness and parameter extraction. *Energy conversion and management*, *vol. 127*, pp.443-460.

Ghani, F., Rosengarten, G., & Duke, M. (2016). The characterisation of crystalline silicon photovoltaic devices using the manufacturer supplied data. *Solar Energy, vol. 132*, pp.15-24.

Gharavi, H., Ardehali, M. M., & Ghanbari-Tichi, S. (2015). Imperial competitive algorithm optimization of fuzzy multi-objective design of a hybrid green power system with considerations for economics, reliability, and environmental emissions. *Renewable Energy*, vol. *78*, pp.427-437.

Ghorbani, N., Kasaeian, A., Toopshekan, A., Bahrami, L., & Maghami, A. (2018). Optimizing a hybrid wind-PV-battery system using GA-PSO and MOPSO for reducing cost and increasing reliability. *Energy*, vol. *154*, pp.581-591.

Giallanza, A., Porretto, M., Puma, G. L., & Marannano, G. (2018). A sizing approach for stand-alone hybrid photovoltaic-wind-battery systems: A Sicilian case study. *Journal of Cleaner Production*, *vol. 199*, pp.817-830.

Gibson, J. A., Kennedy, W. K., & Gibbard, R. W. (1979). Two's complement circuit word division. *Computers & Electrical Engineering*, vol. *6*, no. 4, pp.249-258.

Gioutsos, D. M., Blok, K., van Velzen, L., & Moorman, S. (2018). Cost-optimal electricity systems with increasing renewable energy penetration for islands across the globe. *Applied energy*, *vol. 226*, pp.437-449.

Gnetchejo, P. J., Essiane, S. N., Dadjé, A., & Ele, P. (2021). A combination of Newton-Raphson method and heuristics algorithms for parameter estimation in photovoltaic modules. *Heliyon*, *vol. 7*, no. 4.

© COPYRIGHT UPM

Gnetchejo, P. J., Ndjakomo Essiane, S., Dadjé, A., Ele, P., Mbadjoun Wapet, D. E., Perabi Ngoffe, S., & Chen, Z. (2021). A self-adaptive algorithm with Newton Raphson method for parameters identification of photovoltaic modules and array. *Transactions on Electrical and Electronic Materials*, *vol. 22,* pp.869-888.

Gomes, R. C. M., Vitorino, M. A., de Rossiter Correa, M. B., Fernandes, D. A., & Wang, R. (2016). Shuffled complex evolution on photovoltaic parameter extraction: A comparative analysis. *IEEE Transactions on Sustainable Energy*, *vol. 8*, no. 2, pp.805-815.

González, A., Riba, J. R., Rius, A., & Puig, R. (2015). Optimal sizing of a hybrid grid-connected photovoltaic and wind power system. *Applied energy*, *vol. 154*, pp.752-762.

Hadidian-Moghaddam, M. J., Arabi-Nowdeh, S., & Bigdeli, M. (2016). Optimal sizing of a stand-alone hybrid photovoltaic/wind system using new grey wolf optimizer considering reliability. *Journal of Renewable and Sustainable Energy*, *vol. 8, no.* 3.

Hall, B. H., Hall, R. E., & Hausman, J. A. (1974). Estimation and inference in nonlinear structural models. *Annals of economic and social measurement*, *vol. 3,* pp.653-666.

Hannan, M. A., Wali, S. B., Ker, P. J., Abd Rahman, M. S., Mansor, M., Ramachandaramurthy, V. K., ... & Dong, Z. Y. (2021). Battery energy-storage system: A review of technologies, optimization objectives, constraints, approaches, and outstanding issues. *Journal of Energy Storage*, *vol. 42*, pp.103023.

Hassan, A., Saadawi, M., Kandil, M., & Saeed, M. (2015). Modified particle swarm optimisation technique for optimal design of small renewable energy system supplying a specific load at Mansoura University. *IET Renewable Power Generation*, vol. *9, no.* 5, pp.474-483.

Hezer, S., Gelmez, E., & Özceylan, E. (2021). Comparative analysis of TOPSIS, VIKOR and COPRAS methods for the COVID-19 Regional Safety Assessment. *Journal of infection and public health*, *vol. 14, no.* 6, pp.775-786.

Houssein, E. H., Zaki, G. N., Diab, A. A. Z., & Younis, E. M. (2021). An efficient Manta Ray Foraging Optimization algorithm for parameter extraction of three-diode photovoltaic model. *Computers & Electrical Engineering*, *vol. 94*, pp.107304.

Hu, Y., Wang, J., Liang, J., Wang, Y., Ashraf, U., Yue, C., & Yu, K. (2022). A two-archive model based evolutionary algorithm for multimodal multi-objective optimization problems. *Applied Soft Computing*, vol. *119,* pp.108606.

Huang, Q., Shi, Y., Wang, Y., Lu, L., & Cui, Y. (2015). Multi-turbine wind-solar hybrid system. *Renewable Energy*, *vol. 76,* pp.401-407.

Humada, A. M., Darweesh, S. Y., Mohammed, K. G., Kamil, M., Mohammed, S. F., Kasim, N. K., ... & Mekhilef, S. (2020). Modeling of PV system and parameter extraction based on experimental data: Review and investigation. *Solar Energy, vol. 199*, pp.742-760.

Ibrahim, I. A., Hossain, M. J., & Duck, B. C. (2022). A hybrid wind driven-based fruit fly optimization algorithm for identifying the parameters of a double-diode photovoltaic cell model considering degradation effects. *Sustainable Energy Technologies and Assessments*, *vol. 50*, pp.101685.

Ibrahim, I. A., Hossain, M. J., Duck, B. C., & Fell, C. J. (2019). An adaptive wind-driven optimization algorithm for extracting the parameters of a single-diode PV cell model. *IEEE Transactions on Sustainable Energy*, vol. *11*, *no.* 2, pp.1054-1066.

Ibrahim, I. A., Hossain, M. J., Duck, B. C., & Nadarajah, M. (2020). An improved wind driven optimization algorithm for parameters identification of a triple-diode photovoltaic cell model. *Energy conversion and management*, vol. *213*, pp.112872.

Ibrahim, I. A., Khatib, T., & Mohamed, A. (2017). Optimal sizing of a standalone photovoltaic system for remote housing electrification using numerical algorithm and improved system models. *Energy*, *vol. 126*, pp.392-403.

Ilbahar, E., Cebi, S., & Kahraman, C. (2019). A state-of-the-art review on multi-attribute renewable energy decision making. *Energy Strategy Reviews*, vol. *25*, pp.18-33.

Ishaque, K., & Salam, Z. (2011). A comprehensive MATLAB Simulink PV system simulator with partial shading capability based on two-diode model. *Solar energy*, *vol. 85*, *no.* 9, pp.2217-2227.

Ishaque, K., & Salam, Z. (2011). An improved modeling method to determine the model parameters of photovoltaic (PV) modules using differential evolution (DE). *Solar energy*, *vol. 85, no.* 9, pp.2349-2359.

Ismail, M. S., Moghavvemi, M., & Mahlia, T. M. I. (2013). Characterization of PV panel and global optimization of its model parameters using genetic algorithm. *Energy Conversion and Management*, *vol. 73*, pp.10-25.

Javed, M. S., Song, A., & Ma, T. (2019). Techno-economic assessment of a stand-alone hybrid solar-wind-battery system for a remote island using genetic algorithm. *Energy*, vol. *176*, pp.704-717.

Jiang, B., Lei, H., Li, W., & Wang, R. (2022). A novel multi-objective evolutionary algorithm for hybrid renewable energy system design. *Swarm and Evolutionary Computation*, *vol. 75*, pp.101186.

© COPYRIGHT UPM

Jordehi, A. R. (2016). Time varying acceleration coefficients particle swarm optimisation (TVACPSO): A new optimisation algorithm for estimating parameters of PV cells and modules. *Energy Conversion and Management*, *vol. 129*, pp.262-274.

Jordehi, A. R. (2018). Enhanced leader particle swarm optimisation (ELPSO): An efficient algorithm for parameter estimation of photovoltaic (PV) cells and modules. *Solar Energy*, *vol. 159*, pp.78-87.

Kaabeche, A., & Bakelli, Y. (2019). Renewable hybrid system size optimization considering various electrochemical energy storage technologies. *Energy conversion and management*, vol. *193*, pp.162-175.

Kaabeche, A., Belhamel, M., & Ibtiouen, R. (2011). Sizing optimization of grid-independent hybrid photovoltaic/wind power generation system. *Energy*, *vol. 36*, *no.* 2, pp.1214-1222.

Kahloul, S., Zouache, D., Brahmi, B., & Got, A. (2022). A multi-external archive-guided henry gas solubility optimization algorithm for solving multi-objective optimization problems. *Engineering Applications of Artificial Intelligence*, *vol. 109*, pp.104588.

Kamjoo, A., Maheri, A., Dizqah, A. M., & Putrus, G. A. (2016). Multi-objective design under uncertainties of hybrid renewable energy system using NSGA-II and chance constrained programming. *International journal of electrical power & energy systems*, vol. *74*, pp.187-194.

Kanimozhi, G., & Kumar, H. (2018). Modeling of solar cell under different conditions by Ant Lion Optimizer with LambertW function. *Applied Soft Computing*, *vol. 71*, pp.141-151.

Katsigiannis, Y. A., Georgilakis, P. S., & Karapidakis, E. S. (2012). Hybrid simulated annealing–tabu search method for optimal sizing of autonomous power systems with renewables. *IEEE transactions on sustainable energy*, *vol. 3*, *no.* 3, pp.330-338.

Kaya, I., Çolak, M., & Terzi, F. (2019). A comprehensive review of fuzzy multi criteria decision making methodologies for energy policy making. *Energy Strategy Reviews*, *vol. 24*, pp.207-228.

Kellogg, W. D., Nehrir, M. H., Venkataramanan, G., & Gerez, V. (1998). Generation unit sizing and cost analysis for stand-alone wind, photovoltaic, and hybrid wind/PV systems. *IEEE Transactions on energy conversion*, *vol. 13*, *no.* 1, pp.70-75.

Kellogg, W., Nehrir, M. H., Venkataramanan, G., & Gerez, V. (1996). Optimal unit sizing for a hybrid wind/photovoltaic generating system. *Electric Power Systems Research*, *vol. 39*, *no.* 1, pp.35-38.

© COPYRIGHT UPM

Kerboua, A., Hacene, F. B., Goosen, M. F., & Ribeiro, L. F. (2022). Development of technical economic analysis for optimal sizing of a hybrid power system: a case study of an industrial site in Tlemcen Algeria. *Results in Engineering*, vol. *16*, pp.100675.

Keshavarz Ghorabaee, M., Zavadskas, E. K., Turskis, Z., & Antuchevičienė, J. (2016). A new combinative distance-based assessment (CODAS) method for multi-criteria decision-making.

Khan, A., & Javaid, N. (2020). Jaya learning-based optimization for optimal sizing of stand-alone photovoltaic, wind turbine, and battery systems. *Engineering, vol. 6, no.* 7, pp.812-826.

Khan, F. A., Pal, N., Saeed, S. H., & Yadav, A. (2022). Modelling and techno-economic analysis of standalone SPV/Wind hybrid renewable energy system with lead-acid battery technology for rural applications. *Journal of Energy Storage*, vol. *55*, pp.105742.

Khan, F., Al-Ahmed, A., & Al-Sulaiman, F. A. (2021). Critical analysis of the limitations and validity of the assumptions with the analytical methods commonly used to determine the photovoltaic cell parameters. *Renewable and Sustainable Energy Reviews*, *vol. 140*, pp.110753.

Khan, H. A., & Pervaiz, S. (2013). Technological review on solar PV in Pakistan: Scope, practices and recommendations for optimized system design. *Renewable and sustainable energy reviews*, *vol. 23*, pp.147-154.

Khanna, V., Das, B. K., Bisht, D., & Singh, P. K. (2015). A three diode model for industrial solar cells and estimation of solar cell parameters using PSO algorithm. *Renewable Energy*, *vol. 78*, pp.105-113.

Khanna, V., Das, B. K., Bisht, D., & Singh, P. K. (2015). A three diode model for industrial solar cells and estimation of solar cell parameters using PSO algorithm. *Renewable Energy*, *vol. 78*, pp.105-113.

Khanna, V., Das, B. K., Bisht, D., & Singh, P. K. (2015). A three diode model for industrial solar cells and estimation of solar cell parameters using PSO algorithm. *Renewable Energy*, vol. *78*, pp.105-113.

Khanna, V., Das, B. K., Bisht, D., & Singh, P. K. (2015). A three diode model for industrial solar cells and estimation of solar cell parameters using PSO algorithm. *Renewable Energy*, *vol. 78*, pp.105-113.

Kharchouf, Y., Herbazi, R., & Chahboun, A. (2022). Parameter's extraction of solar photovoltaic models using an improved differential evolution algorithm. *Energy Conversion and Management*, *vol. 251*, pp.114972.

Khatib, T., & Elmenreich, W. (2016). *Modeling of photovoltaic systems using Matlab: Simplified green codes*. John Wiley & Sons.

© COPYRIGHT UPM

Khatib, T., Mohamed, A., & Sopian, K. (2012). Optimization of a PV/wind micro-grid for rural housing electrification using a hybrid iterative/genetic algorithm: Case study of Kuala Terengganu, Malaysia. *Energy and buildings*, *vol. 47*, pp.321-331.

Khatod, D. K., Pant, V., & Sharma, J. (2009). Analytical approach for well-being assessment of small autonomous power systems with solar and wind energy sources. *IEEE Transactions on energy conversion*, vol. *25*, *no.* 2, pp.535-545.

Kler, D., Goswami, Y., Rana, K. P. S., & Kumar, V. (2019). A novel approach to parameter estimation of photovoltaic systems using hybridized optimizer. *Energy Conversion and Management*, *vol. 187*, pp.486-511.

Koohi-Fayegh, S., & Rosen, M. A. (2020). A review of energy storage types, applications and recent developments. *Journal of Energy Storage*, *vol. 27*, pp.101047.

Kumar, C., & Mary, D. M. (2021). Parameter estimation of three-diode solar photovoltaic model using an Improved-African Vultures optimization algorithm with Newton–Raphson method. *Journal of Computational Electronics*, vol. *20*, pp.2563-2593.

Kumar, M., & Kumar, A. (2017). An efficient parameters extraction technique of photovoltaic models for performance assessment. *Solar Energy*, *vol. 158*, pp.192-206.

Laudani, A., Fulginei, F. R., & Salvini, A. (2014). High performing extraction procedure for the one-diode model of a photovoltaic panel from experimental I–V curves by using reduced forms. *Solar Energy*, vol. *103*, pp.316-326.

Li, B., Li, J., Tang, K., & Yao, X. (2014, July). An improved two archive algorithm for many-objective optimization. In *2014 IEEE Congress on Evolutionary Computation (CEC)* (pp. 2869-2876). IEEE.

Li, M., Yang, S., & Liu, X. (2015). Bi-goal evolution for many-objective optimization problems. *Artificial Intelligence*, vol. *228*, pp.45-65.

Li, S., Gong, W., & Gu, Q. (2021). A comprehensive survey on meta-heuristic algorithms for parameter extraction of photovoltaic models. *Renewable and Sustainable Energy Reviews*, *vol. 141*, pp.110828.

Lian, J., Zhang, Y., Ma, C., Yang, Y., & Chaima, E. (2019). A review on recent sizing methodologies of hybrid renewable energy systems. *Energy Conversion and Management*, *vol. 199*, pp.112027.

Liang, J., Qiao, K., Yuan, M., Yu, K., Qu, B., Ge, S., ... & Chen, G. (2020). Evolutionary multi-task optimization for parameters extraction of photovoltaic models. *Energy Conversion and Management*, *vol. 207*, pp.112509.

© COPYRIGHT UPM

Lim, L. H. I., Ye, Z., Ye, J., Yang, D., & Du, H. (2015). A linear identification of diode models from single $ I $–$ V $ characteristics of PV panels. *IEEE Transactions on Industrial Electronics*, *vol. 62, no.* 7, pp.4181-4193.

Liu, J., Chen, X., Cao, S., & Yang, H. (2019). Overview on hybrid solar photovoltaic-electrical energy storage technologies for power supply to buildings. *Energy conversion and management*, *vol. 187*, pp.103-121.

Liu, J., Chen, X., Cao, S., & Yang, H. (2019). Overview on hybrid solar photovoltaic-electrical energy storage technologies for power supply to buildings. *Energy conversion and management*, *vol. 187*, pp.103-121.

Liu, Y., Heidari, A. A., Ye, X., Chi, C., Zhao, X., Ma, C., ... & Le, R. (2021). Evolutionary shuffled frog leaping with memory pool for parameter optimization. *Energy reports*, *vol. 7*, pp.584-606.

López-Castrillón, W., Sepúlveda, H. H., & Mattar, C. (2022). Too many solar panels? Oversizing or undersizing of hybrid renewable energy systems based on different sources of information. *Sustainable Energy Technologies and Assessments*, vol. *52*, pp.102264.

Louzazni, M., Khouya, A., Amechnoue, K., Gandelli, A., Mussetta, M., & Crăciunescu, A. (2018). Metaheuristic algorithm for photovoltaic parameters: comparative study and prediction with a firefly algorithm. *Applied Sciences*, *vol. 8*, no. 3, pp.339.

Louzazni, M., Khouya, A., Amechnoue, K., Mussetta, M., & Crăciunescu, A. (2020). Comparison and evaluation of statistical criteria in the solar cell and photovoltaic module parameters' extraction. *International Journal of Ambient Energy*, *vol. 41*, no. 13, pp.1482-1494.

Lu, K., & Liao, H. (2022). A survey of group decision making methods in Healthcare Industry 4.0: bibliometrics, applications, and directions. *Applied Intelligence*, vol. *52, no.* 12, pp.13689-13713.

Lun, S. X., Du, C. J., Guo, T. T., Wang, S., Sang, J. S., & Li, J. P. (2013). A new explicit I–V model of a solar cell based on Taylor's series expansion. *Solar energy*, *vol. 94*, pp.221-232.

Luo, X., Wang, J., Dooner, M., & Clarke, J. (2015). Overview of current development in electrical energy storage technologies and the application potential in power system operation. *Applied energy*, *vol. 137*, pp.511-536.

Ma, G., Xu, G., Chen, Y., & Ju, R. (2017). Multi-objective optimal configuration method for a standalone wind–solar–battery hybrid power system. *IET Renewable Power Generation*, *vol. 11, no.* 1, pp.194-202.

Ma, T., & Javed, M. S. (2019). Integrated sizing of hybrid PV-wind-battery system for remote island considering the saturation of each renewable energy resource. *Energy conversion and management*, *vol. 182*, pp.178-190.

© COPYRIGHT UPM

Ma, T., Yang, H., & Lu, L. (2014). A feasibility study of a stand-alone hybrid solar–wind–battery system for a remote island. *Applied Energy*, *vol. 121*, pp.149-158.

Ma, T., Yang, H., & Lu, L. (2014). Development of a model to simulate the performance characteristics of crystalline silicon photovoltaic modules/strings/arrays. *Solar Energy*, vol. *100*, pp.31-41.

Ma, X., Huang, W. H., Schnabel, E., Köhl, M., Brynjarsdóttir, J., Braid, J. L., & French, R. H. (2019). Data-driven $ I $–$ V $ feature extraction for photovoltaic modules. *IEEE Journal of Photovoltaics*, *vol. 9*, no. 5, pp.1405-1412.

Ma, X., Li, M., Du, L., Qin, B., Wang, Y., Luo, X., & Li, G. (2019). Online extraction of physical parameters of photovoltaic modules in a building-integrated photovoltaic system. *Energy conversion and management*, *vol. 199*, pp.112028.

Madhlopa, A., Sparks, D., Keen, S., Moorlach, M., Krog, P., & Dlamini, T. (2015). Optimization of a PV–wind hybrid system under limited water resources. *Renewable and Sustainable Energy Reviews*, *vol. 47*, pp.324-331.

Mahdavi, S., Rahnamayan, S., & Deb, K. (2018). Opposition based learning: A literature review. *Swarm and evolutionary computation*, *vol. 39*, pp.1-23.

Maheri, A., Unsal, I., & Mahian, O. (2022). Multiobjective optimisation of hybrid wind-PV-battery-fuel cell-electrolyser-diesel systems: An integrated configuration-size formulation approach. *Energy*, *vol. 241*, pp.122825.

Mahesh, A., & Sandhu, K. S. (2015). Hybrid wind/photovoltaic energy system developments: Critical review and findings. *Renewable and Sustainable Energy Reviews*, vol. *52*, pp.1135-1147.

Mahesh, A., & Sandhu, K. S. (2015). Hybrid wind/photovoltaic energy system developments: Critical review and findings. *Renewable and Sustainable Energy Reviews*, vol. *52*, pp.1135-1147.

Maleki, A., Ameri, M., & Keynia, F. (2015). Scrutiny of multifarious particle swarm optimization for finding the optimal size of a PV/wind/battery hybrid system. *Renewable Energy*, vol. *80*, pp.552-563.

Maleki, A., Khajeh, M. G., & Ameri, M. (2016). Optimal sizing of a grid independent hybrid renewable energy system incorporating resource uncertainty, and load uncertainty. *International Journal of Electrical Power & Energy Systems*, vol. *83*, pp.514-524.

Mallipeddi, R., & Das, K. N. (2022). A twin-archive guided decomposition based multi/many-objective evolutionary algorithm. *Swarm and Evolutionary Computation*, vol. *71*, pp.101082.

© COPYRIGHT UPM

Maouhoub, N. (2018). Photovoltaic module parameter estimation using an analytical approach and least squares method. *Journal of Computational Electronics, vol. 17, no.* 2, pp.784-790.

Markvart, T. (1996). Sizing of hybrid photovoltaic-wind energy systems. *solar energy, vol. 57, no.* 4, pp.277-281.

Merchaoui, M., Sakly, A., & Mimouni, M. F. (2018). Particle swarm optimisation with adaptive mutation strategy for photovoltaic solar cell/module parameter extraction. *Energy Conversion and Management*, vol. *175*, pp.151-163.

Mishra, S., Saini, G., Saha, S., Chauhan, A., Kumar, A., & Maity, S. (2022). A survey on multi-criterion decision parameters, integration layout, storage technologies, sizing methodologies and control strategies for integrated renewable energy system. *Sustainable Energy Technologies and Assessments*, vol. *52*, pp.102246.

Moghaddam, M. J. H., Kalam, A., Nowdeh, S. A., Ahmadi, A., Babanezhad, M., & Saha, S. (2019). Optimal sizing and energy management of stand-alone hybrid photovoltaic/wind system based on hydrogen storage considering LOEE and LOLE reliability indices using flower pollination algorithm. *Renewable energy, vol. 135*, pp.1412-1434.

Moghaddam, S., Bigdeli, M., Moradlou, M., & Siano, P. (2019). Designing of stand-alone hybrid PV/wind/battery system using improved crow search algorithm considering reliability index. *International Journal of Energy and Environmental Engineering, vol. 10, no.* 4, pp.429-449.

Monteiro, R. V., Guimaraes, G. C., Moura, F. A., Albertini, M. R., & Albertini, M. K. (2017). Estimating photovoltaic power generation: Performance analysis of artificial neural networks, Support Vector Machine and Kalman filter. *Electric Power Systems Research, vol. 143,* pp.643-656.

Mughal, M. A., Ma, Q., & Xiao, C. (2017). Photovoltaic cell parameter estimation using hybrid particle swarm optimization and simulated annealing. *Energies, vol. 10, no.* 8, pp.1213.

Muhammad, F. F., Karim Sangawi, A. W., Hashim, S., Ghoshal, S. K., Abdullah, I. K., & Hameed, S. S. (2019). Simple and efficient estimation of photovoltaic cells and modules parameters using approximation and correction technique. *PLoS One*, vol. *14, no.* 5, pp.e0216201.

Muhsen, D. H., Ghazali, A. B., Khatib, T., & Abed, I. A. (2015). Parameters extraction of double diode photovoltaic module's model based on hybrid evolutionary algorithm. *Energy Conversion and Management*, vol. *105*, pp.552-561.

Muhsen, D. H., Ghazali, A. B., Khatib, T., & Abed, I. A. (2015). Extraction of photovoltaic module model's parameters using an improved hybrid differential evolution/electromagnetism-like algorithm. *Solar Energy, vol. 119*, pp.286-297.

© COPYRIGHT UPM

Muhsen, D. H., Ghazali, A. B., Khatib, T., & Abed, I. A. (2015). Extraction of photovoltaic module model's parameters using an improved hybrid differential evolution/electromagnetism-like algorithm. *Solar Energy, vol. 119,* pp.286-297.

Muhsen, D. H., Ghazali, A. B., Khatib, T., Abed, I. A., & Natsheh, E. M. (2016). Sizing of a standalone photovoltaic water pumping system using a multi-objective evolutionary algorithm. *Energy, vol. 109*, pp.961-973.

Mukhtaruddin, R. N. S. R., Rahman, H. A., Hassan, M. Y., & Jamian, J. J. (2015). Optimal hybrid renewable energy design in autonomous system using Iterative-Pareto-Fuzzy technique. *International Journal of Electrical Power & Energy Systems*, vol. *64*, pp.242-249.

Naderipour, A., Kamyab, H., Klemeš, J. J., Ebrahimi, R., Chelliapan, S., Nowdeh, S. A., ... & Marzbali, M. H. (2022). Optimal design of hybrid grid-connected photovoltaic/wind/battery sustainable energy system improving reliability, cost and emission. *Energy*, vol. *257*, pp.124679.

Naderipour, A., Ramtin, A. R., Abdullah, A., Marzbali, M. H., Nowdeh, S. A., & Kamyab, H. (2022). Hybrid energy system optimization with battery storage for remote area application considering loss of energy probability and economic analysis. *Energy, vol. 239*, pp.122303.

Nadjemi, O., Nacer, T., Hamidat, A., & Salhi, H. (2017). Optimal hybrid PV/wind energy system sizing: Application of cuckoo search algorithm for Algerian dairy farms. *Renewable and Sustainable Energy Reviews*, *vol. 70,* pp.1352-1365..

Nassar-Eddine, I., Obbadi, A., Errami, Y., & Agunaou, M. (2016). Parameter estimation of photovoltaic modules using iterative method and the Lambert W function: A comparative study. *Energy Conversion and Management*, *vol. 119,* pp.37-48.

NAZ SOLAR ELECTRIC, (accessed June 7, 2022), Available online: https://www.solar-electric.com/victron-energy-smartsolar-mppt-250-85-tr-ve-can-solar-charge-controller.html.

NAZ SOLAR ELECTRIC, (accessed June 7, 2022), Available online: https://www.solar-electric.com/cotek-sl3000-112-low-frequency-pure-sine-wave-inverter.html.

NAZ SOLAR ELECTRIC, (accessed October 24, 2022), Available Online: https://www.solar-electric.com/centennial-gc2200p-flooded-deep-cycle-battery.html,

Ndegwa, R., Ayieta, E., Simiyu, J., & Odero, N. (2020). A simplified simulation procedure and analysis of a photovoltaic solar system using a single diode model.

© COPYRIGHT UPM

Nogueira, C. E. C., Vidotto, M. L., Niedzialkoski, R. K., de Souza, S. N. M., Chaves, L. I., Edwiges, T., ... & Werncke, I. (2014). Sizing and simulation of a photovoltaic-wind energy system using batteries, applied for a small rural property located in the south of Brazil. *Renewable and Sustainable Energy Reviews, vol. 29*, pp.151-157.

Nunes, H. G. G., Pombo, J. A. N., Bento, P. M. R., Mariano, S. J. P. S., & Calado, M. R. A. (2019). Collaborative swarm intelligence to estimate PV parameters. *Energy Conversion and Management*, vol. *185*, pp.866-890.

Nunes, H. G. G., Pombo, J. A. N., Mariano, S. J. P. S., Calado, M. R. A., & De Souza, J. F. (2018). A new high performance method for determining the parameters of PV cells and modules based on guaranteed convergence particle swarm optimization. *Applied energy*, *vol. 211*, pp.774-791.

Nunes, H. G. G., Silva, P. N. C., Pombo, J. A. N., Mariano, S. J. P. S., & Calado, M. R. A. (2020). Multiswarm spiral leader particle swarm optimisation algorithm for PV parameter identification. *Energy conversion and management*, *vol. 225*, pp.113388.

Oliva, D., Abd El Aziz, M., & Hassanien, A. E. (2017). Parameter estimation of photovoltaic cells using an improved chaotic whale optimization algorithm. *Applied energy*, *vol. 200*, pp.141-154.

Oliva, D., Abd Elaziz, M., Elsheikh, A. H., & Ewees, A. A. (2019). A review on meta-heuristics methods for estimating parameters of solar cells. *Journal of Power Sources*, vol. *435*, pp.126683.

Opricovic, S., & Tzeng, G. H. (2004). Compromise solution by MCDM methods: A comparative analysis of VIKOR and TOPSIS. *European journal of operational research*, *vol. 156, no.* 2, pp.445-455.

Oulcaid, M., El Fadil, H., Ammeh, L., Yahya, A., & Giri, F. (2020). Parameter extraction of photovoltaic cell and module: Analysis and discussion of various combinations and test cases. *Sustainable Energy Technologies and Assessments*, *vol. 40*, pp.100736.

Pamučar, D., & Ćirović, G. (2015). The selection of transport and handling resources in logistics centers using Multi-Attributive Border Approximation area Comparison (MABAC). *Expert systems with applications*, *vol. 42, no.* 6, pp.3016-3028.

Pamučar, D., Stević, Ž., & Sremac, S. (2018). A new model for determining weight coefficients of criteria in mcdm models: Full consistency method (fucom). *Symmetry*, *vol. 10*, no. 9, pp.393.

Pandiyan, P., Sitharthan, R., Saravanan, S., Prabaharan, N., Tiwari, M. R., Chinnadurai, T., ... & Devabalaji, K. R. (2022). A comprehensive review of the prospects for rural electrification using stand-alone and hybrid energy technologies. *Sustainable energy technologies and assessments*, vol. *52*, pp.102155.

© COPYRIGHT UPM

Park, J. Y., & Choi, S. J. (2015). A novel datasheet-based parameter extraction method for a single-diode photovoltaic array model. *Solar Energy*, *vol. 122*, pp.1235-1244.

Park, J. Y., & Choi, S. J. (2017). A novel simulation model for PV panels based on datasheet parameter tuning. *Solar Energy*, vol. *145*, pp.90-98.

Patro, S. K., & Saini, R. P. (2020). Mathematical modeling framework of a PV model using novel differential evolution algorithm. *Solar Energy*, vol. *211*, pp.210-226.

Peng, L., Sun, Y., & Meng, Z. (2014). An improved model and parameters extraction for photovoltaic cells using only three state points at standard test condition. *Journal of power Sources*, *vol. 248*, pp.621-631.

Pindado, S., Roibás-Millán, E., Cubas, J., Álvarez, J. M., Alfonso-Corcuera, D., Cubero-Estalrrich, J. L., ... & Jado-Puente, R. (2021). Simplified lambert w-function math equations when applied to photovoltaic systems modeling. *IEEE Transactions on industry applications*, vol. *57, no.* 2, pp.1779-1788.

Polo, J., Martín-Chivelet, N., Alonso-García, M. C., Zitouni, H., Alonso-Abella, M., Sanz-Saiz, C., & Vela-Barrionuevo, N. (2019). Modeling IV curves of photovoltaic modules at indoor and outdoor conditions by using the Lambert function. *Energy conversion and management*, *vol. 195*, pp.1004-1011.

Ponsich, A., Domenech, B., Ferrer-Martí, L., Juanpera, M., & Pastor, R. (2022). A multi-objective optimization approach for the design of stand-alone electrification systems based on renewable energies. *Expert Systems with Applications*, vol. *199*, pp.116939.

Prasad, A. R., & Natarajan, E. (2006). Optimization of integrated photovoltaic–wind power generation systems with battery storage. *Energy*, *vol. 31, no.* 12, pp.1943-1954.

Qais, M. H., Hasanien, H. M., & Alghuwainem, S. (2019). Identification of electrical parameters for three-diode photovoltaic model using analytical and sunflower optimization algorithm. *Applied Energy*, *vol. 250*, pp.109-117.

Qais, M. H., Hasanien, H. M., & Alghuwainem, S. (2020). Parameters extraction of three-diode photovoltaic model using computation and Harris Hawks optimization. *Energy*, *vol. 195*, pp.117040.

Rajasekar, N., Kumar, N. K., & Venugopalan, R. (2013). Bacterial foraging algorithm based solar PV parameter estimation. *Solar Energy*, vol. *97*, pp.255-265.

Ram, J. P., Babu, T. S., Dragicevic, T., & Rajasekar, N. (2017). A new hybrid bee pollinator flower pollination algorithm for solar PV parameter estimation. *Energy conversion and management*, *vol. 135*, pp.463-476.

© COPYRIGHT UPM

Rao, R. V., Savsani, V. J., & Vakharia, D. P. (2012). Teaching–learning-based optimization: an optimization method for continuous non-linear large scale problems. *Information sciences*, *vol. 183, no.* 1, pp.1-15.

Rathore, A., & Patidar, N. P. (2019). Reliability assessment using probabilistic modelling of pumped storage hydro plant with PV-Wind based standalone microgrid. *International Journal of Electrical Power & Energy Systems*, *vol. 106*, pp.17-32.

Rezaei, J. (2015). Best-worst multi-criteria decision-making method. *Omega*, *vol. 53*, pp.49-57.

Rezaei, J. (2016). Best-worst multi-criteria decision-making method: Some properties and a linear model. *Omega*, *vol. 64*, pp.126-130.

Rezk, H., Babu, T. S., Al-Dhaifallah, M., & Ziedan, H. A. (2021). A robust parameter estimation approach based on stochastic fractal search optimization algorithm applied to solar PV parameters. *Energy Reports*, vol. *7*, pp.620-640.

Ridha, H. M. (2020). Parameters extraction of single and double diodes photovoltaic models using Marine Predators Algorithm and Lambert W function. *Solar Energy*, *vol. 209*, pp.674-693.

Ridha, H. M., Gomes, C., & Hizam, H. (2020). Estimation of photovoltaic module model's parameters using an improved electromagnetic-like algorithm. *Neural Computing and Applications*, *vol. 32*, pp.12627-12642.

Ridha, H. M., Gomes, C., & Hizam, H. (2020). Estimation of photovoltaic module model's parameters using an improved electromagnetic-like algorithm. *Neural Computing and Applications*, vol. *32*, pp.12627-12642.

Ridha, H. M., Gomes, C., Hizam, H., Ahmadipour, M., Heidari, A. A., & Chen, H. (2021). Multi-objective optimization and multi-criteria decision-making methods for optimal design of standalone photovoltaic system: A comprehensive review. *Renewable and Sustainable Energy Reviews*, *vol. 135*, pp.110202.

Ridha, H. M., Heidari, A. A., Wang, M., & Chen, H. (2020). Boosted mutation-based Harris hawks optimizer for parameters identification of single-diode solar cell models. *Energy Conversion and Management*, vol. *209*, pp.112660.

Ridha, H. M., Hizam, H., Gomes, C., Heidari, A. A., Chen, H., Ahmadipour, M., ... & Alghrairi, M. (2021). Parameters extraction of three diode photovoltaic models using boosted LSHADE algorithm and Newton Raphson method. *Energy*, vol. *224*, pp.120136.

Ridha, H. M., Hizam, H., Gomes, C., Heidari, A. A., Chen, H., Ahmadipour, M., ... & Alghrairi, M. (2021). Parameters extraction of three diode photovoltaic models using boosted LSHADE algorithm and Newton Raphson method. *Energy*, *vol. 224*, pp.120136.

© COPYRIGHT UPM

Rizk-Allah, R. M., & El-Fergany, A. A. (2020). Conscious neighborhood scheme-based Laplacian barnacles mating algorithm for parameters optimization of photovoltaic single-and double-diode models. *Energy conversion and management*, *vol. 226*, pp.113522.

Rizk-Allah, R. M., & Hassanien, A. E. (2020). Locomotion-based hybrid salp swarm algorithm for parameter estimation of fuzzy representation-based photovoltaic modules. *Journal of Modern Power Systems and Clean Energy*, vol. *9*, no. 2, pp. 384-394.

Selem, S. I., El-Fergany, A. A., & Hasanien, H. M. (2021). Artificial electric field algorithm to extract nine parameters of triple-diode photovoltaic model. *International Journal of Energy Research*, *vol. 45*, no. 1, pp.590-604.

Sharma, N., & Anpalagan, A. (2015). Differential evolution aided adaptive resource allocation in OFDMA systems with proportional rate constraints. *Applied Soft Computing*, vol. *34*, pp.39-50.

Shayeghi, H., & Hashemi, Y. (2015). Application of fuzzy decision-making based on INSGA-II to designing PV–wind hybrid system. *Engineering Applications of Artificial Intelligence*, *vol. 45*, pp.1-17.

Si, J., Marjanovic-Halburd, L., Nasiri, F., & Bell, S. (2016). Assessment of building-integrated green technologies: A review and case study on applications of Multi-Criteria Decision Making (MCDM) method. *Sustainable cities and society*, vol. *27*, pp.106-115.

Siddiqui, M. U., & Abido, M. (2013). Parameter estimation for five-and seven-parameter photovoltaic electrical models using evolutionary algorithms. *Applied soft computing*, *vol.13*, no. 12, pp.4608-4621.

Sinha, S., & Chandel, S. S. (2014). Review of software tools for hybrid renewable energy systems. *Renewable and sustainable energy reviews*, *vol. 32*, pp.192-205.

Subudhi, B., & Pradhan, R. (2017). Bacterial foraging optimization approach to parameter extraction of a photovoltaic module. *IEEE Transactions on Sustainable Energy*, *vol. 9*, *no.* 1, pp.381-389.

Sufyan, M., Abd Rahim, N., Tan, C., Muhammad, M. A., & Sheikh Raihan, S. R. (2019). Optimal sizing and energy scheduling of isolated microgrid considering the battery lifetime degradation. *PloS one*, *vol. 14*, no. 2, pp.e0211642.

Sun, B. (2021). A multi-objective optimization model for fast electric vehicle charging stations with wind, PV power and energy storage. *Journal of Cleaner Production*, vol. *288*, pp.125564.

© COPYRIGHT UPM

Tahani, M., Babayan, N., & Pouyaei, A. (2015). Optimization of PV/Wind/Battery stand-alone system, using hybrid FPA/SA algorithm and CFD simulation, case study: Tehran. *Energy conversion and management*, vol. *106*, pp.644-659.

Tchakpedeou, A. B., Lare, Y., Napo, K., & Fousseni, A. (2022). An improved levenberg–marquardt approach with a new reduced form for the identification of parameters of the one-diode photovoltaic model. *Journal of Solar Energy Engineering*, *vol. 144, no.* 4, pp.041005.

Tito, S. R., Lie, T. T., & Anderson, T. N. (2016). Optimal sizing of a wind-photovoltaic-battery hybrid renewable energy system considering socio-demographic factors. *Solar Energy*, *vol. 136*, pp.525-532.

Tiwari, S., Koch, P., Fadel, G., & Deb, K. (2008, July). AMGA: an archive-based micro genetic algorithm for multi-objective optimization. In *Proceedings of the 10th annual conference on Genetic and evolutionary computation* (pp. 729-736).

Tossa, A. K., Soro, Y. M., Azoumah, Y., & Yamegueu, D. (2014). A new approach to estimate the performance and energy productivity of photovoltaic modules in real operating conditions. *Solar energy*, *vol. 110*, pp.543-560.

Tutkun, N. (2014). Minimization of operational cost for an off-grid renewable hybrid system to generate electricity in residential buildings through the SVM and the BCGA methods. *Energy and Buildings*, *vol. 76*, pp.470-475.

Tzeng, G. H., & Huang, J. J. (2011). *Multiple attribute decision making: methods and applications*. CRC press..

Vasilj, J., Sarajcev, P., & Jakus, D. (2016). Estimating future balancing power requirements in wind–PV power system. *Renewable energy*, *vol. 99*, pp.369-378.

Venkateswari, R., & Rajasekar, N. (2021). Review on parameter estimation techniques of solar photovoltaic systems. *International Transactions on Electrical Energy Systems*, *vol. 31*, no. 11, pp. e13113.

Villalva, M. G., Gazoli, J. R., & Ruppert Filho, E. (2009). Comprehensive approach to modeling and simulation of photovoltaic arrays. *IEEE Transactions on power electronics*, *vol. 24*, no. 5, pp.1198-1208.

Vincke, J. P., & Brans, P. (1985). A preference ranking organization method. The PROMETHEE method for MCDM. *Management Science*, *vol. 31, no.* 6, pp.647-656.

Wang, J., Yang, B., Li, D., Zeng, C., Chen, Y., Guo, Z., ... & Yu, T. (2021). Photovoltaic cell parameter estimation based on improved equilibrium optimizer algorithm. *Energy Conversion and Management*, vol. *236*, pp.114051.

© COPYRIGHT UPM

Wang, M., Xu, X., Yan, Z., & Wang, H. (2021). An online optimization method for extracting parameters of multi-parameter PV module model based on adaptive Levenberg-Marquardt algorithm. *Energy Conversion and Management*, *vol. 245*, pp.114611.

Wang, S., Yu, Y., & Hu, W. (2021). Static and dynamic solar photovoltaic models' parameters estimation using hybrid Rao optimization algorithm. *Journal of Cleaner Production*, vol. *315*, pp.128080.

Weerasuriya, A. U., Zhang, X., Wang, J., Lu, B., Tse, K. T., & Liu, C. H. (2021). Performance evaluation of population-based metaheuristic algorithms and decision-making for multi-objective optimization of building design. *Building and Environment*, vol. *198*, pp.107855.

Wu, Y., Chen, R., Li, C., Zhang, L., & Cui, Z. (2020). Hybrid symbiotic differential evolution moth-flame optimization algorithm for estimating parameters of photovoltaic models. *IEEE Access*, *vol. 8*, pp.156328-156346.

Xu, C., Ke, Y., Li, Y., Chu, H., & Wu, Y. (2020). Data-driven configuration optimization of an off-grid wind/PV/hydrogen system based on modified NSGA-II and CRITIC-TOPSIS. *Energy Conversion and Management*, vol. *215*, pp.112892.

Yan, Z., Li, C., Song, Z., Xiong, L., & Luo, C. (2019). An improved brain storming optimization algorithm for estimating parameters of photovoltaic models. *IEEE Access*, *vol. 7*, pp.77629-77641.

Yang, B., Wang, J., Zhang, X., Yu, T., Yao, W., Shu, H., ... & Sun, L. (2020). Comprehensive overview of meta-heuristic algorithm applications on PV cell parameter identification. *Energy Conversion and Management*, *vol. 208*, pp.112595.

Yang, H., Lu, L., & Zhou, W. (2007). A novel optimization sizing model for hybrid solar-wind power generation system. *Solar energy*, *vol. 81*, no. 1, pp.76-84.

Yang, X., & Gong, W. (2021). Opposition-based JAYA with population reduction for parameter estimation of photovoltaic solar cells and modules. *Applied Soft Computing*, vol. *104*, pp.107218.

Yang, X., Gong, W., & Wang, L. (2019). Comparative study on parameter extraction of photovoltaic models via differential evolution. *Energy conversion and management*, *vol. 201*, pp.112113.

Yao, X. (2006, November). A new multi-objective evolutionary optimisation algorithm: The two-archive algorithm. In *2006 International Conference on computational intelligence and security* (Vol. 1, pp. 286-291). IEEE.

Yousri, D., Abd Elaziz, M., Oliva, D., Abualigah, L., Al-Qaness, M. A., & Ewees, A. A. (2020). Reliable applied objective for identifying simple and detailed photovoltaic models using modern metaheuristics: Comparative study. *Energy Conversion and Management*, vol. *223*, pp.113279.

© COPYRIGHT UPM

Yousri, D., Allam, D., Eteiba, M. B., & Suganthan, P. N. (2019). Static and dynamic photovoltaic models' parameters identification using chaotic heterogeneous comprehensive learning particle swarm optimizer variants. *Energy conversion and management*, *vol. 182*, pp.546-563.

Yousri, D., Fathy, A., Rezk, H., Babu, T. S., & Berber, M. R. (2021). A reliable approach for modeling the photovoltaic system under partial shading conditions using three diode model and hybrid marine predators-slime mould algorithm. *Energy Conversion and Management*, vol. *243*, pp.114269.

Yousri, D., Rezk, H., & Fathy, A. (2020). Identifying the parameters of different configurations of photovoltaic models based on recent artificial ecosystem-based optimization approach. *International Journal of Energy Research*, *vol. 44*, no. 14, pp.11302-11322.

Yousri, D., Thanikanti, S. B., Allam, D., Ramachandaramurthy, V. K., & Eteiba, M. B. (2020). Fractional chaotic ensemble particle swarm optimizer for identifying the single, double, and three diode photovoltaic models' parameters. *Energy*, *vol. 195*, pp.116979.

Yu, K., Qu, B., Yue, C., Ge, S., Chen, X., & Liang, J. (2019). A performance-guided JAYA algorithm for parameters identification of photovoltaic cell and module. *Applied energy*, *vol. 237*, pp.241-257.

Yuan, Y., Xu, H., Wang, B., & Yao, X. (2015). A new dominance relation-based evolutionary algorithm for many-objective optimization. *IEEE Transactions on Evolutionary Computation*, vol. *20, no.* 1, pp.16-37.

Zaimi, M., El Achouby, H., Ibral, A., & Assaid, E. M. (2019). Determining combined effects of solar radiation and panel junction temperature on all model-parameters to forecast peak power and photovoltaic yield of solar panel under non-standard conditions. *Solar Energy*, *vol. 191*, pp.341-359.

Zhang, G., Wu, B., Maleki, A., & Zhang, W. (2018). Simulated annealing-chaotic search algorithm based optimization of reverse osmosis hybrid desalination system driven by wind and solar energies. *Solar Energy*, vol. *173*, pp.964-975.

Zhang, W., Maleki, A., Rosen, M. A., & Liu, J. (2019). Sizing a stand-alone solar-wind-hydrogen energy system using weather forecasting and a hybrid search optimization algorithm. *Energy conversion and management*, *vol. 180*, pp.609-621.

Zhang, Y., Hao, P., Lu, H., Ma, J., & Yang, M. (2022). Modelling and estimating performance for PV module under varying operating conditions independent of reference condition. *Applied Energy*, *vol. 310*, pp.118527.

Zhang, Y., Ma, M., & Jin, Z. (2020). Backtracking search algorithm with competitive learning for identification of unknown parameters of photovoltaic systems. *Expert Systems with Applications*, *vol. 160*, pp.113750.

© COPYRIGHT UPM

Zhou, W., Lou, C., Li, Z., Lu, L., & Yang, H. (2010). Current status of research on optimum sizing of stand-alone hybrid solar–wind power generation systems. *Applied energy*, *vol. 87*, no. 2, pp.380-389.

Zhou, W., Wang, P., Heidari, A. A., Zhao, X., Turabieh, H., & Chen, H. (2021). Random learning gradient based optimization for efficient design of photovoltaic models. *Energy Conversion and Management*, vol. *230*, pp.113751.

Zitzler, E., & Künzli, S. (2004, September). Indicator-based selection in multiobjective search. In *International conference on parallel problem solving from nature* (pp. 832-842). Berlin, Heidelberg: Springer Berlin Heidelberg.

Zitzler, E., Laumanns, M., & Thiele, L. (2001). SPEA2: Improving the strength Pareto evolutionary algorithm. *TIK report*, *vol. 103*.

Zolfani, S. H., Aghdaie, M. H., Derakhti, A., Zavadskas, E. K., & Varzandeh, M. H. M. (2013). Decision making on business issues with foresight perspective; an application of new hybrid MCDM model in shopping mall locating. *Expert systems with applications*, vol. *40*, *no.* 17, pp.7111-7121.

© COPYRIGHT UPM

APPENDICES

Appendix 1

Methods for optimal design of the standalone WT/PV/Battery system

Ref.	Type of data	Method	Objective function	Outcomes
[196]	Average long-term data	Intuitive	LPSP	Optimum design based average monthly data is selected with considering only the reliability of the system. However, the cost of the system has been not mentioned.
[197]	Monthly average daily	Intuitive	Total cost of the system	Using the summer and winter weather conditions, the optimal design of the system is selected using sizing curve method.
[199,200]	Synthetic hourly	Iterative	Total cost of the system	The optimal design of the system is selected by computing the total cost of the system based on proper capacity of the battery storage to satisfy the required load.
[157]	Average monthly	Iterative	LLP and lowest cost of the system.	The optimal design of the system is proposed by establishing various configurations using numerical method based on LLP. Then, the design with minimum cost is selected.
[201]	Daily	Iterative	Initial cost of the system	Mixed integer linear programming is employed to select the optimal solution based on reducing the initial investment cost needed to satisfy the load demand.
[27]	Hourly	Iterative	LPSP and LCE	The optimal design of the system is chosen based on minimizing the LPSP and LCE using intersection curve between the two objectives.
[202]	Hourly	Iterative	LPSP and LCE	The numerical method is proposed in this study to compute the optimal configuration at LPSP=0. Then, the optimal configuration with minimum LCE is chosen.
[204]	Average monthly	Iterative	LLP, seasonal LLP, and ACS	Fuzzy logic interface is implemented to select optimal design for the proposed system. The technical criteria is based on LLP and seasonal LLP, while ACS is considered as an economic criteria.
[205]	Hourly	Iterative	LPSP, NPC, and SPB	The authors proposed a numerical method to optimize the size of the WT/PV/Battery system using different sizes of the WT. LPSP is considered as a technical factor, while NPC and SPB are considered as economic indicators. The results revealed that a smaller size of the WT offers a better choice as an optimal solution for the proposed system.

© COPYRIGHT UPM

[206]	Monthly average daily	Analytical	Total cost of the system	Analytical method based MCS is proposed to select optimum design of the system based on LOHE and LOLE parameters.
[207]	Hourly	Analytical	LCE	Analytical model is implemented to optimize the size of the system based on minimizing the LCE. However, the technical criteria was excluded in this study, which may lead to over/under sizing.
[208]	Hourly	Analytical	EENS and LOLE	The authors developed analytical method based MSM_{UR} to select popper design for the system. The LOLE and EENS are used as a technical criteria. However, the cost assessment has not mentioned. The results compared with MCS.
[209]	Hourly for 16 days	Analytical	LPSP and LCE	Analytical method was simulated to provide electricity of the typical load demand. The objectives function were LPSP and LCE. The results indicated that the batteries storage occupied a crucial part of the total investment cost of the system.
[31]	Average monthly	Analytical	LPSP and LCC	A simulation method based on a probabilistic method is proposed to optimize the size of the WT/PV/Battery system. LPSP and LCC are addressed as techno-economic objectives to be optimized. However, few number of solutions are conducted during the optimization process.
[211]	Hourly	Stochastic	NPC	GA is proposed to selected optimal design of the proposed system by minimizing NPC as an economic criteria. However, the authors did not consider the reliability of the system in this study.
[212]	Average hourly	Stochastic	TAC	The PSO-CF algorithm is proposed to choose the best design of the system. The TAC is considered as an objective function to be minimized. The results compared with different variants of PSO method. However, the reliability of the system has been not considered.
[213]	Average hourly	Stochastic	PBC, LPSP, and TAC	The authors proposed GWO to find optimal design of the proposed system. The PBC and LPSP are used as a technical parameter, while the TAC is employed as an economic parameter.
[214]	Monthly average daily	Stochastic	LPSP and TAC	The GA is used to optimize the size of the proposed system. The LPSP is assumed to be zero, while the TAC is obtained as an objective function to be optimized.
[215]	Hourly	Stochastic	ELF, LPSP, LOEE, and NPC	The authors proposed ICA based on multi-objective optimization to select optimal design of the proposed WT/PV/FC system. The technical criteria are ELF, LPSP, and LOEE, respectively. The NPC is used as an economic objective. The three objectives are converted to single objective using fuzzy logic approach.

© COPYRIGHT UPM

© COPYRIGHT UPM

[216]	Hourly	Stochastic	Total cost of the system	The authors proposed MBA to optimize the size of the WT/PV/FC system. The DD PV model is used to estimate the output power. The total cost of the system is obtained as an objective function. However, the dependability of the system has been not considered in this study.
[217]	Monthly average data	Stochastic	TIC	The MPSO is used to optimize the size of the WT/PV/Battery system. The TIC is used as an objective function to be minimized. However, the technical criteria is ignored in this study.
[218]	Hourly	Stochastic	ENSP and CSLS	The AEFA is proposed to optimize the size of the proposed hybrid system. The ENSP and CSLS are considered as techno-economic objective to be optimized. The two objectives are converted to single-objective method. The results indicated that the optimal design based on VRB storage is more reliable and cost-effective than LAB storage.
[219]	Average monthly	Stochastic	LPSP and COE	The authors proposed GA to optimize the size of the hybrid system. The LPSP and COE are considered as techno-economic criteria. The GA provided better performance in comparison with HOMER software tools.
[220]	Hourly	Stochastic	LPSP and LCE	Optimal size of the WT/PV/Battery system is proposed to enhance LPSP and LCE criteria based on GA. The two objectives are converted into a single objective function.
[222]	Hourly	Hybrid	TAC	The authors combined MCS and PSO methods to optimize the size of the system. The MCS is used to conduct stochastic load demand profile, while PSO is implemented to optimize the TAC. However, the technical parameter has not considered in this study.
[223]	Hourly	Hybrid	LPSP, minimize CO_2 emissions, and annualized total cost	The authors improved NSGA-II method's diversity using dynamic crowding distance, SBX, and PM to optimize the size of the WT/PV/Battery system. The technical objectives are LPSP and minimize CO_2 emissions, while annualized total cost is obtained as an economic objective. Finally, FDM is used to select best optimal solutions from a set of PF.
[224]	Hourly	Hybrid	DPSP and TAC	The NSGA-II is implemented to optimize the size of the proposed system. The DPSP is employed as a technical factor, while TAC is utilized as an economic parameter. The NSGA-II showed a higher dependability than MCS method.
[225]	Hourly	Hybrid	GPAP and total cost of the system	The CS is combined with on Pareto ε-constraint multi-objective method to optimize the size of the WT/PV/Battery system. The GPAP is considered as a technical criteria, while the total cost of the system is used as an economic criteria. The results showed better performance than PSO.

[226]	Hourly	Hybrid	ENS and TPC	The authors combined BB-BC algorithm with PSO to optimal size of the hybrid renewable energy system. Moreover, the mutation mechanism is applied for exploring new areas in the feature space. The ENS is used as a technical parameter, while TPC is employed as an economic one. The performance results is compared with PSO and HDS.
[227]	Annual average hourly	Hybrid	Total cost of the system	The authors proposed ALO_R for optimal size of the proposed hybrid renewable energy system. The objective function is to minimize the total cost of the system. However, the technical criteria is not mentioned.
[228]	Minutely	Hybrid	Total cost of the system	The authors proposed BCGA based on SVM to minimize the total cost of the WT/PV/Battery system. However, the technical parameter has been not considered in this study.
[229]	Hourly	Hybrid	LPSP and LCC	The authors hybridized chaotic search based on SA (HAS) to optimize the size of the hybrid renewable energy system. LPSP and LCC are used as techno-economic criteria. The proposed method compared with CS and SA.
[230]	Hourly	Hybrid	LPSP and LCC	The authors integrated CS-SA-HS-ANN algorithm to optimize the size of the WT/PV/Hydrogen system LPSP and LCC are used as techno-economic objectives to be optimized. The proposed hybrid method outperformed the traditional methods.
[231]	Hourly	Hybrid	LPSP and total cost of the system	The authors proposed GA-PSO method to optimize the size of the system. The objectives functions to be optimized were LPSP and total cost of the system. The results are verified by using HOMER software.
[232]	Hourly	Hybrid	EIR, dumped load size, and total cost of the system	The Iterative-Pareto-fuzzy (IPF) method is obtained to find optimal size of the hybrid renewable energy system. The reliability indicators are EIR and minimizing untiled surplus energy, while total cost of the system is used as a technical parameter. The results indicated that by considering the unutilized surplus power, the total cost of the system can be significantly lowered.
[233]	Hourly	Hybrid	LPSP and LCC	The authors proposed a natural selection PSO and weight coefficient transform method based on multi-objective optimization principle to find optimal size of the WT/PV/Battery system. LPSP and LCC are considered as techno-economic objectives to be optimized.
[234]	Hourly	Hybrid	LPSP and CHSS	The authors proposed FPASA method to find optimal size of the WT/P/Battery system. The LPSP and CHSS are considered as techno-economic objectives, which are converted to single objective to be minimized.

[238]	Hourly	Hybrid	CO_2, LCE, and life cycle emissions	The authors proposed HOGA software tools to optimize the size of the hybrid system. The HOGA is based on SPEA and SPEA 2 methods, which are used to minimize the costs and emissions. In addition, the GA is used to choose the best control strategy with lower cost for each combination of the components of the system.
[168]	Hourly	Hybrid	LPSP and COE	The authors proposed MOEA/D method to establish set of the optimal PF solutions. LPSP and COE are considered as techno-economic objectives to be optimized. However, the poor diversity is observed in the set of the optimal PF solutions.
[174]	Hourly	Hybrid	LPSP, LCE, and PAR	A modified NSGA method is proposed to find optimal size of the WT/PV/Battery system. LPSP, LCE, and PAR are considered as techno-economic criteria. The CRITIC and TOPSIS are used to weight and rank the set of optimal PF solutions.
[235]	Hourly	Hybrid	CO_2 emissions and LCE	The authors proposed MOPSO method to optimize the size of the hybrid system. TOPSIS is then used to sort the optimal solutions from best to worst. The CO2 and LCE are used as techno-economic objectives.
[240]	Average monthly	Software tools	LLP and auxiliary energy unit cost	The OptQuest software tool is proposed to optimize the size of the proposed hybrid system.
[242]	Half-hourly of year	Software tools	LPSP, EE, and LCC	The authors proposed NSGA-II algorithm to find optimal size of the hybrid renewable energy system. The LPSP and EE are used as technical criteria, while the LCC is utilized as a technical criteria. These objectives are converted into single objective. Various auxiliary energy unit cost and LLP are considered as techno-economic objectives to be optimized.
[239]	Average hourly	Software tools	NPC, LCE, CO2 emissions, excess, energy, generated power, and job formation factor.	The authors proposed HOMER software tools to optimize the size of the WT/PV/Battery system based on several techno-economic-social factors. The technical models of the components of the system are implemented by using Matlab/Simulink.

© COPYRIGHT UPM

LIST OF PUBLICATIONS

Ridha, H. M., Hizam, H., Mirjalili, S., Othman, M. L., Ya'acob, M. E., & Abualigah, L. (2022). A novel theoretical and practical methodology for extracting the parameters of the single and double diode photovoltaic models. *IEEE Access*, *10*, 11110-11137.

Ridha, H. M., Hizam, H., Mirjalili, S., Othman, M. L., Ya'acob, M. E., Ahmadipour, M., & Ismaeel, N. Q. (2022). On the problem formulation for parameter extraction of the photovoltaic model: Novel integration of hybrid evolutionary algorithm and Levenberg Marquardt based on adaptive damping parameter formula. *Energy Conversion and Management*, *256*, 115403.

Ridha, H. M., Hizam, H., Mirjalili, S., Othman, M. L., & Ya'acob, M. E. (2022). Zero root-mean-square error for single-and double-diode photovoltaic models parameter determination. *Neural Computing and Applications*, *34*(14), 11603-11624.

Ridha, H. M., Hizam, H., Mirjalili, S., Othman, M. L., Ya'acob, M. E., & Ahmadipour, M. (2022). Parameter extraction of single, double, and three diodes photovoltaic model based on guaranteed convergence arithmetic optimization algorithm and modified third order Newton Raphson methods. *Renewable and Sustainable Energy Reviews*, *162*, 112436.

Ridha, H. M., Hizam, H., Mirjalili, S., Othman, M. L., Ya'acob, M. E., & Ahmadipour, M. (2022). Novel parameter extraction for Single, Double, and three diodes photovoltaic models based on robust adaptive arithmetic optimization algorithm and adaptive damping method of Berndt-Hall-Hall-Hausman. *Solar Energy*, *243*, 35-61.

Ridha, H. M., Hizam, H., Mirjalili, S., Othman, M. L., Ya'acob, M. E., Ahmadipour, M., & Ismaeel, N. Q. (2022). Multi-objective optimization and multi-criteria decision making aided by numerical method: Framework and a case study of Malaysia and South Africa. *Energy Conversion and Management*, *274*, 116468.

Ridha, H. M., Hizam, H., Mirjalili, S., Othman, M. L., Ya'acob, M. E., & Ahmadipour, M. (2023). Innovative hybridization of the two-archive and PROMETHEE-II triple-objective and multi-criterion decision making for optimum configuration of the hybrid renewable energy system. *Applied Energy*, *341*, 121117.

© COPYRIGHT UPM